SPATIAL COMPARISON OF TWO OKLAHOMA RAINFALL ESTIMATES AS POTENTIAL INPUTS FOR AN EVAPOTRANSPIRATION MODEL

By

SCOTT A. WOODRUFF

Bachelor of Science

Northeastern State University

Tahlequah, Oklahoma

1993

Submitted to the Faculty of the
Graduate College of the
Oklahoma State University
in partial fulfillment of
the requirements for
the Degree of
MASTER OF SCIENCE
December, 2000

SPATIAL COMPARISON OF TWO OKLAHOMA

RAINFALL ESTIMATES AS POTENTIAL INPUTS

FOR AN EVAPOTRANSPIRATION MODEL

Thesis Approved:

Thesis Advisor

Dean of the Graduate College

ACKNOWLEDGEMENTS

I wish to express my appreciation to my advisor Dr. Stephen Stadler. He has provided me with sound advice, guidance, and lots of encouragement. I would also like to express appreciation to my other committee members Dr. Allen Finchum and Dr. Mahesh Rao for their technical advice and valuable input. I would like to thank the Department of Geography and the State of Oklahoma EPSCoR and NASA funds for providing me with this research opportunity and their financial support.

I wish to express my appreciation to all the others who provided statistical, technical and analytical support for his study: Steve Woodruff, Dr. John Comer, Joe Seig, Dr. Ron Elliot, Mike Larson, and the Arkansas-Red Basin River Forecast Center.

I would also like to thank my family members who provided love and encouragement along the way. Especially my wife, Amy Woodruff, who supported my return to school, encouraged me when discouraged, reassured me when I felt over-whelmed, motivated me when I wanted to slow down, and pushed me to complete this thesis.

TABLE OF CONTENTS

Chapter Page

Chapter | Page

LIST OF TABLES

Table Page

Table Page

Table	Page

LIST OF FIGURES

Figure Page

Figure Page

Figure Page

Figure Page

Figure Page

LIST OF ACRONYMS

ABRFC	Arkansas-Red Basin River Forecast Center
GIS	Geographic Information Systems
HDP	Hourly Digital Precipitation
HRAP	Hydrologic Rainfall Analysis Project
IDW	Inverse Distance Weighted Interpolation
MAP	Mean Aerial Precipitation
NetCDF	Network Comma Delimited File
NEXRAD	Next Generation Radar
NWS	National Weather Service
WSR-88D	Weather Service Radar 1988 Doppler

CHAPTER I

INTRODUCTION

The ability to accurately measure the amount of rain that has fallen over a given area is valuable to many areas of research. Hydrologic modeling (useful in flood prediction, pollution runoff, water resources management, and agricultural management) depends on an accurate estimate of rainfall over the area being considered. Variability in this estimate may translate into faulty predictions and management choices (Finnerty, et. al., 1997a).

A simple garden rain gage can give an accurate measurement of rainfall in a particular spot but estimating rainfall for every point across a wide area is a real challenge. In the past, rainfall was measured by rain gages and assumed to be evenly dispersed over the whole area thus, inputting a single rainfall depth for the entire basin. With the demand for hydrologic models of increasing accuracy, it is no longer practical to maintain this assumption (Cedarwall, 1999; Chaubey, 1997).

With the advent of modern precipitation measurement techniques, such as radar and large, automated rain gage networks, it is now possible to measure spatial variability of rainfall easily and more accurately. However, there are shortcomings in both of these estimation methods (Wilson and Brandes, 1979). Rain gage networks give accurate point estimates but fall short when it comes to spatially describing a rainfall event over a large area. This is especially true in areas with non-homogenous rainfall patterns such as Oklahoma (Cedarwall, 1999). Small, concentrated rainfall events can occur between gages giving a false, low rainfall estimation. A rain gage network large enough and with a high concentration of gages per area could give an accurate description but the sheer numbers of gages required would render the network too expensive and unmanageable (Duncan, et. al., 1993). Radar has the advantage of being able to remotely survey large areas and make thousands of measurements in minutes (the equivalent of a dense rain gage network containing thousands of individual gages), but is less accurate than a rain gage for estimating total rainfall for an individual point (Wilson, et. al., 1979). Several researchers have suggested that radar estimated rainfall, when calibrated with rain gage data, can give a rainfall estimate with the point accuracy of gages and the spatial resolution of radar (Pereira and Crawford, 1995; Wilson and Brandes, 1979; Wilson, 1970). Collier (1986a) compared rainfall estimates from a gage network alone, and from radar that was calibrated with data from only a few gages. He suggested that a very dense gage network was needed to measure point rainfall very accurately. However, a less dense gage network with a radar system calibrated using the data from a few of the gages was capable of producing measurements which had the same or better accuracy as a sparse gage network over a large area.

There are several available sources for total rainfall measurement in Oklahoma, from rain-gage networks to radar to rain gage calibrated radar. The Oklahoma Mesonetwork is a dense network of weather stations covering the entire state. The network density is nearly one gage per 35 kilometers and can provide rainfall measurements at 15 minute intervals. The Mesonet point rainfall measurements can be interpolated to create a rainfall surface for the state of Oklahoma.

The Arkansas-Red Basin River Forecast Center (ABRFC) in Tulsa, Oklahoma produces a daily rainfall estimate for the Arkansas and Red river basins using radar calibrated with rain gage data from across the ABRFC study area. This data product provides a rainfall estimate with a resolution of 4 kilometers and provides a detailed spatial description of rainfall events.

1.1 Statement of the Problem

Both of these efforts to measure and describe rainfall events provide a valuable source of data for hydrologic modeling. However, if both of these estimates were used as input into the same model, the difference in how these estimates spatially describe the same rainfall event could result in inconsistent model output. Chaubey (1997) concluded that the spatial variability of rainfall does introduce uncertainty into model outputs.

In that radar and gage-based estimates of rainfall are both readily available for model input in Oklahoma, it is important to examine how these two rainfall estimates differ in their description of the spatial variability of rainfall, ability to accurately estimate various storm events, and estimate of total rainfall volume.

1.2 Objectives

The overall goal of this study is to examine the differences between two available total rainfall estimates, the Oklahoma Mesonet and the ABRFC, and determine if those differences are significant. The specific objectives of this research are:

1) To use both sources to generate rainfall estimates for the same study area, so that the two estimates can be visually compared.

2) To calculate and map the actual volumetric difference between the two estimates.

3) To statistically examine the volumetric differences with reference to location and distance from the measurement components (Mesonet weather stations and radar facilities) of each rainfall estimate.

4) To examine differences in reference to the type of rainfall event, to see if the spatial characteristics of the rainfall event affects the agreement or disagreement between the two rainfall estimates.

5) To repeat the above mentioned objectives for several different time scales (hourly, 6-hour, and daily) to see if time is an important factor in estimate comparisons.

Research Hypothesis: The spatial difference between Mesonet gage estimated rainfall and the ABRFC gage calibrated radar rainfall estimates will be significant.

The goal of this study is to spatially compare these two methods of estimating total rainfall. It is hoped that this comparison will answer many key questions. Do these two sources differ significantly in their estimate of total rainfall? If so, is this due to the added spatial description of the radar estimate? Where is the difference occurring? How important is it to precisely describe the spatial structure of rainfall events? The answers to these questions would be valuable to anyone trying to determine which estimate to apply to a research project or a modeling effort.

1.3 Importance of Study

An evaluation of the spatial differences between the ABRFC and Mesonet rainfall estimates, will be useful in determining the optimal total rainfall input for various hydrologic modeling efforts. Total rainfall is a key input for any many hydrologic models and spatial variation in the rainfall input will result in variation in model output (Chaubey, 1997).

The ABRFC and Mesonet rainfall estimates describe the spatial variability of rainfall in different ways. If the spatial differences between these two rainfall estimates are significant, then the variation in model outputs will be significant depending on which estimate is used as the rainfall input.

CHAPTER II

REVIEW OF LITERATURE

Accurately estimating the amount of total rainfall falling in a given area is the key to modeling the behavior of that rainfall as runoff, soil moisture, ground or surface water. Hydrologic modeling (useful in evapotranspiration estimates, flood prediction, pollution runoff, water resources management, and agricultural management) depends on an accurate estimate of total rainfall over the area being considered. Variability in the estimates may translate into faulty predictions and management choices (Finnerty and Johnson, 1997).

Many hydrologic models depend on a single, or maybe a few, point rainfall measurements to provide a rainfall input. Often, a single, uniform rainfall amount is estimated for the entire model study area from this measurement alone. In areas where the majority of rainfall is spatially uniform, this may be acceptable. In Oklahoma however, one cannot assume a totally uniform rainfall from point rainfall measurements. Even the densest of rain gage networks have difficulty capturing the spatial variability of Oklahoma rainfall events (Legates, 2000).

With the advent of modern precipitation measurement techniques, such as radar and large, automated rain gage networks, an attempt is being made to measure the spatial variability of rainfall and take this variability into account when modeling the numerous hydrologic processes. The following sections will cover the evolution of total rainfall estimation and its impact on hydrologic modeling.

2.1 Rain-Gage Measurement of Rainfall

The amount of rainfall at a given point can be measured easily and effectively with a single common rain gage. This type of measurement can be used to calculate a myriad of hydrologic information, such as soil moisture or runoff, for that one point. If rainfall in the area is evenly distributed, one rain gage can accurately estimate the surrounding rainfall for a large area. Many hydrologic models rely on a single rainfall measurement for an entire watershed and assume that rainfall to be even for the entire area.

A rain gage precipitation measurement is a "biased underestimate" (Legates, 2000) of true precipitation due to error introduced by several factors: 1) the deleterious effects of the wind, 2) wetting losses on the interior walls of the gage, 3) splashing from the gage collector and, 4) and the mechanical limitations of weighing gages and tipping-bucket recorders (Legates and DeLiberty, 1993; Groisman and Legates, 1994). "Wind is the largest source of gage undercatch (Legates, 2000)." Using only one point rainfall measurement, with its inherent bias, can introduce uncertainty in any hydrologic model that relies on that estimate.

A single rain gage cannot measure the spatial variability of rainfall. Cederwall (1999) states that point measurements (rain gages) often are not representative of the amount of precipitation falling over a large area. This particular true where convective rainfall events or spatially variable rainfall events are common.

The use of many rain gages together in the form of a network, can dramatically improve the ability to spatially describe a rainfall event using point rainfall measurements. With the technological advances in this area, it is feasible to have completely automated rain gage networks with the ability to transmit data through telecommunication. Many states, power utilities, military installations, and regional water districts have installed their own gage networks (Legates, 2000).

According to Legates (2000), gage-based precipitation data (with an hourly temporal resolution) are readily available from the NWS through their first order station network. Other regional and local gage networks are available for specific areas of the country through the United States Geological Survey (USGS) and the National Weather Service (NWS) (Legates 2000).

Scientists at Oklahoma State University and the University of Oklahoma proposed a statewide network of weather stations in response to the need for agricultural, hydrological, and meteorological monitoring (Brock, et. al., 1995). The result of this effort was the Oklahoma Mesonet network of weather stations, a joint project of Oklahoma State University and the University of Oklahoma. The Oklahoma Mesonet is an automated network of 114 stations covering the state of Oklahoma. Each station measures air temperature, humidity, barometric pressure, wind speed and direction, rainfall, solar radiation, and soil temperatures. Each station transmits a data message every 15 minutes via radio link to a central site in Norman, Oklahoma. The data is archived and disseminated in real time to a broad community of users. For a complete description of the Oklahoma Mesonet and its functionality, see Brock et. al. (1995).

The Oklahoma Mesonet will be used to provide one of the rainfall estimates compared in this study. Each station uses an unheated tipping bucket gage to measure rainfall. The unheated gage is meant to measure rainfall rather than all precipitation, since the unheated tipping bucket gage is not suited for snow or freezing precipitation measurement (Brock, et al., 1995). This measurement device is suitable for this study since all study dates are taken from the summer season. A Alter-style wind screen is used to reduce the error caused by wind-induced precipitation loss.

The effectiveness of these gage networks often depends upon the density and distribution of the gages within the network. According to Pereira et. al. (1998), the rain gage density and their distribution in a network significantly affect the accuracy of the final rainfall analysis. Brock et. al. (1995) posits the Oklahoma Mesonet weather station network represents "the most intense statewide system, in both space and time, in the country." The average distance between stations is 35 km (19 miles). Morrissey et. al. (1995) studied the distribution of various gage networks and their associated error variances. He determined that rain gages in the Mesonet have an error variance similar to a uniform network.

The rain gage networks only provide an estimate of total rainfall at gage locations. The amount of rainfall between the gages must be estimated. Cruten and Obled (1982) provide a contrast and comparison of the methods that have been proposed for mapping rainfall fields from point rainfall data. Cruten and Obled (1982) found that for regions with intense and strongly varying rainfall events, sophisticated techniques provide a much better estimation than any of the more commonly used techniques. They included spline-surface fitting, optimal interpolation, kriging, and interpolation based on empirical orthogonal functions in the category of sophisticated techniques.

Legates (2000) points out that one of the problems associated with gage network measurements is that "they are only point measurements." Even for many high spatial-resolution, regional networks, including the Oklahoma Mesonet, distances between stations often exceed 50 kilometers. The NWS first-order station network has inter-station distances that exceed 100 km. There is a large amount of space where rainfall is not measured with gages. Convective showers and even large-scale stratiform precipitation events can often be completely contained in areas this small. As a consequence, many precipitation events are misrepresented spatially by the traditional gage networks. This results in an under-representation of the more intense rainfall regions, thereby further underestimating the true precipitation (Legates, 2000). NWS river forecasters also acknowledge that rain gage networks often do not fully capture the intensity and spatial characteristics of heavy precipitation events (Finnerty, et al., 1997).

Network density can be increased by adding new gages, thus producing a more accurate spatial description of rainfall. However, the number of gage additions required to produce the desired accuracy, could be unfeasible. Duncan et. al. (1993) used simulated rain gage networks of different gage densities to study the effect of gage sampling density on the accuracy of a stream flow model. Duncan attempted to determine the required gage density to estimate model parameters within 5% accuracy. He determined that a very dense gage network would be required and that for large watersheds, the number of gages required would be prohibitive.

2.2 Radar Measurement of Rainfall

Radar measures the electromagnetic energy reflected off of airborne water particles (liquid or solid) in the atmosphere. The amount reflected energy is used to estimate the amount of water present in the atmosphere. Radar has an advantage over rain gage networks because it can directly measure reflected energy over a large area and at an enormous sample density. However, the amount of rainfall is not measured directly and has to be estimated based on the estimated relationship between reflectivity and actual atmospheric moisture.

The use of the federal government's Next Generation Radar (NEXRAD) precipitation estimates is expected to improve hydrologic forecasting because of the distinct advantage of radar over rain gage networks in estimating the spatial coverage of heavy rainfall (Seo and Smith, 1996; Smith et al., 1996). Although radar is not a direct measure of precipitation, it provides much better spatial description of rainfall (Cederwall, 1999).

By the late 1980s, the advent of the National Weather Service (NWS) Weather Surveillance Radar-1988 Doppler (WSR-88D) weather radar, was greatly enhancing weather forecasting across the country (Legates, 2000). According to Legates (2000), these radars provide a new and improved tool for hydro-climatological and hydro-meteorological data acquisition. The WSR-88D radar network provides real-time precipitation estimates with a more-than-adequate temporal resolution and a spatial resolution that far surpasses anything available from traditional precipitation gage networks (Legates, 2000).

The main problem with the radar precipitation estimates, however, is their accuracy. Sources of error include the reflectivity to rainfall factor, which is not constant from storm to storm. Raindrop size distributions can vary widely among different storms. Other sources of error stem from the variation in drop-size distribution as well as the evaporation and advection of precipitation before it reaches the ground (Wilson and Brandes, 1979).

Several studies indicate the extreme biases associated with radar based precipitation estimates used to determine storm total precipitation. In a study by Woodley et. al. (1975), it was found that convective rainfall estimates were seriously underestimated. And Pereira and Crawford (1995) found that uncalibrated radar underestimated the rainfall volume during most events in the study period. The direct use of radar rainfall data in quantitative operational hydrologic forecasting, however, is not in general an acceptable practice because of various sources of error associated with radar observation of rainfall (Wilson and Brandes, 1979).

2.3 Comparison of Rain Gage Data with Radar Data

Both rain gage networks and radar have their advantages and disadvantages in estimating rainfall. Rain gage networks directly measure rainfall and, through interpolation or other statistical methods, can produce useful areal estimates of total rainfall for a large area. However, they lack the ability to spatially describe a rainfall event, especially for rainfall that exhibits high spatial variability. Radar can create a clear spatial description of a rainfall event by accurately delineating areas of high, low, and no rainfall. However, radar does not directly measure rainfall and an estimate of rainfall from reflectivity is susceptible to various sources of error.

The meteorological literature contains numerous papers on the comparison of radar and rain gage measurements of precipitation amounts. These papers are reviewed in Wilson and Brandes (1979).

Wilson and Brandes (1979) found that "areal and point rainfall estimates are often in error by a factor of two or more." They also found an average difference of 24% between radar and gage point measurements for all 14 storms studied, after removing the mean storm bias.

In a study by Smith et. al. (1996), values from rain gages were interpolated to the same grid used by a WSR-88D rainfall estimate through an inverse distance squared algorithm. When the two estimates were compared, the analysis suggested systematic underestimation of rainfall by radar in comparison to rain gage, for paired gage-radar observations. The gage-radar analysis indicated underestimation by most WSR-88D sites. Underestimation was most severe at far range and close range, but at most sites, underestimation occurred at all ranges.

It is difficult to determine which estimate is better suited for a particular application. Agreement or disagreement between the estimation methods can depend on factors such as rain gage network density, radar range, and intensity of rainfall.

Rain gage network density can negate the need for the added spatial description of radar. Hildebrand et. al. (1979) found that radar data are no more accurate than gage only data for gage densities greater than one gage per 100 km^2. Hildebrand et. al. (1979) used a high-density gage network to show that radar adds little information to high-density gage network estimates of areal rainfall, particularly when rainfall is light.

Radar range can affect the differences between radar and rain gage estimates for different areas. Wilson and Brandes (1979) found that agreement between radar and surface (gage) rainfall estimates generally decreases with increasing radar range. Increasing radar sampling volume and height of the beam above the ground at far ranges leads to a higher probability that the precipitation observed aloft is different from that reaching the ground.

A study by Smith et. al. (1996) suggests both close-range and far-range bias in a radar precipitation estimate. Smith et. al. (1996) found that rain gage observations were 48% larger than WSR-88D rainfall estimates in the range 0-40 km, 18% in the range 40-160 km, and 40% in the range greater than 160 km for the warm season. Underestimation was most pronounced at close range and far range.

The two estimate types can also be best suited for different spatial types of rainfall. As mentioned earlier, Hildebrand et. al. (1979) states that radar adds little information to high-density gage network estimates of areal rainfall, particularly when rainfall is light. If rainfall is evenly distributed over a large area, individual gages can capture the low spatial variability.

Accurate delineation of the no-rain area has long been held to be a particular strength of radar rainfall estimates, especially for convective precipitation. The study by Smith et. al. (1996) found that for sites within 200 kilometers of one WSR-88D, radar and gage measurements agreed at 98% of the locations where gages showed zero rainfall accumulation.

Accurate delineation of heavy rain areas is as equally important as delineating zero rainfall areas. For a typical heavy rainfall event in the Southern Great Plains of Oklahoma, Smith et. al. (1996) found that the gage rainfall estimate indicated that no rainfall in the area exceeded 25 millimeters, while the radar derived estimate found a total of 1,730 km^2 that exceeded 25 millimeters of rainfall. Smith et. al. (1996) also found that "more than 200 hours from the WSR-88D products had greater than 1000 km^2 with hourly accumulations exceeding 25 mm," while only 20 hours of the gage accumulations showed the same results. Numerous storm systems producing WSR-88D-measured hourly rainfall accumulations exceeding 50 mm, were completely missed by the rain gage network. The results of Smith's et. al. (1996) study illustrate the inability of rain gage networks, even of relatively high density, to detect and measure heavy rainfall. The WSR-88D has far superior capability for monitoring heavy rainfall than rain gage networks.

2.4 Calibration of Radar Estimates with Rain-Gage Data

Some researchers suggested that radar and rain gage data be combined to take advantage of the positive qualities of both estimates, while at the same time, negating the disadvantages of both estimates. Collier (1986a) stated that "it is important to blend the different methods of measurement operationally to generate a measurement system, which performs better overall than any one of its constituent parts."

The meteorological literature contains numerous papers on the comparison of radar and rain gage measurements of precipitation amounts and on adjustment techniques for their optimum combination. These papers are reviewed in Wilson and Brandes (1979).

Wilson and Brandes (1979) found that the most successful technique for improving radar rainfall estimates has been to calibrate the radar with rain gages. They suggest that even a single gage observation can provide useful storm calibration information and more than one gage used to calibrate will reduce the expected error even more. Collier (1986b) suggested that a gage network would have to be very dense to a very high accuracy of point rainfall measurement. However, a radar system calibrated with a few gages from a less dense gage network, is capable of producing measurements which have the same or better accuracy as a sparse gage network over a large area. And He predicted that there would be high accuracy in the region of the gages, which could be deliberately sited in areas of particular hydrological interest.

When Wilson (1970) adjusted radar-derived thunder-storm rainfalls for a 3500 km^2 watershed by a single centrally located gage, the average error was reduced from 51% (unadjusted measurements) to 35%. Wilson (1970) also illustrated that radar derived precipitation estimates, when calibrated with gage densities as low as one gage per 3400 km^2, are more accurate than estimates from gages alone spaced one per 860 km^2.

Brandes (1975) found that areal precipitation estimates derived from rainfalls observed by rain gages alone produced errors ranging from 21% to 24%. However, when calibrated by networks of rain gages with densities of 900 km^2 and 1600 km^2, the estimate error was reduced to between 13% and 14%. Brandes (1975) also found that radar data added to gage observations also increased the explained variance in point rainfall estimates above that from gages alone, from 53% to 77% and 46% to 72% for rain gage network densities of 1 gage per 900 km^2 and 1600 km^2 respectively.

Collier (1986a) found that using five tele-metering rain gages significantly improves the accuracy, as compared with independent rain gage data, of estimates of surface rainfall within 75 kilometers of the radar site on most occasions. And Collier (1986b) stated that to produce more accurate rainfall estimates than calibrated radar data would require the use of a rain gage network with gage spacing not greater than 20 kilometers.

Pereirea and Crawford (1995) used hydrologic simulations to show that the statistical integration of radar estimates and Mesonet measurements produced a more accurate final analysis than using either individual estimate. "Consequently, more accurate hydrologic forecasts are possible in the near real time." Hildebrand et. al. (1979) concluded that for lower gage densities (less than one gage per 250 km^2) and for the Illinois climate, a combination of gage and radar data may be more accurate than gage only mean convective rainfall measurements.

Collier (1986a) suggested that rainfall spatial characteristics may change the effects of calibration on improving radar estimates. He found that gage calibration of radar has on average a smaller effect, "although it may have a large effect in individual cases."

The Arkansas-Red Basin River Forecast Center (ABRFC) in Tulsa, Oklahoma produces rainfall data products based on this concept of calibrating radar data with rain gage measurements. The ABRFC is responsible for predicting the flash flood danger and monitoring flow for streams and rivers throughout the Arkansas and Red river watershed.

An accurate rainfall input is necessary for forecasting flash flood danger and issuing accurate flood warnings. The ABRFC depends on a rainfall input that is generated by calibrating WSR-88D radar with rain gage data. Besides being used for the ABRFC forecast, the ABRFC provides the rainfall data to the public.

The ABRFC rainfall data product, called Stage III, is a combination of data from 18 overlapping WSR-88D radars and rainfall gage network data from across the ABRFC coverage area, including the Oklahoma Mesonet. This is an hourly product with 4 kilometer resolution, corresponding with the Hydrologic Rainfall Analysis Project (HRAP) grid.

> *The Stage III data merges the hourly digital precipitation array (HDP) and gage precipitation estimates by using the gage data to remove mean and local biases contained in the radar derived 1-hour precipitation estimates. The Stage III data assumes the gage sensor is 'ground truth' precipitation and uses the HDP gridded precipitation estimates to fill in the spatial distribution and rate of rainfall between the gages. The NWS Hydrologic Rainfall Analysis Project grid system (HRAP) uses a polar stereographic projection grid to merge optimal rainfall estimates from multi-radars and rain gages. The HRAP grid size is a function of latitude and is approximately 4 x 4 km^2 over the area of study (Finnerty, et al., 1997).*

The ABRFC staff hydrologists often performs supplementary corrections, as they think necessary, to account for gage network or radar discrepancies. Therefore, the data product in not produced purely from objective formulas. Problems such as faulty gages or radar are accounted for on an hourly basis. There is no metadata available to indicate the actual number of gages used for any particular product. The Stage III data will be refered to as the ABRFC rainfall estimate for the remainder of the study.

2.5 Effects of Spatial Variability of Rainfall on Hydrologic Model Outputs

Rainfall is a key input variable used in hydrologic and water quality models. Many studies emphasize the importance of spatially describing rainfall for accurately modeling hydrologic processes and that spatial variability in the rainfall estimate may cause variability in model outputs. Rudra et. al. (1993) suggests that failure to take these variations into account during calibration could lead to highly distorted estimates of model parameters; and failure to consider the detailed variations during model application could lead to serious inaccuracies in predicted results.

Dawdy and Bergman (1969) studied the effect of rainfall variability on stream flow simulation in a small basin in Southern California. They concluded that predicting peak discharge based on a single rain gage observation resulted in a standard error on the magnitude of 20%. Wilson et. al. (1979) and other researchers (Beven and Hornberger, 1982; Corradini and Singh, 1985; Obled et al., 1994) have concluded that storm runoff hydrographs are sensitive to the spatial distribution and accuracy of the precipitation inputs. Chaubey's (1997) study also confirms the importance of accurately describing the spatial characteristics of rainfall. His goal was to study the variability introduced into the runoff model due to the spatial variability in rainfall. His study showed that for all rainfall events studied, variability in the measured rainfall resulted in variability in model outputs. The complex relationship between the degree of spatial variability of rainfall, watershed characteristics (topography, channel network, soils, etc.), antecedent soil moisture conditions and catchment response is poorly understood (Chaubey 1997).

Hydrologic model response to precipitation inputs of various spatial and temporal resolutions has been the subject of numerous investigations. Many studies have approached this problem from the standpoint of rain gage sampling and density. Recently, the implementation of radar has enabled hydrologists to begin the evaluation of model response to gridded precipitation estimates. Intuitively, one would hypothesize that the higher resolution data leads to better model results. Surprisingly, there does not seem to be a clear trend in the literature that supports this hypothesis (Finnerty, et. al., 1997).

In an oft-referenced work, Wilson et. al. (1979) concluded that ignoring the spatial variability of precipitation input, given when the total depth of rainfall is preserved, could have significant influences on the runoff hydrograph. Their findings were based on the analysis of a 67 square kilometer basin and two levels of synthetic precipitation definition: in the first case, one gage was used to define the input to a lumped parameter model, while in the second, 20 gages were used. Based on limited testing, Shanhltz et. al. (1981) arrived at a similar conclusion, as did Beven and Hornberger (1982) who suggested that the incorporation of distributed inputs would lead to improvements in simulating catchment hydrographs (Finnerty, et. al., 1997).

On the other hand, Obled et. al. (1994) used 21 rain gages to define the input to 9 sub-basins representing a 71 square kilometer basin. They presumed that providing distributed inputs to the model would improve simulations, especially if parameter re-optimization was allowed. However, their semi-distributed representation of the basin produced slightly worse results than a lumped representation combined with coarser precipitation input, even after recalibration of the model parameters. The authors were unable to prove the value of using distributed rainfall inputs to improve hydrologic predictions, noting that: "better dynamics expected in the discharge from better information on rainfall pattern is not demonstrated in the goodness-of-fit criteria."

Any modeling effort that includes a rainfall input, must seriously consider the effects of rainfall spatial variability on model outputs. This study will examine two rainfall estimates that could potentially be used as rainfall inputs for a variety of models. The Mesonet estimates in this thesis interpolate point rainfall measurements from the 114 Mesonet weather station sites. Rainfall is measured directly but the amount of rainfall between measurement points has to be estimated and the spatial structure of a rainfall event can be overlooked. The ABRFC estimate combines the benefits of radar (spatial description) and rain gages (direct rainfall measurement) to produce a rainfall estimate. The differences in how these two estimates spatially describe the same rainfall event could result in significantly different rainfall volumes and therefore, significantly different model outputs.

CHAPTER III

METHODS

3.1 DESIGN

Objectives

The purpose of this study is to investigate the spatial and temporal differences between two total rainfall estimates available in Oklahoma. The spatial differences between Arkansas-Red Basin River Forecast Center (ABRFC) estimates and Oklahoma Mesonet estimates were examined by computing the difference in estimated total rainfall in 4 x 4 km grid cells across the state of Oklahoma. The temporal differences between the two types of estimates will be examined by comparing data from various time scales, such as hourly, six hour, and daily rainfall data.

For a description of the specific study objectives, please refer to the list of objectives outlined in chapter one.

Study Area

The state of Oklahoma will be used as the study area for this thesis. The study area was chosen based on the overlap between the coverage area of the two sources of rainfall estimates. The study area must coincide with areas covered by both data sources. Figure 3.1 illustrates the ABRFC coverage area, which corresponds with the Hydrologic

Rainfall Analysis Project (HRAP) grid. This area covers the entire state of Oklahoma as well as most of the surrounding states. Figure 3.2 illustrates the Oklahoma Mesonet network of weather stations, which does not extend beyond the Oklahoma state borders. A list of the Mesonet sites with 4 letter identifier is contained in Appendix A. Therefore, any area within the Oklahoma state borders is covered by both data sources.

The entire state of Oklahoma, rather than a smaller subdivision, will be used as the study area for several reasons. Large statewide rainfall events can be examined, the largest sample of Mesonet stations and ABRFC grid cells can be used, and the effects of distance can be best examined if the largest possible study area is used.

Map Projection

No projection was used when mapping the data. The rainfall data was initially described using the HRAP coordinate of each grid cell. The HRAP coordinates were converted to latitude and longitude coordinate system, which is compatible with the Geographic Information Systems (GIS) software. Latitude and longitude coordinates were used to describe the location of the rainfall data throughout the study. The GIS software used in this study (ESRI, 1999) is capable of completing all the necessary functions and calculations without projecting the data. Therefore, no projection was used and the data remained in their unprojected forms.

Figure 3.1: The Arkansas-Red Basin River Forecast Center coverage area.

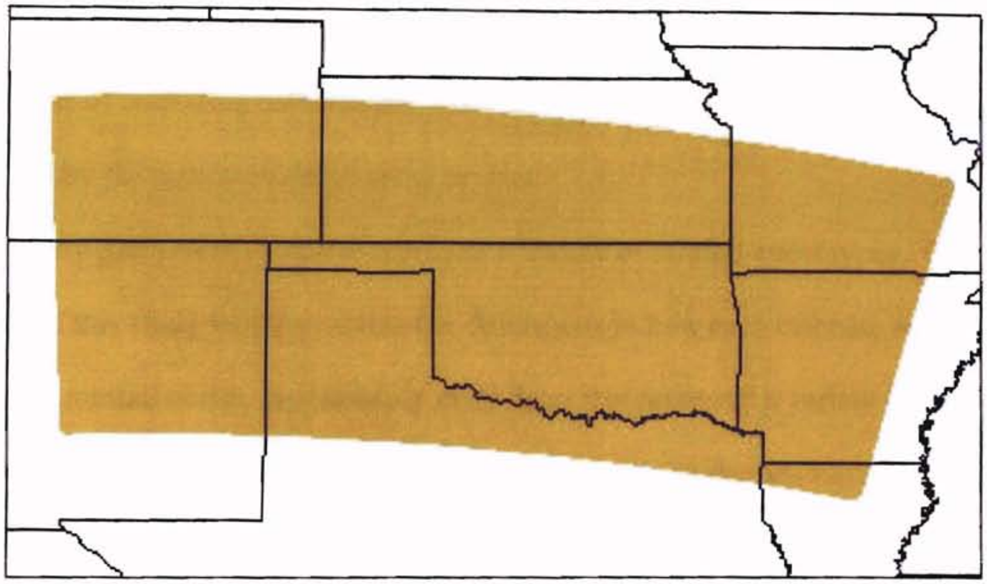

Figure 3.2: Mesonet Weather Station sites with 4-letter identifier.

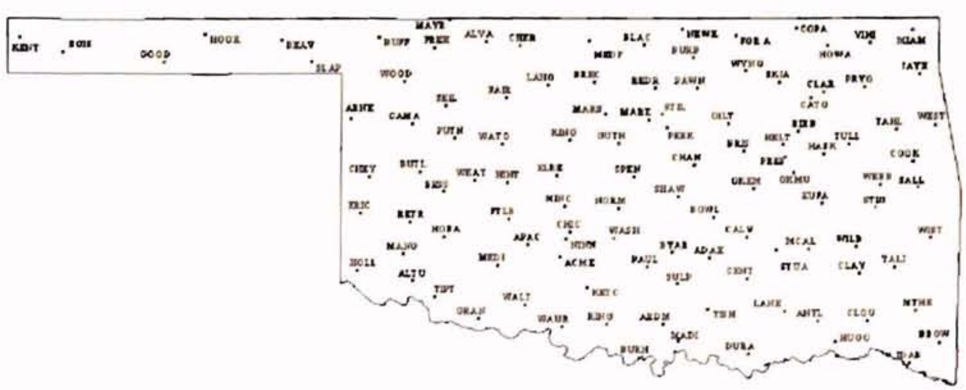

Study Dates

A total of 9 study dates were chosen from the three summer months (June, July, and August) of 1997. The dates were chosen to represent a broad range of rainfall types. The purpose of excluding cold weather study dates was to avoid the error that could be introduced by the measurement of snow or sleet.

Study dates were chosen to represent a variety of rainfall event types. One of the purposes of this study was to examine the differences in how each estimate spatially describes a rainfall event. By choosing study dates that represent a variety of rainfall patterns, the effects of storm type on the differences between the two rainfall estimates can be examined. The study dates exhibited rainfall patterns ranging from light to heavy rainfall, local to widespread rainfall, or homogenous to concentrated rainfall events.

Figure 3.3 through Figure 3.11 contain images of rainfall dates taken from the ABRFC website and represent the 24-hour accumulated rainfall. The amount of rainfall is color-coded according to the original ABRFC scale (inches) at the bottom of the images. For the purposes of this study, millimeters were used when comparing the ABRFC to the Mesonet data.

Figure 3.5: 24-hour accumulated rainfall image for June 28, 1997 (ABRFC, 1999).

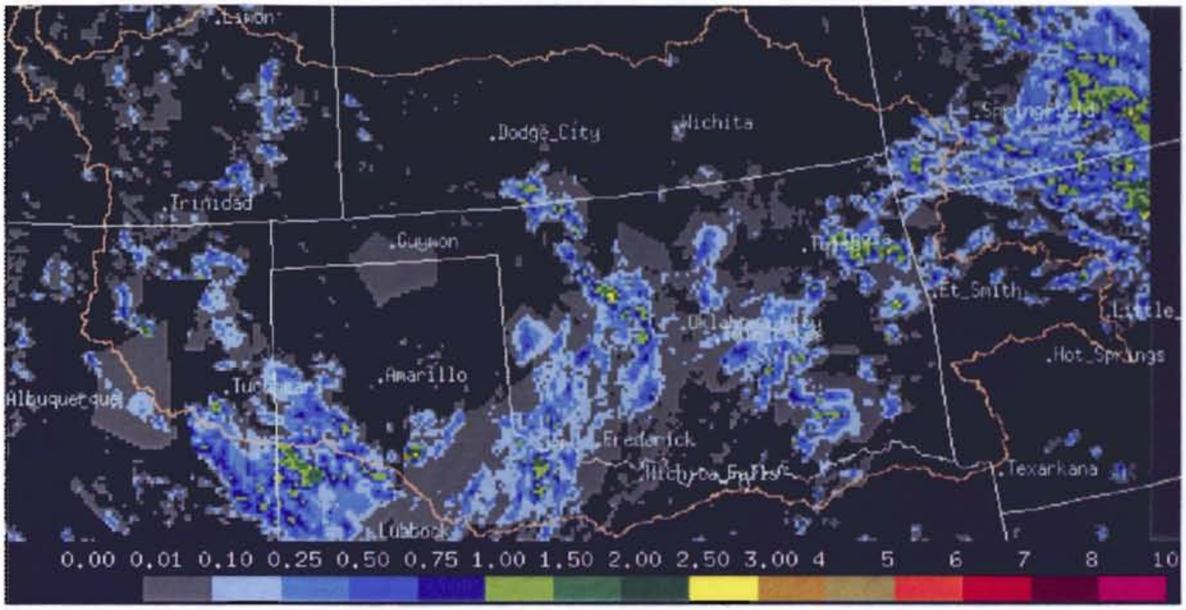

Figure 3.6: 24-hour accumulated rainfall image for July 11, 1997 (ABRFC, 1999).

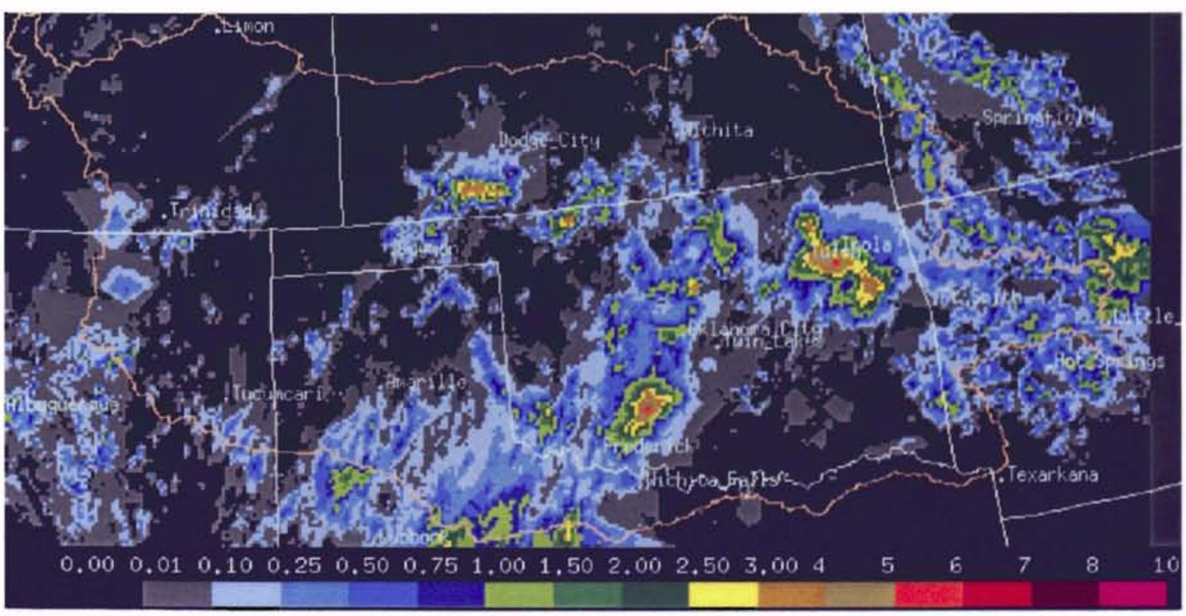

Figure 3.7: 24-hour accumulated rainfall image for July 16, 1997 (ABRFC, 1999).

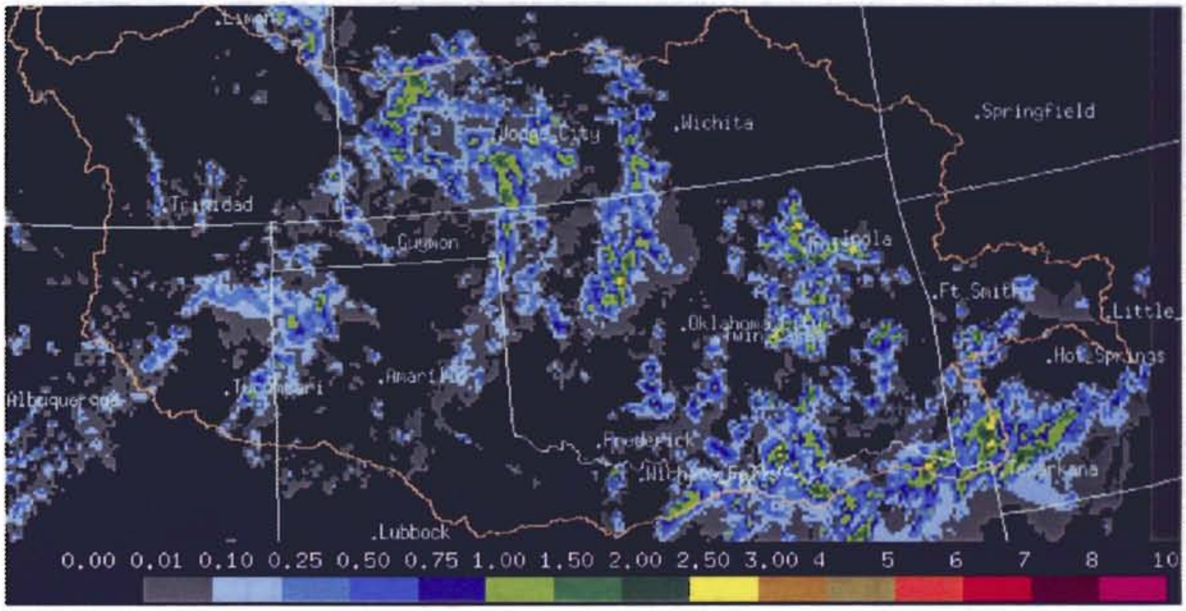

Figure 3.8: 24-hour accumulated rainfall image for July 18, 1997 (ABRFC, 1999).

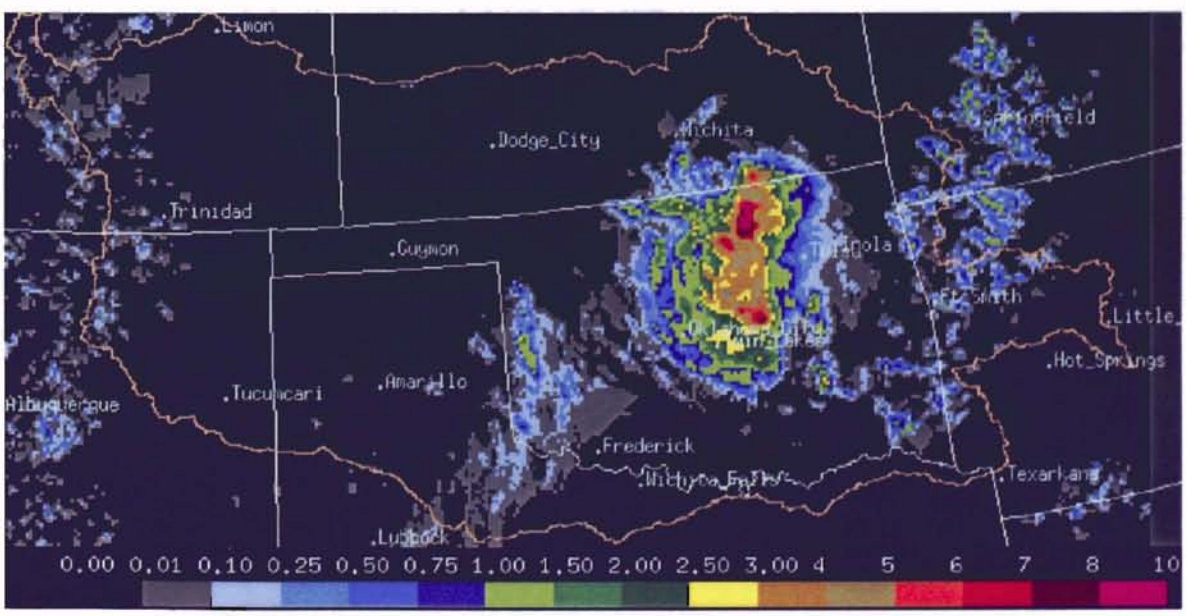

Figure 3.9: 24-hour accumulated rainfall image for August 13, 1997 (ABRFC, 1999).

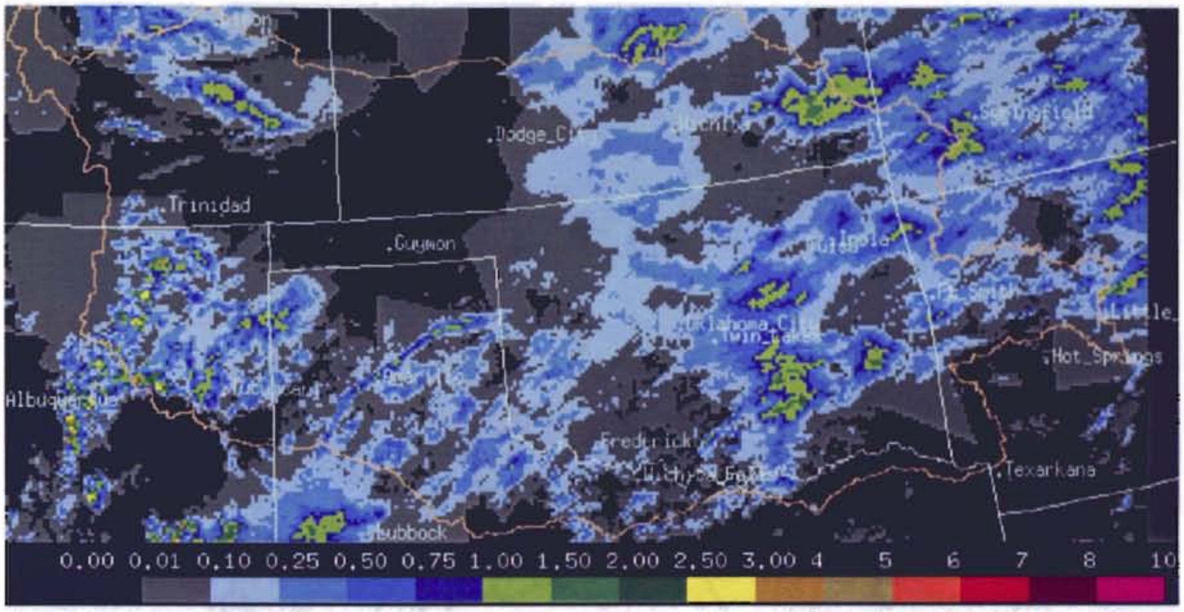

Figure 3.10: 24-hour accumulated rainfall image for August 19, 1997 (ABRFC, 1999).

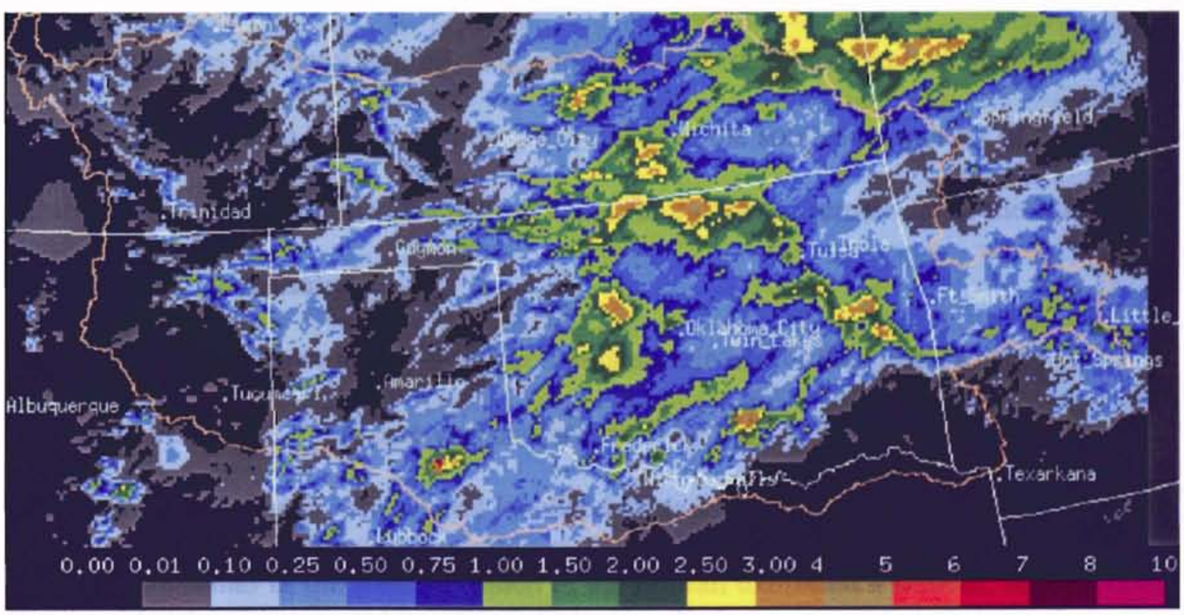

Figure 3.11: 24-hour accumulated rainfall image for August 22, 1997 (ABRFC, 1999).

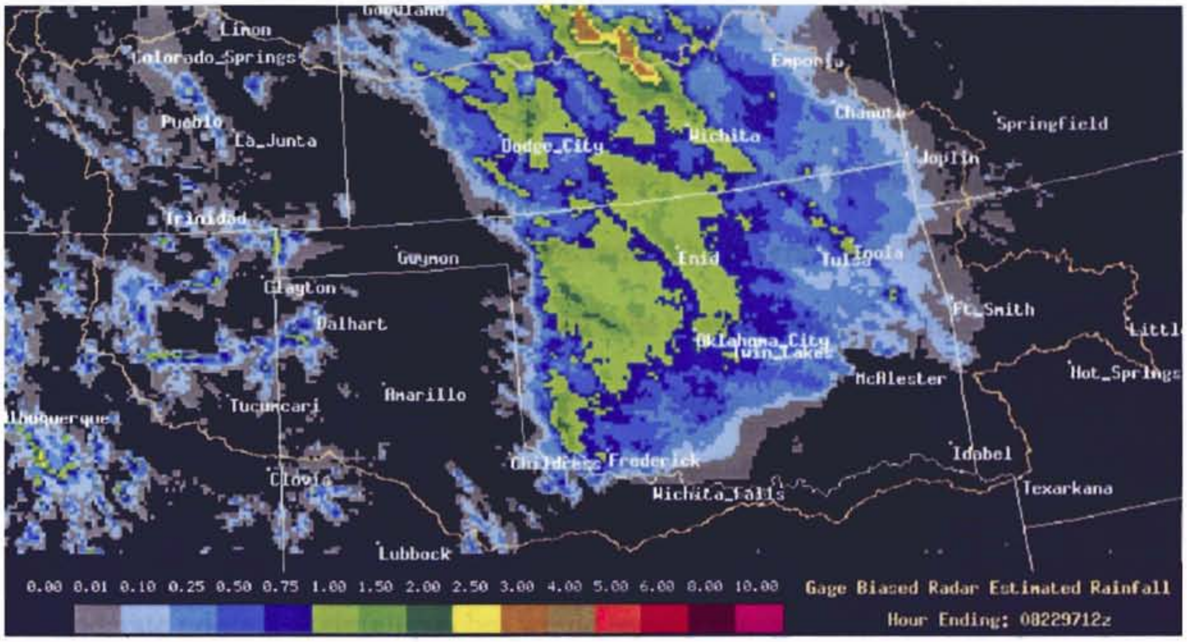

Figure 3.3 shows the 24-hour accumulated rainfall for the June 9, 1997 study date (ABRFC, 1999). This date was characterized by mostly light to moderate rainfall with scattered patches of heavy rainfall. The rainfall was widespread but broken up into separate, concentrated rainfall events. The rainfall in the southwest quarter of the state exhibited a smooth, homogenous pattern while rainfall in the remainder of the state was localized and concentrated.

Figure 3.4 shows the 24-hour accumulated rainfall for the June 24, 1997 study date (ABRFC, 1999). This date was characterized by light to moderate rainfall across most of the state. There were several localized areas of heavy rainfall in the panhandle and the eastern half of the state but much of the rainfall exhibited a smooth, homogenous pattern.

Figure 3.5 shows the 24-hour accumulated rainfall for the June 28, 1997 study date (ABRFC, 1999). This date was characterized by random, scattered patches of light to moderate rainfall. Rainfall patches exhibited sharp transitions from moderately heavy rainfall at the center to little or no rainfall around the edges.

Figure 3.6 shows the 24-hour accumulated rainfall for the July 11, 1997 study date (ABRFC, 1999). This date was characterized by several large,heavy rainfall maxima. These events were widespread with the heaviest rainfall at the center and gradually decreased rainfall amounts towards the edges.

Figure 3.7 shows the 24-hour accumulated rainfall for the July 16, 1997 study date (ABRFC, 1999). This date was characterized by random, scattered patches of light to moderate rainfall. Rainfall patches would rapidly change from moderately heavy rainfall at the center to little or no rainfall around the edges.

Figure 3.8 shows the 24-hour accumulated rainfall for the July 18, 1997 study date (ABRFC, 1999). This date was characterized by a single, extremely heavy rainfall event. This event was widespread, covering almost the whole northeast quarter of the state, with the heaviest rainfall in the center and gradually decreasing rainfall towards the edges of the rainfall event.

Figure 3.9 shows the 24-hour accumulated rainfall for the August 13, 1997 study date (ABRFC, 1999). This date was characterized by widespread areas of light to moderate rainfall. Changes in rainfall amount were gradual from the center to the edges of rainfall events.

Figure 3.10 shows the 24-hour accumulated rainfall for the August 19, 1997 study date (ABRFC, 1999). This date was characterized by widespread, heavy rainfall.

Figure 3.5 shows the 24-hour accumulated rainfall for the June 28, 1997 study date (ABRFC, 1999). This date was characterized by random, scattered patches of light to moderate rainfall. Rainfall patches exhibited sharp transitions from moderately heavy rainfall at the center to little or no rainfall around the edges.

Figure 3.6 shows the 24-hour accumulated rainfall for the July 11, 1997 study date (ABRFC, 1999). This date was characterized by several large, heavy rainfall maxima. These events were widespread with the heaviest rainfall at the center and gradually decreased rainfall amounts towards the edges.

Figure 3.7 shows the 24-hour accumulated rainfall for the July 16, 1997 study date (ABRFC, 1999). This date was characterized by random, scattered patches of light to moderate rainfall. Rainfall patches would rapidly change from moderately heavy rainfall at the center to little or no rainfall around the edges.

Figure 3.8 shows the 24-hour accumulated rainfall for the July 18, 1997 study date (ABRFC, 1999). This date was characterized by a single, extremely heavy rainfall event. This event was widespread, covering almost the whole northeast quarter of the state, with the heaviest rainfall in the center and gradually decreasing rainfall towards the edges of the rainfall event.

Figure 3.9 shows the 24-hour accumulated rainfall for the August 13, 1997 study date (ABRFC, 1999). This date was characterized by widespread areas of light to moderate rainfall. Changes in rainfall amount were gradual from the center to the edges of rainfall events.

Figure 3.10 shows the 24-hour accumulated rainfall for the August 19, 1997 study date (ABRFC, 1999). This date was characterized by widespread, heavy rainfall.

Rainfall amount changed gradually from areas of heavy rainfall at the center to moderate rainfall at the edges of rainfall events.

Figure 3.11 shows the 24-hour accumulated rainfall for the August 22, 1997 study date (ABRFC, 1999). This date was characterized by widespread, moderate rainfall. A single, widespread rainfall event covered almost the entire study area. Rainfall was very homogenous, with gradual change from areas of high rainfall to areas of low rainfall at the edges of the rainfall event.

Units of Measurement

System Internationale (SI) units are the standard for scientific investigations so this study will follow the international convention of using millimeters as the basic units. Any statistical measurement of rainfall, such as minimum, maximum, mean, or standard deviation, will also be expressed in millimeters. The difference between the two rainfall estimates will be measured in millimeters as well. Distance will be measured in kilometers.

Both sources of rainfall data, the Oklahoma Mesonet and the Arkansas-Red Basin River Forecast Center, are based on Coordinated Universal Time (UTC). A single ABRFC 24-hour rainfall day is measured from 12:00 UTC to 12:00 UTC. For convenience sake, the study days in this investigation will be measured in the same way. For example, the study date of June 9, 1997 will consist of the 24 hours between 12:00 UTC June 8, 1997 and 12:00 UTC June 9, 1997.

Spatial and Temporal Resolution

A 4 km^2 spatial resolution will be used in this study. The spatial resolution used in this study was decided on the basis of which resolution is optimal for both the Mesonet and ABRFC rainfall estimates. The geographic software (ESRI, 1999) used to interpolate the Mesonet data also allows the user to interpolate to a user determined grid resolution. Because the Mesonet data were in the form of point data and can be interpolated to match any grid cell size, the resolution for the ABRFC rainfall data was used as the determining factor. The ABRFC rainfall data is reported as a 4 x 4 kilometer grid with rainfall values for each grid cell center point.

Temporal resolutions of 1 hour, 6 hours, and 24 hours were used in this study. By examining the rainfall estimates over several different time scales, the effects of time scale on variation between the two estimates were examined. The ABRFC rainfall data is available in 1, 6, and 24 hour files based on UTC time. The Mesonet rainfall data is also available in an hourly format from which 6 hour and 24 hour totals and hourly data can be derived. However, the Mesonet data in these files is based on Central Daylight Time and must be converted to match the ABRFC time scale.

Equipment and Tools

All software functions were performed using an IBM compatible personal computer (PC) with a 266 Megahertz Intel processor and 32 Megabytes of random access memory (RAM) and Windows NT as the operating system.

Software

ARC/INFO 7.0. The ARC/INFO 7.0 (ESRI, 1999) geographic information systems (GIS) software was used in this study. ARC/INFO was used to interpolate the Mesonet point rainfall data to a grid matching the ABRFC rainfall data. ARC/INFO is the GIS software developed by Environmental Systems Research Institute (ESRI). ARC/INFO has both raster and vector capability. The GRID module of ARC/INFO was used for raster or grid functions.

ArcView GIS 3.1. ArcView GIS 3.1 software (ESRI, 1999) was also used in this study. ArcView was used to perform spatial joins, distance calculations, and create the maps displaying the geographic information. ArcView GIS is software developed by ESRI that is complimentary to the ARC/INFO GIS software. ArcView GIS 3.1 has fewer of the robust geographic functions of ARC/INFO such as interpolation, but uses a graphic user interface (GUI) to conveniently manipulate and display the geographic data produced by ARC/INFO.

SPSS 7.5. The statistical analysis was performed using the SPSS 7.5 for Windows software (SPSS, 1996). Once the rainfall data was converted into database tables, it was imported into SPSS for analysis. SPSS has a graphic user interface and can generate statistical charts and graphs.

3.2 PROCEDURES

Preparing Daily Meteorological Data

ABRFC Data. The ABRFC rainfall data files are available at the ABRFC web site, located at the following address: http://info.abrfc.noaa.gov/index.html. The archive section of the web site contains 1, 6, and 24-hour rainfall data files back to January of 1994. For each rainfall data file, there is an image available illustrating the amount of rainfall for that date and time period. For example, Figure 3.7 is the image associated with the 24-hour rainfall file for the date of July 16, 1997. Each image contains a color scale that represents the amount of rainfall in inches. No other metadata are included with these files.

The data files can be downloaded from the ABRFC archive section in a compressed format that need to be decompressed with a utility such as WinZip. WinZip can be found at the following web site address: http://www.winzip.com.

The ABRFC rainfall data files are in an archive format known as NetCDF (NetCDF, 1999). NetCDF is an archive format that is commonly used to store scientific data. Since the data files are in an archive format, they cannot be read with a standard text editor such as WordPad or NotePad. The file must be converted from the NetCDF format to an ASCII format before further manipulation.

There are several tools available for manipulating NetCDF files. A package of NetCDF software tools is available for download at the following website address: http://www.unidata.ucar.edu/packages/netcdf.

Two utilities called "NCDump" and "NCGen" were used to convert a NetCDF file to an ASCII file and back into the NetCDF format. The "NCDump" utility was used to convert the 1 hour, 6 hour, and 24 hour ABRFC rainfall files for each of the nine study dates.

Figure 3.12 contains the ASCII text version of the 24-hour NetCDF file for the July 16, 1997 study date. Each NetCDF file contains an introductory section with pertinent information on the data contained within the file and how it is stored. The remaining sections store a series of rainfall values for the center point of the approximately 50,000 4 x 4 kilometer HRAP grid cells. Rainfall values are stored according to their respective x and y HRAP coordinates. Figure 3.1 shows the HRAP grid coverage area, which also serves to define the ABRFC coverage area.

The data contained in the ASCII version of the NetCDF file are unusable by the GIS and statistical software used in the study. The data is not immediately usable for several reasons. The HRAP coordinate system, used to refer to the location of individual rainfall values, is not compatible with the GIS software. The rainfall values are stored in units of $1/100^{th}$ of millimeters and need to be converted to millimeters. And the data is not in a tabular format that can be imported into the GIS and statistical software. The data must be converted to a useable format.

Figure 3.12: ASCII text version of the NetCDF data archive file with header information and rainfall data for one row of the HRAP grid.

```
netcdf 071697 {
dimensions:
	hrapy = 159 ;
	hrapx = 335 ;
	latlong = 4 ;
	dates = 9 ;

variables:
	short amountofprecip(hrapy, hrapx) ;
		amountofprecip:long_name = "24 hourly precipitatio" ;
		amountofprecip:units = "1/100 mm" ;
		amountofprecip:grid = "hrap_grid=1/40th lfm grid" ;
		amountofprecip:resolution = "4km*4km" ;
		amountofprecip:dateofdata = "07169712Z" ;
		amountofprecip:dateofcreation = "07169720Z" ;
		amountofprecip:source = "arkansas red basin river forecast
center tulsa ok" ;
		amountofprecip:comments = "preliminary data...subject to
change" ;
	float lat(latlong) ;
		lat:order = "bottom_left,bottom_right,top_right,top_left" ;
	float lon(latlong) ;
		lon:order = "bottom_left,bottom_right,top_right,top_left" ;
	float true_lat ;
	float true_lon ;
	char timeofdata(dates) ;
	char timeofcreation(dates) ;
	float hrap_xor ;
		hrap_xor:comments = "offset in x direction of hrap grid" ;
	float hrap_yor ;
		hrap_yor:comments = "offset in y direction of hrap grid" ;

data:
 amountofprecip =
  // amountofprecip(hrapy = 0, hrapx 0-334)
    0, 29, 0, 0, 0, 0, 0, 0, 0, 0, 29, 0, 0, 0, 0, 0, 0, 0, 0, 0, 0, 0,
0, 0, 108, 0, 0, 0, 0, 0, 0, 0, 0, 0, 0, 0, 0, 0, 0, 0, 0, 0, 0, 0, 0,
0, 0, 0, 0, 0, 0, 0, 0, 0, 0, 0, 0, 0, 0, 0, 0, 0, 0, 0, 0, 0, 0, 0, 0,
0, 0, 0, 0, 0, 0, 0, 0, 0, 0, 0, 0, 0, 0, 0, 0, 0, 0, 0, 0, 0, 0, 0, 0,
0, 0, 0, 0, 0, 0, 0, 0, 0, 0, 0, 0, 0, 0, 0, 0, 0, 0, 0, 0, 0, 0, 0, 0,
0, 0, 0, 0, 0, 0, 0, 0, 0, 0, 0, 0, 0, 0, 0, 0, 0, 0, 0, 0, 0, 0, 0, 0,
0, 0, 0, 0, 0, 0, 0, 0, 0, 0, 0, 0, 0, 0, 0, 0, 0, 0, 0, 0, 0, 0, 0, 0,
0, 0, 0, 0, 0, 0, 0, 0, 0, 0, 0, 0, 0, 0, 0, 0, 0, 0, 0, 0, 0, 0, 0, 0,
0, 48, 129, 58, 38, 29, 0, 0, 0, 0, 0, 0, 0, 0, 0, 0, 0, 0, 0, 0, 29,
0, 603, 1728, 1430, 300, 156, 21, 18, 17, 29, 94, 124, 278, 178, 69,
28, 16, 671, 2279, 1792, 2044, 945, 90, 52, 42, 32, 17, 388, 2790,
2161, 137, 92, 716, 1315, 1523, 2445, 2119, 3321, 3477, 2508, 1162,
1129, 1294, 335, 487, 479, 405, 332, 308, 374, 361, 424, 481, 576, 584,
463, 384, 975, 231, 654, 1011, 179, 205, 121, 130, 124, 108, 66, 61,
55, 49, 43, 38, 32, 27, 23, 0, 0, 0, 0, 0, 0, 0, 0, 0, 0, 0, 0, 0, 0,
0, 0, 0, 0, 0, 38, 29, 0, 0, 0, 0, 0, 0, 0, 0, 0, 0, 0, 0, 0, 0, 0, 0,
0, 0, 0, 0, 0, 0, 0, 0, 0, 0, 0, 0,
```

The present author wrote a computer program that converts the data contained in the NetCDF ASCII file into a useable format. The program will hereafter be referred to as "NetCDF Converter."

The NetCDF Converter program performs the following functions on the data contained in the ASCII NetCDF file:

1. Opens the ASCII NetCDF file and accesses the data for the first rainfall cell.
2. Converts the HRAP x and y coordinates of an individual rainfall cell and converts them to corresponding latitude and longitude coordinates.
3. Converts the rainfall value from units of 1/100th of a millimeter to millimeter units.
4. Writes a record for the individual rainfall cell to an output file in a comma-delimited table format.
5. Repeats steps 2-4 for each of the approximately 53,000 rainfall grid cells.

The final product is a comma delimited text table containing a single-line record for each of the approximately 50,000 HRAP grid cells. Table 3.1 contains a portion of the output table for the 24-hour NetCDF file for the July 16, 1997 study date. Each record in the table contains the HRAP X coordinate, HRAP Y coordinate, latitude coordinate, longitude coordinate, and the amount of estimated rainfall in millimeters for that particular grid cell. The HRAP coordinates refer to the position within the HRAP grid, which consists of 335 rows and 159 columns. For example, HRAP coordinates of X = 100 and Y = 50, would refer to the 101st grid cell in the 51st row (row and column

Table 3.1: NetCDF Converter program output table July 16, 1997.

HRAPX	HRAPY	LATITUDE	LONGITUDE	RAINFALL (MM)
0	0	33.6375	-106.4567	0.00
1	0	33.6384	-106.4139	0.29
2	0	33.6392	-106.3711	0.00
3	0	33.6401	-106.3282	0.00
4	0	33.6409	-106.2854	0.00
5	0	33.6417	-106.2426	0.00
6	0	33.6424	-106.1997	0.00
7	0	33.6432	-106.1569	0.00
8	0	33.6439	-106.1141	0.00
9	0	33.6446	-106.0712	0.00
10	0	33.6452	-106.0284	0.29
11	0	33.6458	-105.9855	0.00
12	0	33.6464	-105.9427	0.00
⋮	⋮	⋮	⋮	⋮
323	158	38.1337	-91.2271	0.00
324	158	38.1249	-91.1812	0.00
325	158	38.116	-91.1354	0.00
326	158	38.1071	-91.0896	0.00
327	158	38.0982	-91.0438	0.00
328	158	38.0892	-90.9981	0.00
329	158	38.0802	-90.9523	0.00
330	158	38.0712	-90.9066	0.00
331	158	38.0621	-90.8609	0.00
332	158	38.053	-90.8152	0.00
333	158	38.0439	-90.7695	0.00
334	158	38.0348	-90.7239	0.00

counts start at zero). Once the ABRFC data is in the comma-delimited text format, it can be imported into the GIS software.

The process described above was repeated for the 1, 6, and 24-hour data of each of the nine study dates to create a total of twenty-seven individual data tables. The table data was then imported into the ArcView GIS software by a process called "adding event themes." In this process, ArcView GIS uses the geographic coordinates in the tables to map the location of every grid cell center-point and stores a rainfall value for each individual cell. The mapped points can be color-coded according to their rainfall values to produce a map of total rainfall. Figure 3.13 contains a map of rainfall produced by ArcView GIS, using the data table from the 24-hour file of the July 16, 1997 study date. Notice the visual similarity to the rainfall image in Figure 3.7 downloaded from the ABRFC web-site for the same date and time period. Figure 3.7 contains only a Graphics Interchange File (GIF) image of ABRFC rainfall and is not numerically comparable to the map of ABRFC rainfall produced by the ArcView GIS software in Figure 3.13. A similar color scale is used for both images however the ABRFC image displays rainfall in inches while the map produced by ArcView GIS is displayed in millimeters.

Adding data as an "event theme" is a temporary way to add table data to the ArcView GIS software. Before ArcView GIS can perform geographic operations on the data, the "event themes" must be converted to a permanent ArcView GIS data format called a "shapefile." An ArcView GIS shapefile contains the data needed to map the point, arc, or polygon features and an associated database containing values tied to the point, arc, or

Figure 3.14: Diagram of ArcView clipping function selecting Oklahoma rainfall points.

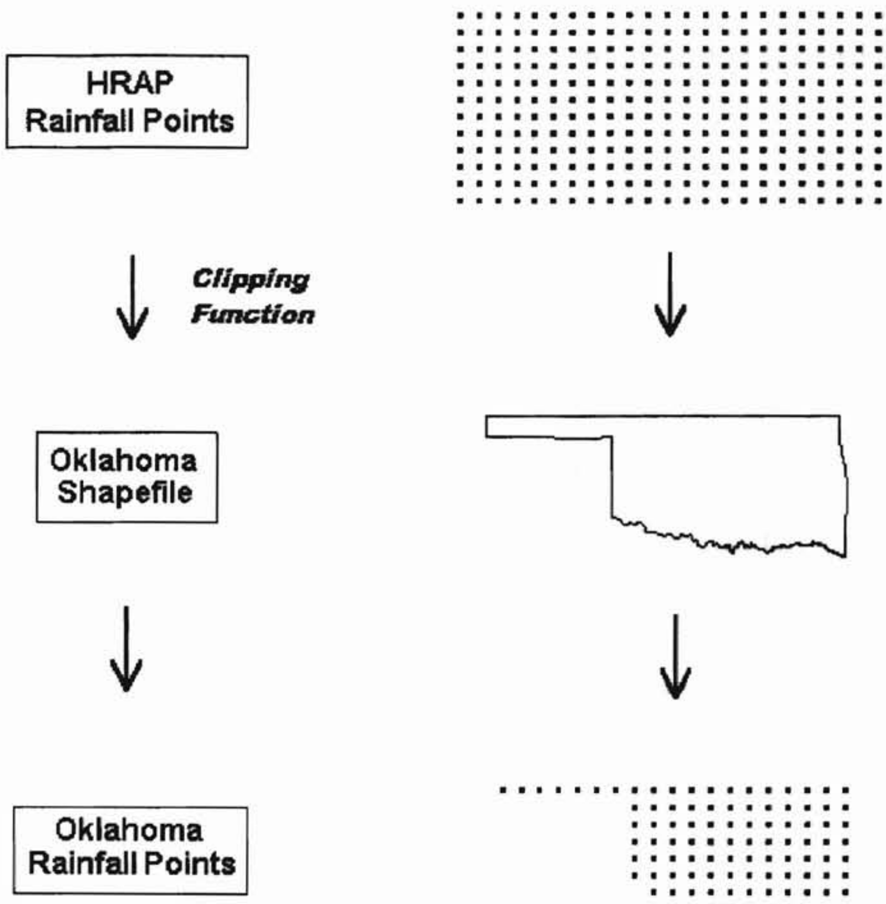

new shapefiles. Figure 3.14 shows a command flow chart of how this function was used and provides an illustration of the results.

The ABRFC rainfall data, as a result of the process described above, was now contained in twenty-seven individual ArcView shapefiles representing the 1 hour, 6 hour, and 24 hour data for each of the nine study dates. In this format, it is possible to combine the ABRFC rainfall data with the Mesonet rainfall data.

Preparing Mesonet Data. The overall goal in preparing the Mesonet rainfall data was to end up with a format that can be used to pair the Mesonet rainfall data with the ABRFC rainfall data so that total rainfall can be compared on a grid-cell by grid-cell basis. To reach this goal, the Mesonet data was transformed from zero-dimensional rainfall data to a two-dimensional rainfall surface by interpolation of the point rainfall data. Finally, a GIS software function called a "spatial join" was used to overlay the lattice or grid of ABRFC rainfall points over the two-dimensional Mesonet rainfall surface to extract total rainfall values. This process is explained in the paragraphs below.

The Oklahoma Mesonet collects a variety of weather parameters including wind speed and direction, solar radiation, temperature, and humidity (Brock, et al., 1995). For this study, only total rainfall data was required. Due to the format in which the Mesonet data were stored, some processing was necessary before the Mesonet data could be matched with the time period of the ABRFC rainfall data. For example, the 1 hour (11 UTC to 12 UTC) ABRFC rainfall data must be paired with the total amount of Mesonet estimated rainfall for that same time period. However, the Mesonet rainfall data were stored as hourly cumulative rainfall, the sum of that hours rainfall plus all the previous hours rainfall, and the rainfall amount was returned to zero at 0000 UTC each day.

Figure 3.14: Schematic diagram of ArcView clipping function selecting Oklahoma rainfall points.

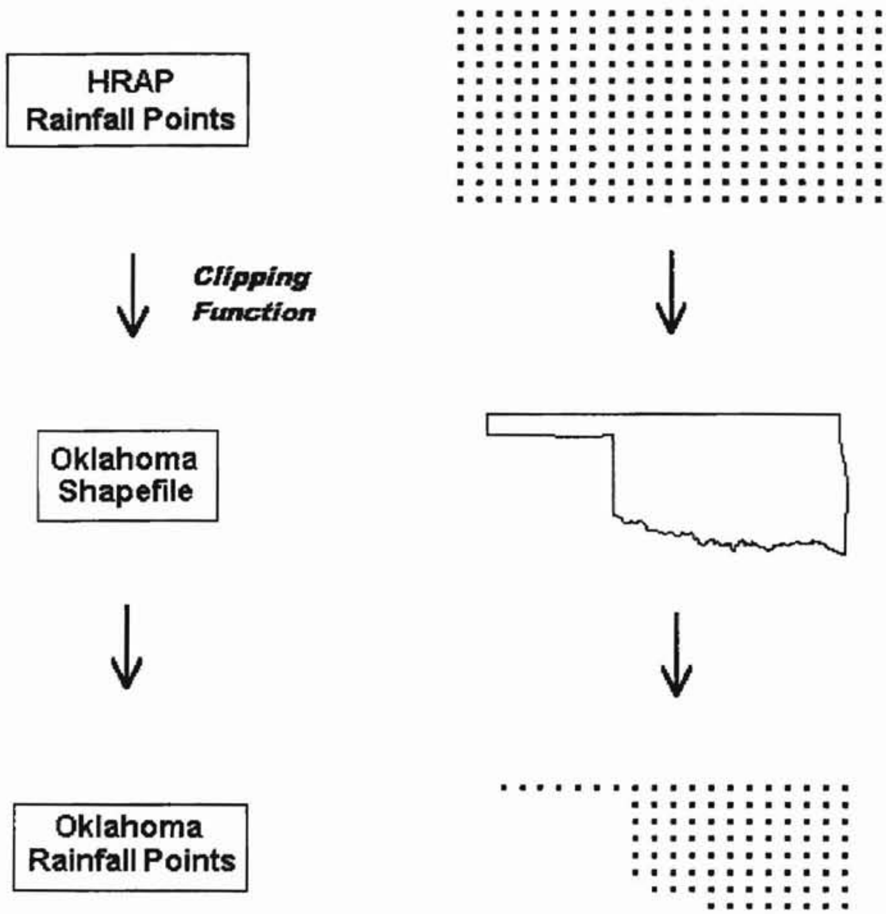

Therefore, to get the amount of rainfall for the hour between 11 UTC and 12 UTC, the rainfall amount for 11 UTC was subtracted from that of the 12 UTC. To match the ABRFC 6 hour rainfall (6 UTC to 12 UTC), the Mesonet 6z rainfall amount was subtracted from the 12 UTC rainfall amount. To match the ABRFC 24 hour rainfall (12 UTC to 12 UTC), the Mesonet rainfall for 12 UTC to 0 UTC was added to the rainfall for 0 UTC to 12 UTC of the next day.

Total rainfall data was collected for each of the 114 Mesonet weather stations. For each of the nine study dates, 1 hour, 6 hour, and 24 hour total rainfall data was obtained, making a total of twenty-seven data files.

Before the Mesonet data were processed by the GIS software, the Mesonet weather stations were assigned geographic coordinates. Appendix A contains a list of the 114 Mesonet sites and their latitude and longitude coordinates. See Figure 3.2 for a map of these Mesonet locations.

The rainfall data and geographic coordinate data were combined in a final data table for all twenty-seven files. Table 3.2 contains an example of the final Mesonet data table for the 24 hour data of the July 16, 1997 study date. Each data table contains a single record for each Mesonet site and each record contains a field for site name, latitude coordinate, longitude coordinate, and rainfall amount in millimeters. In this format, the Mesonet data can be imported into the GIS software.

The Mesonet rainfall tables were imported into the ArcView GIS software as "event themes" and converted to ArcView shapefiles in the same manner as described for the ABRFC data. These files need to be in an ArcView shapefile format before they can

Table 3.2: Table of Mesonet sites with coordinate and rainfall data.

SITE	LATITUDE	LONGITUDE	RAINFALL (MM)
ACME	34.8056	-98.0056	5.55
ADAX	34.7989	-96.6692	0.00
ALTU	34.5872	-99.3378	0.00
ALVA	36.7797	-98.6717	0.00
ANTL	34.2242	-95.7006	0.49
APAC	34.9139	-98.2917	1.30
ARDM	34.1922	-97.0850	0.00
ARNE	36.0728	-99.9014	0.00
BBOW	34.0144	-94.6131	0.00
BEAV	36.8022	-100.5300	0.00
BESS	35.4017	-99.0589	0.00
BIXB	35.9625	-95.8661	18.00
BLAC	36.7544	-97.2539	0.00
BOIS	36.6925	-102.4927	1.00
BOWL	35.1717	-96.6314	0.00
BREC	36.4119	-97.6942	0.00
BRIS	35.7808	-96.3539	0.25
BUFF	36.8314	-99.6408	0.73
BURB	36.6342	-96.8111	1.01
BURN	33.8939	-97.2692	2.48
BUTL	35.5914	-99.2706	9.32
BYAR	34.8497	-97.0033	0.00
CALV	34.9925	-96.3342	0.00
CAMA	36.0283	-99.3464	2.22
CATO	36.2619	-95.7572	4.25
CENT	34.6086	-96.3331	0.00
CHAN	35.6528	-96.8042	0.00
CHER	36.7481	-98.3628	2.81
CHEY	35.5458	-99.7275	0.00
CHIC	35.0319	-97.9144	0.00
CLAR	36.3172	-95.6417	3.38
CLAY	34.6556	-95.3281	1.05
CLOU	34.2231	-95.2494	0.49
COOK	35.6794	-94.8486	0.25
COPA	36.9097	-95.8853	0.00
⋮	⋮	⋮	⋮
WEAT	35.5081	-98.7753	0.00
WEBB	35.4728	-95.1322	0.00
WEST	36.0111	-94.6450	0.00
WILB	34.9008	-95.3478	0.00
WIST	34.9847	-94.6881	0.00
WOOD	36.4233	-99.4169	1.36
WYNO	36.5172	-96.3422	0.25

be further processed by the ARC/INFO GIS software. Although shapefiles are not the standard input format to ARC/INFO, they can be converted to ARC/INFO coverages.

The twenty-seven Mesonet shapefiles were converted to ARC/INFO coverages using the SHAPEARC function. The GRID module of the ARC/INFO GIS software contains the functions for interpolating. The ARC/INFO POINTINTERP function was used to access the Mesonet station coordinates and rainfall values to interpolate total rainfall across the study area. The POINTINTERP command can be set to control the method of interpolation, output cell size, and weight factor. The Inverse Distance Weighted (IDW) method of interpolation was used with a weight factor of two and an output cell size of 4 kilometers. The product of this function was a 4 x 4 kilometer grid of interpolated Mesonet rainfall.

The IDW method of interpolation was chosen because it was one of the more sophisticated interpolation techniques that are recommended for areas of intense and strongly varying rainfall (Cruten and Obled, 1982). It is also one of the few available interpolation functions within ARC/INFO and the parameters of weight and output grid cell size were easily set. Although it would be interesting to use a variety of interpolation methods for comparison, this would be beyond the scope of this study. In Yuen's (1994) study of the effects kriging on estimating evapotranspiration, he used several methods of interpolation and compared resulting grids. He found that there was no significant difference between the interpolation methods in estimating evapotranspiration. Therefore, the IDW method was used because it was appropriate.

The ARC/INFO GRID module function GRIDPOLY was then used to convert the Mesonet rainfall grid coverage to a polygon coverage. This polygon coverage was

Figure 3.15: Command flow chart and illustrations of the interpolation process.

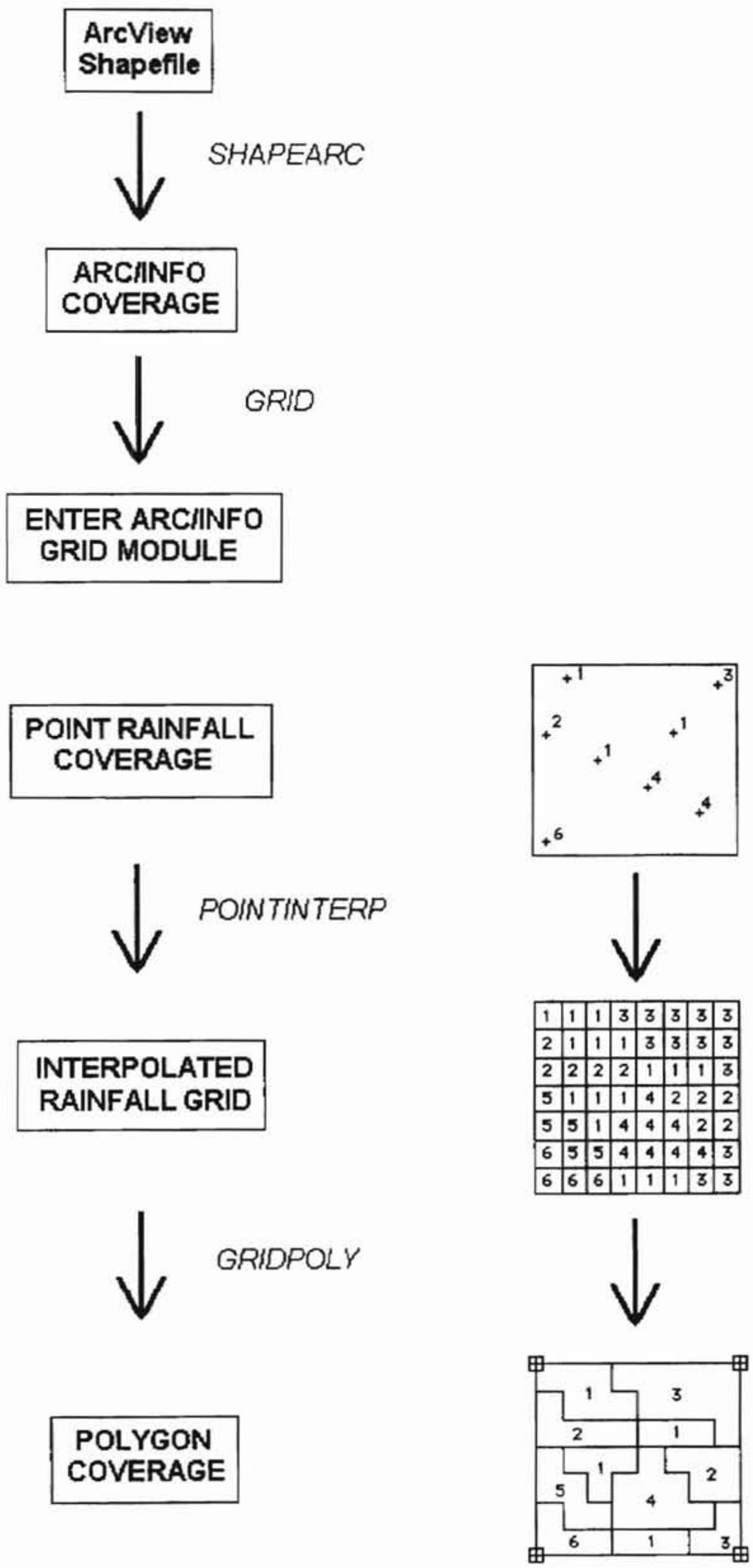

imported into the ArcView GIS software to be compared with the previously produced ABRFC shapefiles. Figure 3.15 contains a flow chart of the command functions used in ARC/INFO to complete the interpolation process and also provides an illustration.

Combining ABRFC and Mesonet Rainfall Data. Before the two rainfall estimates can be statistically compared, the rainfall values for the ABRFC and Mesonet need to exist in the same database table. Following the process leading to the final step in Figure 3.15, the rainfall data for the two estimates are contained in two separate database tables. The ABRFC rainfall data is contained in an ArcView shapefile and its associated data table while the Mesonet data is contained in an ARC/INFO polygon coverage with its own data table.

Using the ArcView function called a SPATIAL JOIN, the ABRFC lattice or grid of rainfall points were, in effect, superimposed on the Mesonet polygon coverage. The Mesonet rainfall values were extracted from the ARC/INFO polygon coverage based on the location of the ABRFC rainfall points. The extracted Mesonet rainfall values were then added as an extra field in the ABRFC shapefile database table. Figure 3.16 illustrates the SPATIAL JOIN process. Table 3.3 is an example of the resulting table, which now contains an ABRFC and a Mesonet estimated rainfall value for each individual point within the study area.

The process described above was repeated for the 1 hour, 6 hour, and 24 hour data for each of the nine study dates. With the rainfall data from both data sources contained in the same database table, the rainfall values for individual points are directly comparable.

Figure 3.16: Illustration of the SPATIAL JOIN function process.

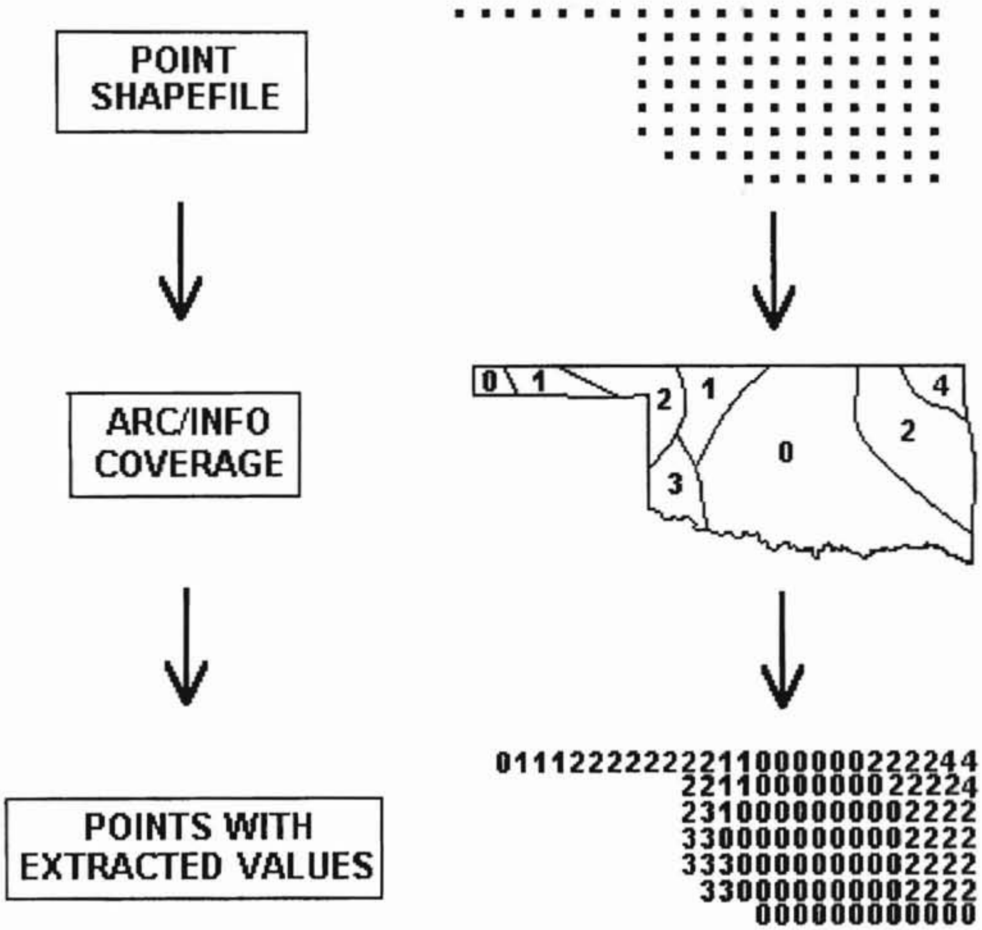

Table 3.3: Example portion of the output database table produced by the SPATIAL JOIN function. The table now contains both ABRFC and Mesonet rainfall data. resulting from the SPATIAL JOIN function.

HRAPX	HRAPY	LATITUDE	LONGITUDE	ABRFC (MM)	MESONET (MM)
216	15	33.7432	-97.1614	1.00	1.87
217	15	33.7383	-97.1188	0.92	1.80
216	16	33.7786	-97.1555	0.46	1.90
217	16	33.7737	-97.1129	2.97	1.80
197	17	33.9020	-97.9605	0.00	0.98
198	17	33.8976	-97.9177	0.00	1.00
199	17	33.8902	-97.8750	0.40	1.00
200	17	33.8887	-97.8322	8.71	1.05
209	17	33.8475	-97.4480	17.23	1.87
210	17	33.8428	-97.4054	3.00	1.81
211	17	33.8380	-97.3627	3.91	2.10
215	17	33.8188	-97.1922	1.84	2.10
216	17	33.8140	-97.1496	2.82	1.94
217	17	33.8091	-97.1070	3.39	1.79
235	17	33.7166	-98.3419	22.34	2.32
198	18	33.9331	-97.9124	0.00	0.92
199	18	33.9286	-97.8696	0.00	0.95
200	18	33.9242	-97.8269	0.88	0.99
201	18	33.9197	-97.7841	2.27	1.09
209	18	33.8829	-97.4423	14.52	1.87
210	18	33.8782	-97.3997	2.72	1.98
211	18	33.8735	-97.3570	3.24	2.18
216	18	33.8494	-97.1437	1.28	1.95
217	18	33.8445	-97.1011	3.10	1.87
234	18	33.7572	-98.3779	15.78	2.35
235	18	33.7519	-98.3355	6.23	2.35
⋮	⋮	⋮	⋮	⋮	⋮
197	19	33.9730	-97.9499	0.00	0.79
198	19	33.9686	-97.9071	0.00	0.80
199	19	33.9641	-97.8643	1.11	0.88
200	19	33.9597	-97.8215	2.81	0.92
201	19	33.9552	-97.7787	5.20	1.02
202	19	33.9507	-97.7359	9.52	1.08
206	19	33.9324	-97.5649	14.92	1.23
207	19	33.9277	-97.5221	19.94	1.31
208	19	33.9231	-97.4794	23.14	1.41

3.3 Method of Investigation

Difference between ABRFC and Mesonet

The difference between the ABRFC estimated rainfall and the Mesonet estimated rainfall for each rainfall point was calculated and added to an extra field in the rainfall database tables. The amount of difference (mm) was calculated by simply subtracting the Mesonet estimated rainfall value from the ABRFC estimated rainfall value. For example, an individual rainfall point has an ABRFC estimated rainfall of 5 millimeters and a Mesonet estimated rainfall of 10 millimeters, resulting in a difference of -5 millimeters. Negative differences indicate a greater Mesonet estimated rainfall and positive differences indicate a greater ABRFC estimated rainfall.

The pattern of difference was mapped based on the location of the rainfall point and the difference value. The difference value was used within ArcView GIS to create maps of difference based on rainfall point location and the difference value for that point. Individual points were color-coded according to their positive or negative value as well as the amount of difference. By mapping out the amount of difference between the two estimates, spatial patterns can be examined and possible reasons for disagreement between the estimates may be determined.

Distance from Mesonet Stations

One of the goals of this study is to examine if the differences between the two rainfall estimates are associated with distance from the Mesonet stations. Individual rainfall points may occur many kilometers from the nearest Mesonet site. Do differences increase or decrease in comparison with rainfall points closer to Mesonet sites? How do correlation coefficients vary as distances increase? An attempt to answer these questions will be made by examining differences between the two rainfall estimates at various distances from the Mesonet stations.

A variety of geographic functions were used within ArcView GIS to divide the rainfall points into categories based on the distance from their nearest Mesonet station. The SPATIAL JOIN function was used to assign a distance value to each rainfall point and the BUFFER and SELECT BY SHAPE functions were used to select categories of cells based on distance from Mesonet stations. The distance categories used to divide the points were 5, 10, 15, and 20 kilometers. The rainfall points were also divided into distance ranges of between 0-5 kilometers, 5-10 kilometers, 10-15 kilometers, and 15-20 kilometers. New database files will be created for the points falling into these categories.

Using the Mesonet station coordinates, the SPATIAL JOIN function of the ArcView GIS software was used to assign a distance value to each rainfall point based on the distance to its nearest Mesonet site. A distance field was added to the rainfall database table and the "distance to Mesonet" value was added for each rainfall point. With the distance field added to the database table, rainfall points were queried and selected according to distance ranges. SPSS statistical software contains a query and select function that was used to select rainfall points based on distance ranges. For example, a query was performed to select all the rainfall points that fell between 10 and 15 kilometers from a Mesonet site. SPSS could then able to run statistical analysis on just those selected rainfall points. SPSS was used to perform a correlation within each distance range of rainfall cells to determine if the correlation coefficient of the cells in a particular distance group increased or decreased with distance from Mesonet station.

Using the Mesonet station coordinates, the BUFFER function in the ArcView GIS software was used to create buffer polygons at 5, 10, 15, and 20 kilometers from each Mesonet site. These polygons were used to select out all the rainfall points that fall within that area using the SELECT BY THEME function. Once the desired points are selected, the ArcView EXPORT function was used to write the database information to a new database table. For example, the 20 kilometer buffer polygon was used to select all rainfall points within 20 kilometers of a Mesonet site. These points were exported to a new database table. Figure 3.17 illustrates the GIS operations used to perform this process. This was performed for the points falling within 5, 10, 15 and 20 kilometers from a Mesonet site. By performing separate correlation on these distances, it was determined if correlation coefficients increase or decrease with distance from Mesonet stations.

Distance from Radar

Another goal of this study is to examine if the differences between the two rainfall estimates are associated with distance from the radar facilities used to produce the ABRFC rainfall estimate. As distance from radar increases, radar signals may be scattered or deflected or overshoot their target due to the curvature of the earth. Wilson

Figure 3.17: Illustration of the BUFFER and SELECT BY THEME functions. Map A shows the 20 kilometer buffer areas and Map B illustrates the rainfall points selected by the buffer areas.

Map A

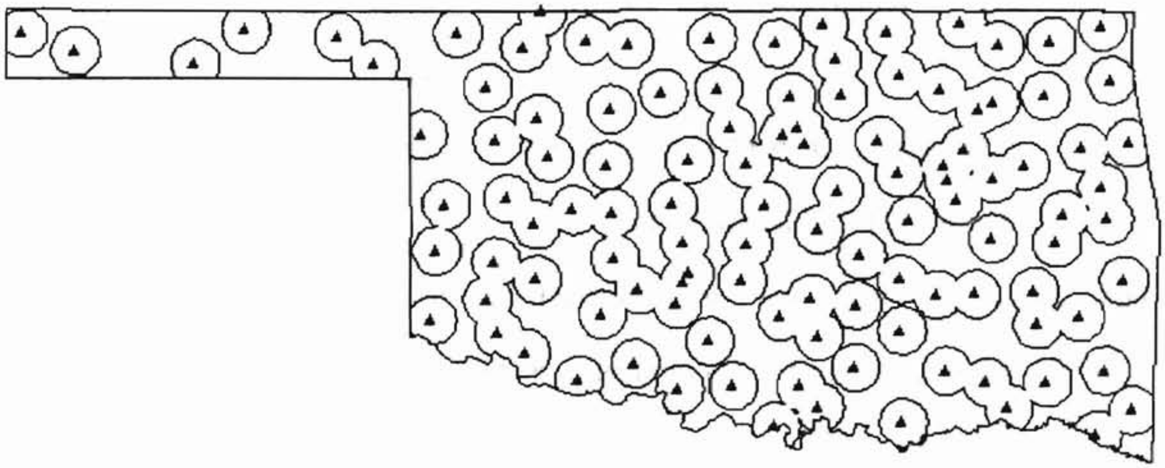

Map B

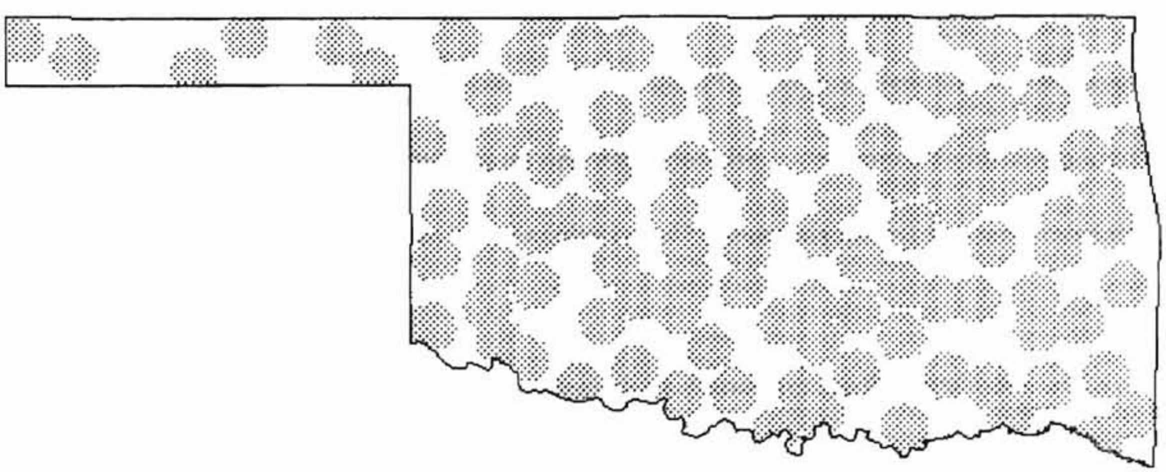

and Brandes (1979) state that agreement between radar and gage rainfall estimates generally decreases with increasing radar range. Do differences between the Mesonet and ABRFC rainfall estimates increase in areas with low radar coverage? How do correlation coefficients vary as distances increase? An attempt to answer these questions was made by examining differences between the two rainfall estimates at various distances from the radar locations.

A variety of geographic functions were used to divide the rainfall points into categories based on the distance from their nearest radar facility. The SPATIAL JOIN function was used to assign a distance value to each rainfall point and the BUFFER and SELECT functions were used to select out categories of cells based on distance from radar facility. The distance categories used to divide the points were 50, 100 and 150 kilometers. New database files were created for the points falling into these categories.

Table 3.4 lists the radar facilities used to produce the ABRFC rainfall estimates and the geographic coordinates of each site. Figure 3.18 is a map of the radar facilities nearest to the study area. Only those sites with ranges extending into the study area were used to calculate Oklahoma rainfall. Using the radar site coordinates, the SPATIAL JOIN function of the ArcView GIS software was used to assign a distance value to each rainfall point based on the distance to its nearest radar site. A distance field was added to the rainfall database table and the "distance to radar" value was added for each rainfall point.

Using the radar site coordinates, the BUFFER function in the ArcView GIS software was used to create buffer polygons at 50, 100, and 150 kilometers from each

Table 3.5: Table of ABRFC radar sites with geographic coordinates.

ID	NAME	STATE	LATITUDE	LONGITUDE
KICT	Witchita	KS	37.6500	-97.4400
KTLX	Twin Lakes	OK	35.3300	-97.2800
KAMA	Amarillo	TX	35.2300	-101.7100
KDDC	Dodge City	KS	37.7600	-99.9700
KLZK	Little Rock	AR	34.8400	-92.2600
KSHV	Shreveport	LA	32.4500	-93.8400
KFWS	Rot Worth	TX	32.5700	-97.3000
KINX	Tulsa	OK	36.1800	-95.5600
KFDR	Frederick	OK	34.3600	-98.9800
KGLD	Goodland	KS	39.3700	-101.7000
KPUX	Pueblo	CO	38.4600	-104.1800
KLBB	Lubbock	TX	33.6500	-101.8100
KFDX	Cannon AFB	NM	34.6400	-103.6300
KTWX	Topeka	KS	39.0000	-96.2300
KABX	Albuquerque	NM	35.1500	-106.8200
KDYS	Dyess AFB	TX	32.5400	-99.2500
KFTG	Denver	CO	39.7900	-104.5500
KSGF	Springfield	MO	37.2400	-93.4000
KNQA	Memphis	TN	35.3400	-89.8700
KSRX	Fort Smith	AR	35.2900	-94.3600
KVNX	Vance AFB	OK	36.7400	-98.1300

Figure 3.18: Map of nearest ABRFC radar sites.

Figure 3.19: Illustration of the BUFFER and SELECT BY THEME functions. Map A shows the 50 kilometer buffer areas and Map B illustrates the rainfall points selected by the buffer areas.

Map A

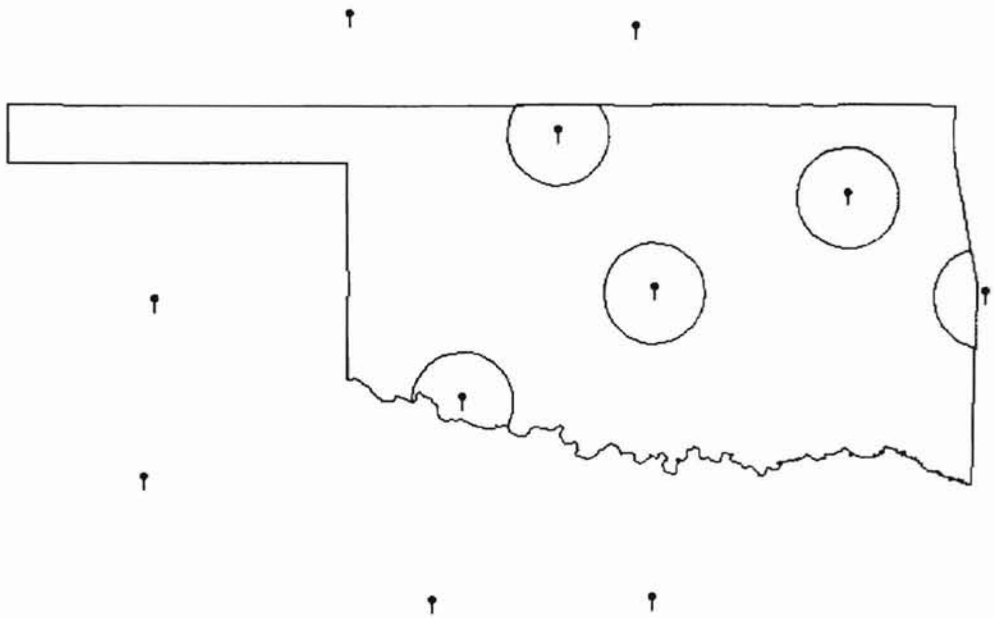

Map B

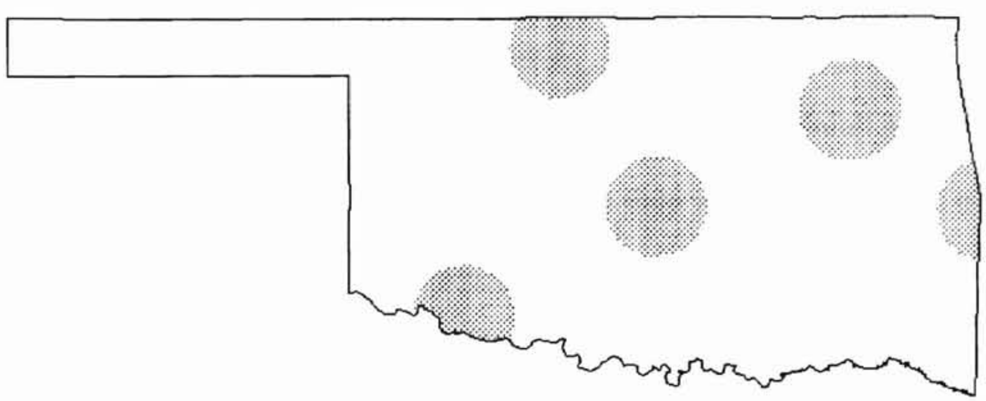

radar site. Using the SELECT BY THEME function, these polygons were used to select out all the rainfall points that fall within that area. Once the desired points are selected, the ArcView EXPORT function was used to write the database information to a new database table. For example, the 50 kilometer buffer polygon was used to select all rainfall points within 50 kilometers of a radar facility. Figure 3.19 provides and illustration of this process. These points were "exported' to a new database table. This was repeated for the points falling within 100 and 150 kilometers from a radar facility. By performing correlation on these files separately, it can be determined if correlation coefficients increase or decrease with distance from radar site.

Final Rainfall Database

For each of the nine study dates, database tables were created for the 1 hour, 6 hour, and 24 hour rainfall data. From each of the one, six, and twenty-four hour rainfall database tables, separate database tables were created for all rainfall points falling within 5, 10, 15, and 20 kilometers of a Mesonet station. Also from each of the one, six, and twenty-four hour rainfall database tables, separate database tables were created for all rainfall points falling within 50, 100, and 150 kilometers of a radar facility. There were a total of 216 separate database tables produced.

Each database table contained a single record for each rainfall point contained within that database table. Each record contained field values for HRAP X coordinate, HRAP Y coordinate, latitude coordinate (decimal degrees), longitude coordinate (decimal degrees), ABRFC estimated rainfall (mm), Mesonet estimated rainfall (mm), difference between estimates (mm), distance from nearest Mesonet station (km), and distance from nearest radar facility (km). Table 3.5 contains an example of the final database table for the 24 hour data of the July 16, 1997 study date.

Statistical Analysis

With a database table for each study date, time period, and distance category, and with database fields containing all the required data values, the rainfall data was statistically analyzed. The results of the analysis are given in Chapter 4.

For each database table, SPSS statistical software was used to run a two-tailed Pearson's correlation (r) (McGrew and Monroe, 1993) of the ABRFC and Mesonet estimated rainfall data. Correlation values were deemed of practical significance if they were statistically significant at the 0.01 level. The minimum, maximum, and mean rainfall, as well as the standard deviation, were determined for both the ABRFC and Mesonet rainfall data.

Table 3.5: Final Output table with complete rainfall and distance data.

HRAPX	HRAPY	LATITUDE	LONGITUDE	ABRFC (MM)	MESONET (MM)	DISTANCE FROM RADAR (KM)	DISTANCE FROM MESONET (KM)
216	15	33.7432	-97.1614	1.00	1.87	118.1	18.5
217	15	33.7383	-97.1188	0.92	1.80	118.2	21.6
216	16	33.7786	-97.1555	0.46	1.90	121.7	16.2
217	16	33.7737	-97.1129	2.97	1.80	121.8	19.7
197	17	33.9020	-97.9605	0.00	0.98	111.8	26.7
198	17	33.8976	-97.9177	0.00	1.00	115.9	27.9
199	17	33.8932	-97.8750	0.40	1.03	120.0	29.7
200	17	33.8887	-97.8322	8.71	1.05	124.1	32.0
209	17	33.8475	-97.4480	17.23	1.67	128.6	18.5
210	17	33.8428	-97.4054	3.03	1.81	127.7	14.5
211	17	33.8380	-97.3627	3.91	2.10	127.0	10.9
215	17	33.8188	-97.1922	1.84	2.10	125.3	10.8
216	17	33.8140	-97.1496	2.82	1.94	125.3	14.4
217	17	33.8091	-97.1070	3.39	1.79	125.4	18.3
⋮	⋮	⋮	⋮	⋮	⋮	⋮	⋮
235	17	33.7166	-96.3419	22.34	2.32	149.4	20.5
198	18	33.9331	-97.9124	0.00	0.92	115.0	24.7
199	18	33.9286	-97.8696	0.00	0.95	119.1	26.7
200	18	33.9242	-97.8269	0.68	0.99	123.3	29.2
201	18	33.9197	-97.7841	2.27	1.09	127.4	32 1
209	18	33.8829	-97.4423	14.52	1.67	132.1	17.3
210	18	33.8782	-97.3997	2.72	1.98	131.2	13.1
211	18	33.8735	-97.3570	3.24	2.18	130.5	9.0
216	18	33.8494	-97.1437	1.28	1.95	128.9	13.3
217	18	33.8445	-97.1011	3.10	1.67	129.0	17.5

CHAPTER 4

RESULTS

4.1 Rainfall Estimates

A total of nine study dates were chosen from the months of June, July and August of 1997. Study dates were chosen to represent the various patterns of Oklahoma rainfall. The study dates exhibited rainfall patterns ranging from light to heavy rainfall, local to widespread rainfall, and homogenous to concentrated rainfall events. Figure 4.1 shows a scatterplot of rainfall intensity verses spatial variability for each of the study dates (24 hour accumulated rainfall). For each study date, 1 hour, 6 hour, and 24 hour rainfall data were collected for each study date.

The Oklahoma state boundaries were used to define the study area. This area contains 11,132 of the Hydrologic Rainfall Analysis Project (HRAP) grid points, each representing the center point of a 4 x 4 kilometer area. The total area equals 178,112 square kilometers.

The total volume of rainfall estimated by each of the estimate methods was compared. The total volume of rainfall for any given study date was calculated by multiplying the mean rainfall for the 11,132 4x4 kilometer cells by the total study area of 178,112 square kilometers. For example, a mean rainfall of 1 mm (or 0.001 meters) per cell would yield a total rainfall volume of 178,112,000 m^3 for the entire study area.

Figure 4.1: Scatterplot of rainfall intensity verses spatial variability rank of the 9 study dataes (24 hour accumulated rainfall).

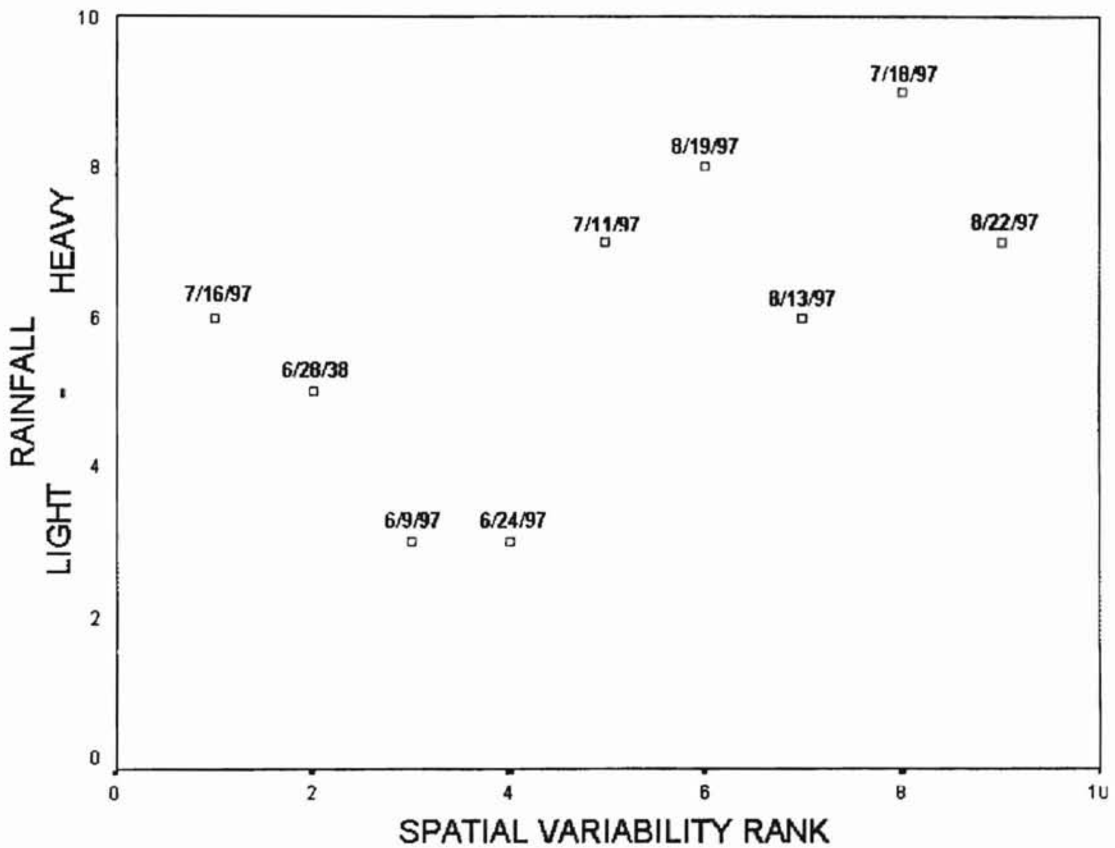

On each of the nine study dates and for each of the time periods (1 hour , 6 hours, and 24 hours of rainfall accumulation) a rainfall amount in millimeters was calculated for each of the 11,132 grid cells. The cells were color coded according to the amount of rainfall. By color-coding the grid cell based on its total rainfall amount, maps of total rainfall were produced for the study area. Maps were produced for both the Mesonet interpolated rainfall estimate and the radar derived Arkansas-Red Basin River Forecast Center (ABRFC) rainfall estimate.

The difference (in millimeters of total rainfall) between the two estimates was compared on a cell by cell basis. The difference between corresponding cells was obtained by simply subtracting the rainfall value of a cell in the Mesonet interpolated rainfall estimate from the rainfall value of the same cell in the ABRFC rainfall estimate. A positive value would indicate a higher ABRFC rainfall estimate than the Mesonet interpolated estimate. Alternatively, a negative value would indicate a higher Mesonet rainfall estimate than the ABRFC estimate. A difference value was calculated for each of the 11,132 4x4 kilometer cells in the study area and these values were used to create a map of difference for each study data and each time period of 1, 6 and 24 hours. The difference in estimated rainfall for each cell was color coded according to the amount of difference between the cells. Cells that had little or no difference between the estimates were shaded a neutral white. Positive differences were shaded red with the darkness of the shade increasing with value. Negative differences were shaded in blue with the darkness of the shade increasing with negative value.

When comparing the maps of total rainfall and difference, it is helpful to view the Mesonet and Radar sites for reference. Figure 3.2 shows the location of the Mesonet weather stations across the state of Oklahoma. Total rainfall values at these locations were interpolated to derive total rainfall for the entire study area. Figure 3.18 shows the location of radar facilities that are used by the ABRFC in developing their total rainfall estimate.

June 9, 1997

The study date of June 9, 1997 covers the 24 hours between June 8, 1997 12 UTC and June 9, 1997 12 UTC. This date was characterized by mostly light to moderate rainfall with scattered patches of heavy rainfall. The rainfall was widespread but broken up into separate, concentrated rainfall events. The rainfall in the southwest quarter of the state exhibited a smooth, homogenous pattern while rainfall in the remainder of the state was localized and concentrated. Rainfall estimates were collected for the last hour (11 UTC – 12 UTC), the last six hours (6 UTC – 12 UTC), and the entire 24-hour period.

June 9, 1997 – 1 Hour Rainfall Estimate. The 1-hour estimate covers the last hour of the June 9, 1997 study period from 11 UTC to 12 UTC. For each of the 11,132 4x4 kilometer cells in the study area, an ABRFC and a Mesonet interpolated rainfall value was obtained. Each cell was color-coded according the rainfall amount and the results are displayed in Figure 4.2. Map A of Figure 4.2 represents the Mesonet-interpolated total rainfall while Map B represents the ABRFC estimated total rainfall.

There is general agreement between the two rainfall estimates on where rainfall is occurring across the study area. But there is a noticeable difference in the spatial resolution of the rainfall descriptions. Both indicate concentrated areas of rainfall occurring in the northwest and southeast quarters of the state. Both indicate little or no

Figure 4.2: Estimated rainfall for June 9, 1997 (1 Hour from 11 UTC to 12 UTC). Map A – Rainfall estimate from interpolated Mesonet data. Map B – Rainfall estimate from ABRFC Stage III radar rainfall data.

Map A

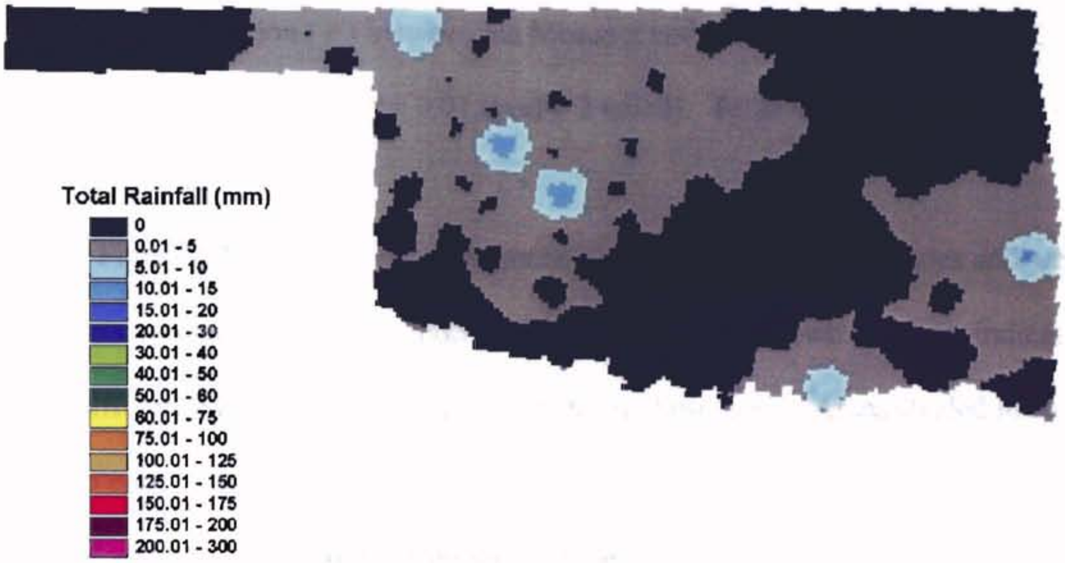

Map B

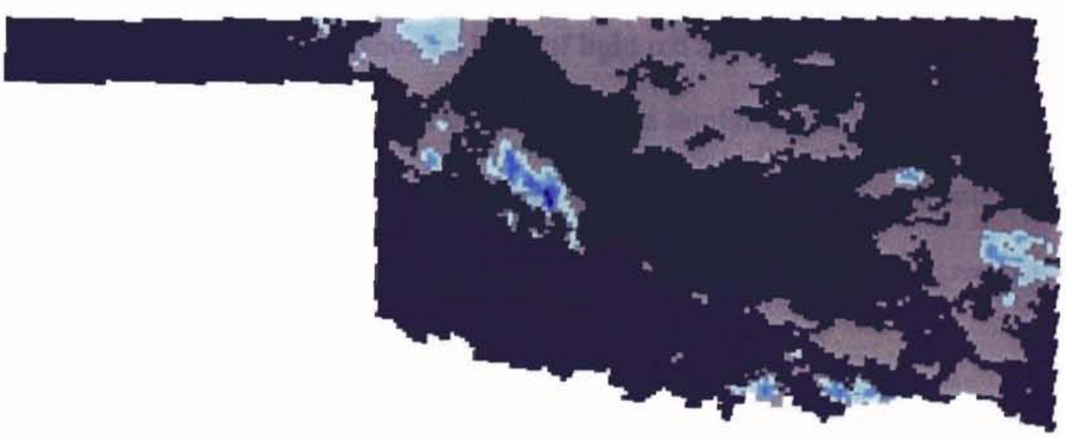

Table 4.1: June 9, 1997
1 Hour (11 UTC to 12 UTC)

Method	Min (mm)	Max (mm)	Mean (mm)	Standard Deviation (mm)	Volume (m3)
ABRFC	0	25	0.38	1.35	68,555,309
MESONET	0	13	0.52	0.90	92,974,464

rainfall for remainder of the study area. Patterns of light rainfall (shades of gray) are similar for both estimates but the Mesonet estimate indicates widespread light rainfall in these areas while the ABRFC estimate indicates light rainfall in more concentrated patches.

The correlation (r) between the Mesonet and ABRFC estimate was 0.536 (correlation is significant at the 0.01 level – 2 tailed). Table 4.1 lists some basic statistics for both estimates.

Figure 4.3 illustrates the differences between the rainfall estimates and where those differences occur. The majority of the study area is shown in white, indicating little or no difference between the rainfall estimates in these areas. Areas shaded in red or blue seem to correspond with areas of localized, concentrated rainfall. Areas of greater ABRFC estimated rainfall (red) are localized and concentrated while areas of greater Mesonet estimated rainfall (blue) exhibit a smoother, more homogenous pattern.

The difference map shows a band of light red areas extending from the north-central Oklahoma border towards the concentrated rainfall in the southeast quarter of the state. Both rainfall estimates indicate light rainfall throughout this area but the ABRFC estimate indicates slightly greater amounts of rainfall where these small, red patches occur.

Where localized, concentrated rainfall events occur, there is a pattern of intense red areas at the center of the event skirted by areas of light blue. This appears to be due rainfall occurring between Mesonet stations or if only the edge of a rainfall event is detected by a Mesonet station. An example of this would be the strong rainfall event in the west-central part of the study area. Looking at the rainfall maps, this rainfall event

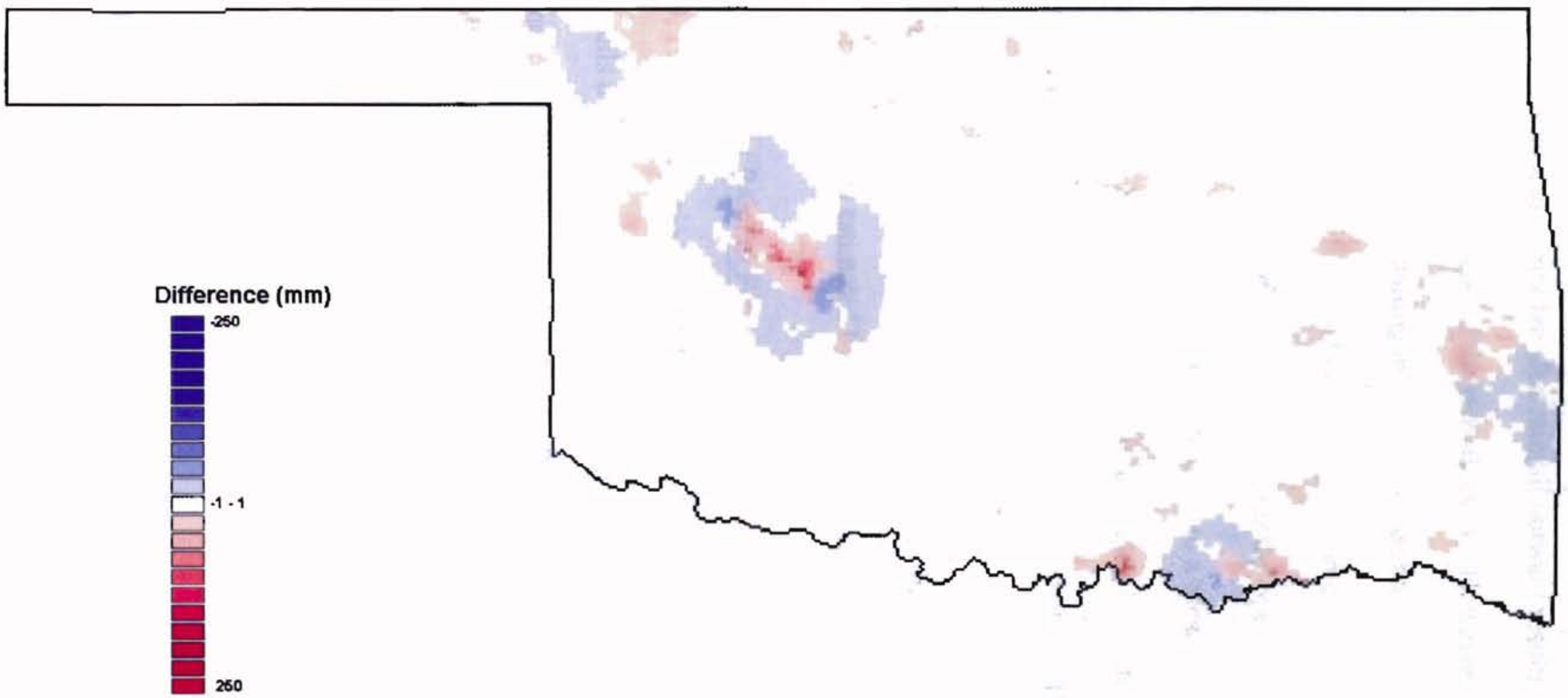

Figure 4.3: Difference in Radar and Mesonet Rainfall (mm) for June 9, 1997 - 1 Hour from 11 UTC to 12 UTC. Difference = Radar Rainfall – Mesonet Rainfall. Positive values indicate greater Radar estimated rainfall. Negative values indicate greater Mesonet estimated rainfall.

fall almost directly between two Mesonet stations. The gages pick up heavy rainfall at each end of this event and interpolate that rainfall outward resulting in the blue areas extending outward from each end of the rainfall event. However the gages miss the heaviest rainfall in between resulting in the intense red area.

There is not much difference between the estimates when describing the rainfall event in the northwest quarter of the study area, near the opening of the panhandle. The rainfall event is small and occurs in close proximity to a Mesonet station. The rainfall amount detected by the Mesonet station was interpolated in a pattern that closely resembles the rainfall pattern estimated by the ABRFC method. The difference between the two estimates is due to the fact that the Mesonet station detected a rainfall amount on the western edge of the rainfall event and interpolation, in effect, misplaces the rainfall event farther west than is estimated by the ABRFC method.

June 9, 1997 - 6 Hour Rainfall Estimate. The 6 hour estimate covers the last 6 hours of the June 9, 1997 study period from 6 UTC to 12 UTC. For each of the 11,132 4x4 kilometer cells in the study area, an ABRFC and a Mesonet interpolated rainfall value was obtained. Each cell is color-coded according the rainfall amount and the results are displayed in Figure 4.4. Map A of Figure 4.4 represents the Mesonet-interpolated total rainfall while Map B represents the ABRFC estimated total rainfall. There is general agreement between the two rainfall estimates on the location and intensity of rainfall occurring across the study area. But there is a noticeable difference in the spatial resolution of the rainfall descriptions.

Both indicate concentrated areas of rainfall occurring in the northwest and southeast quarters of the state. However, the intense rainfall event along the central

Figure 4.4: Estimated rainfall for June 9, 1997 (6 Hour from 6 UTC to 12 UTC). Map A – Rainfall estimate from interpolated Mesonet data. Map B – Rainfall estimate from ABRFC Stage III radar rainfall data.

Map A

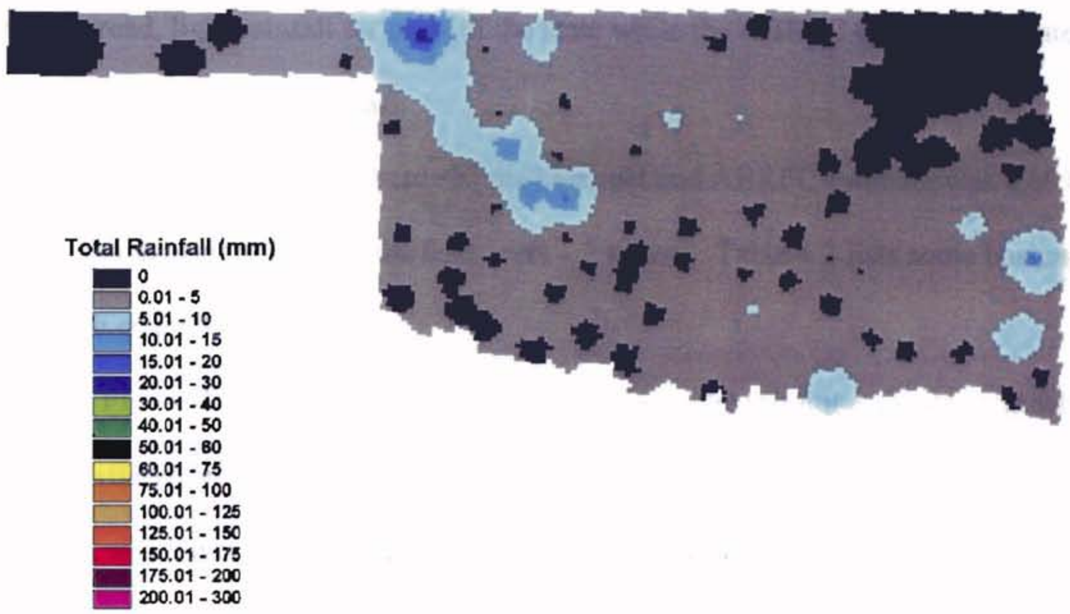

Map B

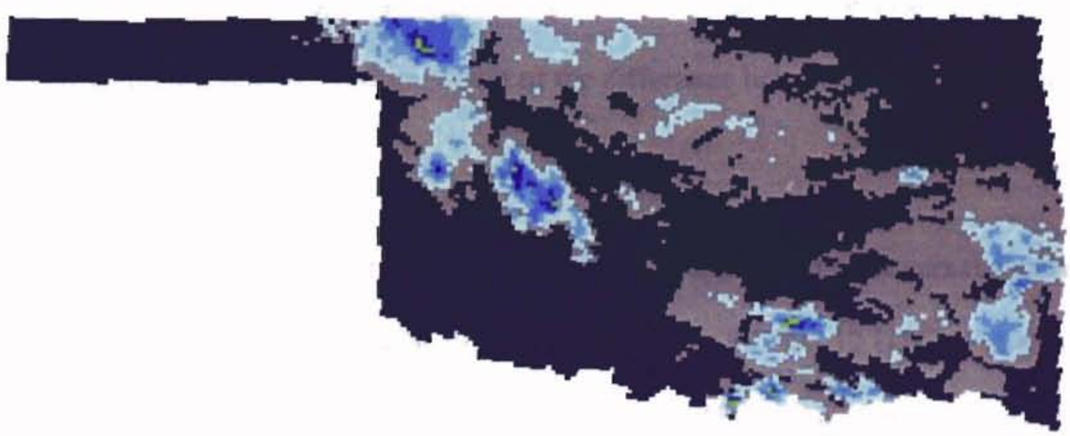

Table 4.2: June 9, 1997
6 Hour (6 UTC to 12 UTC)

Method	Min (mm)	Max (mm)	Mean (mm)	Standard Deviation (mm)	Volume (m3)
ABRFC	0	32	1.18	2.88	210,884,608
MESONET	0	21	1.12	1.63	199,841,664

southern border of the study area is almost completely missed by the Mesonet estimate. Both indicate little or no rainfall for the same parts of the study area. Patterns of light rainfall (shades of gray) are similar for both estimates but the Mesonet estimate indicates widespread, light rainfall for most of the state while the ABRFC estimate indicates light rainfall in more defined areas.

The correlation (r) between the Mesonet and ABRFC estimate was 0.691 (correlation is significant at the 0.01 level – 2 tailed). Table 4.2 lists some basic statistics for both estimates.

Figure 4.5 illustrates the differences between the rainfall estimates and where those differences occur. There is little or no difference shown in areas where light or no rainfall was indicated by both estimates. The 0.01 m to 5 mm rainfall (light gray) indicated by the Mesonet estimate covers a greater area than the ABRFC estimate but very little of this area shows up as a difference on the difference map. Differences of less than 1 mm are shown as white. Most of the difference between the estimates occurs near areas of high rainfall.

June 9, 1997 - 24 Hour Rainfall Estimate. The 24-hour estimate covers the entire June 9, 1997 study period from June 8, 1997 12 UTC to June 9, 1997 12 UTC. For each of the 11,132 4x4 kilometer cells in the study area, an ABRFC and a Mesonet interpolated rainfall value was obtained. Each cell is color-coded according the rainfall amount and the results are displayed in Figure 4.6. Map A of Figure 4.6 represents the Mesonet-interpolated total rainfall while Map B represents the ABRFC estimated total rainfall. There is general agreement between the two rainfall estimates on where rainfall is

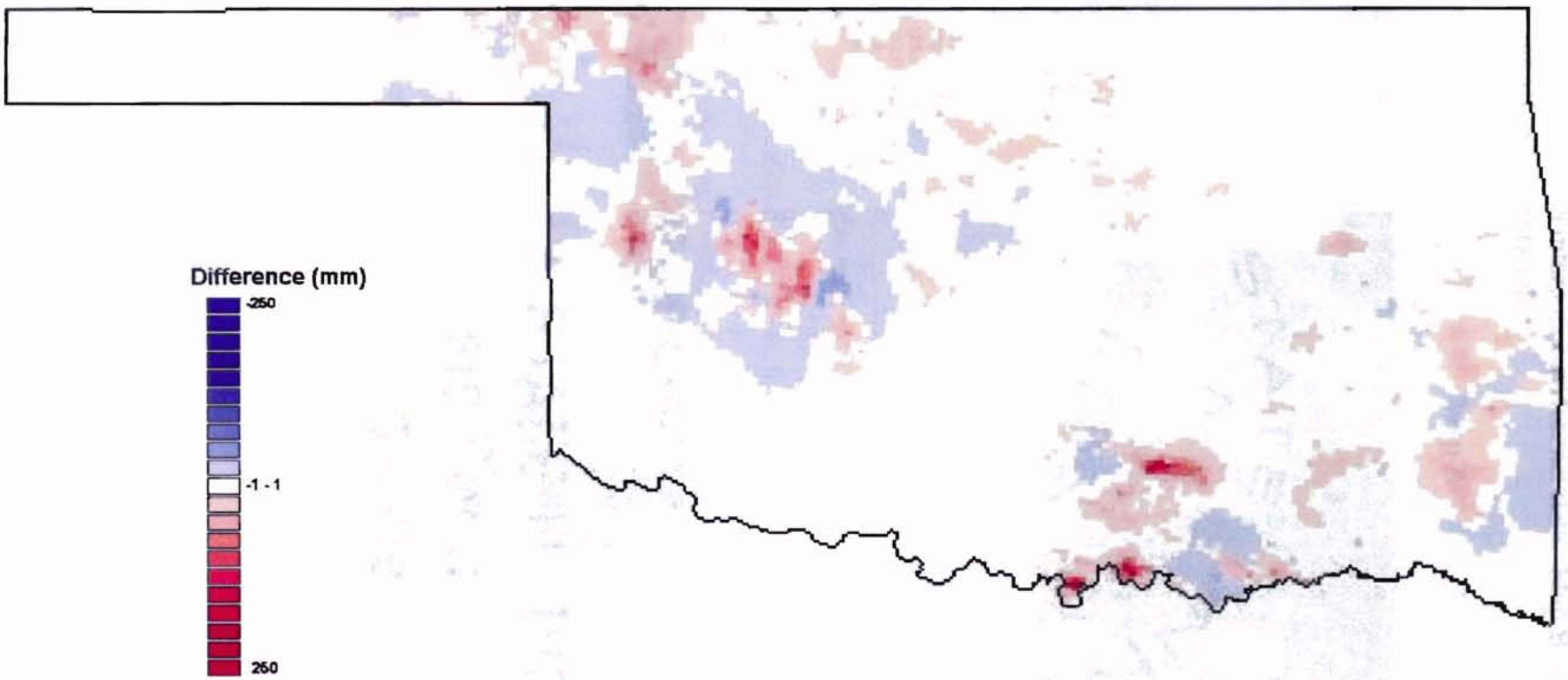

Figure 4.5: Difference in Radar and Mesonet Rainfall (mm) for June 9, 1997 - 6 Hour from 6 UTC to 12 UTC. Difference = Radar Rainfall – Mesonet Rainfall. Positive values indicate greater Radar estimated rainfall. Negative values indicate greater Mesonet estimated rainfall.

Figure 4.6: Estimated rainfall for June 9, 1997 (24 Hour from 12 UTC to 12 UTC). Map A – Rainfall estimate from interpolated Mesonet data. Map B – Rainfall estimate from ABRFC Stage III radar rainfall data.

Map A

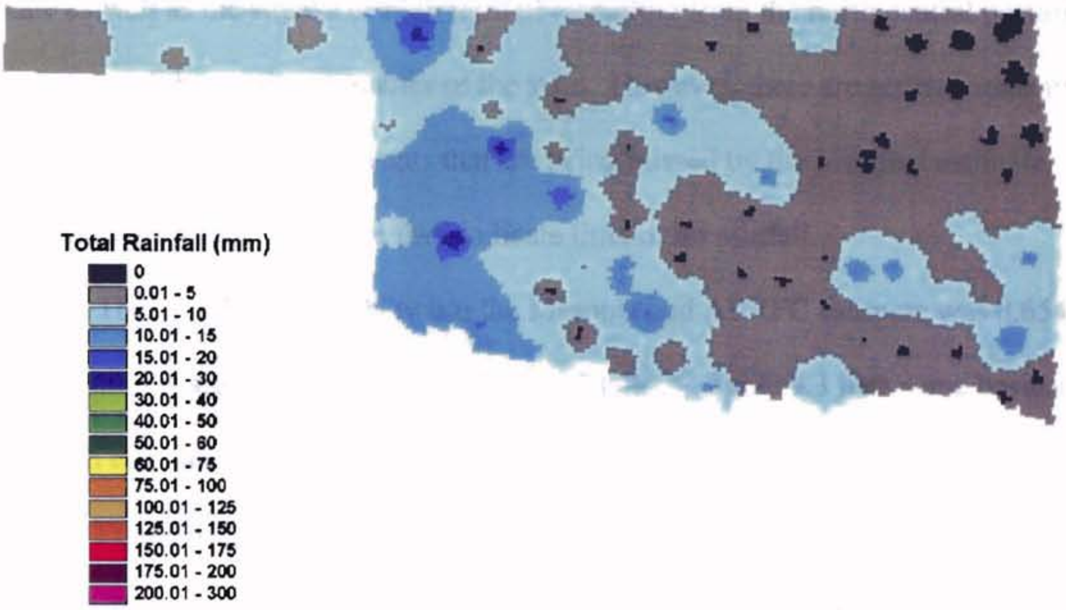

Map B

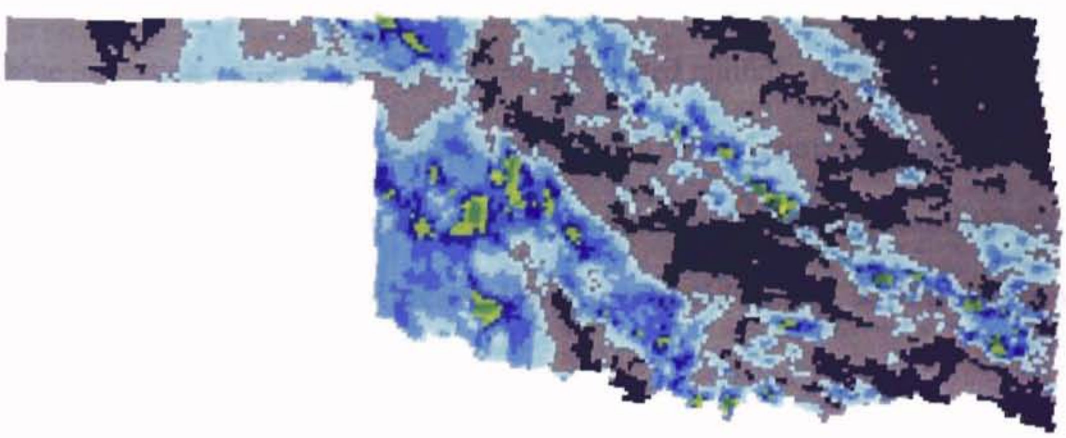

Table 4.3: June 9, 1997
24 Hour (12 UTC to 12 UTC)

Method	Min (mm)	Max (mm)	Mean (mm)	Standard Deviation (mm)	Volume (m3)
ABRFC	0	69	4.54	6.67	808,842,214
MESONET	0	22	3.51	3.04	625,547,155

occurring across the study area. But there is a noticeable difference in the spatial resolution of the rainfall descriptions.

Both estimates indicate the very high rainfall in the southwestern quarter of the state as well as the streaks of high rainfall extending from the north central portion of the state toward the southeast quarter of the state. However, there are several areas near these concentrated rainfall events that are being missed by the Mesonet estimate. Both estimates are similar in where they indicate little or no rainfall.

The correlation (r) between the Mesonet and ABRFC estimate was 0.654 (correlation is significant at the 0.01 level – 2 tailed). Table 4.3 lists some basic statistics for both estimates.

Figure 4.7 illustrates the differences between the rainfall estimates and where those differences occur. The far northeast corner indicates little or no difference between the estimates. The remainder of the state shows a large amount of difference, usually corresponding with areas of intense rainfall. Areas of light rainfall are dominated by light blue indicating a slightly greater Mesonet estimated rainfall. Areas of high rainfall are dominated by red or dark red indicating a greater ABRFC estimated rainfall. Most of the areas of greater Mesonet estimated rainfall are characterized by very low differences. However, where there are areas of greater ABRFC estimated rainfall, the differences are often very large.

June 24, 1997

The study date of June 24, 1997 covers the 24 hours between June 23, 1997 12 UTC and June 24, 1997 12 UTC. This date was characterized by light to moderate

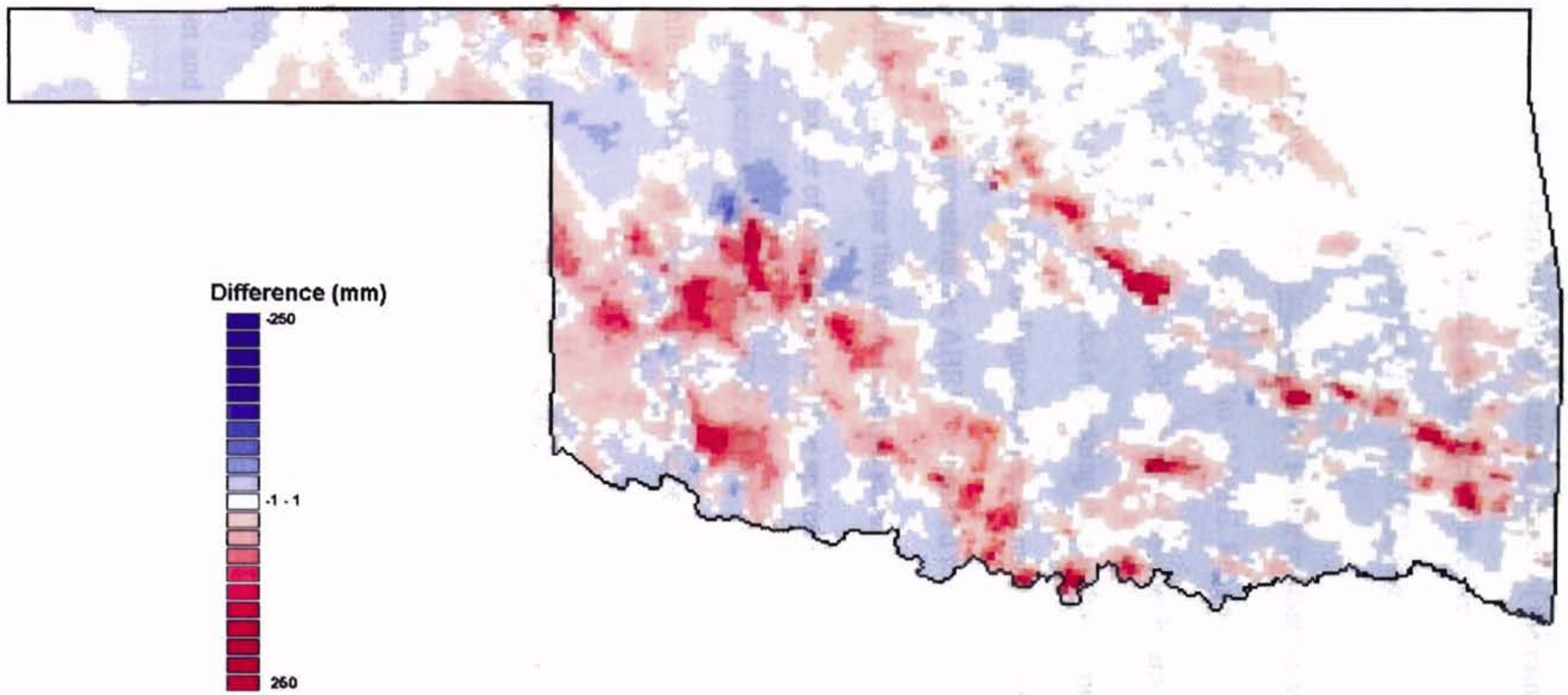

Figure 4.7: Difference in Radar and Mesonet Rainfall (mm) for June 9, 1997 - 24 Hour from 12 UTC to 12 UTC. Difference = Radar Rainfall – Mesonet Rainfall. Positive values indicate greater Radar estimated rainfall. Negative values indicate greater Mesonet estimated rainfall.

rainfall across most of the state. There were several localized areas of heavy rainfall in the panhandle and the eastern half of the state but much of the rainfall exhibited a smooth, homogenous pattern. Rainfall estimates were collected for the last hour (11 UTC - 12 UTC), the last six hours (6 UTC - 12 UTC), and the entire 24-hour period.

June 24, 1997 - 1Hour Rainfall Estimate. The 1-hour estimate covers the last hour of the June 24, 1997 study period from 11 UTC to 12 UTC. For each of the 11,132 4x4 kilometer cells in the study area, an ABRFC and a Mesonet interpolated rainfall value was obtained. Each cell is color-coded according the rainfall amount and the results are displayed in Figure 4.8. Map A of Figure 4.8 represents the Mesonet-interpolated total rainfall while Map B represents the ABRFC estimated total rainfall.

Both estimates agree that there is only a small amount of rainfall occurring near the north central border of the study area. The spatial description of this rainfall by the two estimates appears very different. The ABRFC estimate shows only a small patch of rainfall while the Mesonet estimate shows extremely light rainfall spread over a large area.

The correlation (*r*) between the Mesonet and ABRFC estimate was 0.284 (correlation is significant at the 0.01 level – 2 tailed). Table 4.4 lists some basic statistics for both estimates.

Figure 4.9 illustrates the differences between the rainfall estimates and where those differences occur. The map of difference shows that there were no areas in which the Mesonet and ABRFC estimates differed by more than one millimeter.

Figure 4.8: Estimated rainfall for June 24, 1997 (1 Hour from 11 UTC to 12 UTC). Map A – Rainfall estimate from interpolated Mesonet data. Map B – Rainfall estimate from ABRFC Stage III radar rainfall data.

Map A

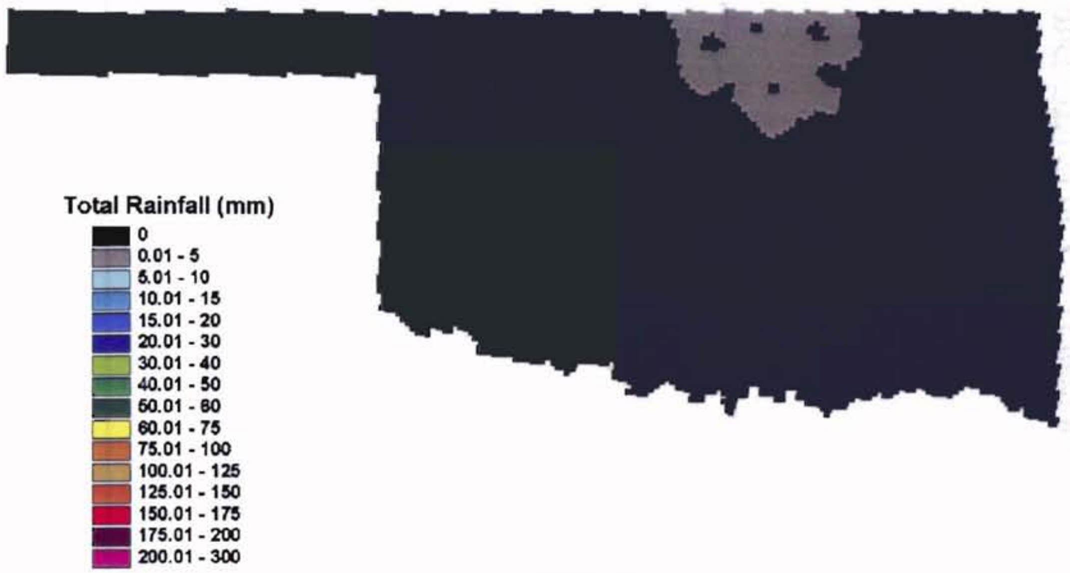

Map B

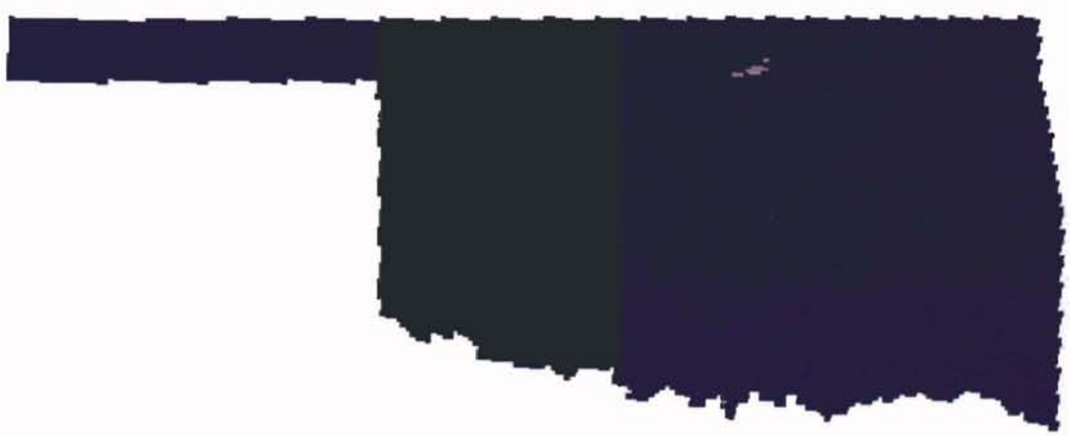

Table 4.4: June 24, 1997
1 Hour (11 UTC to 12 UTC)

Method	Min (mm)	Max (mm)	Mean (mm)	Standard Deviation (mm)	Volume (m3)
ABRFC	0	1	0.00	0.02	79,687
MESONET	0	0	0.00	0.01	247,754

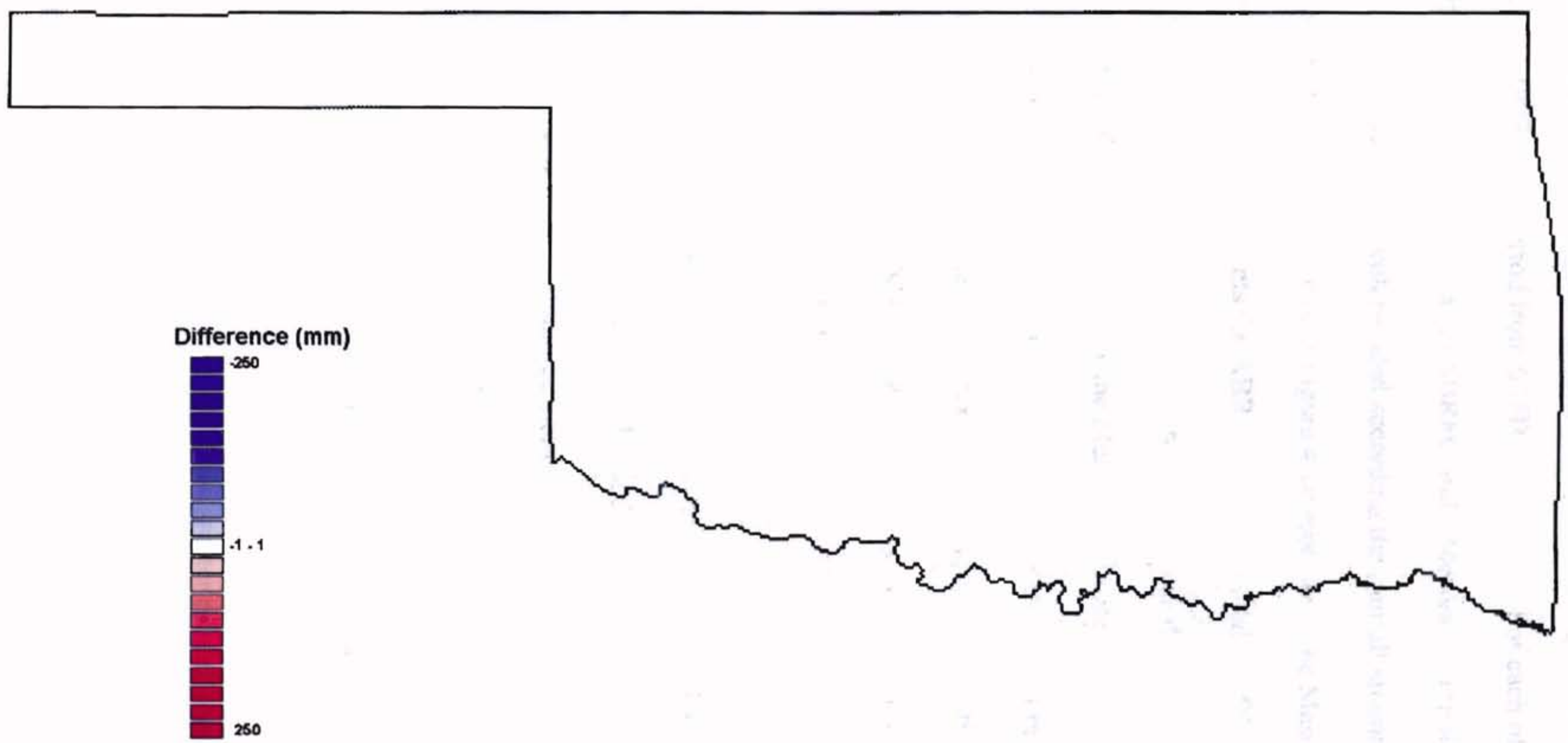

Figure 4.9: Difference in Radar and Mesonet Rainfall (mm) for June 24, 1997 - 1 Hour from 11 UTC to 12 UTC. Difference = Radar Rainfall – Mesonet Rainfall. Positive values indicate greater Radar estimated rainfall. Negative values indicate greater Mesonet estimated rainfall. In this case there were no differences greater than 1 mm.

June 24, 1997 - 6 Hour Rainfall Estimate. The 6-hour estimate covers the last 6 hours of the June 24, 1997 study period from 6 UTC to 12 UTC. For each of the 11,132 4x4 kilometer cells in the study area, an ABRFC and a Mesonet interpolated rainfall value was obtained. Each cell is color-coded according the rainfall amount and the results are displayed in Figure 4.10. Map A of Figure 4.10 represents the Mesonet-interpolated total rainfall while Map B represents the ABRFC estimated total rainfall.

There was only a small amount of rainfall indicated in both estimates. It appears that no new rainfall was indicated by the Mesonet estimate from the 1-hour estimate. The ABRFC estimate, however, indicates a concentrated area of light rainfall along the northern Oklahoma border that is not indicated by the Mesonet estimate.

The correlation (r) between the Mesonet and ABRFC estimate was 0.014 (correlation is NOT significant at the 0.01 level – 2 tailed). Table 4.5 lists some basic statistics for both estimates.

Figure 4.11 illustrates the differences between the rainfall estimates and where those differences occur. The majority of the study area is shown in white, indicating little or no difference between the rainfall estimates for most of the study area. There is some difference indicated by the concentrated area of red along the northern Oklahoma border. The red indicates that the ABRFC estimate indicates greater rainfall for this area than the Mesonet estimate. This corresponds with the rainfall event that was indicated by the ABRFC estimate and not indicated by the Mesonet estimate. There are no areas of difference where the Mesonet estimate indicates greater rainfall than the ABRFC estimate.

Figure 4.8: Estimated rainfall for June 24, 1997 (1 Hour from 11 UTC to 12 UTC). Map A – Rainfall estimate from interpolated Mesonet data. Map B – Rainfall estimate from ABRFC Stage III radar rainfall data.

Map A

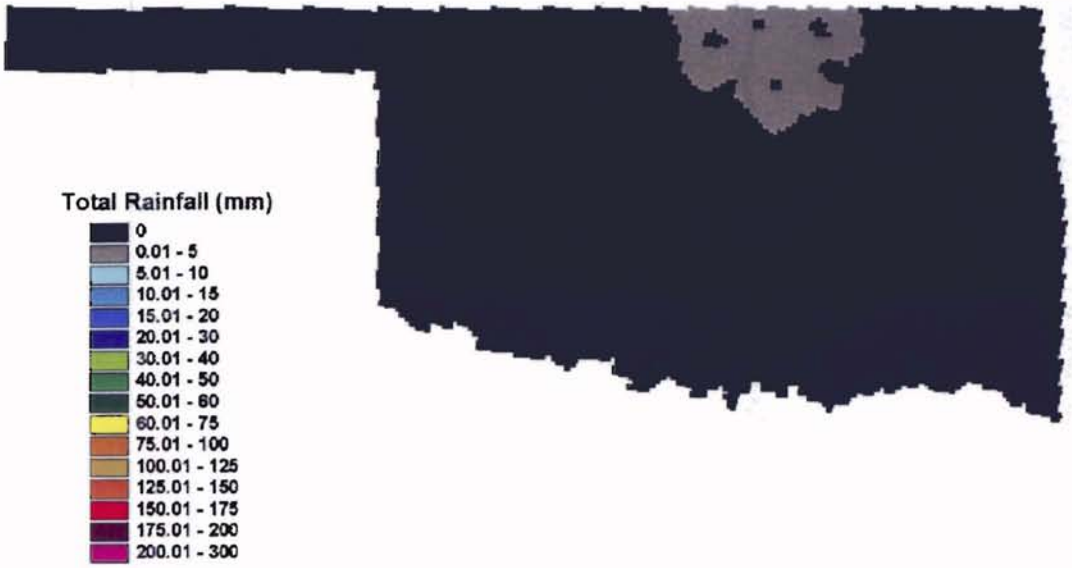

Map B

Table 4.4: June 24, 1997
1 Hour (11 UTC to 12 UTC)

Method	Min (mm)	Max (mm)	Mean (mm)	Standard Deviation (mm)	Volume (m3)
ABRFC	0	1	0.00	0.02	79,687
MESONET	0	0	0.00	0.01	247,754

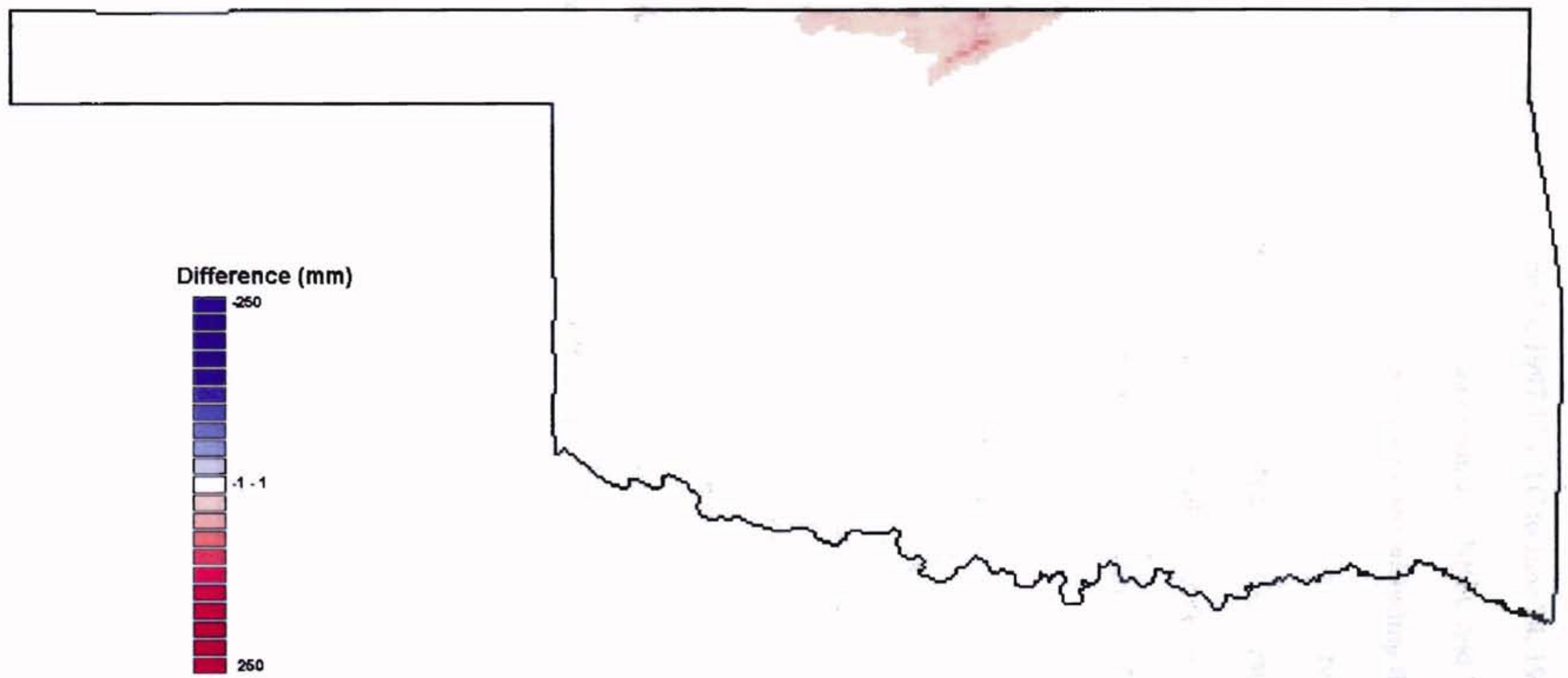

Figure 4.11: Difference in Radar and Mesonet Rainfall (mm) for June 24, 1997 - 6 Hour from 6 UTC to 12 UTC. Difference = Radar Rainfall – Mesonet Rainfall. Positive values indicate greater Radar estimated rainfall. Negative values indicate greater Mesonet estimated rainfall.

June 24, 1997 - 24 Hour Rainfall Estimate. The 24-hour estimate covers the entire June 24, 1997 study period from June 23, 1997 12 UTC to June 24, 1997 12 UTC. For each of the 11,132 4x4 kilometer cells in the study area, an ABRFC and Mesonet interpolated rainfall value was obtained. Each cell is color-coded according the rainfall amount and the results are displayed in Figure 4.12. Map A of Figure 4.12 represents the Mesonet-interpolated total rainfall while Map B represents the ABRFC estimated total rainfall. There is general agreement between the two rainfall estimates on where rainfall is occurring across the study area. However, there is a noticeable difference in the spatial resolution of the rainfall descriptions.

Both estimates generally agree on where rainfall occurred across the study area. They both indicate a band of heavy rainfall stretching from the northeast quarter to the central border of the study area. Both estimates indicate light concentrations of rainfall near the eastern end of the Oklahoma panhandle as well as an indication of light rainfall for the remainder of the study area. However, the ABRFC estimate describes the rainfall event along the north-central Oklahoma border as elongated while the Mesonet estimate only indicates a single spot. The ABRFC also indicates a small, concentrated rainfall event in the central panhandle whereas the Mesonet does not.

The correlation (r) between the Mesonet and ABRFC estimate was 0.676 (correlation was significant at the 0.01 level – 2 tailed). Table 4.6 lists some basic statistics for both estimates.

Figure 4.13 illustrates the differences between the rainfall estimates and where those differences occur. There is a large amount of difference across the study area. Areas where the ABRFC estimate indicates greater rainfall than the Mesonet (red) seem

Figure 4.12: Estimated rainfall for June 24, 1997 (24 Hour from 12 UTC to 12 UTC). Map A – Rainfall estimate from interpolated Mesonet data. Map B – Rainfall estimate from ABRFC Stage III radar rainfall data.

Map A

Map B

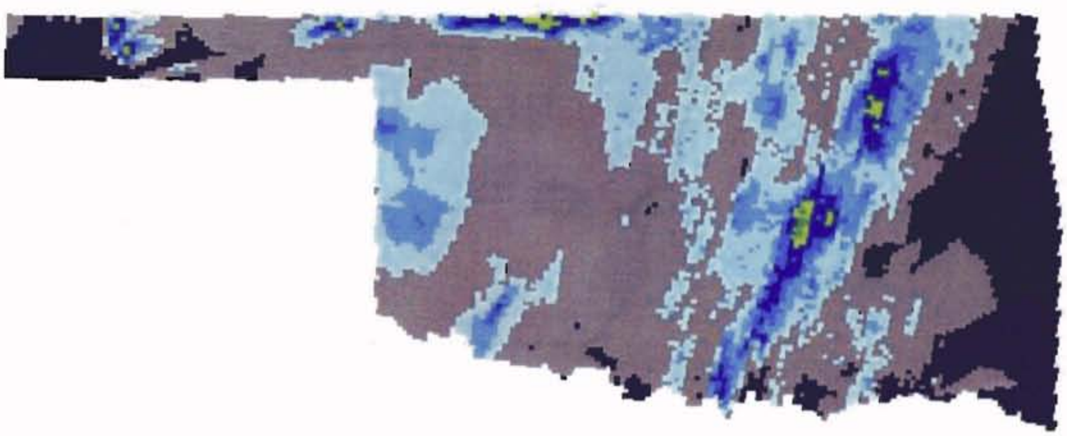

Table 4.6: June 24, 1997
24 Hour (12 UTC to 12 UTC)

Method	Min (mm)	Max (mm)	Mean (mm)	Standard Deviation (mm)	Volume (m3)
ABRFC	0.00	42.84	4.80	5.68	854,545,754
MESONET	0.00	26.43	4.67	3.14	831,409,005

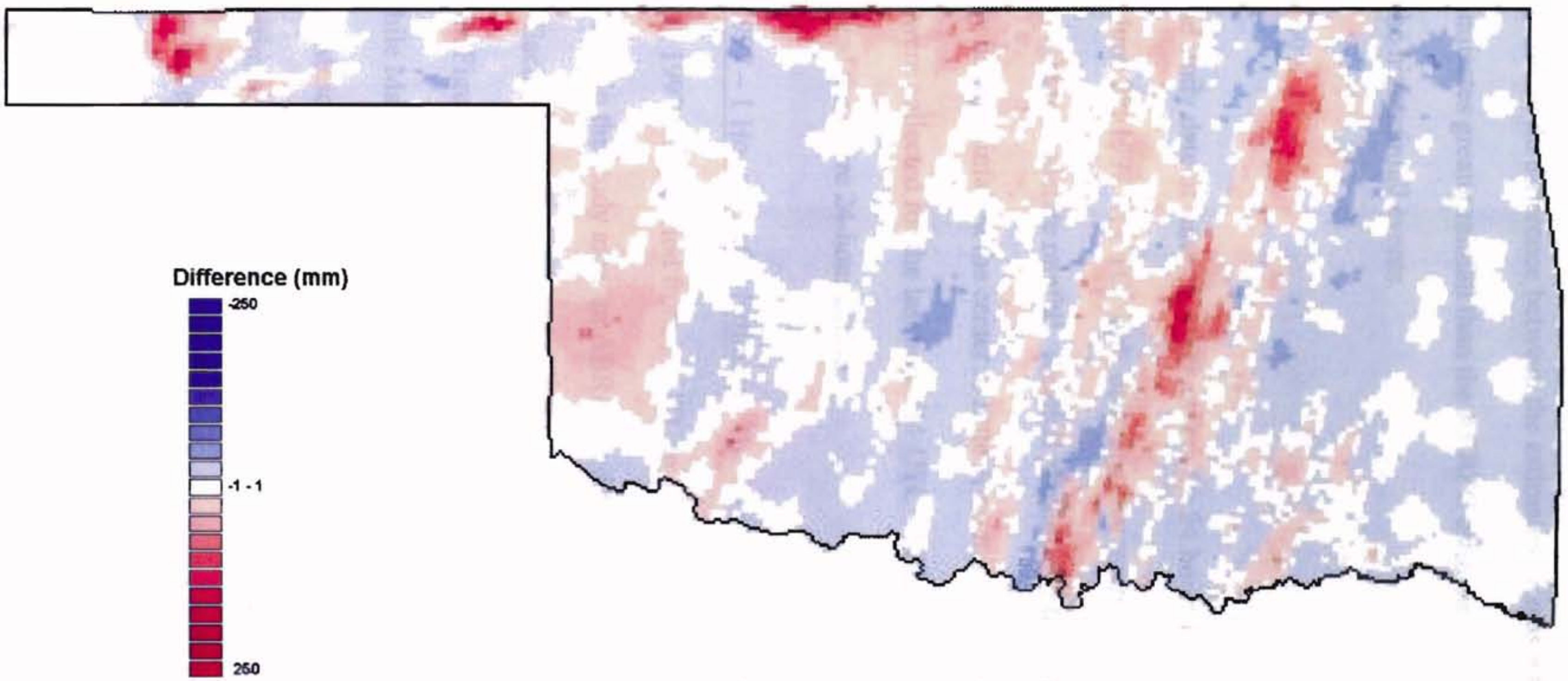

Figure 4.13: Difference in Radar and Mesonet Rainfall (mm) for June 24, 1997 - 24 Hour from 12 UTC to 12 UTC. Difference = Radar Rainfall – Mesonet Rainfall. Positive values indicate greater Radar estimated rainfall. Negative values indicate greater Mesonet estimated rainfall.

to correspond with the areas of the heaviest rainfall. These areas are skirted by white indicating little or no difference between the estimates. Areas where the Mesonet estimate indicates greater rainfall than the ABRFC estimate seem to fill in the areas between the high rainfall events.

June 28, 1997

The study date of June 28, 1997 covers the 24 hours between June 27, 1997 12 UTC and June 28, 1997 12 UTC. This date was characterized by random, scattered patches of light to moderate rainfall. Rainfall patches exhibited sharp transitions from moderately heavy rainfall at the center to little or no rainfall around the edges. Rainfall estimates were collected for the last hour (11 UTC - 12 UTC), the last six hours (6 UTC - 12 UTC), and the entire 24-hour period.

June 28, 1997 – 1 Hour Rainfall Estimate. The 1-hour estimate covers the last hour of the June 28, 1997 study period from 11 UTC to 12 UTC. For each of the 11,132 4x4 kilometer cells in the study area, an ABRFC and Mesonet interpolated rainfall value was obtained. Each cell is color-coded according the rainfall amount and the results are displayed in Figure 4.14. Map A of Figure 4.14 represents the Mesonet-interpolated total rainfall while Map B represents the ABRFC estimated total rainfall.

The Mesonet estimate indicates light rainfall for most of the study area. The ABRFC estimate indicates light rainfall in much more concentrated areas than indicated by the Mesonet estimate. The ABRFC estimate indicates three small, concentrated rainfall events occurring in the west-central, central and northeast portions of the study area. The Mesonet only indicates the west-central and northeast rainfall events. The

Figure 4.14: Estimated rainfall for June 28, 1997 (1 Hour from 11 UTC to 12 UTC). Map A – Rainfall estimate from interpolated Mesonet data. Map B – Rainfall estimate from ABRFC Stage III radar rainfall data.

Map A

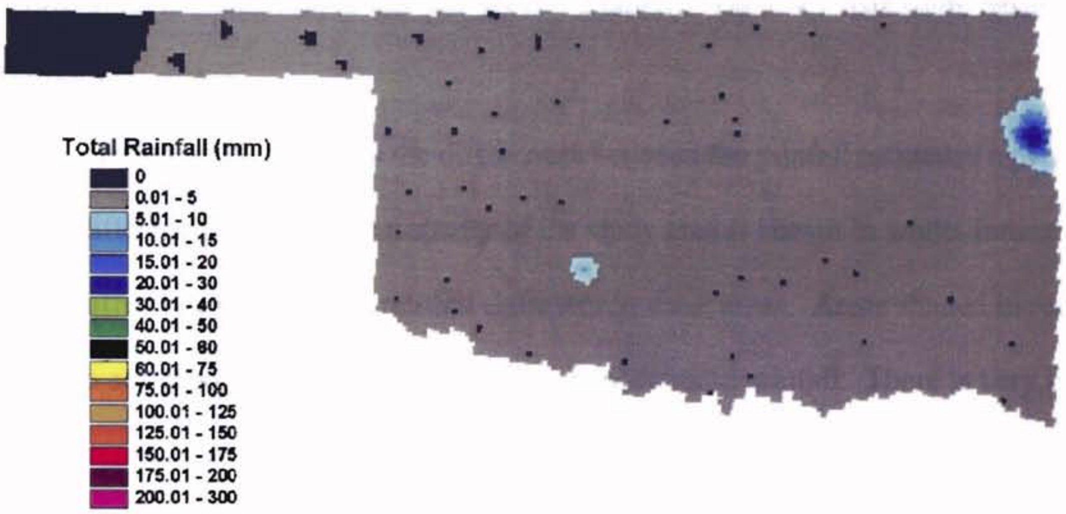

Map B

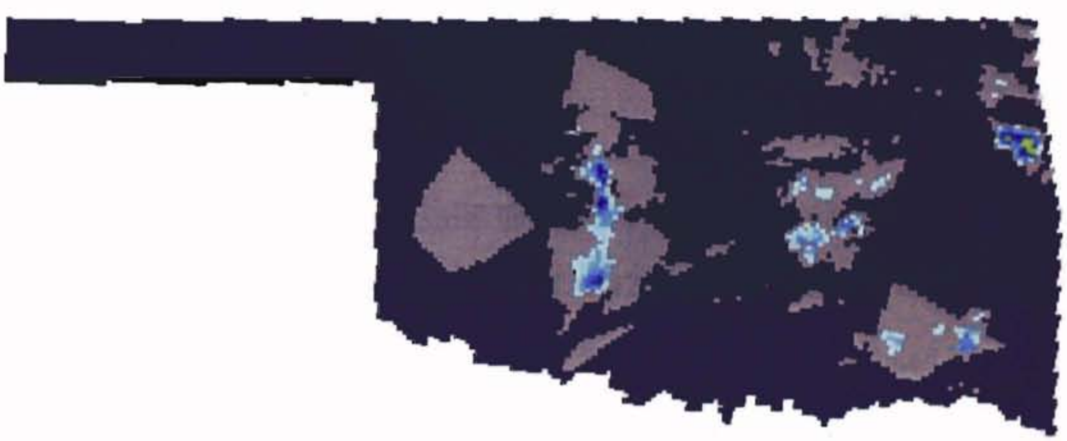

Table 4.7: June 28, 1997
1 Hour (11 UTC to 12 UTC)

Method	Min (mm)	Max (mm)	Mean (mm)	Standard Deviation (mm)	Volume (m3)
ABRFC	0	39	0.48	2.21	86,330,886
MESONET	0	29	0.43	1.47	77,336,230

ABRFC estimate describes the west-central rainfall event as elongated and extending toward the north. The Mesonet estimate describes it as a single spot.

The correlation (r) between the Mesonet and ABRFC estimate was 0.515 (correlation is significant at the 0.01 level – 2 tailed). Table 4.7 lists some basic statistics for both estimates.

Figure 4.15 illustrates the differences between the rainfall estimates and where those differences occur. The majority of the study area is shown in white, indicating little or no difference between the rainfall estimates in these areas. Areas shaded in red or blue seem to correspond with areas of localized, concentrated rainfall. There is very little area of greater Mesonet estimated rainfall (blue) except for the rainfall event occurring in the northeast. It appears that the Mesonet estimate places the rainfall event just northeast of where the ABRFC estimate places it. This results in the pattern of difference seen the in the northeast corner of the study area.

June 28, 1997 - 6 Hour Rainfall Estimate. The 6-hour estimate covers the last 6 hours of the June 28, 1997 study period from 6 UTC to 12 UTC. For each of the 11,132 4x4 kilometer cells in the study area, an ABRFC and a Mesonet interpolated rainfall value was obtained. Each cell is color-coded according the rainfall amount and the results are displayed in Figure 4.16. Map A of Figure 4.16 represents the Mesonet-interpolated total rainfall while Map B represents the ABRFC estimated total rainfall.

As in the 1-hour estimate, the ABRFC estimate indicates rainfall events occurring in the west-central, central and northeast portions of the study area. These are indicated by the Mesonet estimate as well but, are described differently. The Mesonet estimate

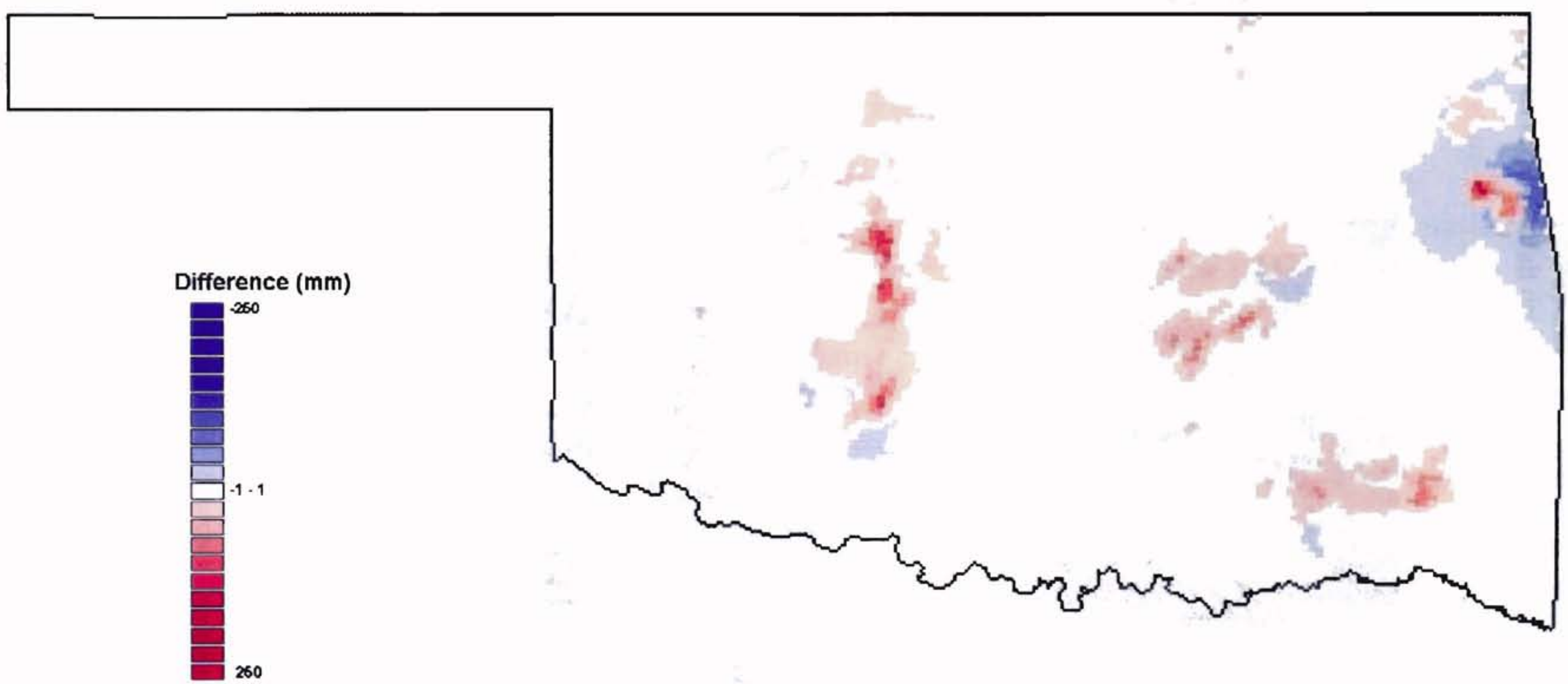

Figure 4.15: Difference in Radar and Mesonet Rainfall (mm) for June 28, 1997 - 1 Hour from 11 UTC to 12 UTC. Difference = Radar Rainfall – Mesonet Rainfall. Positive values indicate greater Radar estimated rainfall. Negative values indicate greater Mesonet estimated rainfall.

Figure 4.16: Estimated rainfall for June 28, 1997 (6 Hour from 6 UTC to 12 UTC). Map A – Rainfall estimate from interpolated Mesonet data. Map B – Rainfall estimate from ABRFC Stage III radar rainfall data.

Map A

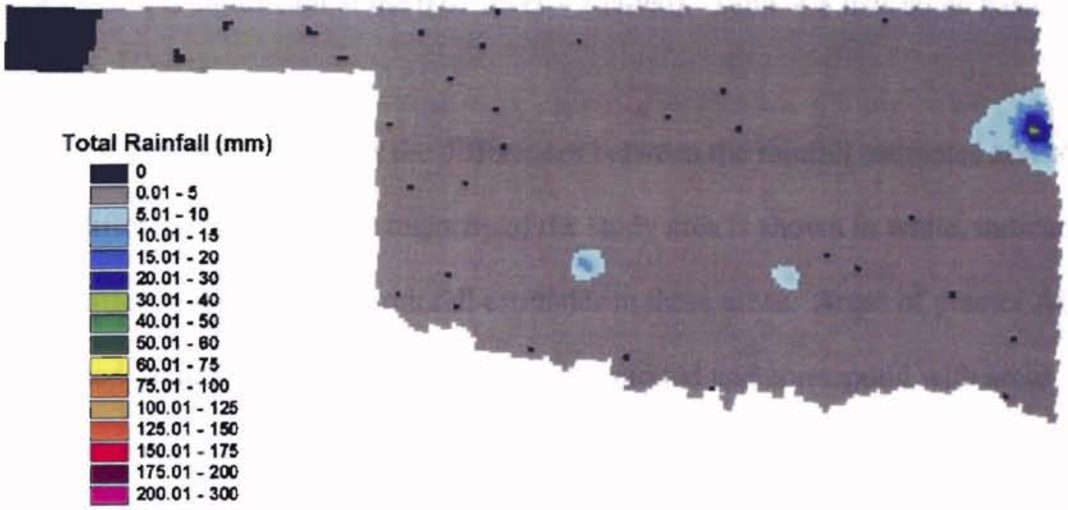

Map B

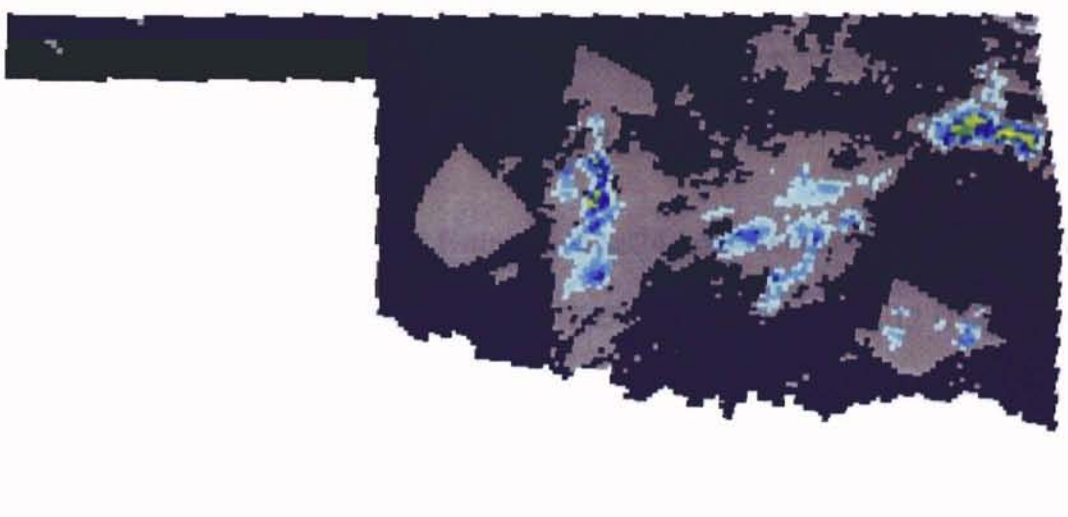

Table 4.8: June 28, 1997
6 Hour (6 UTC to 12 UTC)

Method	Min (mm)	Max (mm)	Mean (mm)	Standard Deviation (mm)	Volume (m3)
ABRFC	0.00	64.75	1.11	3.80	198,523,635
MESONET	0.00	32.34	0.76	1.81	134,474,560

describes them as single points corresponding with Mesonet gage locations while the ABRFC describes them as occurring over a larger area.

The correlation (r) between the Mesonet and ABRFC estimate was 0.450 (correlation is significant at the 0.01 level – 2 tailed). Table 4.8 lists some basic statistics for both estimates.

Figure 4.17 illustrates the differences between the rainfall estimates and where those differences occur. The majority of the study area is shown in white, indicating little or no difference between the rainfall estimates in these areas. Areas of greater ABRFC estimated rainfall (red) are localized and concentrated and correspond with areas of high rainfall. Areas of greater Mesonet estimated rainfall (blue) occur at the periphery of these high rainfall areas and exhibit a smoother, more homogenous pattern. As in the 1-hour difference map, the rainfall event in the northeast is placed farther northeast by the Mesonet estimate than it is placed by the ABRFC estimate resulting in the areas of dark red and blue difference in the northeast portion of the map.

<u>June 28, 1997 - 24 Hour Rainfall Estimate</u>. The 24-hour estimate covers the entire June 28, 1997 study period from June 27, 1997 12 UTC to June 28, 1997 12 UTC. For each of the 11,132 4x4 kilometer cells in the study area, an ABRFC and a Mesonet interpolated rainfall value was obtained. Each cell is color-coded according the rainfall amount and the results are displayed in Figure 4.18. Map A of Figure 4.18 represents the Mesonet-interpolated total rainfall while Map B represents the ABRFC estimated total rainfall.

Both estimates agree that there are numerous patches of small, concentrated rainfall events occurring across most of the study area. These events are more numerous

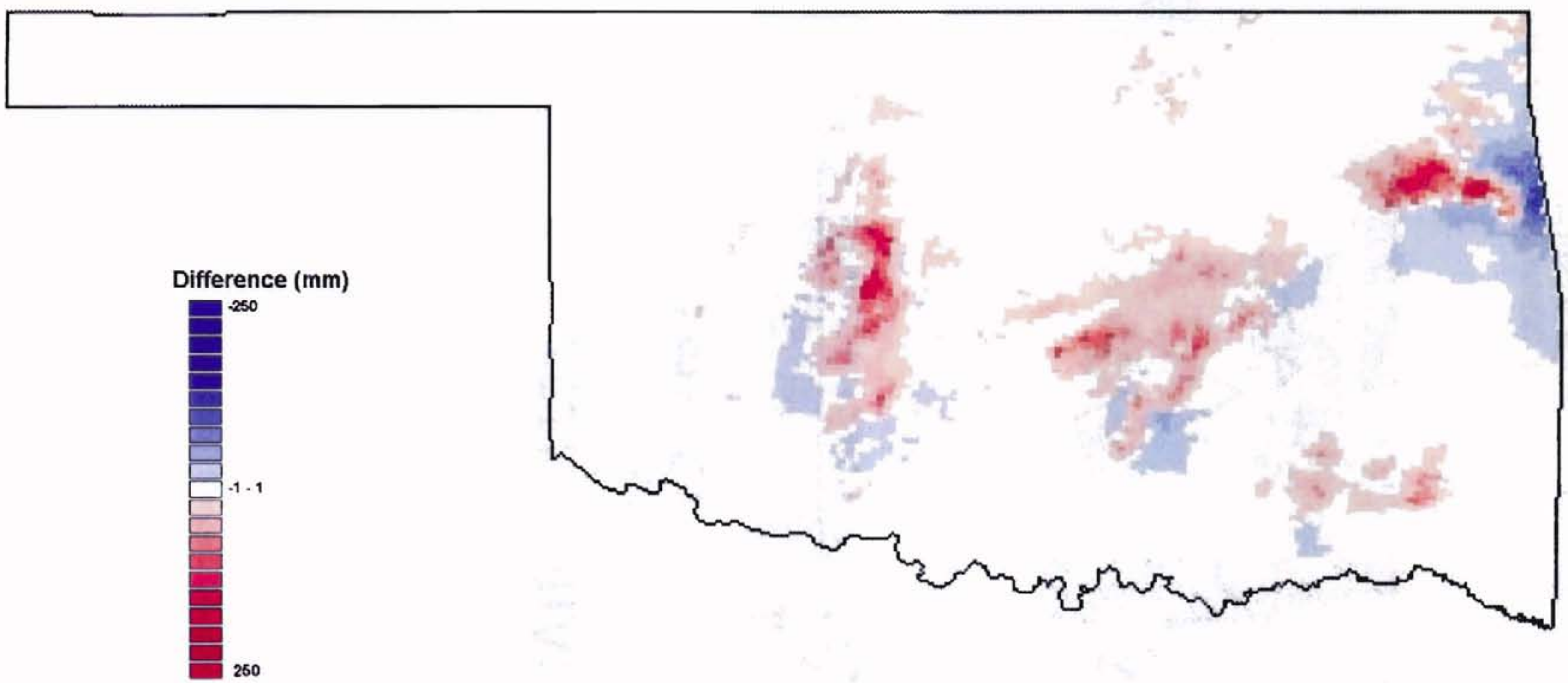

Figure 4.17: Difference in Radar and Mesonet Rainfall (mm) for June 28, 1997 - 6 Hour from 6 UTC to 12 UTC. Difference = Radar Rainfall – Mesonet Rainfall. Positive values indicate greater Radar estimated rainfall. Negative values indicate greater Mesonet estimated rainfall.

Figure 4.18: Estimated rainfall for June 28, 1997 (24 Hour from 12 UTC to 12 UTC). Map A – Rainfall estimate from interpolated Mesonet data. Map B – Rainfall estimate from ABRFC Stage III radar rainfall data.

Map A

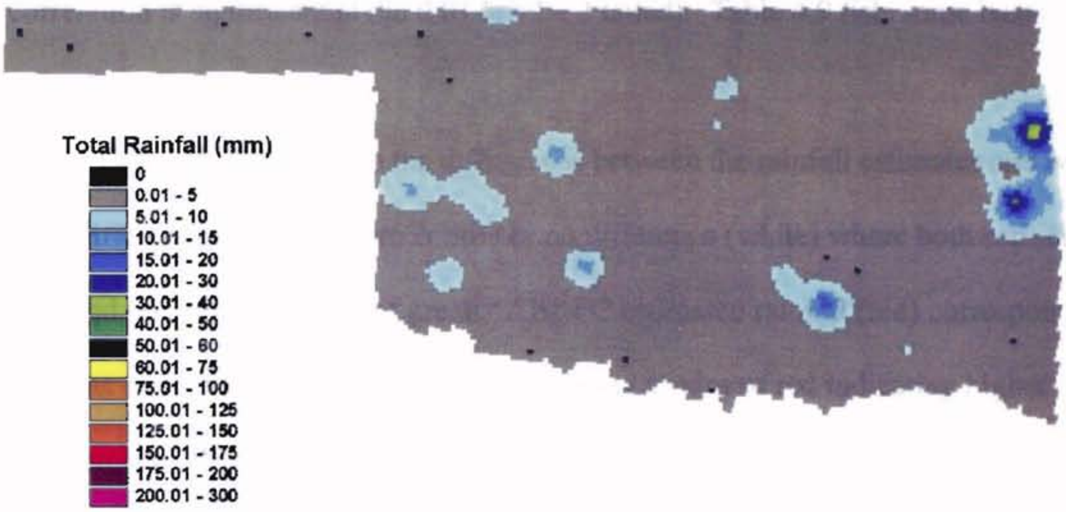

Map B

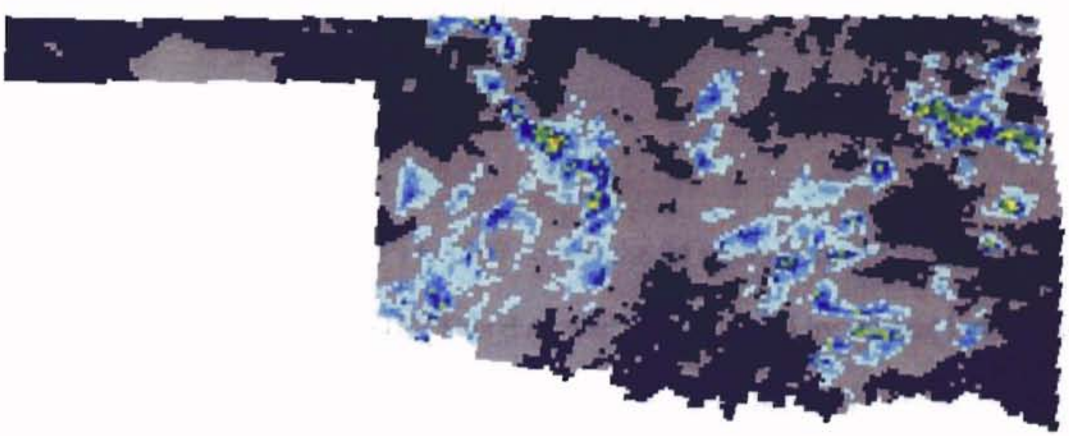

Table 4.9: June 28, 1997
24 Hour (12 UTC to 12 UTC)

Method	Min (mm)	Max (mm)	Mean (mm)	Standard Deviation (mm)	Volume (m3)
ABRFC	0	75	3.07	6.45	547,088,819
MESONET	0	34	2.12	2.71	377,294,650

and described in greater spatial detail by the ABRFC estimate. Both estimates agree that light rainfall fills the areas between the concentrated rainfall events.

The correlation (r) between the Mesonet and ABRFC estimate was 0.380 (correlation is significant at the 0.01 level – 2 tailed). Table 4.9 lists some basic statistics for both estimates.

Figure 4.19 illustrates the differences between the rainfall estimates and where those differences occur. There is little or no difference (white) where both estimates have indicated no rainfall. Areas of greater ABRFC estimated rainfall (red) correspond with the areas of heaviest rainfall and are often darker shades of red indicating higher amounts of difference. Areas of greater Mesonet estimated rainfall (blue) correspond with areas where both estimates indicate light rainfall and are usually lighter shades of blue indicating lower amounts of difference.

July 11, 1997

The study date of July 11, 1997 covers the 24 hours between July 10, 1997 12 UTC and July 11, 1997 12 UTC. This date was characterized by several large, heavy rainfall maxima. These events were widespread with the heaviest rainfall at the center and gradually decreased rainfall amounts towards the edges. Rainfall estimates were (11 UTC - 12 UTC), the last six hours (6 UTC - 12 UTC), and the entire 24-hour period.

July 11, 1997 - 1Hour Rainfall Estimate. The 1-hour estimate covers 11 UTC to 12 UTC of the July 11, 1997 study period. For each of the 11,132 4x4 kilometer cells in the study area, an ABRFC and a Mesonet interpolated rainfall value was obtained. Each cell is

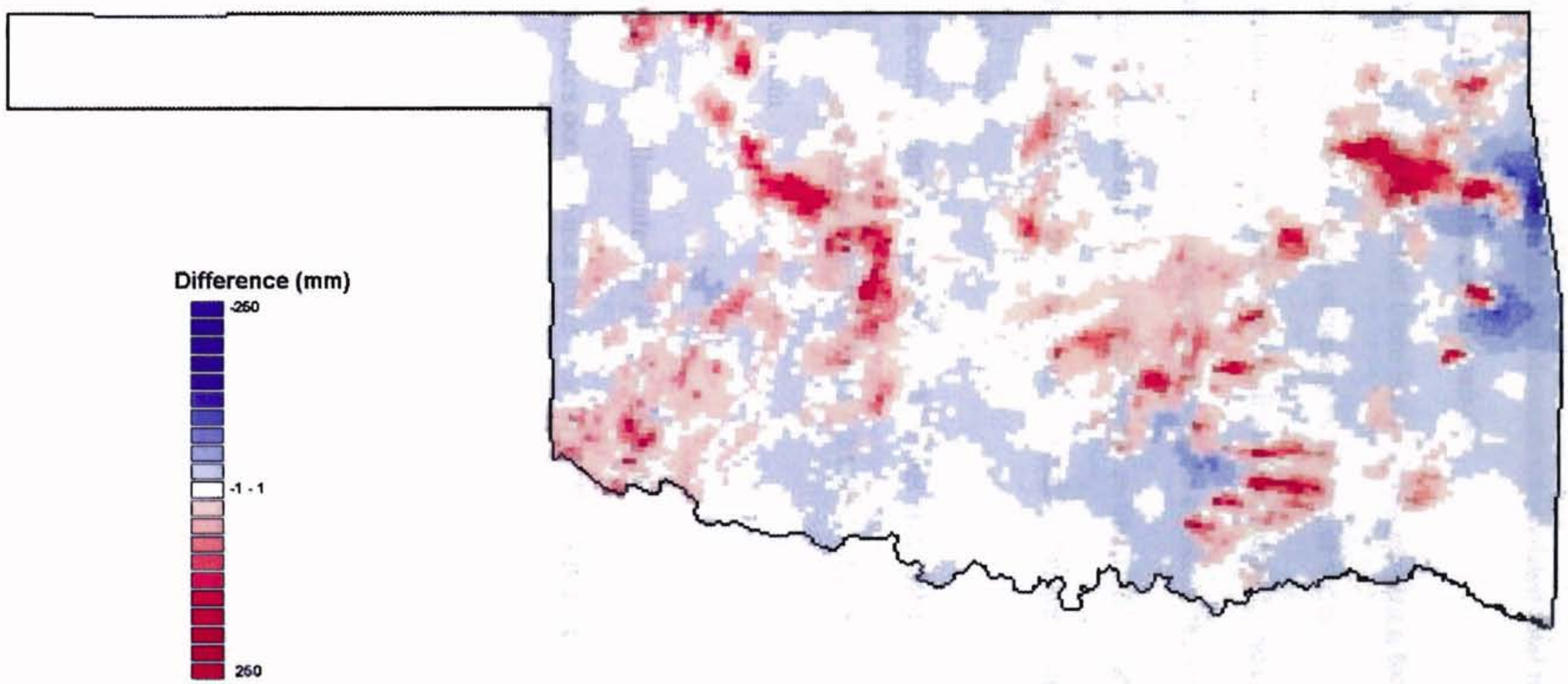

Figure 4.19: Difference in Radar and Mesonet Rainfall (mm) for June 28, 1997 - 24 Hour from 12 UTC to 12 UTC. Difference = Radar Rainfall – Mesonet Rainfall. Positive values indicate greater Radar estimated rainfall. Negative values indicate greater Mesonet estimated rainfall.

color-coded according the rainfall amount and the results are displayed in Figure 4.20. Map A of Figure 4.20 represents the Mesonet-interpolated total rainfall while Map B represents the ABRFC estimated total rainfall.

Both estimates agree that there is no rainfall occurring for the eastern half of the study area and that any rainfall occurring in the rest of the state is very light. The ABRFC estimate indicates only two small areas of rainfall, one on the north central border and the other in the extreme southwestern corner of the study area. The Mesonet estimate also indicates the same rainfall events as the ABRFC estimate, but indicates extremely light rainfall for the whole western half of the study area while the ABRFC estimate does not.

The correlation (r) between the Mesonet and ABRFC estimate was 0.605 (correlation is significant at the 0.01 level – 2 tailed). Table 4.10 lists some basic statistics for both

estimates.

Figure 4.21 illustrates the differences between the rainfall estimates and where those differences occur. Since there was very little rainfall across the study area for this date and time period, the majority of the study area is shown in white, indicating little or no difference between the rainfall estimates in these areas. When looking at the rainfall maps, it appears that there is a great deal of rainfall indicated by the Mesonet estimate that is not indicated by the ABRFC. The difference map, however, shows that differences in this area do not exceed 1 mm. There are no areas of greater Mesonet estimated rainfall (blue). There are two areas of greater ABRFC estimated rainfall (red)

Figure 4.20: Estimated rainfall for July 11, 1997 (1 Hour from 11 UTC to 12 UTC). Map A – Rainfall estimate from interpolated Mesonet data. Map B – Rainfall estimate from ABRFC Stage III radar rainfall data.

Map A

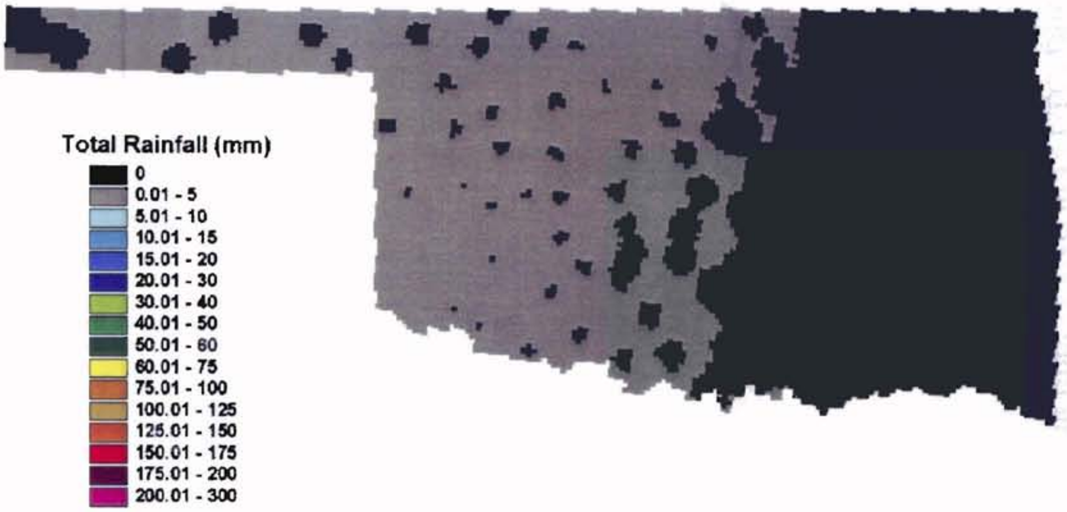

Map B

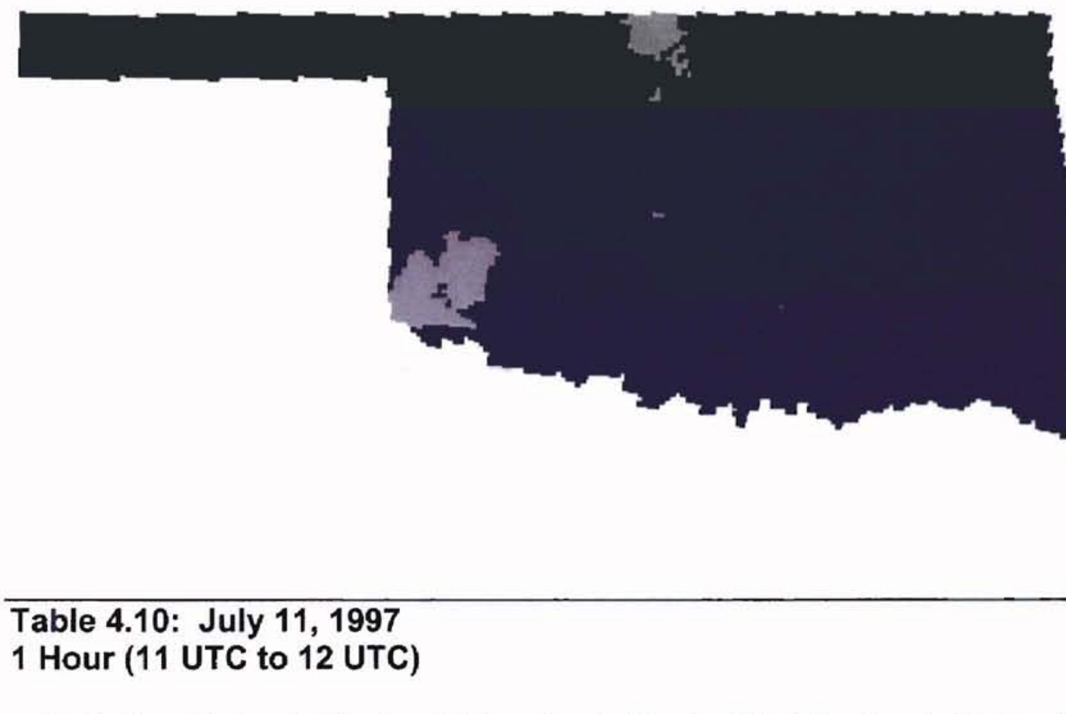

Table 4.10: July 11, 1997
1 Hour (11 UTC to 12 UTC)

Method	Min (mm)	Max (mm)	Mean (mm)	Standard Deviation (mm)	Volume (m3)
ABRFC	0	4	0.03	0.20	4,604,195
MESONET	0	2	0.03	0.10	4,700,376

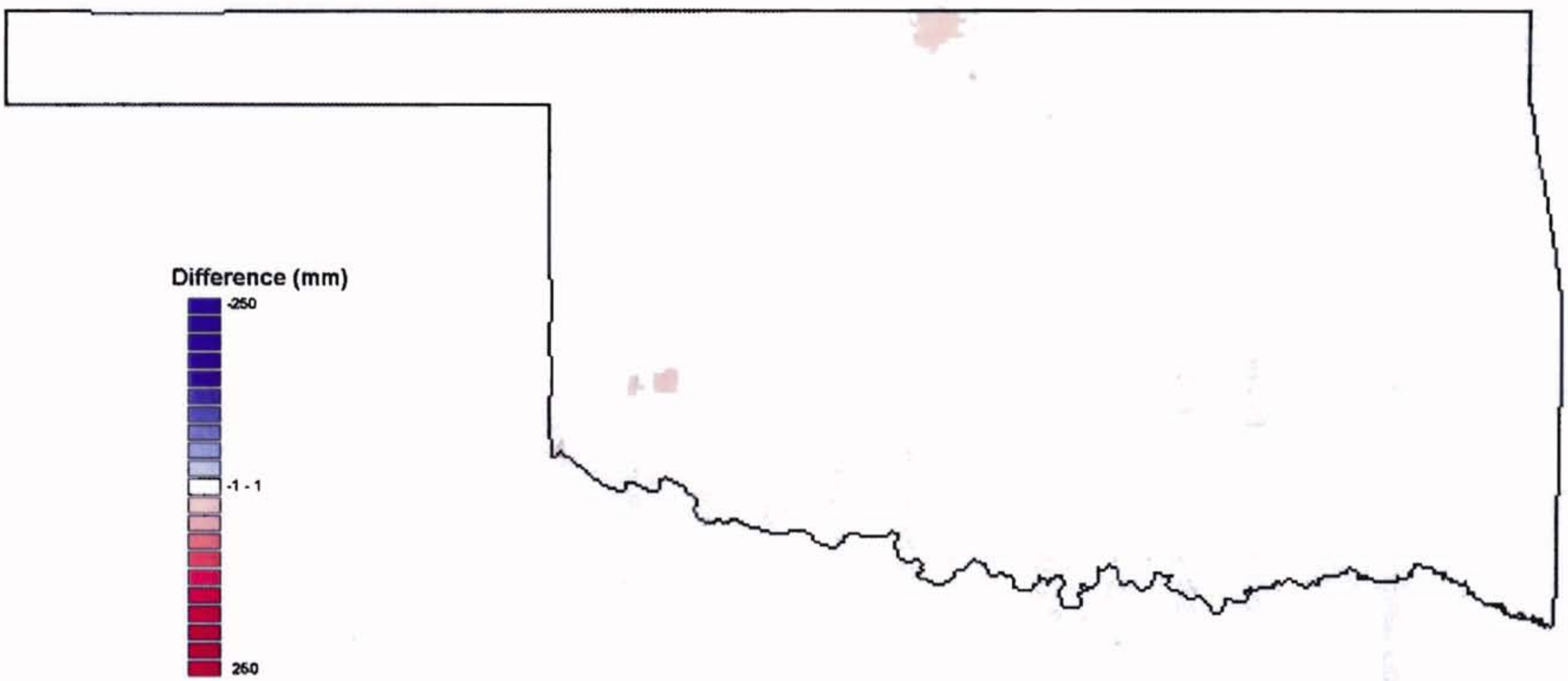

Figure 4.21: Difference in Radar and Mesonet Rainfall (mm) for July 11, 1997 - 1 Hour from 11 UTC to 12 UTC. Difference = Radar Rainfall – Mesonet Rainfall. Positive values indicate greater Radar estimated rainfall. Negative values indicate greater Mesonet estimated rainfall.

corresponding with the rainfall events in the extreme southwest corner and along the north central border of the study area.

<u>July 11, 1997 - 6 Hour Rainfall Estimate</u>. The 6-hour rainfall estimate covers the last 6 hours, from 6 UTC to 12 UTC, of the July 11, 1997 study period. For each of the 11,132 4x4 kilometer cells in the study area, an ABRFC and a Mesonet interpolated rainfall value was obtained. Each cell is color-coded according the rainfall amount and the results are displayed in Figure 4.22. Map A of Figure 4.22 represents the Mesonet-interpolated total rainfall while Map B represents the ABRFC estimated total rainfall.

Both estimates agree that there is no rainfall for most of the eastern half of the study area and that any rainfall occurring in the rest of the state is light. The ABRFC estimate indicates only two small areas of rainfall, one on the north central border and the other in the extreme southwestern corner of the study area. The Mesonet estimate also indicates the same rainfall events as the ABRFC estimate, but indicates extremely light rainfall for the whole western half of the study area while the ABRFC estimate does not. The ABRFC estimate indicates small patches of higher rainfall (5-15 mm) along the southwestern border that are not indicated by the Mesonet estimate.

The correlation (*r*) between the Mesonet and ABRFC estimate was 0.731 (correlation is significant at the 0.01 level – 2 tailed). Table 4.11 lists some basic statistics for both estimates.

Figure 4.23 illustrates the differences between the rainfall estimates and where those differences occur. Since there was very little rainfall across the study area for this date and time period, the majority of the study area is shown in white, indicating little or

Figure 4.22: Estimated rainfall for July 11, 1997 (6 Hour from 6 UTC to 12 UTC). Map A – Rainfall estimate from interpolated Mesonet data. Map B – Rainfall estimate from ABRFC Stage III radar rainfall data.

Map A

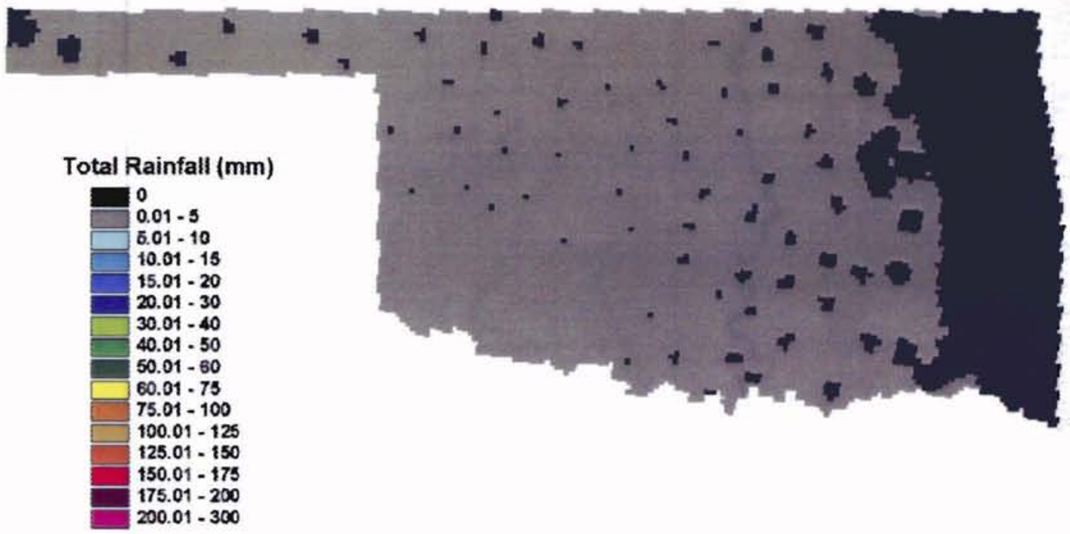

Map B

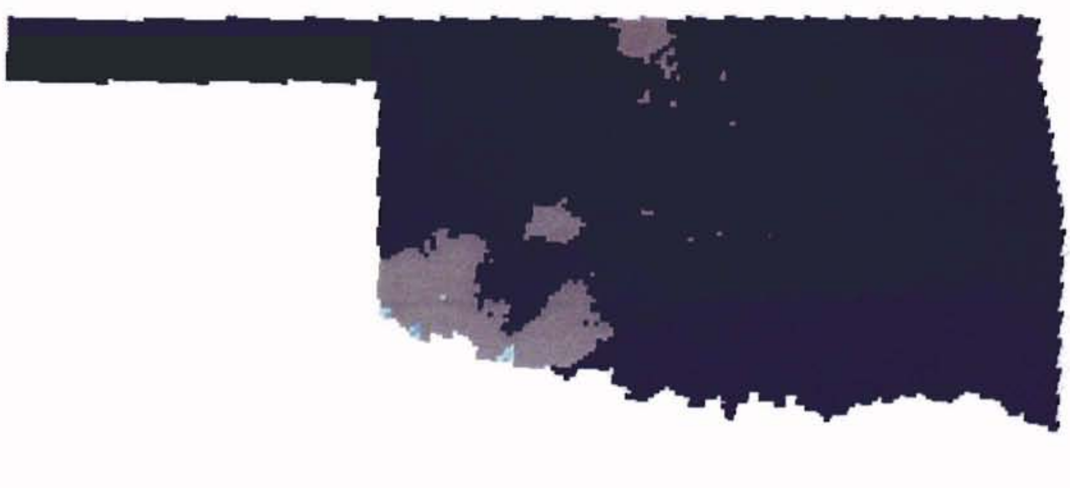

Table 4.11: July 11, 1997
6 Hour (6 UTC to 12 UTC)

Method	Min (mm)	Max (mm)	Mean (mm)	Standard Deviation (mm)	Volume (m3)
ABRFC	0	11	0.11	0.55	19,788,243
MESONET	0	4	0.09	0.26	16,717,592

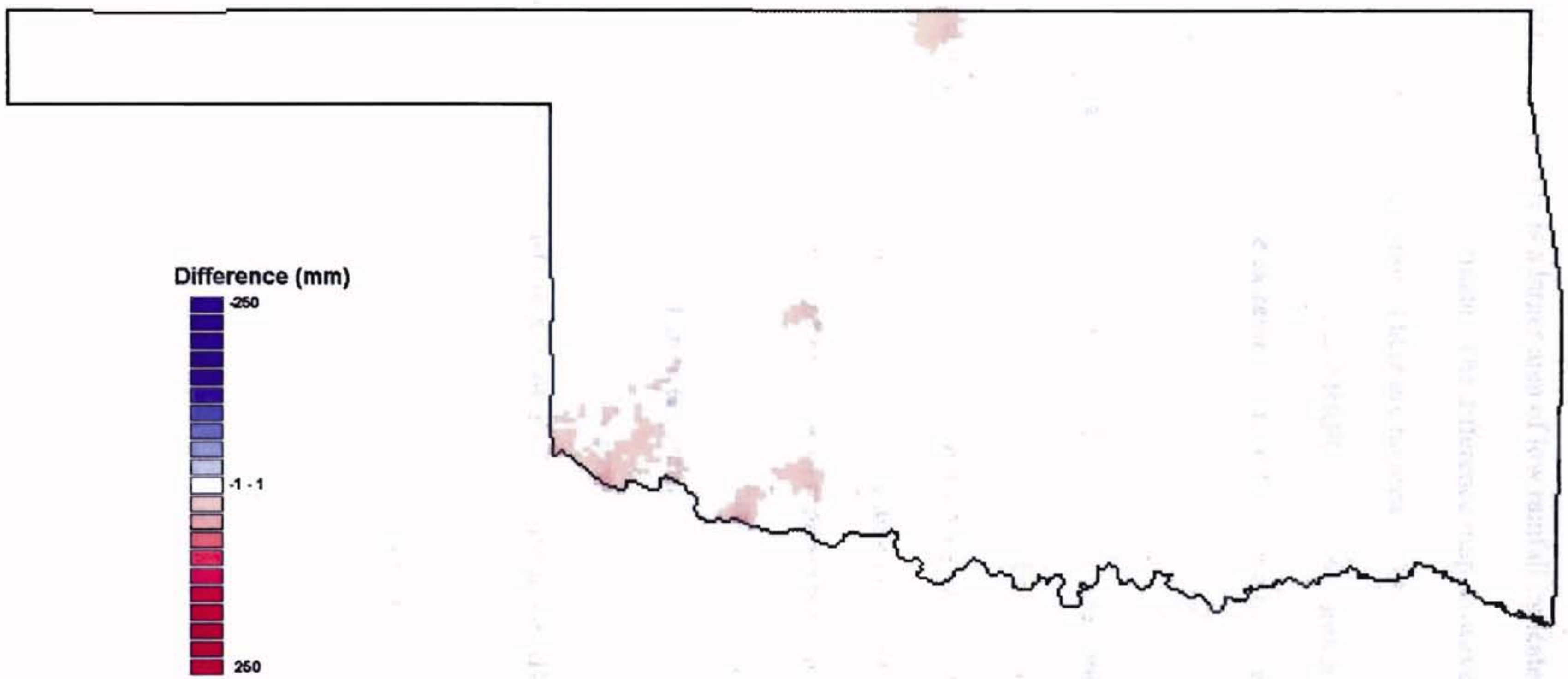

Figure 4.23: Difference in Radar and Mesonet Rainfall (mm) for July 11, 1997 - 6 Hour from 6 UTC to 12 UTC. Difference = Radar Rainfall – Mesonet Rainfall. Positive values indicate greater Radar estimated rainfall. Negative values indicate greater Mesonet estimated rainfall.

no difference between the rainfall estimates in these areas. When looking at the rainfall maps, it appears that there is a larger area of low rainfall indicated by the Mesonet estimate than the ABRFC estimate. The difference map, however, shows that differences in this area do not exceed 1 mm. There are no areas of greater Mesonet estimated rainfall (blue). There are two areas of greater ABRFC estimated rainfall (red) corresponding with the rainfall events in the extreme southwest corner and along the north central border of the study area.

July 11, 1997 - 24 Hour Rainfall Estimate. The 24-hour estimate covers the time period from July 10, 1997 12 UTC to July 11, 1997 12 UTC. For each of the 11,132 4x4 kilometer cells in the study area, an ABRFC and a Mesonet interpolated rainfall value was obtained. Each cell is color-coded according the rainfall amount and the results are displayed in Figure 4.24. Map A of Figure 4.24 represents the Mesonet-interpolated total rainfall while Map B represents the ABRFC estimated total rainfall.

Both estimates agree that there were areas of intense rainfall across the central and northeast portions of the study area. There were two, extremely heavy rainfall events in the southwest and northeast quarters of the state. Both the ABRFC and Mesonet estimates had similar spatial descriptions of these events. Both estimates agree that there was little or no rainfall in the southeast and south central portions of the study area. The ABRFC estimate provides a detailed spatial description of the light rainfall in this area while the Mesonet estimate indicates an even blanket of light rainfall for the whole area. The ABRFC estimate indicates a significant rainfall event (50 – 60 mm) in the panhandle that is not indicated by the Mesonet estimate.

Figure 4.24: Estimated rainfall for July11, 1997 (24 Hour from 12 UTC to 12 UTC). Map A – Rainfall estimate from interpolated Mesonet data. Map B – Rainfall estimate from ABRFC Stage III radar rainfall data.

Map A

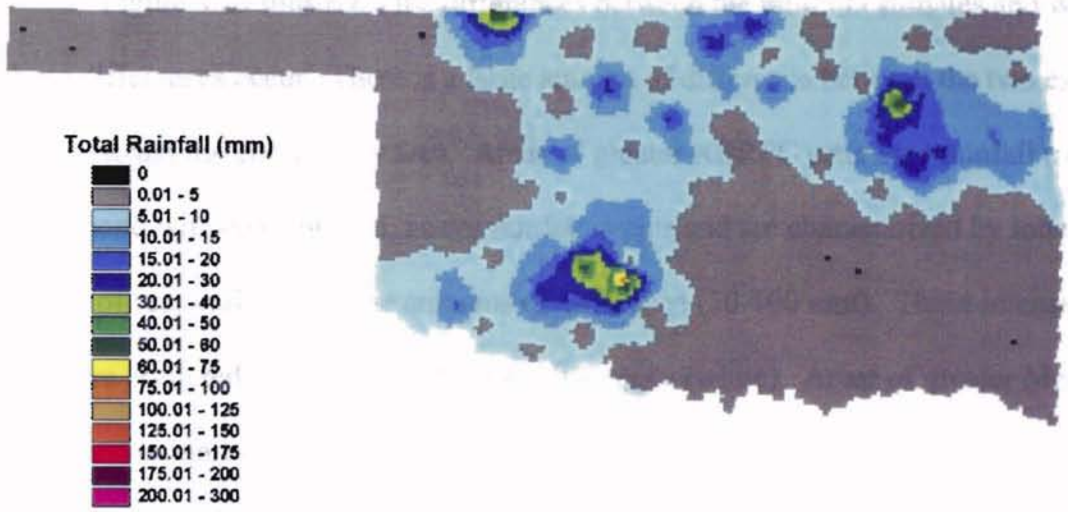

Map B

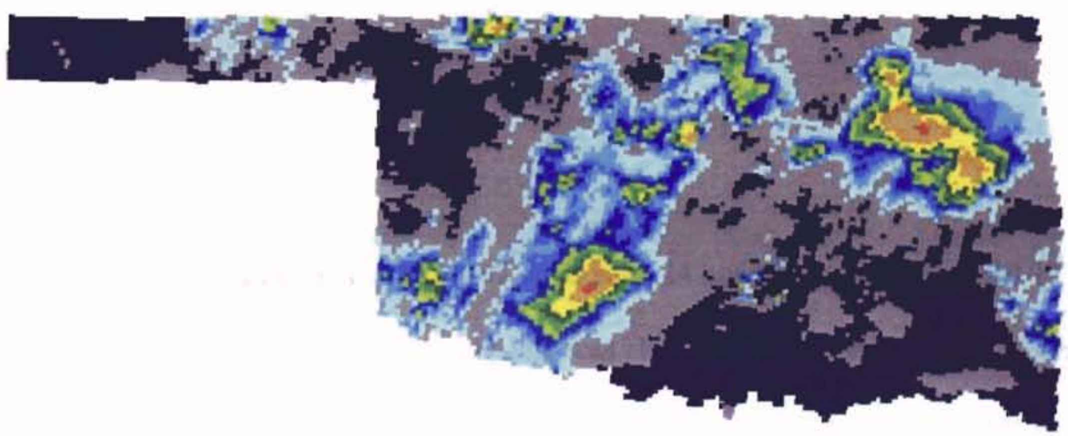

Table 4.12: July 11, 1997
24 Hour (12 UTC to 12 UTC)

Method	Min (mm)	Max (mm)	Mean (mm)	Standard Deviation (mm)	Volume (m3)
ABRFC	0	146	9.03	17.11	1,608,867,885
MESONET	0	81	6.27	6.31	1,116,085,414

The correlation (r) between the Mesonet and ABRFC estimate was 0.701 (correlation is significant at the 0.01 level – 2 tailed). Table 4.12 lists some basic statistics for both estimates.

Figure 4.25 illustrates the differences between the rainfall estimates and where those differences occur. There is a large amount of difference between the two estimates shown across the entire study area. Areas of greater ABRFC estimated rainfall (red) correspond with concentrated, heavy rainfall events and are characterized by intense shades of red, indicating large amounts of difference (50-100 mm). These intense red areas are bordered by areas of little or no difference (white). Areas of greater Mesonet estimated rainfall (blue) are widespread, evenly distributed between intense red areas, and mostly consist of lighter shades of blue (indicating low amounts of difference). There are several patches of intense blue and all correspond with the edges of heavy rainfall events.

<u>July 16, 1997</u>

The study date of July 16, 1997 covers the 24 hours between July 15, 1997 12 UTC and July 16, 1997 12 UTC. This date was characterized by random, scattered patches of light to moderate rainfall. Rainfall patches would rapidly change from moderately heavy rainfall at the center to little or no rainfall around the edges. Rainfall estimates were collected for the last hour (11 UTC - 12 UTC), the last six hours (6 UTC - 12 UTC), and the entire 24-hour period.

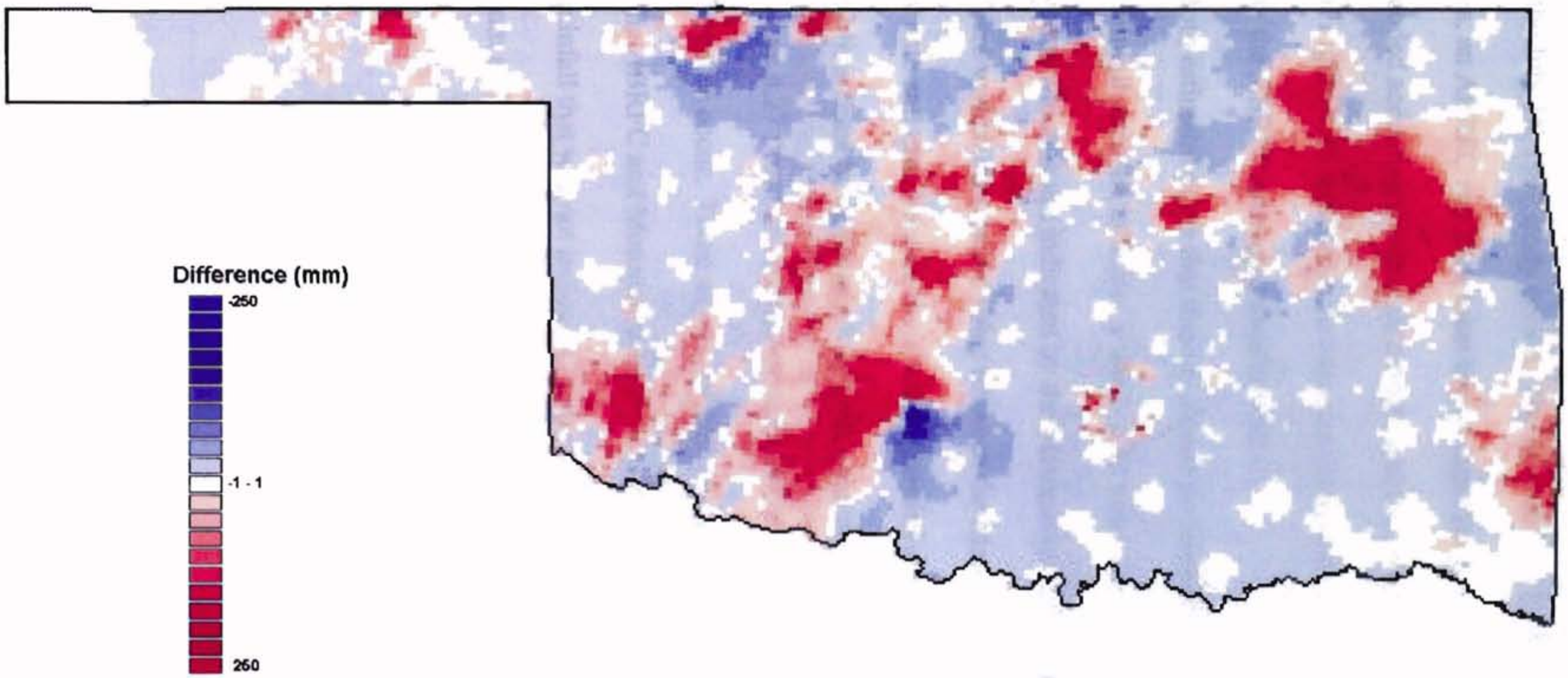

Figure 4.25: Difference in Radar and Mesonet Rainfall (mm) for July 11, 1997 - 24 Hour from 12 UTC to 12 UTC. Difference = Radar Rainfall – Mesonet Rainfall. Positive values indicate greater Radar estimated rainfall. Negative values indicate greater Mesonet estimated rainfall.

July 16, 1997 – 1 Hour Rainfall Estimate. The 1-hour estimate covers 11 UTC to 12 UTC of the July 16, 1997 study period. For each of the 11,132 4x4 kilometer cells in the study area, an ABRFC and a Mesonet interpolated rainfall value was obtained. Each cell is color-coded according the rainfall amount and the results are displayed in Figure 4.26. Map A of Figure 4.26 represents the Mesonet-interpolated total rainfall while Map B represents the ABRFC estimated total rainfall.

Both estimates agree that there is almost no rainfall for the entire study area. The ABRFC rainfall estimate indicates a small, light rainfall event in the northwest quarter of the study area which is not indicated by the Mesonet rainfall estimate.

There was no correlation value between the Mesonet and ABRFC estimate for this study date and time because there was no rainfall at all for the Mesonet estimate. Table 4.13 lists some basic statistics for both estimates.

Figure 4.27 illustrates the differences between the rainfall estimates and where those differences occur. There was no difference indicated on the difference map between the ABRFC and Mesonet rainfall estimates. The ABRFC did indicate a small patch of rainfall that was not indicated by the Mesonet estimate but the difference did not exceed 1mm and therefore did not show up on the difference map.

Figure 4.26: Estimated rainfall for July 16, 1997 (1 Hour from 11 UTC to 12 UTC). Map A – Rainfall estimate from interpolated Mesonet data. Map B – Rainfall estimate from ABRFC Stage III radar rainfall data.

Map A

Map B

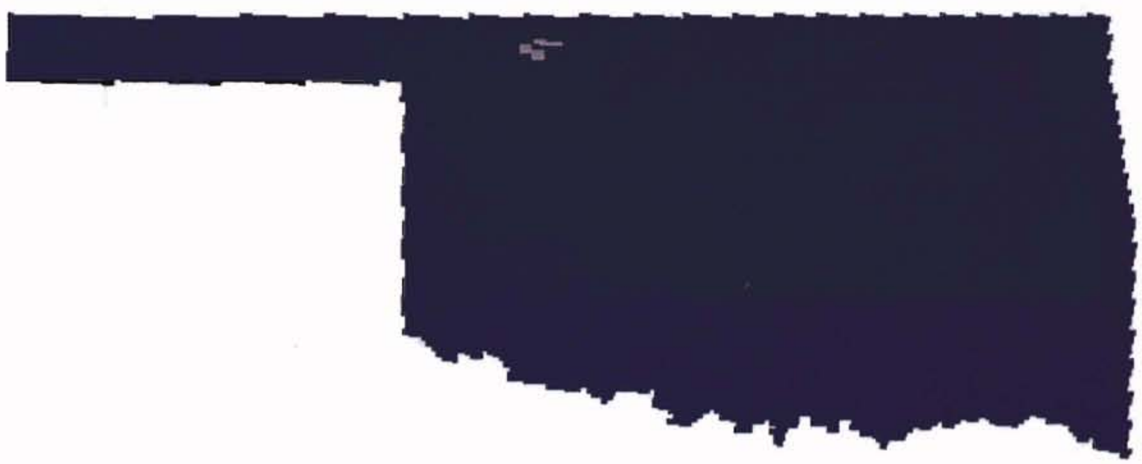

Table 4.13: July 16, 1997
1 Hour (11 UTC to 12 UTC)

Method	Min (mm)	Max (mm)	Mean (mm)	Standard Deviation (mm)	Volume (m3)
ABRFC	0	1	0.00	0.02	89,056
MESONET	0	0	0.00	0.00	0

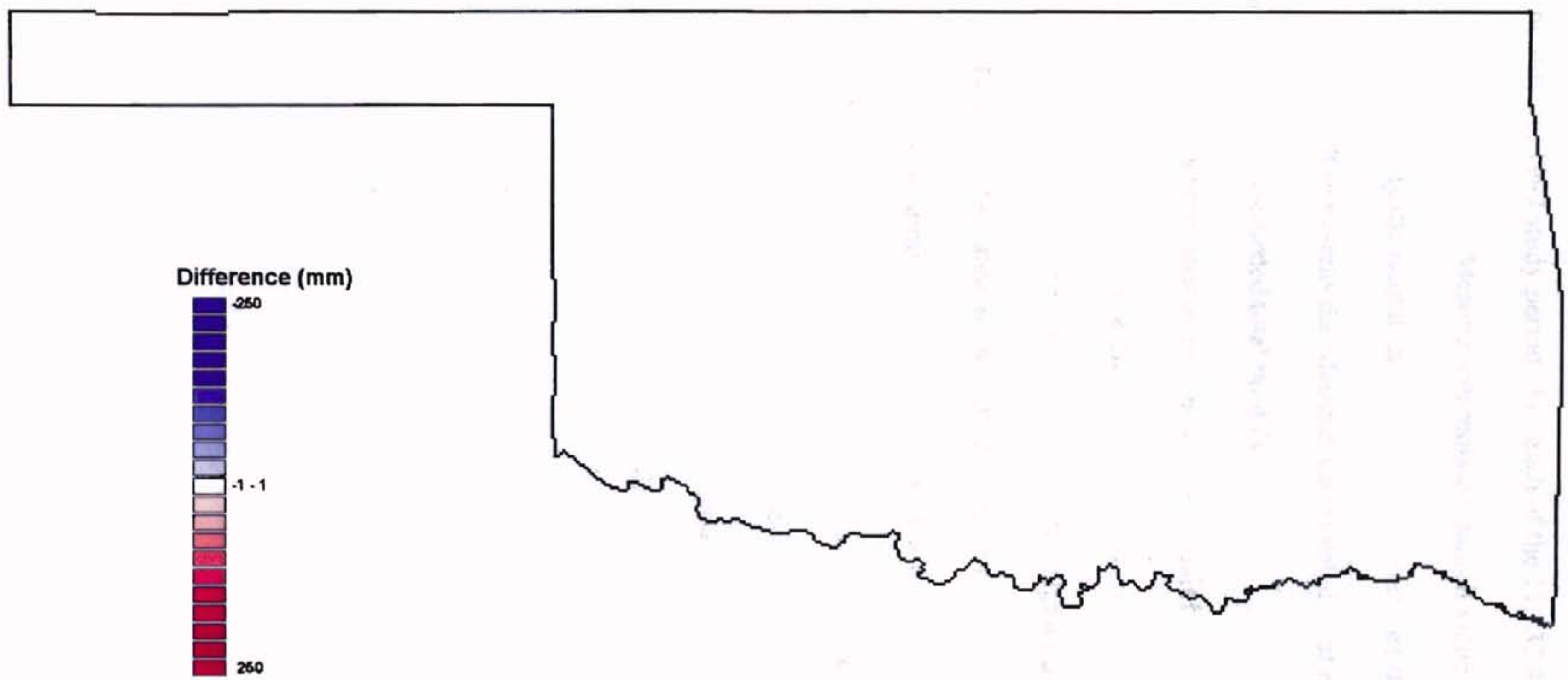

Figure 4.27: Difference in Radar and Mesonet Rainfall (mm) for July 16, 1997 - 1 Hour from 11 UTC to 12 UTC. Difference = Radar Rainfall – Mesonet Rainfall. Positive values indicate greater Radar estimated rainfall. Negative values indicate greater Mesonet estimated rainfall.

July 16, 1997 - 6 Hour Rainfall Estimate. The 6-hour estimate covers from 6 UTC to 12 UTC of the July 16, 1997 study period. For each of the 11,132 4x4 kilometer cells in the study area, an ABRFC and a Mesonet interpolated rainfall value was obtained. Each cell is color-coded according the rainfall amount and the results are displayed in Figure 4.28. Map A of Figure 4.28 represents the Mesonet-interpolated total rainfall while Map B represents the ABRFC estimated total rainfall.

Both estimates agree that there was little or no rainfall for most of the study area. The ABRFC estimate indicated a rainfall event near the mouth of the panhandle with small patches of rainfall exceeding 15 mm of rainfall. Although the Mesonet estimate does indicate rainfall in this area, it only indicates light rainfall (< 5 mm). This instance is repeated for the small rainfall event indicated by the ABRFC estimate in the north central portion of the study area. The Mesonet estimate indicates widespread, extremely light rainfall that is not indicated by the ABRFC estimate.

The correlation (r) between the Mesonet and ABRFC estimate was 0.396 (correlation is significant at the 0.01 level – 2 tailed). Table 4.14 lists some basic statistics for both estimates.

Figure 4.29 illustrates the differences between the rainfall estimates and where those differences occur. There is very little difference between the rainfall estimates across the study area. The widespread, extremely light rainfall indicated by the Mesonet estimate, did not differ from the ABRFC estimate by more than 1 mm. Therefore, no areas of greater Mesonet estimated rainfall are present. There are areas of greater ABRFC estimated rainfall (red) corresponding with the two rainfall events near the north central border and the mouth of the panhandle.

Figure 4.28: Estimated rainfall for July 16, 1997 (6 Hour from 6 UTC to 12 UTC). Map A – Rainfall estimate from interpolated Mesonet data. Map B – Rainfall estimate from ABRFC Stage III radar rainfall data.

Map A

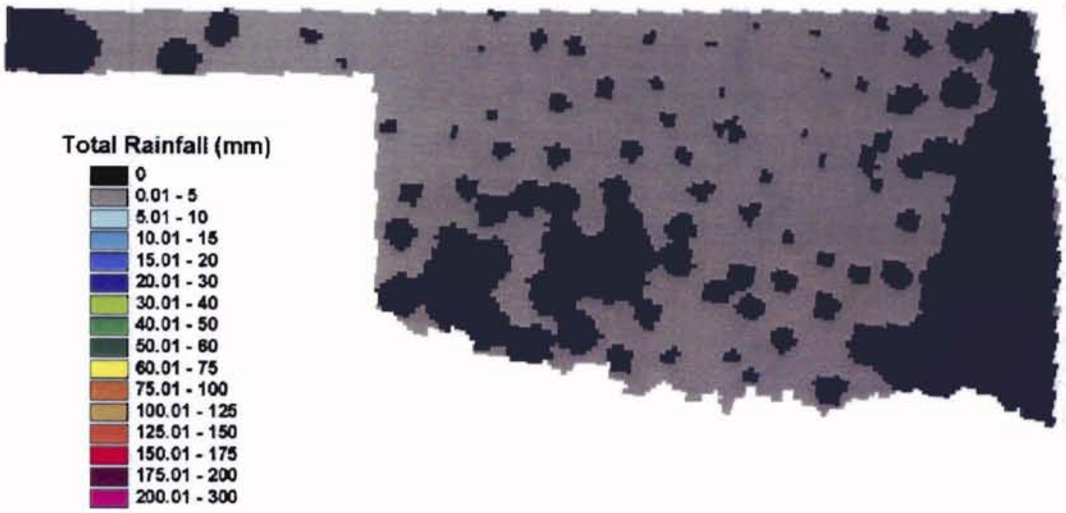

Map B

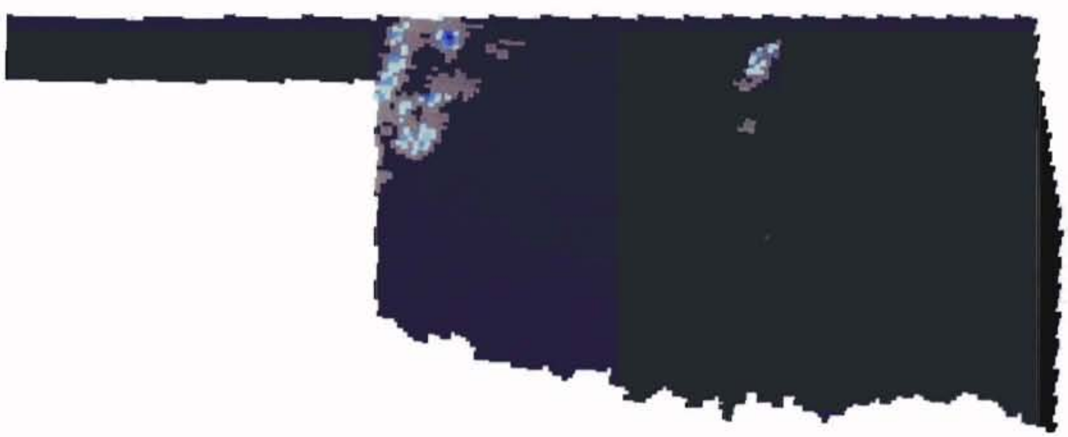

Table 4.14: July 16, 1997
6 Hour (6 UTC to 12 UTC)

Method	Min (mm)	Max (mm)	Mean (mm)	Standard Deviation (mm)	Volume (m3)
ABRFC	0	21	0.13	1.01	23,261,427
MESONET	0	1	0.02	0.06	3,562,240

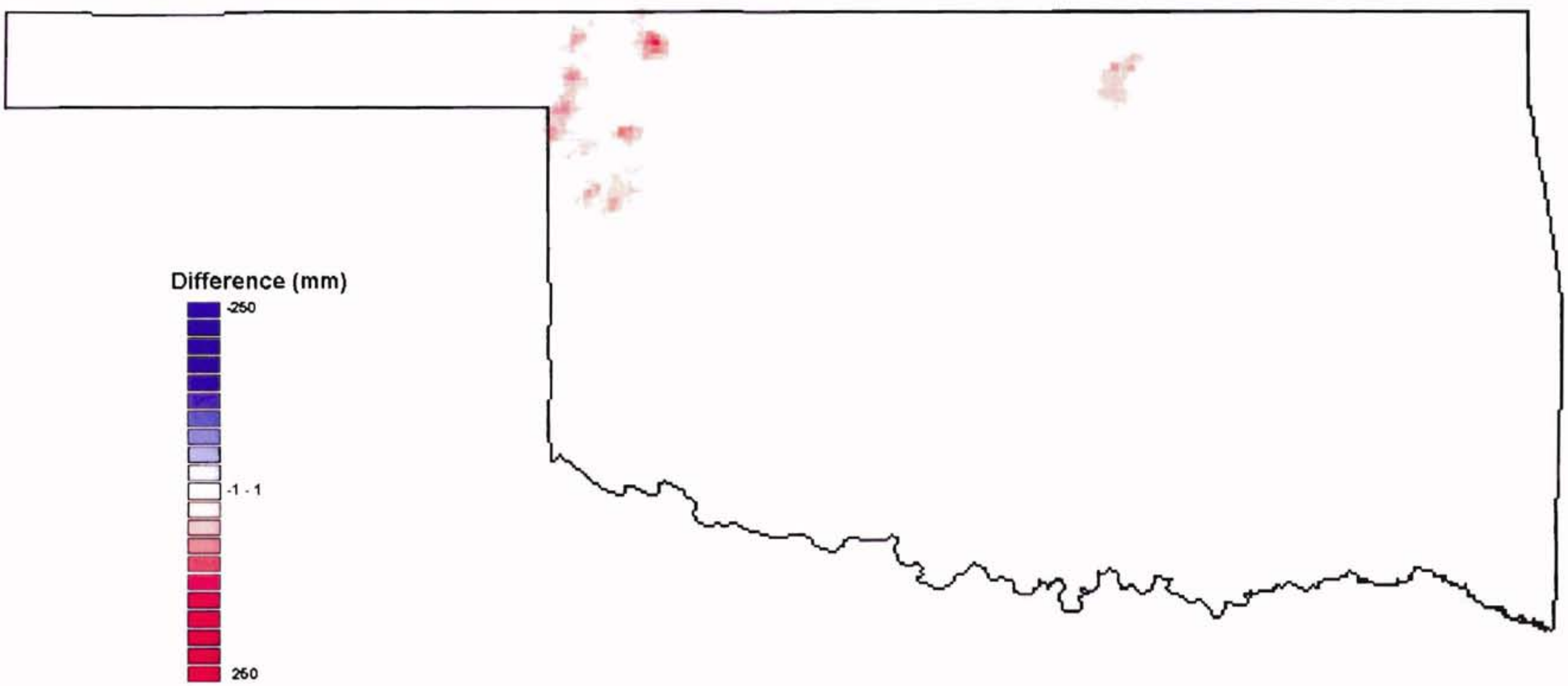

Figure 4.29 Difference in Radar and Mesonet Rainfall (mm) for July 16, 1997 - 6 Hour from 6 UTC to 12 UTC. Difference = Radar Rainfall – Mesonet Rainfall. Positive values indicate greater Radar estimated rainfall. Negative values indicate greater Mesonet estimated rainfall.

July 16, 1997 - 24 Hour Rainfall Estimate. The 24-hour estimate covers the entire July 16, 1997 study period from July 15, 1997 12 UTC to July 16, 1997 12 UTC. For each of the 11,132 4x4 kilometer cells in the study area, an ABRFC and a Mesonet interpolated rainfall value was obtained. Each cell is color-coded according the rainfall amount and the results are displayed in Figure 4.30. Map A of Figure 4.30 represents the Mesonet-interpolated total rainfall while Map B represents the ABRFC estimated total rainfall.

There appears to be little agreement between the estimates about where and in what amount rainfall is occurring across the study area. The Mesonet estimate indicates light rainfall for the entire state while the ABRFC indicates light rainfall only around concentrated rainfall events. The ABRFC estimate indicates widespread patches of concentrated rainfall occurring across the study area. Although the Mesonet estimate indicates heavy rainfall in areas corresponding with the ABRFC estimate, the spatial description of the rainfall events are a very different. The Mesonet indicates only light rainfall (<5 mm) in the northwest quarter and the panhandle while the ABRFC estimate indicates several heavy rainfall events across this area.

The correlation (*r*) between the Mesonet and ABRFC estimate was 0.454 (correlation is significant at the 0.01 level – 2 tailed). Table 4.15 lists some basic statistics for both estimates.

Figure 4.31 illustrates the differences between the rainfall estimates and where those differences occur. There is a large of amount of difference between the two rainfall estimates. Areas of greater ABRFC estimated rainfall (red) correspond with the heavy rainfall events indicated in the ABRFC rainfall estimate and usually shaded in dark red

Figure 4.30: Estimated rainfall for July 16, 1997 (24 Hour from 12 UTC to 12 UTC). Map A – Rainfall estimate from interpolated Mesonet data. Map B – Rainfall estimate from ABRFC Stage III radar rainfall data.

Map A

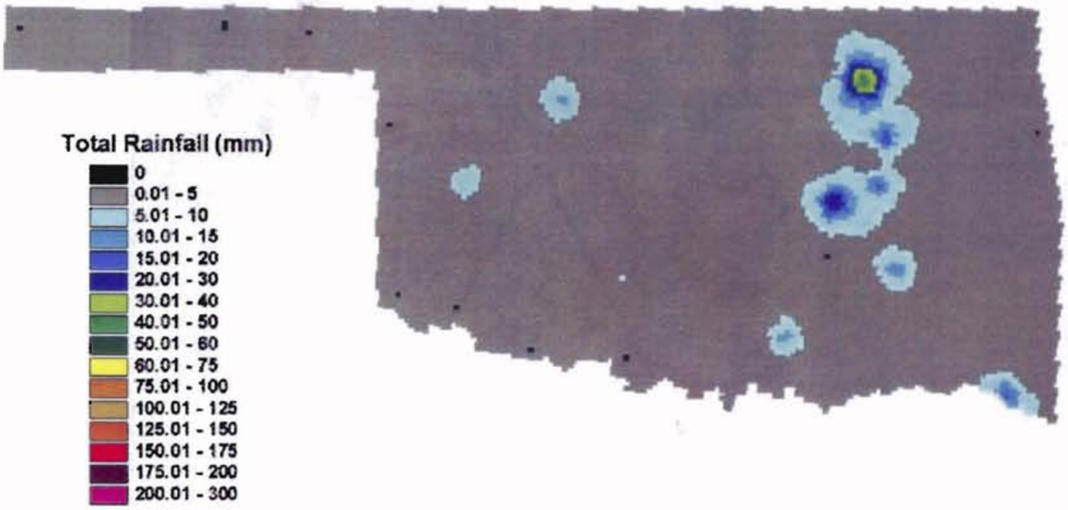

Map B

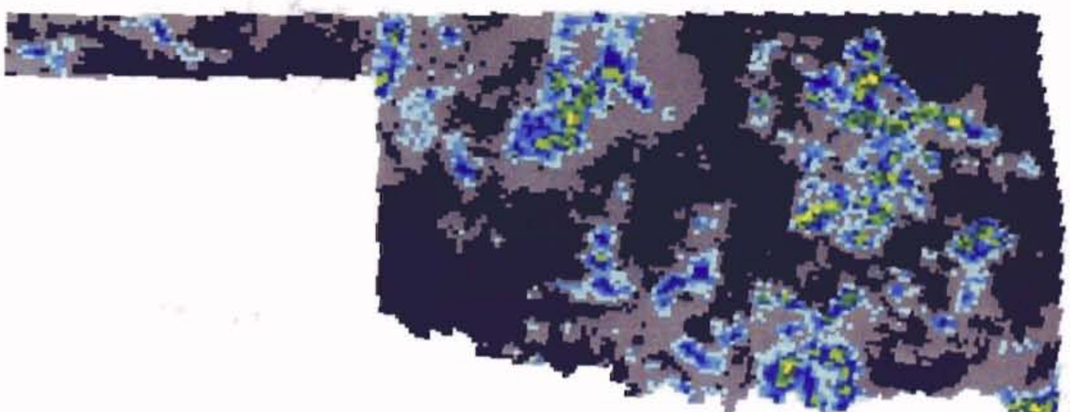

Table 4.15: July 16, 1997
24 Hour (12 UTC to 12 UTC)

Method	Min (mm)	Max (mm)	Mean (mm)	Standard Deviation (mm)	Volume (m3)
ABRFC	0	87	4.40	9.24	784,031,213
MESONET	0	49	1.92	2.87	342,206,586

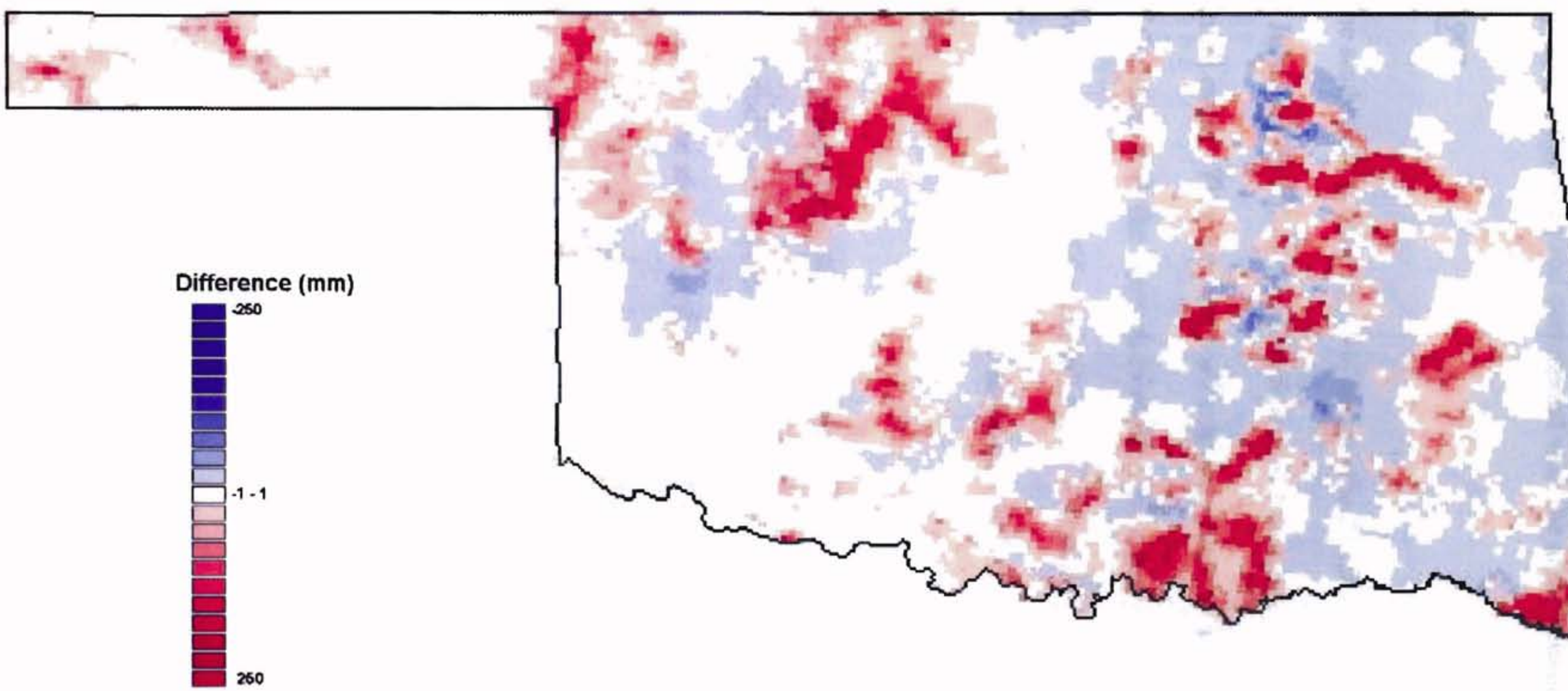

Figure 4.31: Difference in Radar and Mesonet Rainfall (mm) for July 16, 1997 - 24 Hour from 12 UTC to 12 UTC. Difference = Radar Rainfall – Mesonet Rainfall. Positive values indicate greater Radar estimated rainfall. Negative values indicate greater Mesonet estimated rainfall.

(large difference). Areas of greater Mesonet estimated rainfall are mostly lighter shades of blue (smaller difference) and correspond with the areas between heavy rainfall events.

July 18, 1997

The study date of July 18, 1997 covers the 24 hours between July 17, 1997 12 UTC and July 18, 1997 12 UTC. This date was characterized by a single, extremely heavy rainfall event. This event was widespread, covering almost the whole northeast quarter of the state, with the heaviest rainfall in the center and gradually decreasing rainfall towards the edges of the rainfall event. Rainfall estimates were collected for the last hour (11 UTC - 12 UTC), the last six hours (6 UTC - 12 UTC), and the entire 24-hour period.

July 18, 1997 - 1Hour Rainfall Estimate. The 1-hour estimate covers the last hour of the July 18, 1997 study period from 11 UTC to 12 UTC. For each of the 11,132 4x4 kilometer cells in the study area, an ABRFC and a Mesonet interpolated rainfall value were obtained. Each cell is color-coded according the rainfall amount and the results are displayed in Figure 4.32. Map A of Figure 4.32 represents the Mesonet-interpolated total rainfall while Map B represents the ABRFC estimated total rainfall.

The spatial description of rainfall is similar for both estimates. The Mesonet estimate indicates widespread, extremely light rainfall for the entire state but the difference between the two estimates in these areas is very low. The Mesonet estimate agrees with the ABRFC estimate that there is a heavy rainfall event in the center of the study area. The Mesonet estimate also describes the small rainfall event in the extreme southwestern corner of the study area.

Figure 4.32: Estimated rainfall for July 18, 1997 (1 Hour from 11 UTC to 12 UTC). Map A – Rainfall estimate from interpolated Mesonet data. Map B – Rainfall estimate from ABRFC Stage III radar rainfall data.

Map A

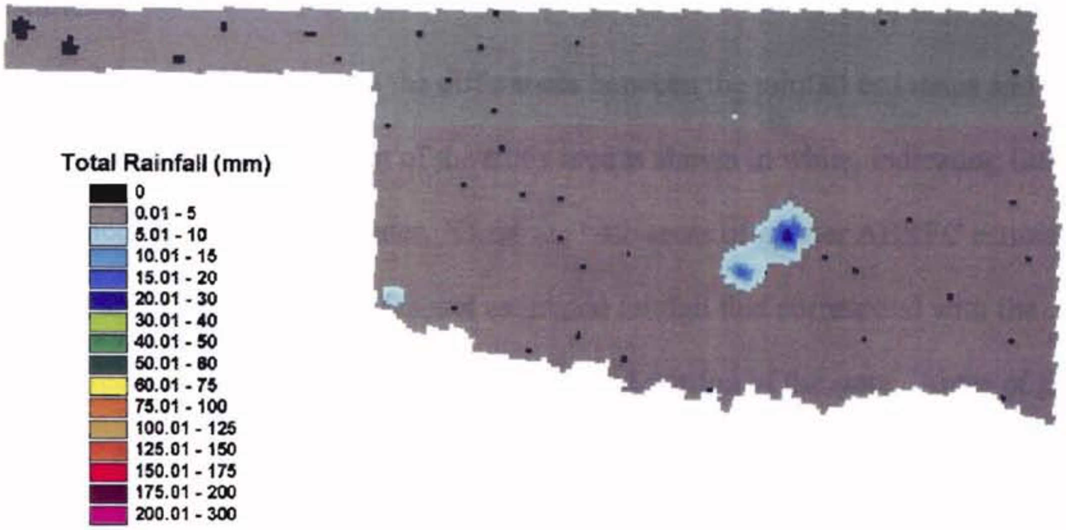

Map B

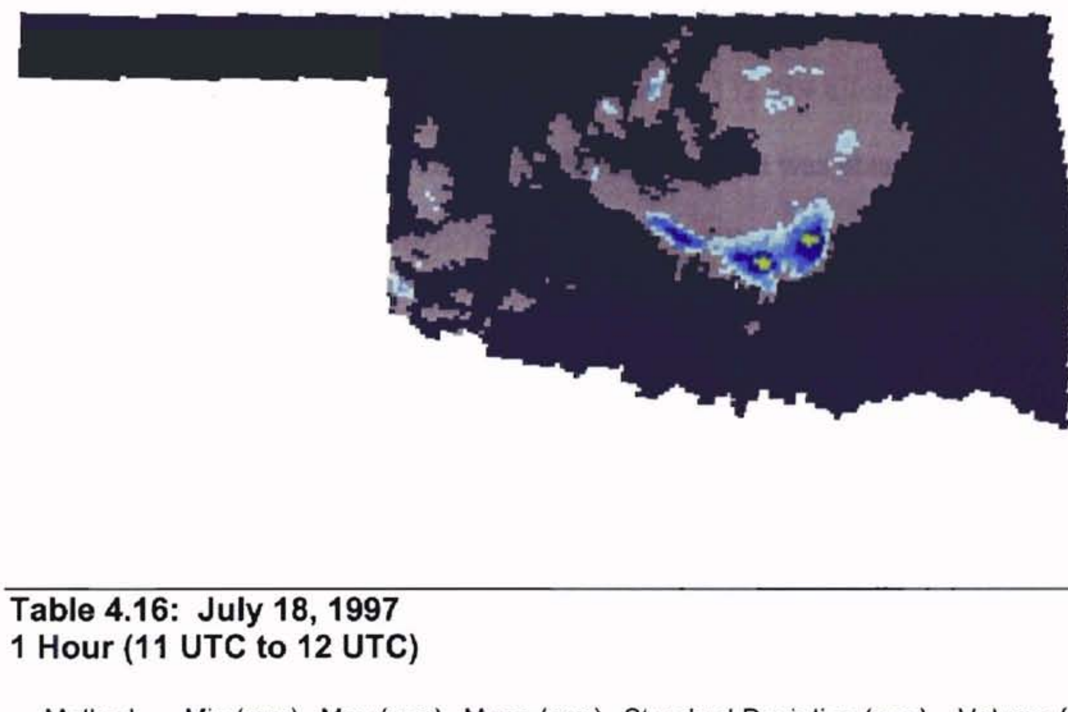

Table 4.16: July 18, 1997
1 Hour (11 UTC to 12 UTC)

Method	Min (mm)	Max (mm)	Mean (mm)	Standard Deviation (mm)	Volume (m3)
ABRFC	0	36	0.70	2.74	124,393,421
MESONET	0	24	0.76	1.41	135,774,778

The correlation (r) between the Mesonet and ABRFC estimate was 0.728 (correlation is significant at the 0.01 level – 2 tailed). Table 4.16 lists some basic statistics for both

estimates.

Figure 4.33 illustrates the differences between the rainfall estimates and where those differences occur. Most of the study area is shown in white, indicating little or no difference between the estimates. There are both areas of greater ABRFC estimated rainfall and areas of greater Mesonet estimated rainfall that correspond with the widespread rainfall event occurring in the central portion of the state. Areas of greater ABRFC estimated rainfall (red) correspond with heavy rainfall while areas of greater Mesonet estimated rainfall correspond with the surrounding lighter rainfall areas.

<u>July 18, 1997 - 6 Hour Rainfall Estimate</u>. The 6-hour estimate covers 6 UTC to 12 UTC of the July 18, 1997 study period. For each of the 11,132 4x4 kilometer cells in the study area, an ABRFC and a Mesonet interpolated rainfall value was obtained. Each cell is color-coded according the rainfall amount and the results are displayed in Figure 4.34. Map A of Figure 4.34 represents the Mesonet-interpolated total rainfall while Map B represents the ABRFC estimated total rainfall.

The spatial description of rainfall is similar for both rainfall estimates. Both estimates describe the concentrated, heavy rainfall event occurring in the center of the study area. The description of the size and scope of the rainfall event is similar in both estimates. Both estimates describe a heavy rainfall event along the western edge of the study area but describe the event differently. The Mesonet estimate describes an event with extremely heavy rainfall (>150 mm) while the ABRFC estimate indicates a

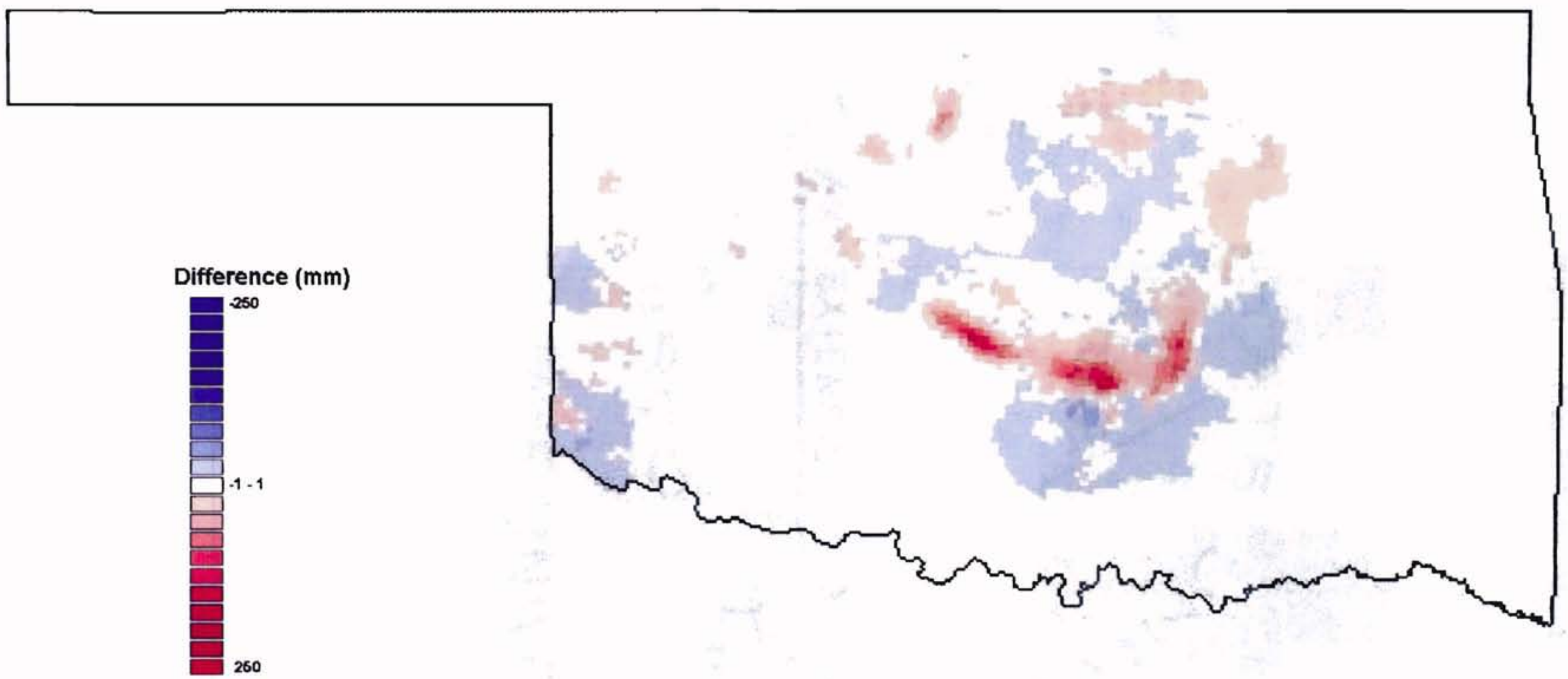

Figure 4.33: Difference in Radar and Mesonet Rainfall (mm) for July 18, 1997 - 1 Hour from 11 UTC to 12 UTC. Difference = Radar Rainfall – Mesonet Rainfall. Positive values indicate greater Radar estimated rainfall. Negative values indicate greater Mesonet estimated rainfall.

Figure 4.34: Estimated rainfall for July 18, 1997 (6 Hour from 6 UTC to 12 UTC). Map A – Rainfall estimate from interpolated Mesonet data. Map B – Rainfall estimate from ABRFC Stage III radar rainfall data.

Map A

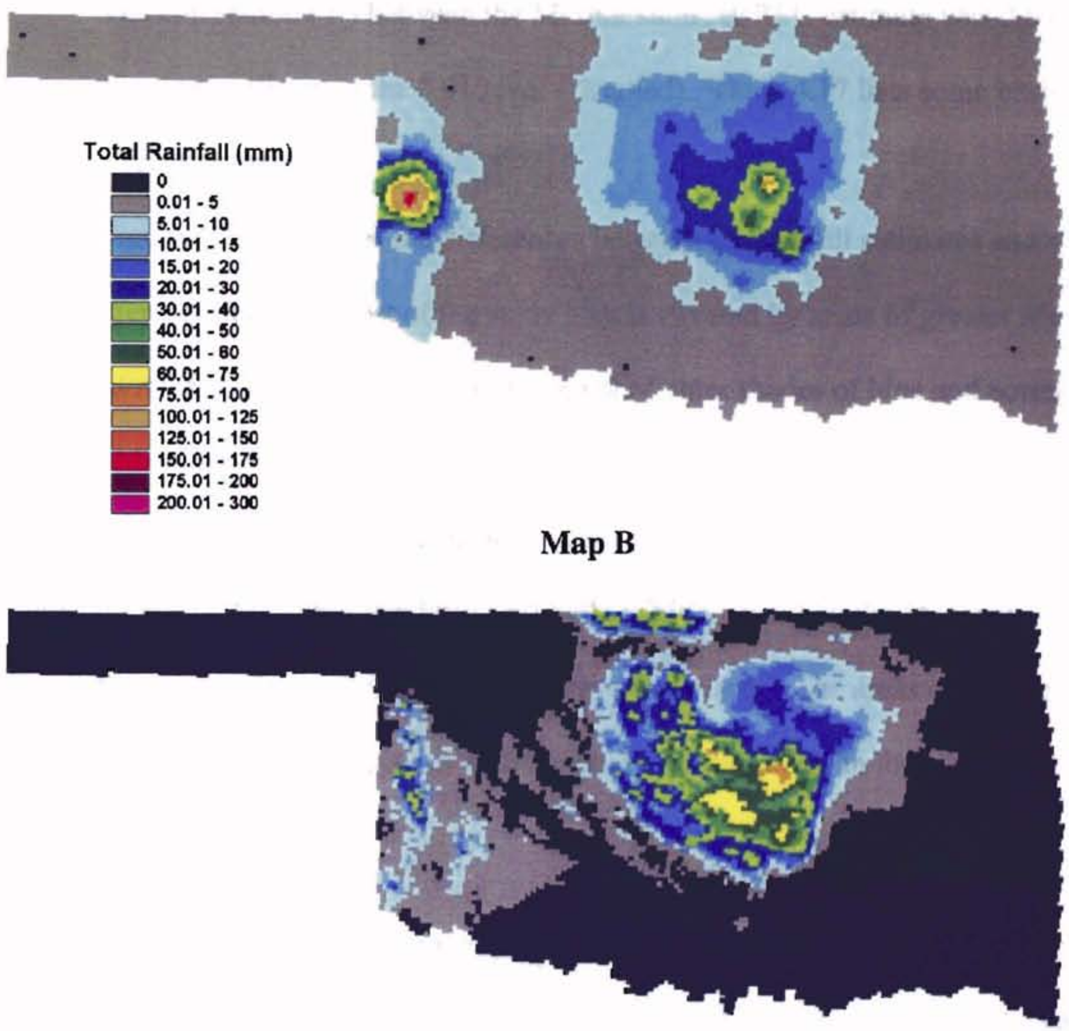

Table 4.17: July 18, 1997
6 Hour (6 UTC to 12 UTC)

Method	Min (mm)	Max (mm)	Mean (mm)	Standard Deviation (mm)	Volume (m3)
ABRFC	0	88	5.42	12.39	965,562,963
MESONET	0	158	6.37	10.55	1,135,036,531

maximum of only 30-40 mm of rainfall for this event. The Mesonet also indicates light rainfall for the remainder of the study area while the ABRFC estimate indicates light rainfall only around the heavy rainfall events and no rainfall for the rest of the study area.

The correlation (r) between the Mesonet and ABRFC estimate was 0.646 (correlation is significant at the 0.01 level – 2 tailed). Table 4.17 lists some basic statistics for both estimates.

Figure 4.35 illustrates the differences between the rainfall estimates and where those differences occur. Most of the study area is covered by areas of greater Mesonet estimated rainfall (blue). These areas are mostly lighter shades of blue and correspond with the Mesonet estimated light rainfall for most of the study area. The area of greater Mesonet estimated rainfall (dark shade of blue) along the western edge of the state corresponds with the extremely heavy rainfall event indicated by the Mesonet estimate. The difference in this area exceeds 150 mm in some places. The areas of greater ABRFC estimated rainfall (red) correspond with the heavy rainfall event in the central portion of the study area.

July 18, 1997 - 24 Hour Rainfall Estimate. The 24-hour estimate covers the study period from July 17, 1997 12 UTC to July 18, 1997 12 UTC. For each of the 11,132 4x4 kilometer cells in the study area, an ABRFC and a Mesonet interpolated rainfall value was obtained. Each cell is color-coded according the rainfall amount and the results are displayed in Figure 4.36. Map A of Figure 4.36 represents the Mesonet-interpolated total rainfall while Map B represents the ABRFC estimated total rainfall.

The spatial description of rainfall is similar for both rainfall estimates. Both estimates describe the concentrated, heavy rainfall event occurring in the center of the

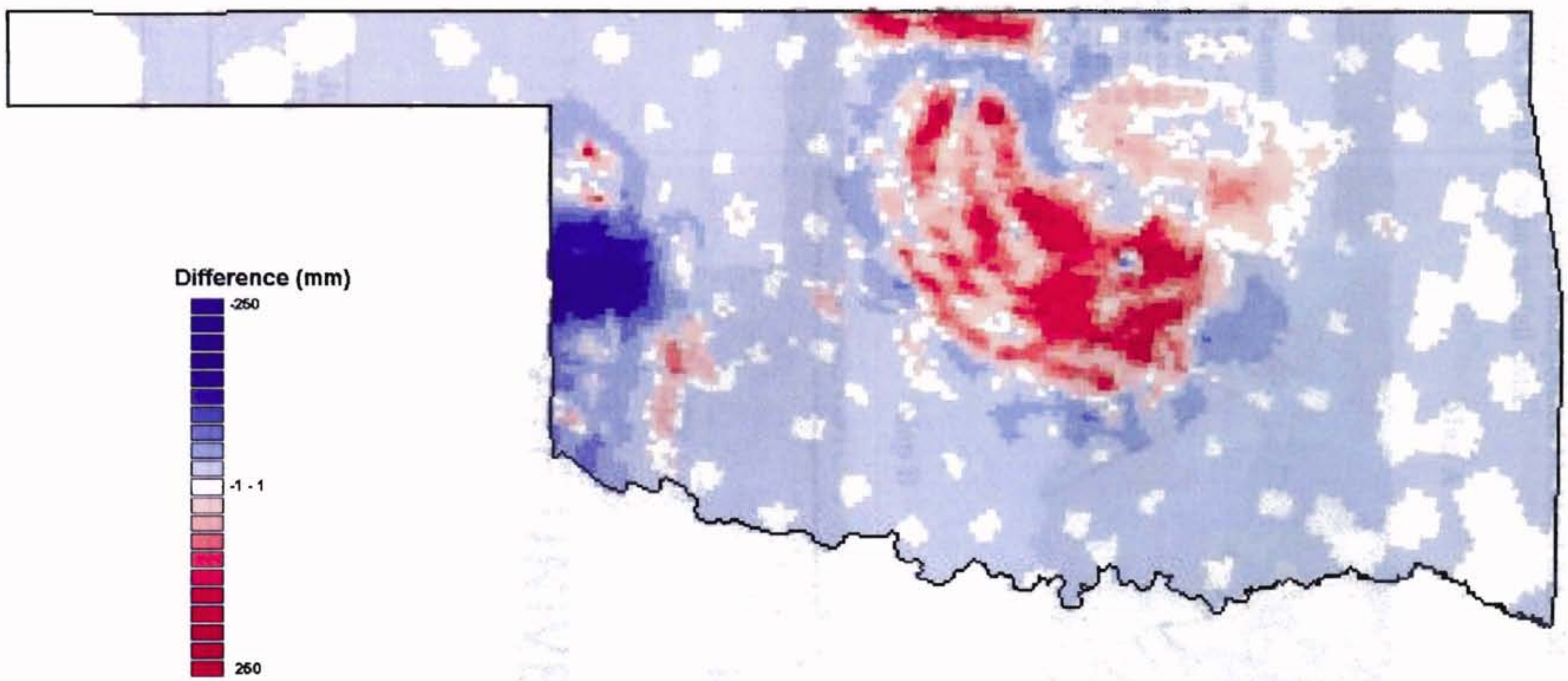

Figure 4.35: Difference in Radar and Mesonet Rainfall (mm) for July 18, 1997 - 6 Hour from 6 UTC to 12 UTC. Difference = Radar Rainfall – Mesonet Rainfall. Positive values indicate greater Radar estimated rainfall. Negative values indicate greater Mesonet estimated rainfall.

Figure 4.36: Estimated rainfall for July 18, 1997 (24 Hour from 12 UTC to 12 UTC). Map A – Rainfall estimate from interpolated Mesonet data. Map B – Rainfall estimate from ABRFC Stage III radar rainfall data.

Map A

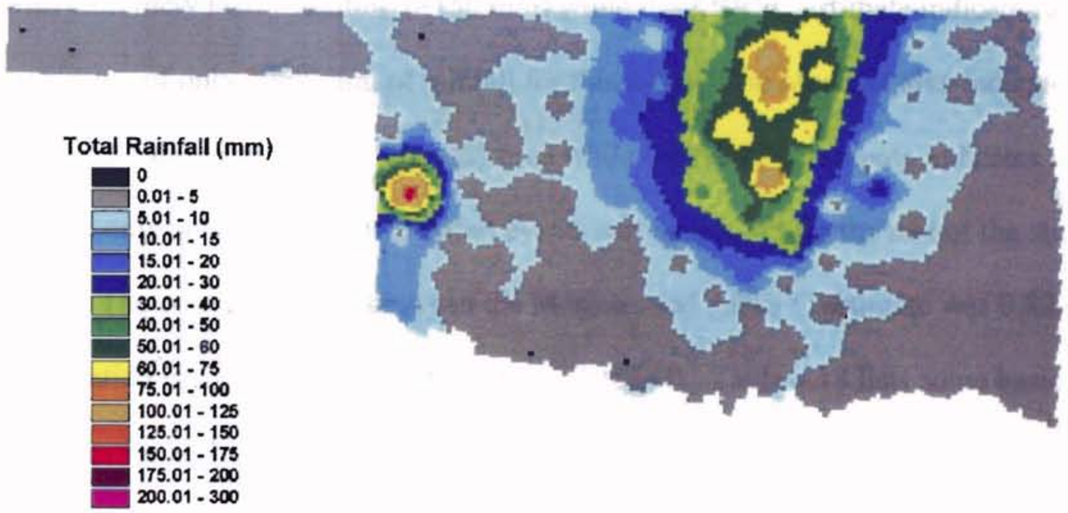

Map B

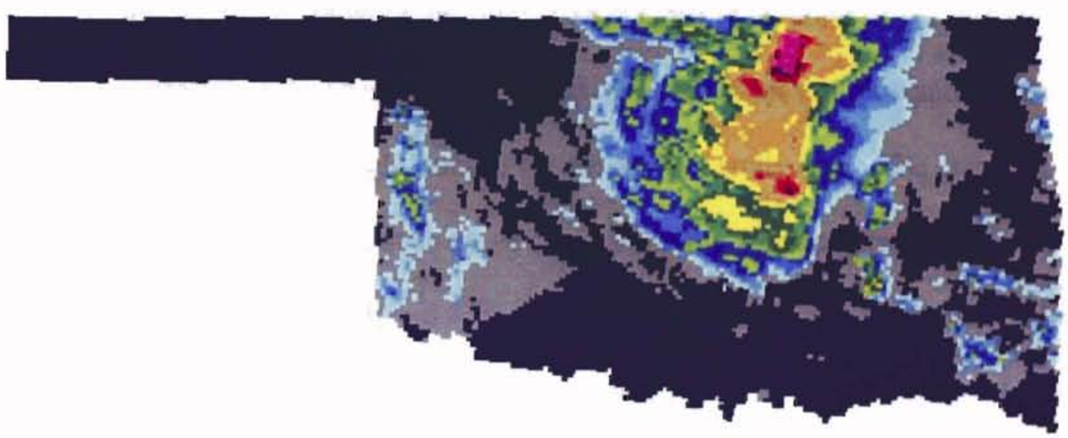

Table 4.18: July 18, 1997
24 Hour (12 UTC to 12 UTC)

Method	Min (mm)	Max (mm)	Mean (mm)	Standard Deviation (mm)	Volume (m3)
ABRFC	0	275	12.51	27.94	2,227,433,050
MESONET	0	158	12.69	18.04	2,259,956,301

study area. The description of the size and scope of the rainfall event is similar in both estimates. Both estimates describe a heavy rainfall event along the western edge of the study area but describe the event differently. The Mesonet estimate describes an event with extremely heavy rainfall (>150 mm) while the ABRFC estimate indicates a maximum of only 30-40 mm of rainfall for this event. The Mesonet also indicates light rainfall for the remainder of the study area while the ABRFC estimate indicates light rainfall only around the heavy rainfall events and no rainfall for the rest of the study area.

The correlation (r) between the Mesonet and ABRFC estimate was 0.823 (correlation is significant at the 0.01 level – 2 tailed). Table 4.18 lists some basic statistics for both estimates.

Figure 4.37 illustrates the differences between the rainfall estimates and where those differences occur. Most of the study area is covered by areas of greater Mesonet estimated rainfall (blue). These areas are mostly lighter shades of blue and correspond with the Mesonet estimated light rainfall for most of the study area. The area of greater Mesonet estimated rainfall (dark shade of blue) along the western edge of the state corresponds with the extremely heavy rainfall event indicated by the Mesonet estimate. The difference in this area exceeds 150 mm in some places. The areas of greater ABRFC estimated rainfall (red) correspond with the heavy rainfall event in the central portion of the study area.

<u>August 13, 1997</u>

The study date of August 13, 1997 covers the 24 hours between August 12, 1997 12 UTC and August 13, 1997 12 UTC. This date was characterized by widespread areas

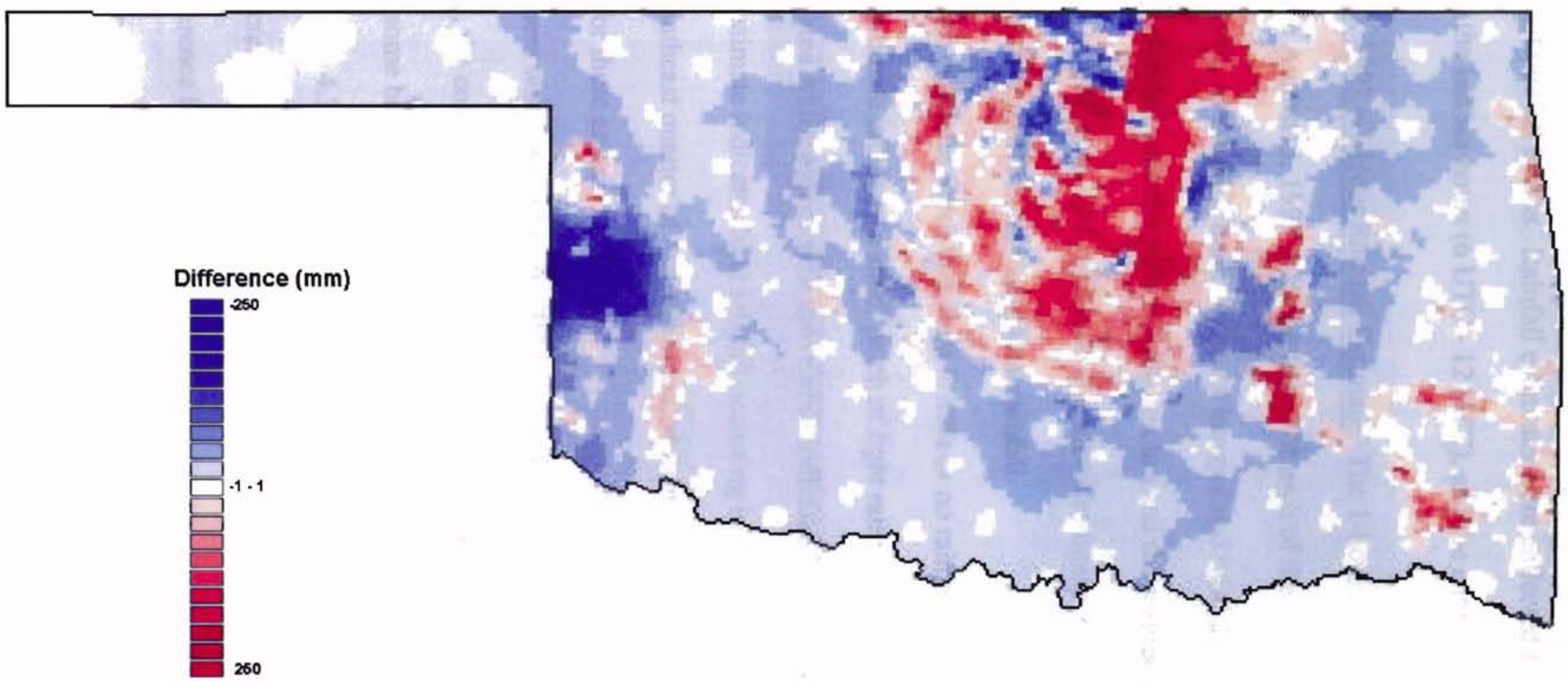

Figure 4.37: Difference in Radar and Mesonet Rainfall (mm) for July 18, 1997 - 24 Hour from 12 UTC to 12 UTC. Difference = Radar Rainfall – Mesonet Rainfall. Positive values indicate greater Radar estimated rainfall. Negative values indicate greater Mesonet estimated rainfall.

of light to moderate rainfall. Changes in rainfall amount were gradual from the center to the edges of rainfall events. Rainfall estimates were collected for the last hour (11 UTC - 12 UTC), the last six hours (6 UTC - 12 UTC), and the entire 24-hour period.

August 13, 1997 – 1 Hour Rainfall Estimate. The 1-hour estimate covers 11 UTC to 12 UTC of the August13, 1997 study period, For each of the 11,132 4x4 kilometer cells in the study area, an ABRFC and a Mesonet interpolated rainfall value was obtained. Each cell is color-coded according the rainfall amount and the results are displayed in Figure 4.38. Map A of Figure 4.38 represents the Mesonet-interpolated total rainfall while Map B represents the ABRFC estimated total rainfall

Both estimates agree that there is little or no rainfall for the entire study area. The Mesonet estimate indicates a small patch of light rainfall in the western central portion of the study area which agrees with the rainfall indicated by the ABRFC estimate. The ABRFC estimate indicates light rainfall occurring in isolated patches in the panhandle and the southeast quarter of the study area while no rainfall is indicated by the Mesonet estimate for these areas.

There was very little rainfall indicated in either the Mesonet or ABRFC estimate. Therefore, the correlation between the Mesonet and ABRFC estimate was zero. Table 4.19 lists some basic statistics for both estimates.

Figure 4.39 illustrates the differences between the rainfall estimates and where those differences occur. The majority of the study area is shown in white, indicating little or no difference between the rainfall estimates in these areas. There are no areas of greater Mesonet estimated rainfall (blue) and only a few patches of greater ABRFC estimated rainfall (red).

Figure 4.38: Estimated rainfall for August 13, 1997 (1 Hour from 11 UTC to 12 UTC). Map A – Rainfall estimate from interpolated Mesonet data. Map B – Rainfall estimate from ABRFC Stage III radar rainfall data.

Map A

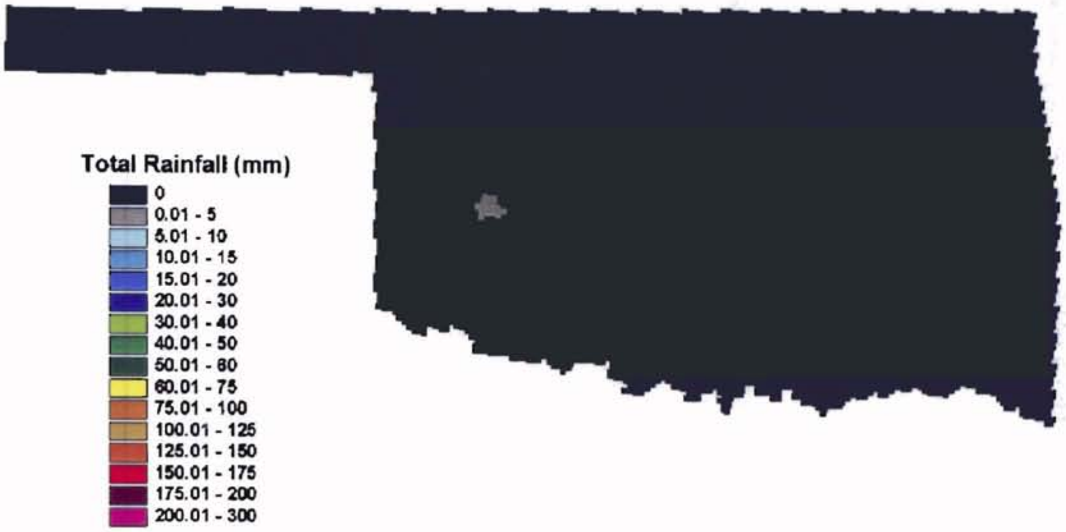

Map B

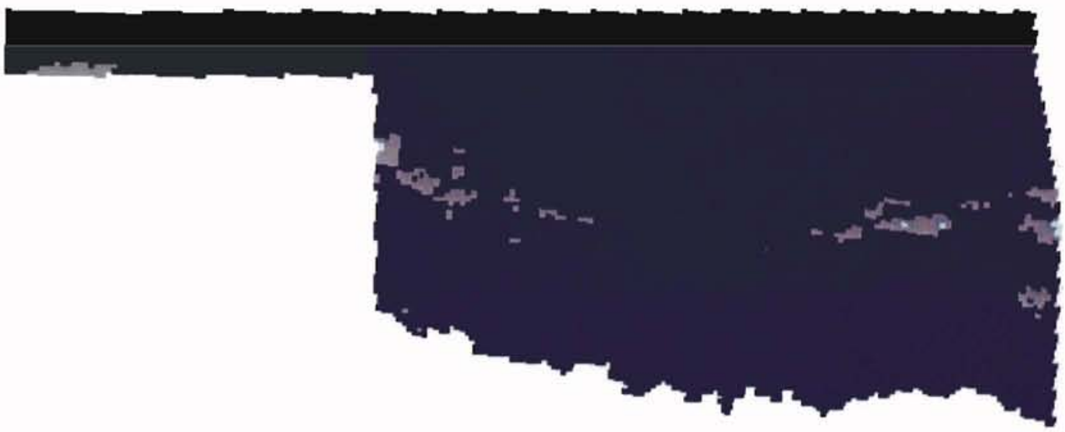

Table 4.19: August 13, 1997
1 Hour (11 UTC to 12 UTC)

Method	Min (mm)	Max (mm)	Mean (mm)	Standard Deviation (mm)	Volume (m3)
ABRFC	0.00	7.27	0.03	0.27	5,532,159
MESONET	0.00	0.01	0.00	0.00	3,519

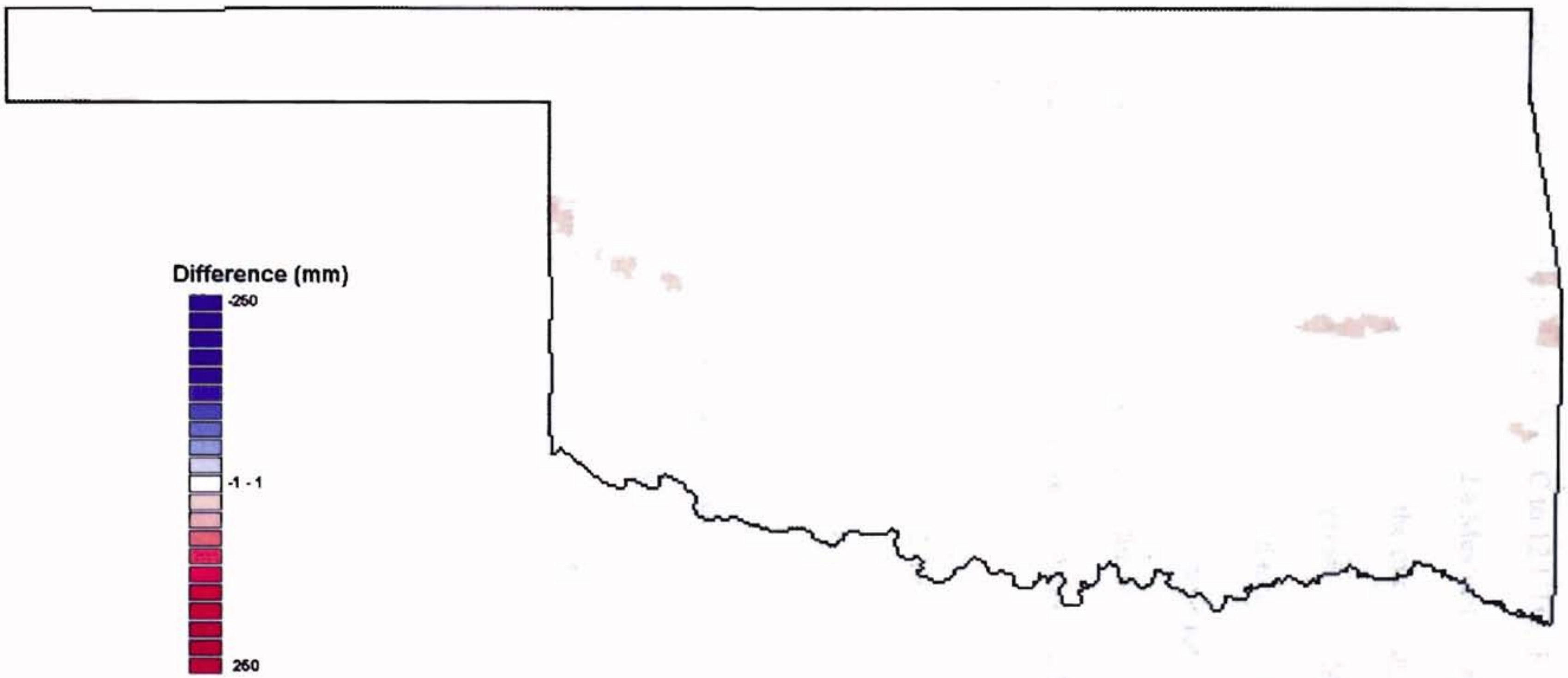

Figure 4.39: Difference in Radar and Mesonet Rainfall (mm) for August 13, 1997 - 1 Hour from 11 UTC to 12 UTC. Difference = Radar Rainfall – Mesonet Rainfall. Positive values indicate greater Radar estimated rainfall. Negative values indicate greater Mesonet estimated rainfall.

August 13, 1997 - 6 Hour Rainfall Estimate. The 6-hour estimate covers the last 6 hours of the August 13, 1997 study period from 6 UTC to 12 UTC. For each of the 11,132 4x4 kilometer cells in the study area, an ABRFC and a Mesonet interpolated rainfall value was obtained. Each cell is color-coded according the rainfall amount and the results are displayed in Figure 4.40. Map A of Figure 4.40 represents the Mesonet-interpolated total rainfall while Map B represents the ABRFC estimated total rainfall.

Both estimates agree that there is little or no rainfall for most of the study area. Both estimates indicate a rainfall event occurring in the southeastern quarter of the state with patches moderate rainfall (5-15 mm). However, there is difference in how each estimate spatially describes this rainfall event.

The correlation (r) between the Mesonet and ABRFC estimate was 0.446 (correlation is significant at the 0.01 level – 2 tailed). Table 4.20 lists some basic statistics for both estimates.

Figure 4.41 illustrates the differences between the rainfall estimates and where those differences occur. The majority of the study area is shown in white, indicating little or no difference between the rainfall estimates in these areas. Besides the small area of greater ABRFC estimated rainfall along the western edge of the state, most of the difference corresponds with the rainfall event in the southeastern quarter of the study area. Although both estimates describe a similar rainfall event in the southeast quarter of the study area, they disagree in where the rainfall is occurring. Areas of greater ABRFC estimated rainfall (red) are localized and concentrated while areas of greater Mesonet estimated rainfall (blue) exhibit a smoother, more homogenous pattern.

Figure 4.40: Estimated rainfall for August 13, 1997 (6 Hour from 6 UTC to 12 UTC). Map A – Rainfall estimate from interpolated Mesonet data. Map B – Rainfall estimate from ABRFC Stage III radar rainfall data.

Map A

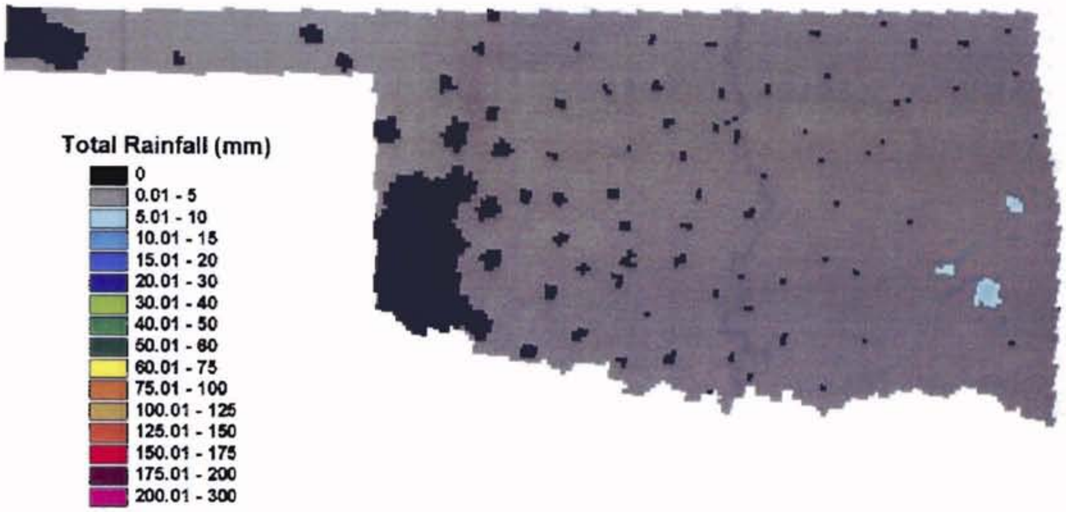

Map B

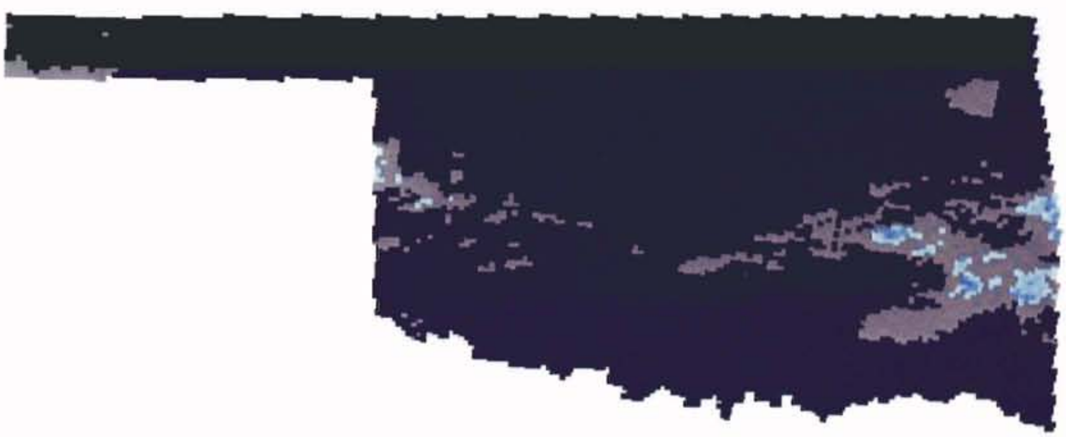

Table 4.20: August 13, 1997
6 Hour (6 UTC to 12 UTC)

Method	Min (mm)	Max (mm)	Mean (mm)	Standard Deviation (mm)	Volume (m3)
ABRFC	0	17	0.23	1.10	41,606,963
MESONET	0	7	0.24	0.64	42,265,978

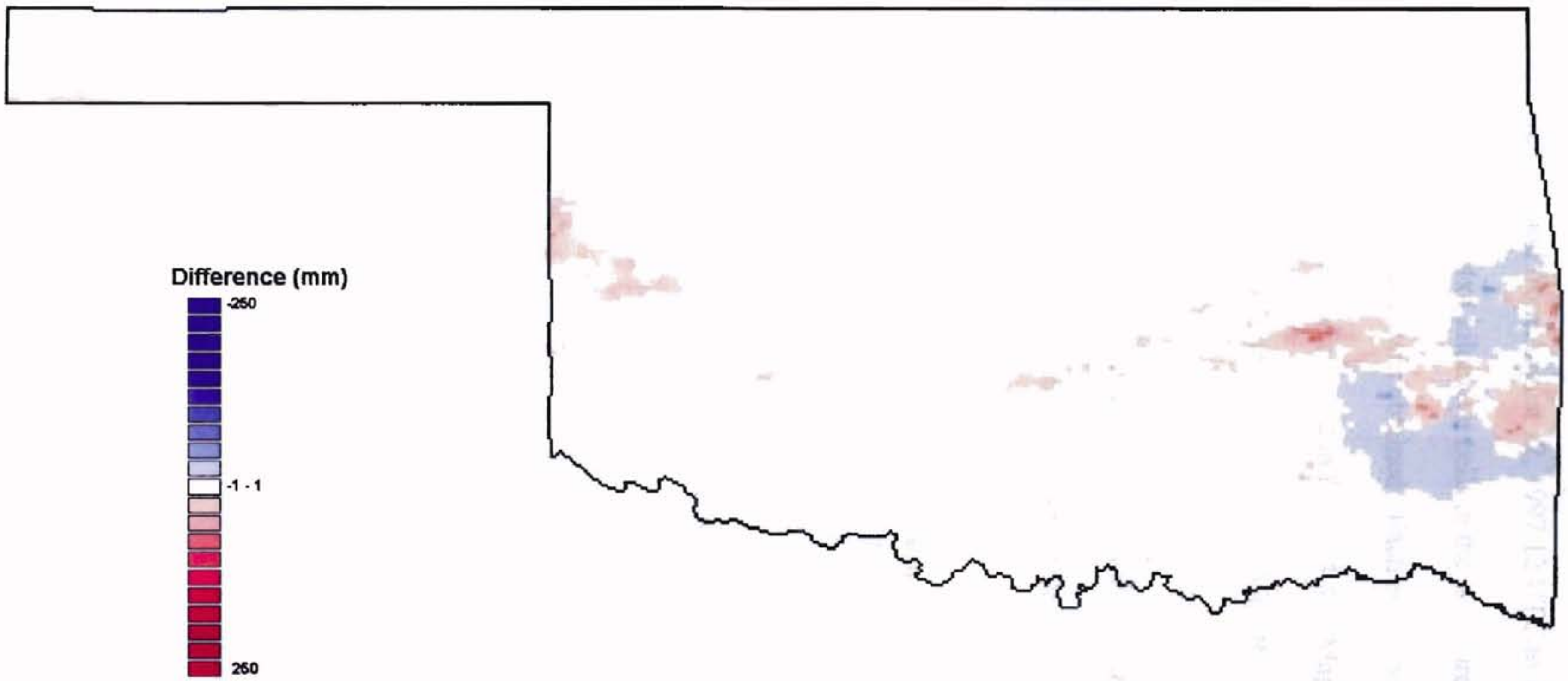

Figure 4.41: Difference in Radar and Mesonet Rainfall (mm) for August 13, 1997 - 6 Hour from 6 UTC to 12 UTC. Difference = Radar Rainfall – Mesonet Rainfall. Positive values indicate greater Radar estimated rainfall. Negative values indicate greater Mesonet estimated rainfall.

August 13, 1997 - 24 Hour Rainfall Estimate. The 24-hour estimate covers the entire August 13, 1997 study period from August 12, 1997 12 UTC to August 13, 1997 12 UTC. For each of the 11,132 4x4 kilometer cells in the study area, an ABRFC and a Mesonet interpolated rainfall value was obtained. Each cell is color-coded according the rainfall amount and the results are displayed in Figure 4.42. Map A of Figure 4.42 represents the Mesonet-interpolated total rainfall while Map B represents the ABRFC estimated total rainfall.

The description of rainfall is similar for both rainfall estimates. Both estimates describe a heavy rainfall event in the central portion of the state and the spatial description of this event is similar for both estimates. Light rainfall is indicated for the remainder of the study area. The Mesonet rainfall estimate shows light rainfall for the entire panhandle while the ABRFC estimate indicates almost no rainfall for the same area.

The correlation (r) between the Mesonet and ABRFC estimate was 0.785 (correlation is significant at the 0.01 level – 2 tailed). Table 4.21 lists some basic statistics for both estimates.

Figure 4.43 illustrates the differences between the rainfall estimates and where those differences occur. The difference map indicates widespread disagreement between the two rainfall estimates. However, where there is greater Mesonet estimated rainfall (blue) or greater ABRFC estimated rainfall (red), lighter color shades are dominant, indicating lower differences. Areas of greater ABRFC estimated rainfall (red) correspond with areas of concentrated rainfall. Areas of greater Mesonet estimated

Figure 4.42: Estimated rainfall for August 13, 1997 (24 Hour from 12 UTC to 12 UTC). Map A – Rainfall estimate from interpolated Mesonet data. Map B – Rainfall estimate from ABRFC Stage III radar rainfall data.

Map A

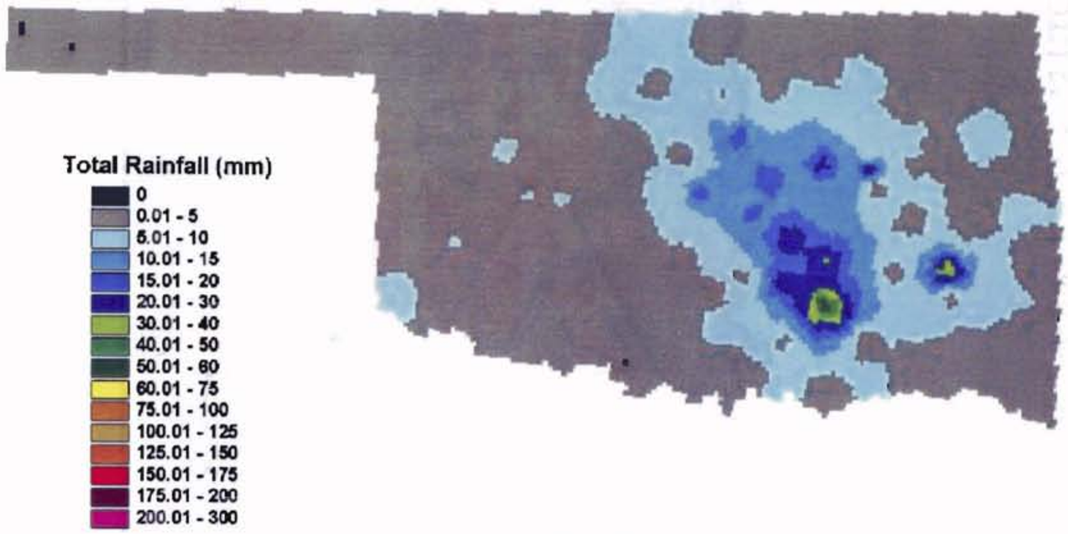

Map B

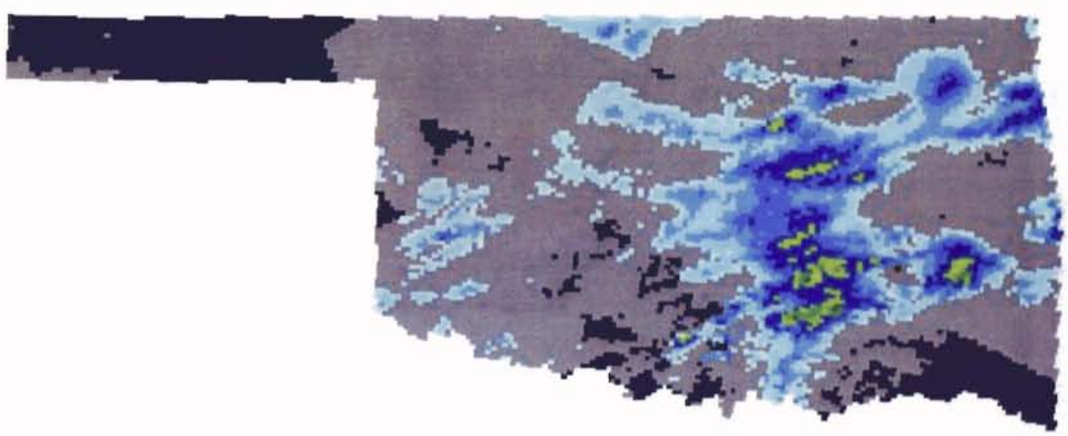

Table 4.21: August 13, 1997
24 Hour (12 UTC to 12 UTC)

Method	Min (mm)	Max (mm)	Mean (mm)	Standard Deviation (mm)	Volume (m3)
ABRFC	0	58	5.25	6.96	935,800,448
MESONET	0	58	5.12	4.91	911,880,006

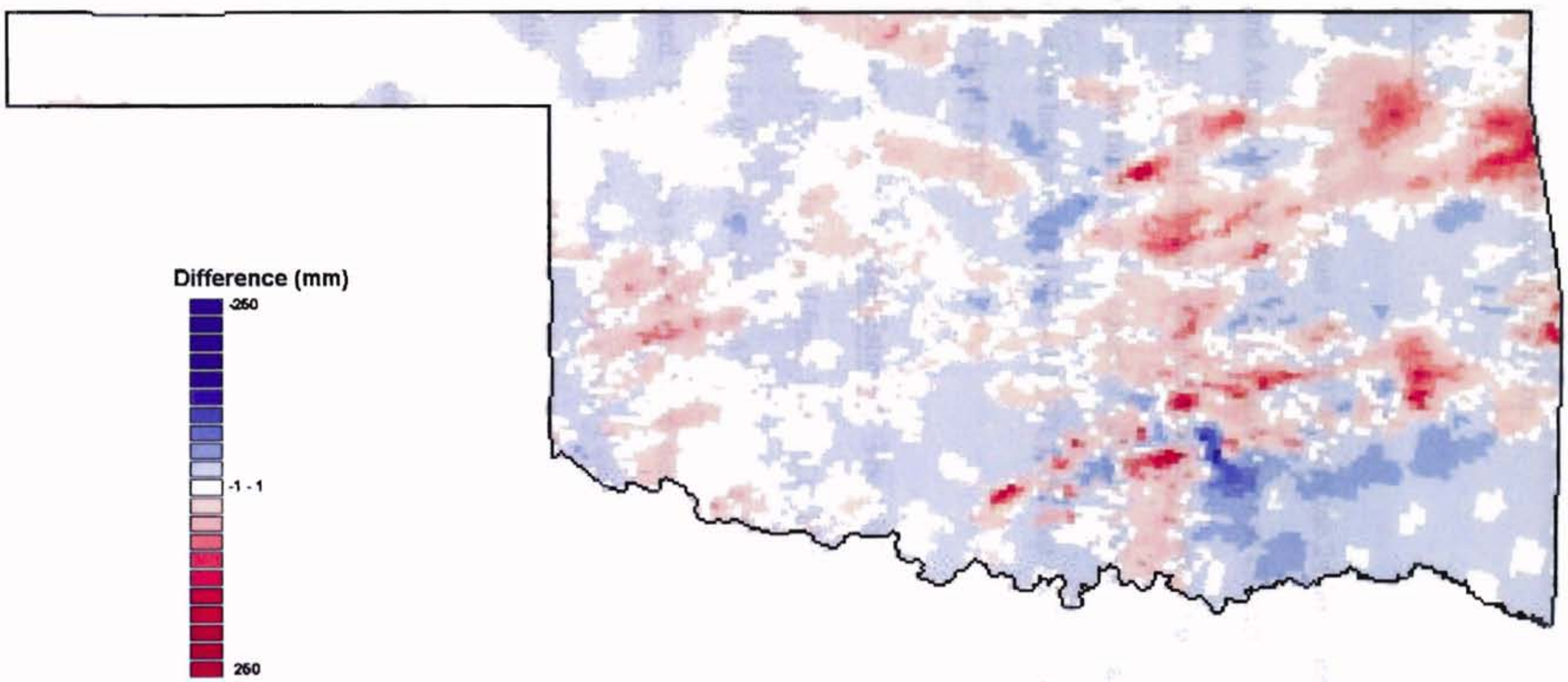

Figure 4.43: Difference in Radar and Mesonet Rainfall (mm) for August 13, 1997 - 24 Hour from 12 UTC to 12 UTC. Difference = Radar Rainfall – Mesonet Rainfall. Positive values indicate greater Radar estimated rainfall. Negative values indicate greater Mesonet estimated rainfall.

rainfall correspond with the areas between rainfall events or with areas of light rainfall and exhibit a smooth, homogenous pattern.

August 19, 1997

The study date of August 19, 1997 covers the 24 hours between August 18, 1997 12 UTC and August 19, 1997 12 UTC. This date was characterized by widespread, heavy rainfall. Rainfall amount changed gradually from areas of heavy rainfall at the center to moderate rainfall at the edges of rainfall events. Rainfall estimates were collected for the last hour (11 UTC - 12 UTC), the last six hours (6 UTC - 12 UTC), and the entire 24-hour period.

August 19, 1997 - 1Hour Rainfall Estimate. The 1-hour estimate covers the last hour of the August 19, 1997 study period from 11 UTC to 12 UTC. For each of the 11,132 4x4 kilometer cells in the study area, an ABRFC and a Mesonet interpolated rainfall value was obtained. Each cell is color-coded according the rainfall amount and the results are displayed in Figure 4.44. Map A of Figure 4.44 represents the Mesonet-interpolated total rainfall while Map B represents the ABRFC estimated total rainfall.

The two rainfall estimates provide a similar spatial description of rainfall for this date and time period. Both estimates agree that there is little or no rainfall in the panhandle, northwest quarter and southeast quarter of the state. Although the Mesonet estimate indicates light rainfall for most of the study area, this rainfall is extremely light and the amount closely matches that indicated by the ABRFC estimate. Both estimates describe a small but concentrated rainfall event along the northern border of the state as

Figure 4.44: Estimated rainfall for August 19, 1997 (1 Hour from 11 UTC to 12 UTC). Map A – Rainfall estimate from interpolated Mesonet data. Map B – Rainfall estimate from ABRFC Stage III radar rainfall data.

Map A

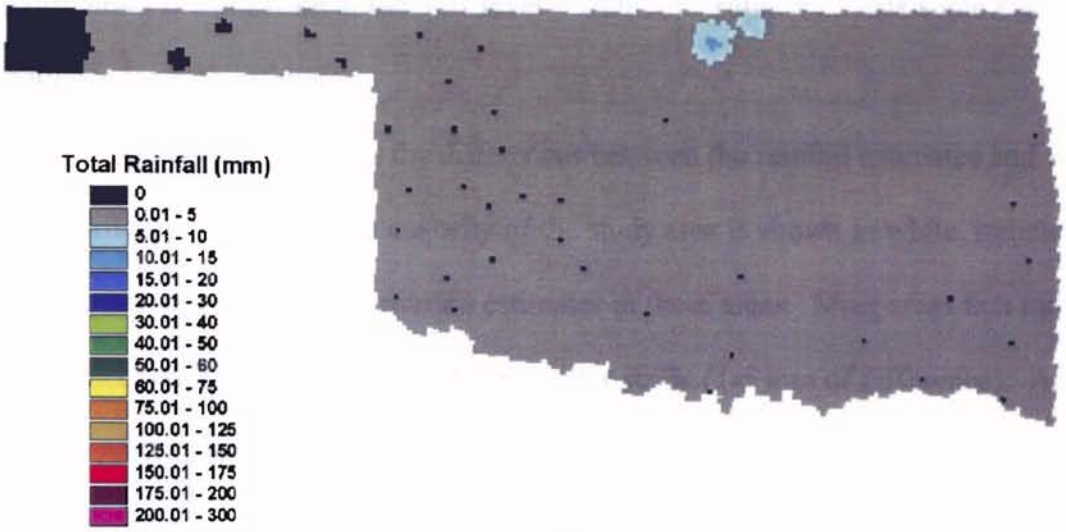

Map B

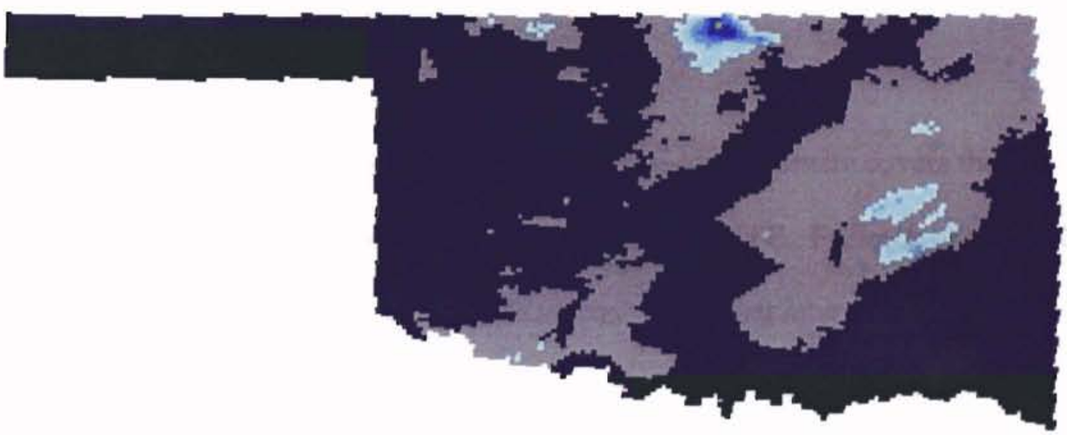

Table 4.22: August 19, 1997
1 Hour (11 UTC to 12 UTC)

Method	Min (mm)	Max (mm)	Mean (mm)	Standard Deviation (mm)	Volume (m3)
ABRFC	0.00	30.48	0.58	1.79	102,841,869
MESONET	0.00	12.01	0.52	0.80	92,208,582

well as a large area of light rainfall (1-5 mm) extending from the extreme northeast corner toward the center of the study area.

The correlation (*r*) between the Mesonet and ABRFC estimate was 0.742 (correlation is significant at the 0.01 level – 2 tailed). Table 4.22 lists some basic statistics for both estimates.

Figure 4.45 illustrates the differences between the rainfall estimates and where those differences occur. The majority of the study area is shown in white, indicating little or no difference between the rainfall estimates in these areas. Most areas that indicate a difference (red or blue) are of the lightest color shade (1-5 mm of difference). Areas of greater ABRFC estimate rainfall correspond with the areas of higher rainfall indicated in the ABRFC estimate. Areas of greater Mesonet estimated rainfall correspond with the edges of these areas of high rainfall and are separated by areas of little or no difference (white).

<u>August 19, 1997 - 6 Hour Rainfall Estimate</u>. The 6-hour estimate covers the last 6 hours of the August 19, 1997 study period from 6 UTC to 12 UTC. For each of the 11,132 4x4 kilometer cells in the study area, an ABRFC and a Mesonet interpolated rainfall value was obtained. Each cell is color-coded according the rainfall amount and the results are displayed in Figure 4.46. Map A of Figure 4.46 represents the Mesonet-interpolated total rainfall while Map B represents the ABRFC estimated total rainfall.

The two rainfall estimates provide a similar spatial description of rainfall for this date and time period. Both estimates agree that there is little or no rainfall in the panhandle, northwest quarter and southeast quarter of the state. Although the Mesonet estimate indicates light rainfall for most of the study area, this rainfall is extremely light

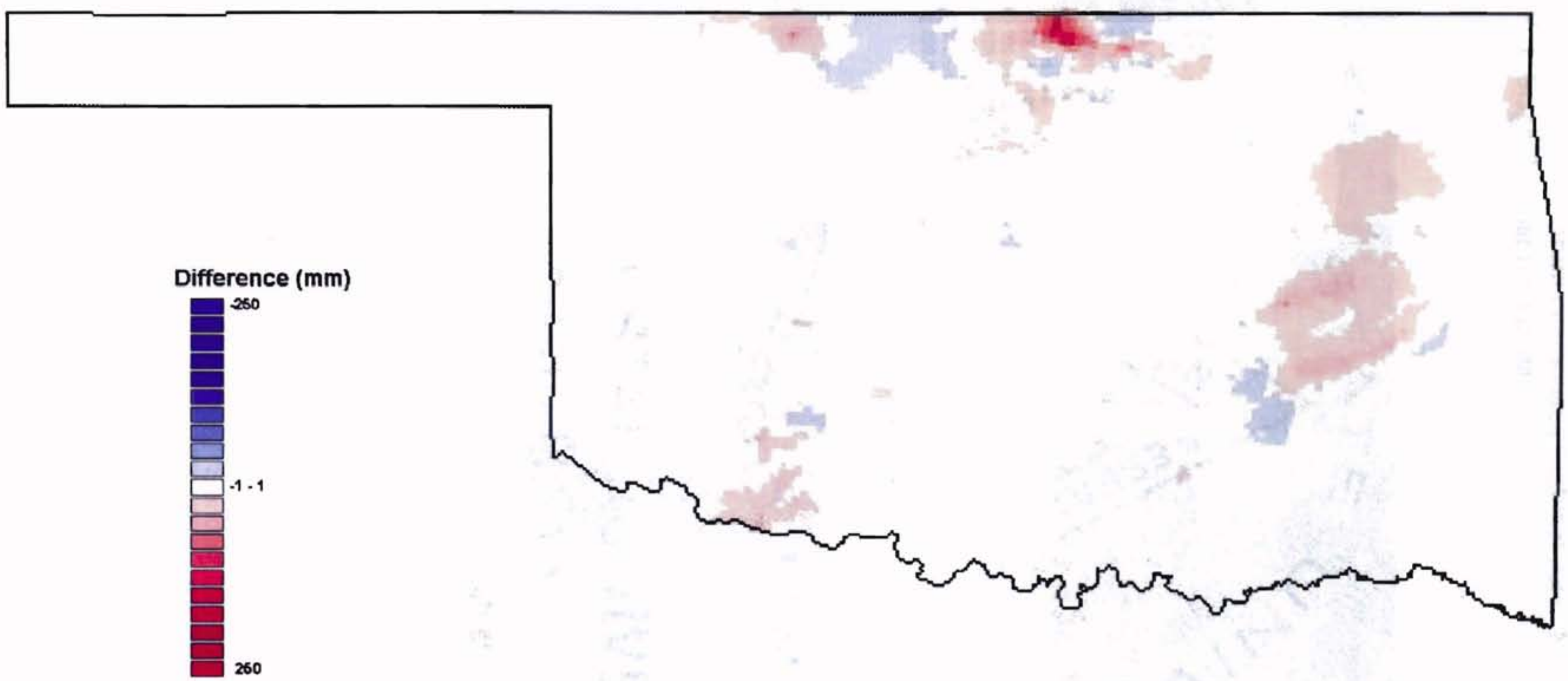

Figure 4.45: Difference in Radar and Mesonet Rainfall (mm) for August 19, 1997 - 1 Hour from 11 UTC to 12 UTC. Difference = Radar Rainfall – Mesonet Rainfall. Positive values indicate greater Radar estimated rainfall. Negative values indicate greater Mesonet estimated rainfall.

Figure 4.46: Estimated rainfall for August 19, 1997 (6 Hour from 6 UTC to 12 UTC). Map A – Rainfall estimate from interpolated Mesonet data. Map B – Rainfall estimate from ABRFC Stage III radar rainfall data.

Map A

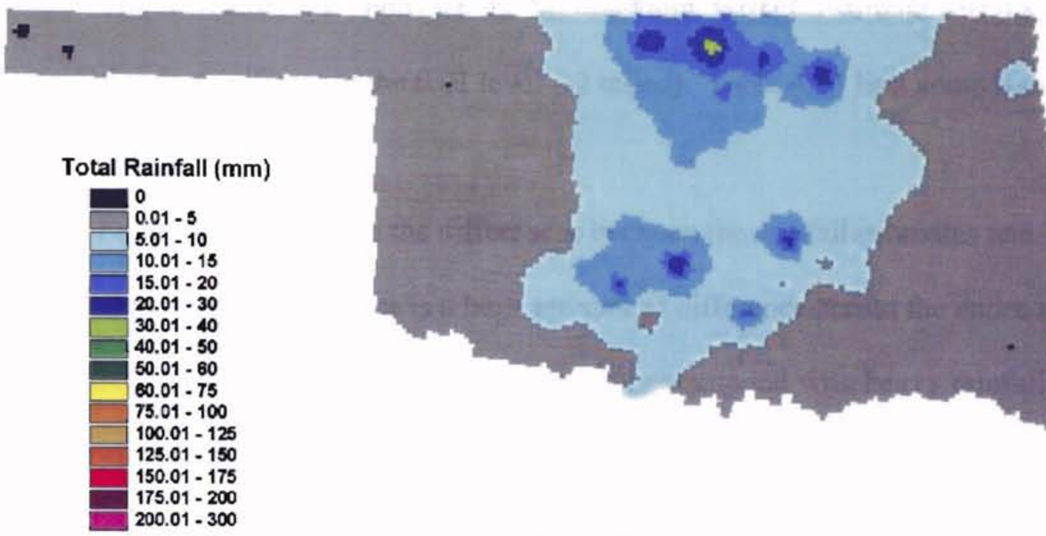

Map B

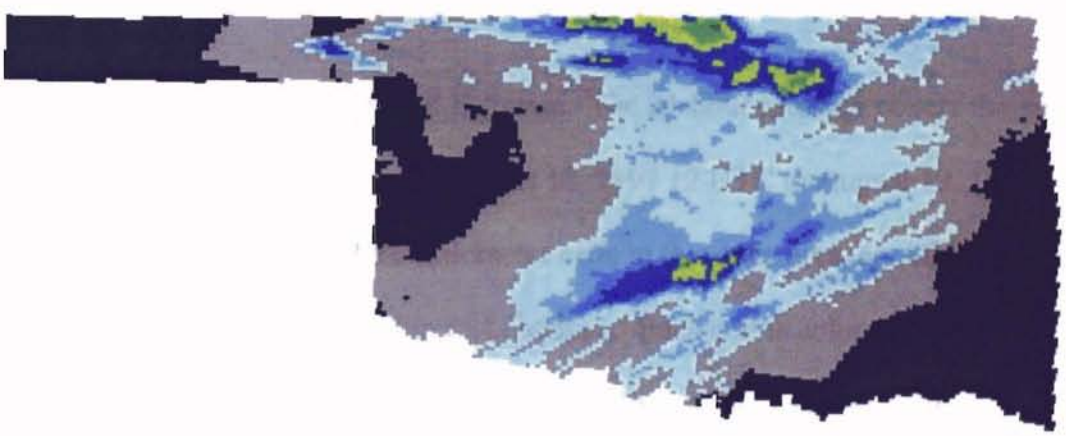

Table 4.23: August 19, 1997
6 Hour (6 UTC to 12 UTC)

Method	Min (mm)	Max (mm)	Mean (mm)	Standard Deviation (mm)	Volume (m3)
ABRFC	0	57	5.24	7.11	933,520,614
MESONET	0	34	5.03	4.43	895,689,626

and the amount closely matches that indicated by the ABRFC estimate. Both estimates describe heavy rainfall events in the north central and south central portions of the state. The spatial description of these rainfall events is similar for both rainfall estimates.

The correlation (r) between the Mesonet and ABRFC estimate was 0.834 (correlation is significant at the 0.01 level – 2 tailed). Table 4.23 lists some basic statistics for both estimates.

Figure 4.47 illustrates the differences between the rainfall estimates and where those differences occur. There is a large amount of difference across the entire study area. Areas of greater ABRFC estimated rainfall correspond with heavy rainfall areas and are characterized by concentrated patches of high difference. Areas of greater Mesonet estimated rainfall correspond with the edges of these high rainfall areas and are characterized by widespread areas of low difference.

August 19, 1997 - 24 Hour Rainfall Estimate. The 24-hour estimate covers the entire August 19, 1997 study period from August 18, 1997 12 UTC to August 19, 1997 12 UTC. For each of the 11,132 4x4 kilometer cells in the study area, an ABRFC and a Mesonet interpolated rainfall value was obtained. Each cell is color-coded according the rainfall amount and the results are displayed in Figure 4.48. Map A of Figure 4.48 represents the Mesonet-interpolated total rainfall while Map B represents the ABRFC estimated total rainfall.

Both estimates provide a similar spatial description of the rainfall for this date and time period. Both estimates indicate heavy, concentrated rainfall events covering the majority of the study area. There is general agreement between the estimates on the location and extent of high rainfall areas. However, the spatial variability of these areas

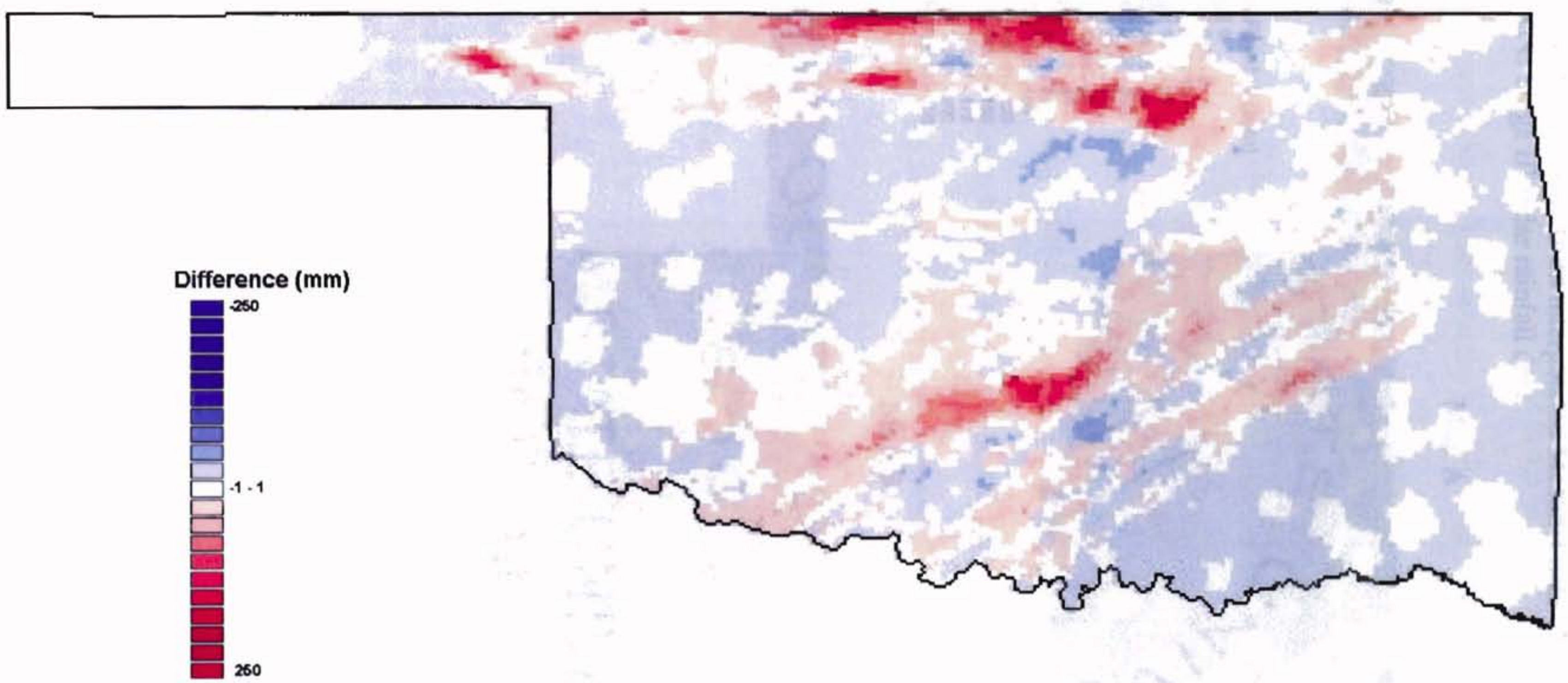

Figure 4.47: Difference in Radar and Mesonet Rainfall (mm) for August 19, 1997 - 6 Hour from 6 UTC to 12 UTC. Difference = Radar Rainfall – Mesonet Rainfall. Positive values indicate greater Radar estimated rainfall. Negative values indicate greater Mesonet estimated rainfall.

Figure 4.48: Estimated rainfall for August 19, 1997 (24 Hour from 12 UTC to 12 UTC). Map A – Rainfall estimate from interpolated Mesonet data. Map B – Rainfall estimate from ABRFC Stage III radar rainfall data.

Map A

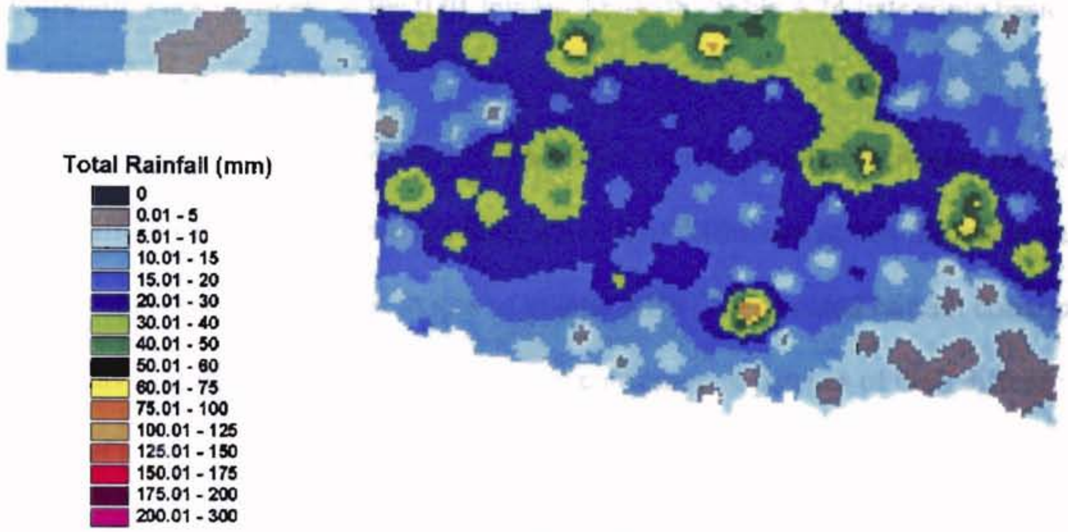

Map B

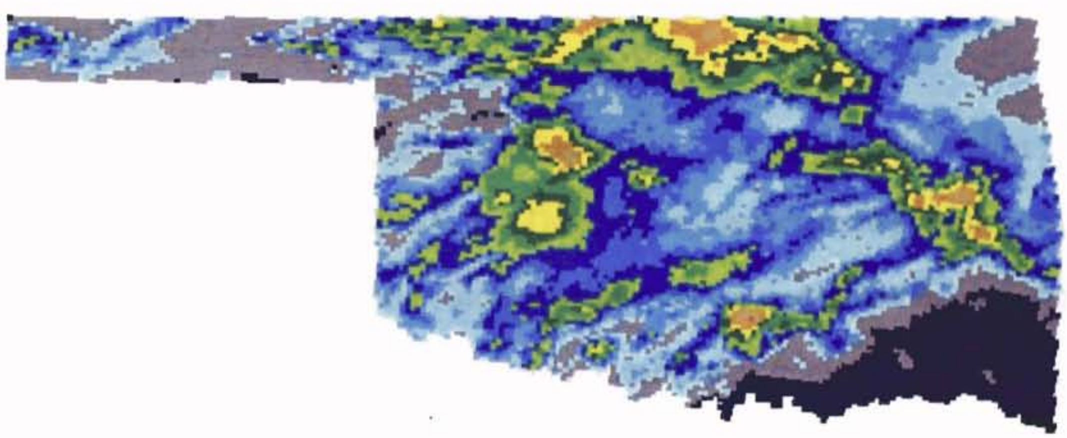

Table 4.24: August 19, 1997
24 Hour (12 UTC to 12 UTC)

Method	Min (mm)	Max (mm)	Mean (mm)	Standard Deviation (mm)	Volume (m3)
ABRFC	0	128	19.51	18.49	3,474,323,917
MESONET	0	111	20.16	11.48	3,590,203,584

is better defined for the ABRFC estimate and there are areas of high rainfall indicated by the ABRFC estimate that are not indicated in the Mesonet estimate.

The correlation (r) between the Mesonet and ABRFC estimate was 0.778 (correlation is significant at the 0.01 level – 2 tailed). Table 4.24 lists some basic statistics for both estimates.

Figure 4.49 illustrates the differences between the rainfall estimates and where those differences occur. There is a large amount of difference across the entire study area for this study data and period. Areas of greater ABRFC estimated rainfall correspond with heavy rainfall and are characterized by concentrated patches of high difference. Areas of greater Mesonet estimated rainfall correspond with the edges of these high rainfall areas and are also characterized by concentrated patches of high difference.

August 22, 1997

The study date of August 22, 1997 covers the 24 hours between August 21, 1997 12 UTC and August 22, 1997 12 UTC. This date was characterized by widespread, moderate rainfall. A single, widespread rainfall event covered almost the entire study area. Rainfall was very homogenous, with gradual change from areas of high rainfall to areas of low rainfall at the edges of the rainfall event. Rainfall estimates were collected for the last hour (11 UTC - 12 UTC), the last six hours (6 UTC - 12 UTC), and the entire 24-hour period.

August 22, 1997 - 1Hour Rainfall Estimate. The 1-hour estimate covers 11 UTC to 12 UTC of the August 22, 1997 study period. For each of the 11,132 4x4 kilometer cells in the study area, an ABRFC and a Mesonet interpolated rainfall value was obtained. Each

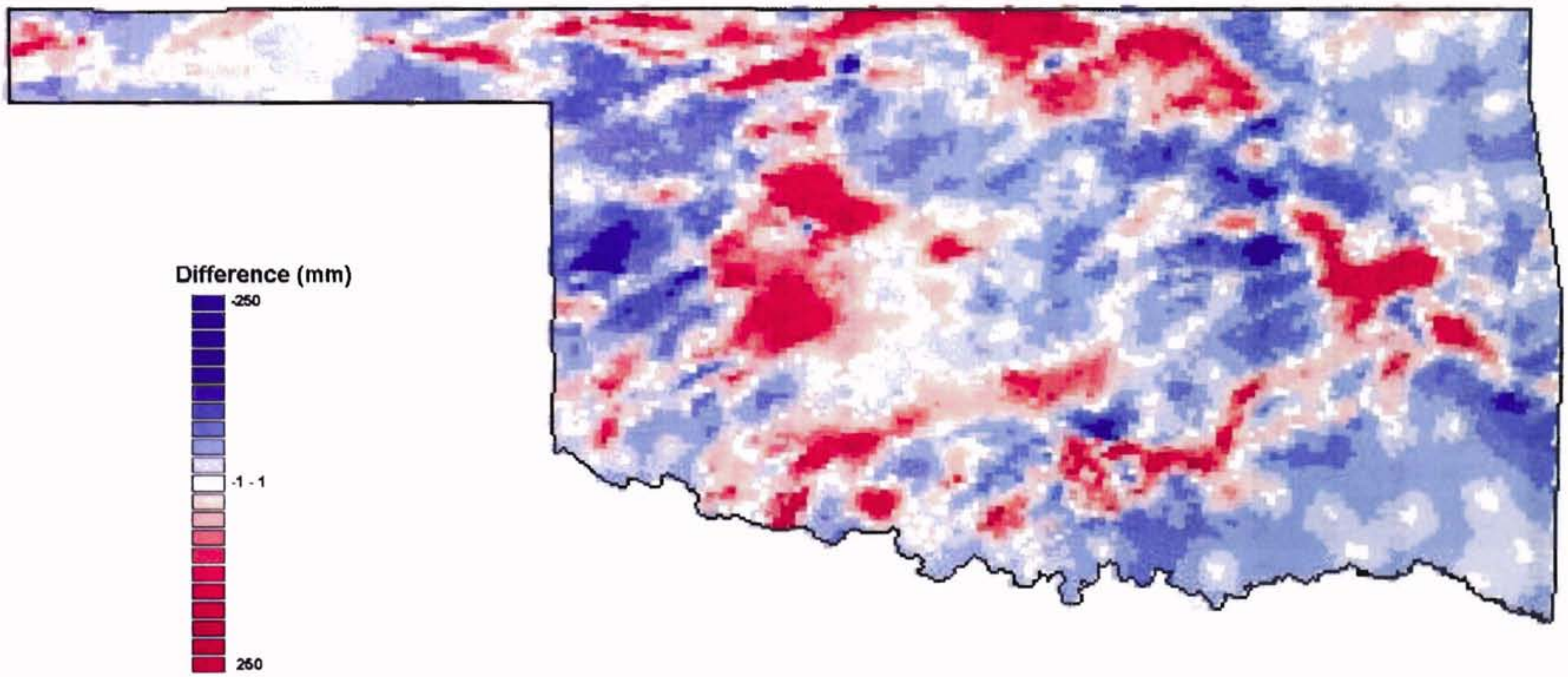

Figure 4.49: Difference in Radar and Mesonet Rainfall (mm) for August 19, 1997 - 24 Hour from 12 UTC to 12 UTC. Difference = Radar Rainfall – Mesonet Rainfall. Positive values indicate greater Radar estimated rainfall. Negative values indicate greater Mesonet estimated rainfall.

cell is color-coded according the rainfall amount and the results are displayed in Figure 4.50. Map A of Figure 4.50 represents the Mesonet-interpolated total rainfall hile Map B represents the ABRFC estimated total rainfall.

Both estimates describe a large rainfall event extending from the extreme southwest quarter towards the center of the study area. The description of the intensity and extent of this event are similar for both estimates. The Mesonet estimate indicates light rainfall covering the remainder of the study area while the ABRFC estimate indicates light rainfall only in areas surrounding the large rainfall event.

The correlation (r) between the Mesonet and ABRFC estimate was 0.874 (correlation is significant at the 0.01 level – 2 tailed). Table 4.25 lists some basic statistics for both estimates.

Figure 4.51 illustrates the differences between the rainfall estimates and where those differences occur. Areas of greater ABRFC estimated rainfall corresponds with the large rainfall event in the south central portion of the study area. Both rainfall estimates indicate the same rainfall event but the ABRFC estimate indicates a greater amount of rainfall than the Mesonet estimate. There is little or no difference between the estimates in the area surrounding this large rainfall event, which is manifested as a buffer of white. Areas of greater Mesonet estimated rainfall (blue) are widespread but are characterized by lighter shades of blue, indicated differences of less than 5 mm.

August 22, 1997 - 6 Hour Rainfall Estimate. The 6-hour estimate covers 6 UTC to 12 UTC of the August 22, 1997 study period. For each of the 11,132 4x4 kilometer cells in the study area, an ABRFC and a Mesonet interpolated rainfall value was obtained. Each cell is color-coded according the rainfall amount and the results are displayed in Figure

Figure 4.50: Estimated rainfall for August 22, 1997 (1 Hour from 11 UTC to 12 UTC). Map A – Rainfall estimate from interpolated Mesonet data. Map B – Rainfall estimate from ABRFC Stage III radar rainfall data.

Map A

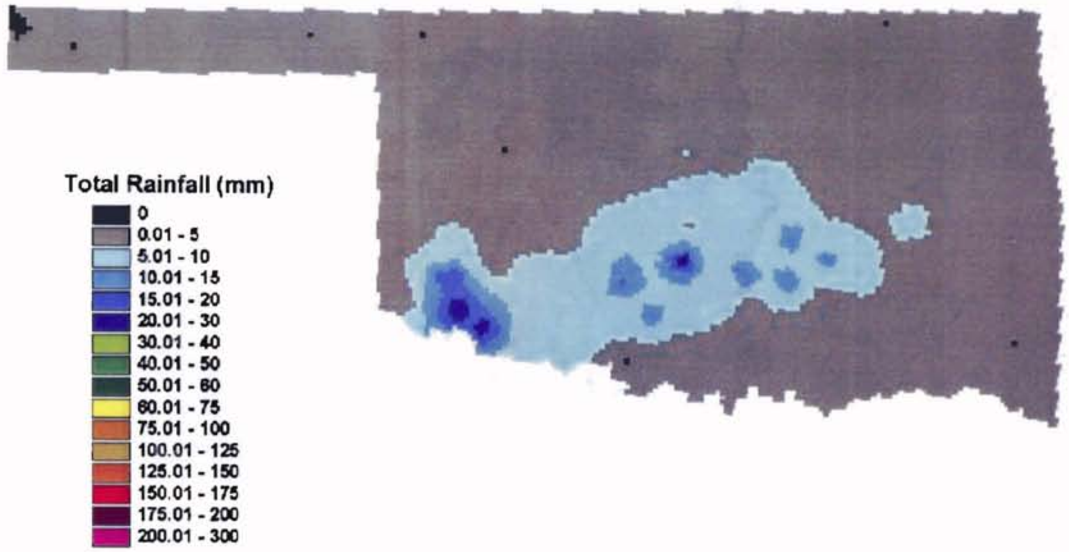

Map B

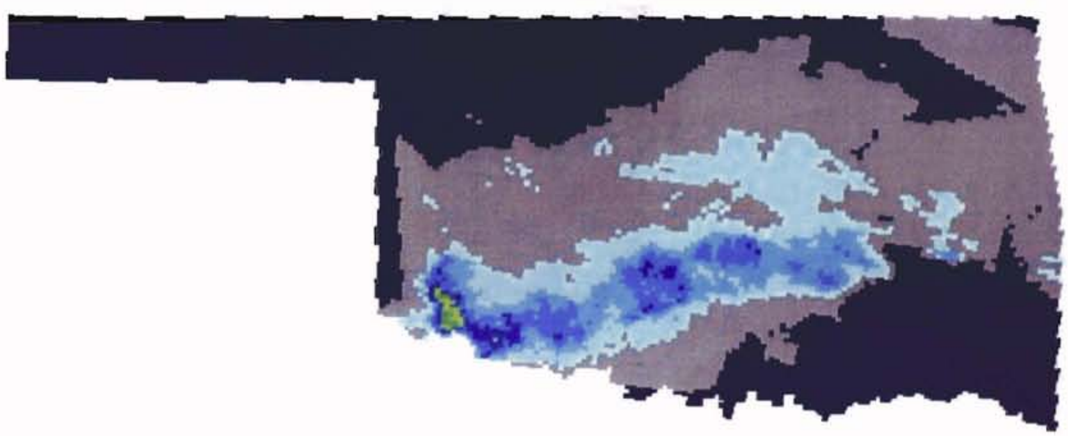

Table 4.25: August 22, 1997
1 Hour (11 UTC to 12 UTC)

Method	Min (mm)	Max (mm)	Mean (mm)	Standard Deviation (mm)	Volume (m3)
ABRFC	0	46	2.91	4.88	518,377,165
MESONET	0	25	3.16	3.21	563,635,424

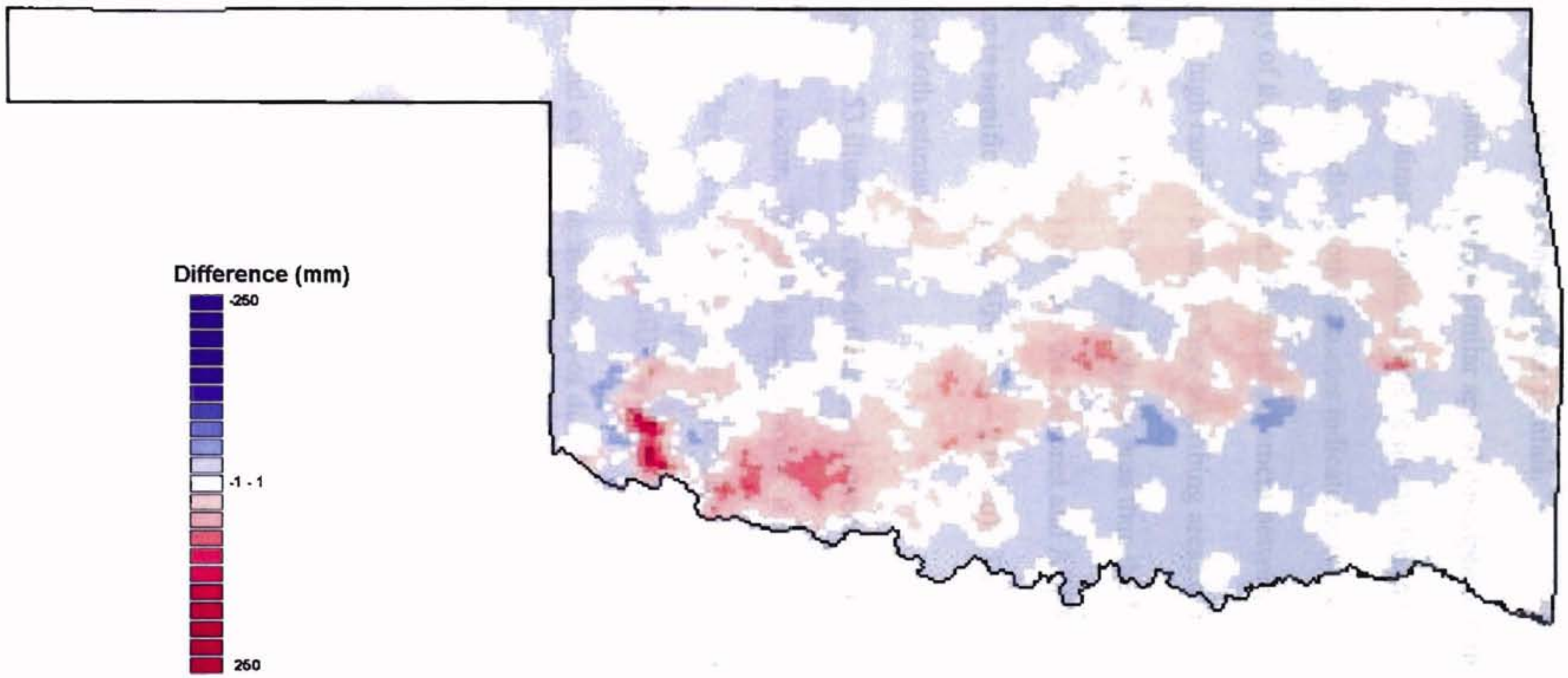

Figure 4.51: Difference in Radar and Mesonet Rainfall (mm) for August 22, 1997 - 1 Hour from 11 UTC to 12 UTC. Difference = Radar Rainfall – Mesonet Rainfall. Positive values indicate greater Radar estimated rainfall. Negative values indicate greater Mesonet estimated rainfall.

4.52. Map A of Figure 4.52 represents the Mesonet-interpolated total rainfall while Map B represents the ABRFC estimated total rainfall.

Both estimates provide a similar spatial description of the rainfall for this date and time period. Both estimates indicate little or no rainfall in the extreme southeastern corner and the panhandle. Both estimates indicate heavy, concentrated rainfall covering the majority of the study area. There is agreement between the estimates on the location and extent of high rainfall areas. When describing areas of very high rainfall (30-60 mm), the ABRFC estimate indicates a larger area than the Mesonet estimate.

The correlation (r) between the Mesonet and ABRFC estimate was 0.865 (correlation is significant at the 0.01 level – 2 tailed). Table 4.26 lists some basic statistics for both estimates.

Figure 4.53 illustrates the differences between the rainfall estimates and where those differences occur. There is a large amount of difference across the study area. Areas of high difference (darkest shades of red and blue) correspond with the heaviest rainfall areas. Areas of greater ABRFC estimated rainfall generally correspond with high rainfall areas and exhibit higher levels of difference. Areas of greater Mesonet estimated rainfall correspond with the edges of high rainfall areas and are characterized by lighter shades of blue, indicating lower levels of difference.

August 22, 1997 - 24 Hour Rainfall Estimate. The 24-hour estimate covers the study period from August 21, 1997 12 UTC to August 22, 1997 12 UTC. For each of the 11,132 4x4 kilometer cells in the study area, an ABRFC and a Mesonet interpolated rainfall value was obtained. Each cell is color-coded according the rainfall amount and

Figure 4.52: Estimated rainfall for August 22, 1997 (6 Hour from 6 UTC to 12 UTC). Map A – Rainfall estimate from interpolated Mesonet data. Map B – Rainfall estimate from ABRFC Stage III radar rainfall data.

Map A

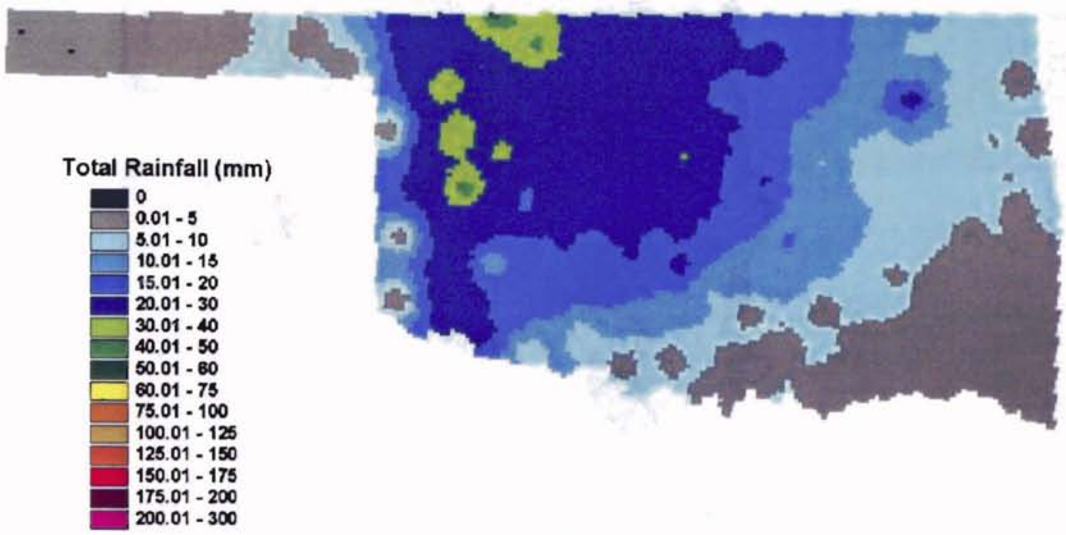

Map B

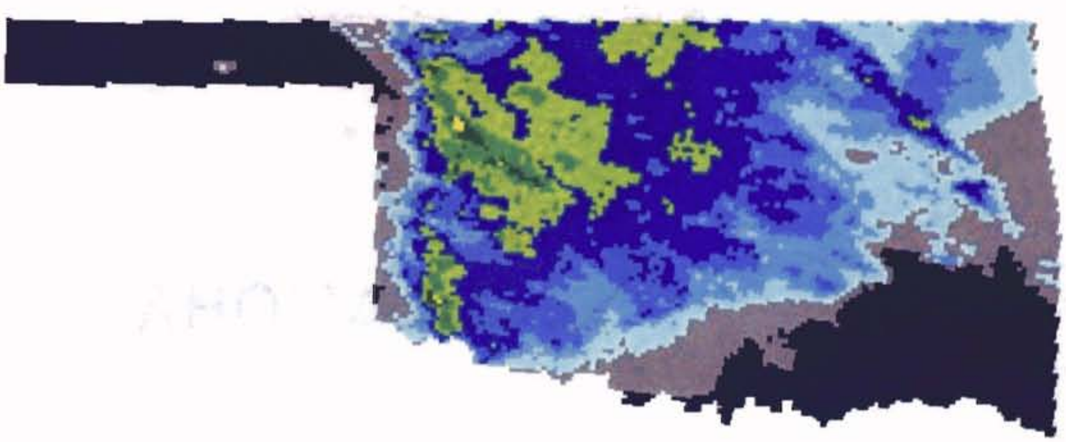

Table 4.26: August 22, 1997
6 Hour (6 UTC to 12 UTC)

Method	Min (mm)	Max (mm)	Mean (mm)	Standard Deviation (mm)	Volume (m3)
ABRFC	0.00	63.37	13.38	12.29	2,383,583,840
MESONET	0.00	51.47	13.49	8.96	2,402,196,544

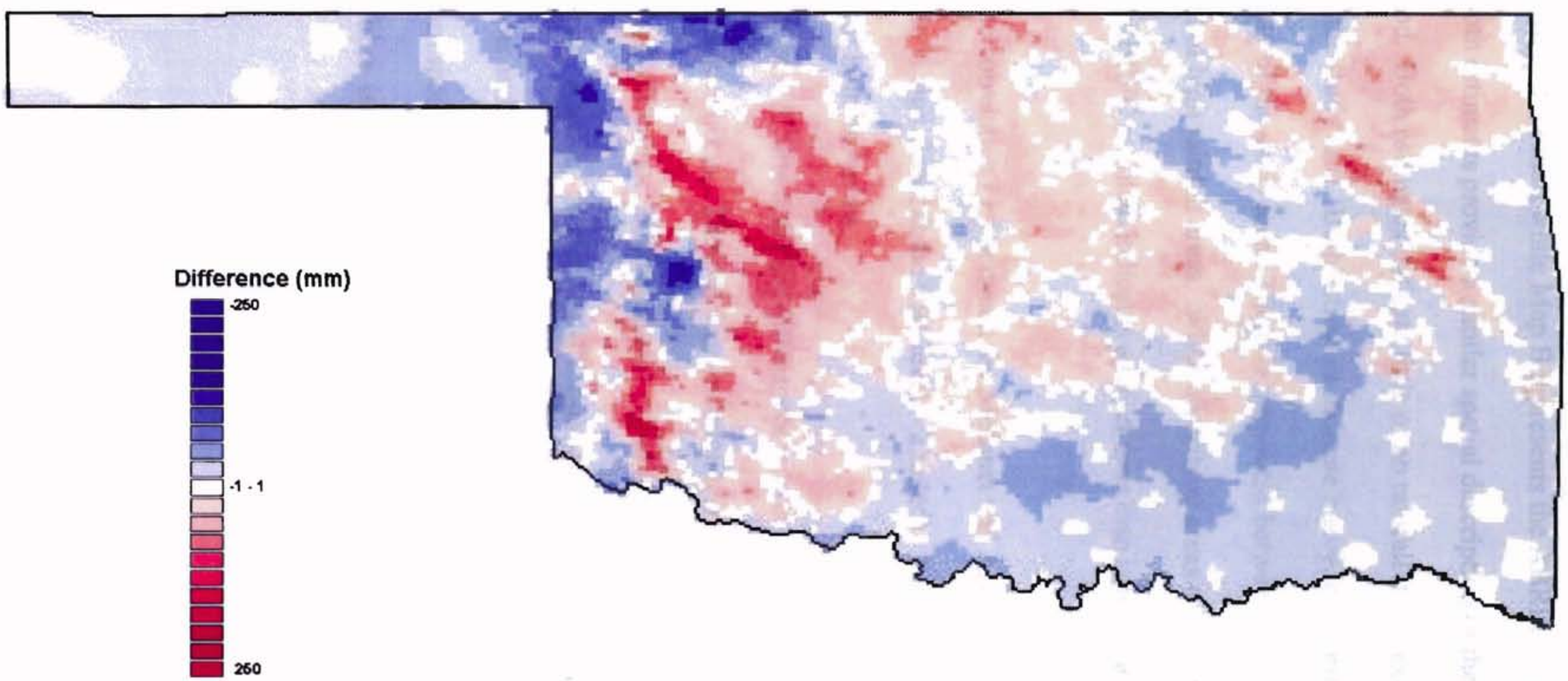

Figure 4.53: Difference in Radar and Mesonet Rainfall (mm) for August 22, 1997 - 6 Hour from 6 UTC to 12 UTC. Difference = Radar Rainfall – Mesonet Rainfall. Positive values indicate greater Radar estimated rainfall. Negative values indicate greater Mesonet estimated rainfall.

the results are displayed in Figure 4.54. Map A of Figure 4.54 represents the Mesonet-interpolated total rainfall while Map B represents the ABRFC estimated total rainfall.

Both estimates provide a similar spatial description of the rainfall for this date and time period. Both estimates indicate little or no rainfall in the extreme southeastern corner of the study area. Both estimates indicate heavy, concentrated rainfall covering the majority of the study area. There is agreement between the estimates on the location and extent of high rainfall areas. When describing areas of very high rainfall (60-100 mm), the ABRFC estimate indicates a larger area than is indicated by the Mesonet estimate.

The correlation (r) between the Mesonet and ABRFC estimate was 0.865 (correlation is significant at the 0.01 level – 2 tailed). Table 4.27 lists some basic statistics for both estimates.

Figure 4.55 illustrates the differences between the rainfall estimates and where those differences occur. There is a large amount of difference across the study area. Areas of high difference (darkest shades of red and blue) correspond with the heaviest rainfall areas. Areas of greater ABRFC estimated rainfall generally correspond with high rainfall areas and exhibit higher levels of difference. Areas of greater Mesonet estimated rainfall correspond with the edges of high rainfall areas and are characterized by lighter shades of blue, indicating lower levels of difference.

Figure 4.54: Estimated rainfall for August 22, 1997 (24 Hour from 12 UTC to 12 UTC). Map A – Rainfall estimate from interpolated Mesonet data. Map B – Rainfall estimate from ABRFC Stage III radar rainfall data.

Map A

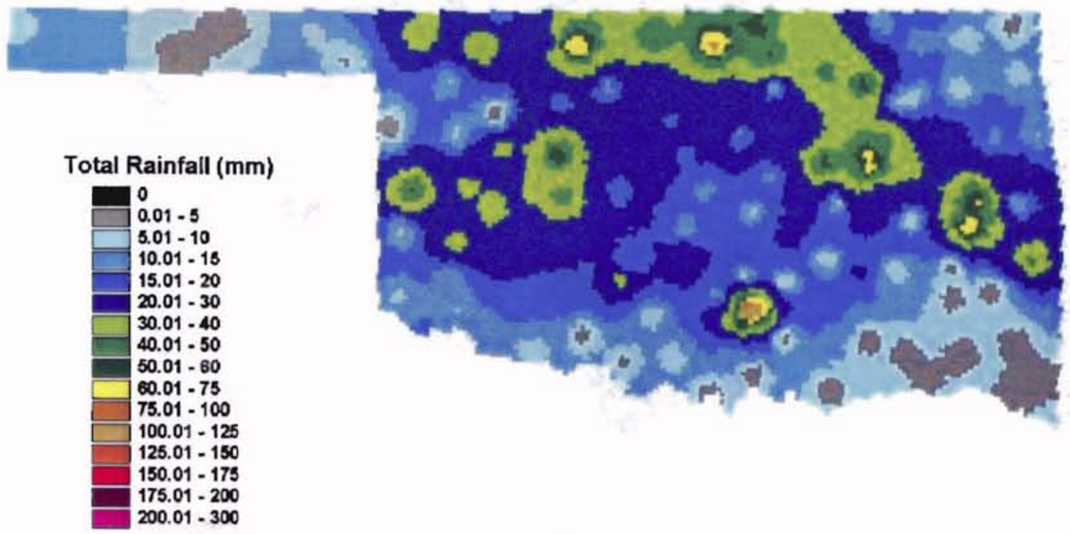

Map B

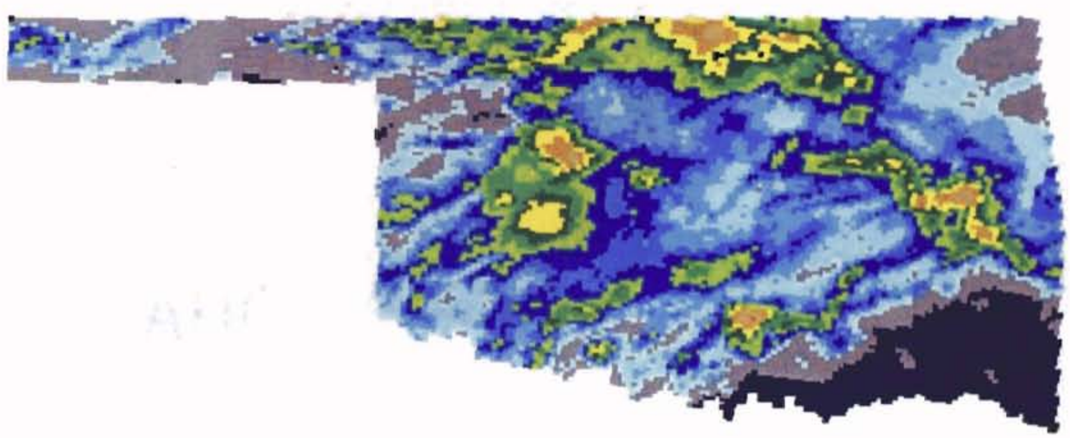

Table 4.27: August 22, 1997
24 Hour (12 UTC to 12 UTC)

Method	Min (mm)	Max (mm)	Mean (mm)	Standard Deviation (mm)	Volume (m3)
ABRFC	0	63	13.78	12.68	2,454,846,451
MESONET	0	51	13.81	8.99	2,458,925,216

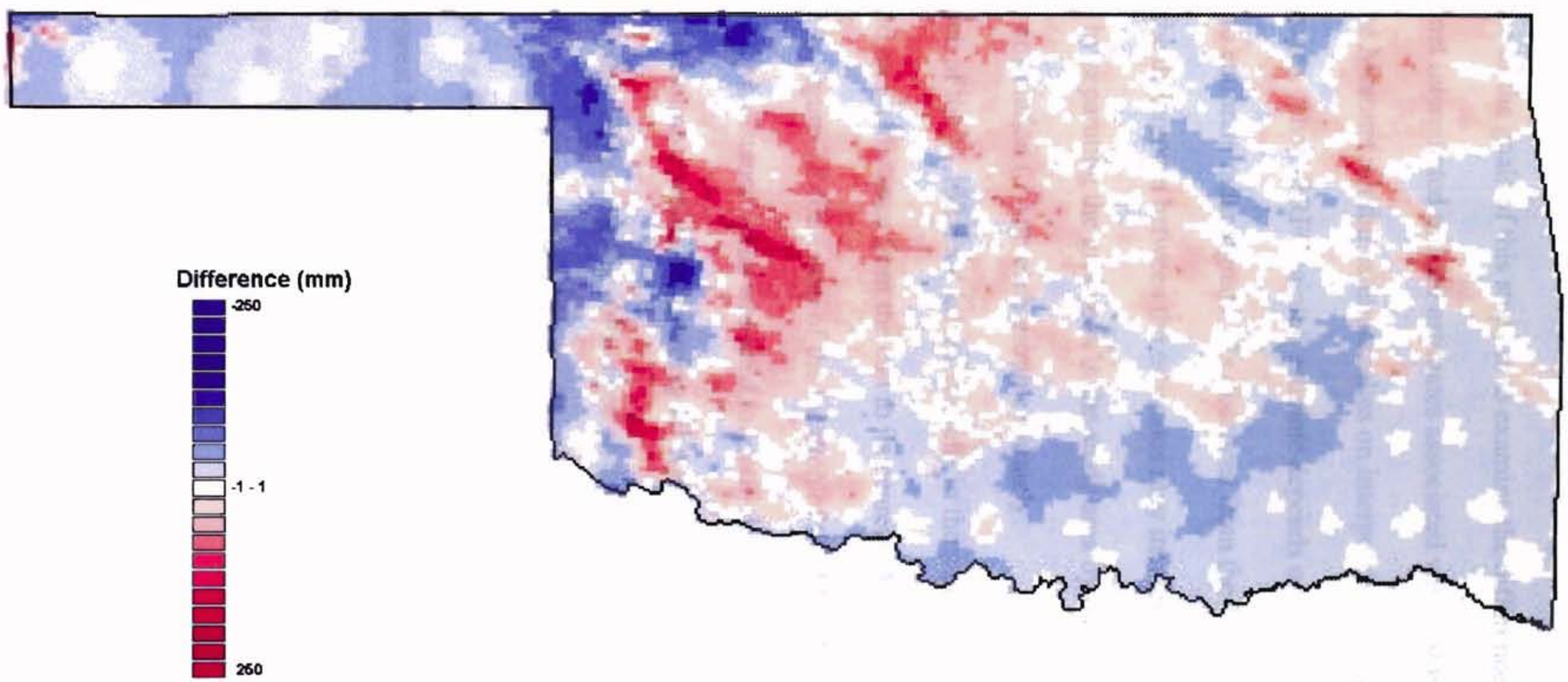

Figure 4.55: Difference in Radar and Mesonet Rainfall (mm) for August 22, 1997 - 24 Hour from 12 UTC to 12 UTC. Difference = Radar Rainfall – Mesonet Rainfall. Positive values indicate greater Radar estimated rainfall. Negative values indicate greater Mesonet estimated rainfall.

4.2 Distance From Mesonet Stations

One of the goals of this study is to examine the differences between the ABRFC and Mesonet interpolated rainfall estimates associated with distance from the Mesonet gages. The Mesonet rainfall estimate relies on interpolation to estimate rainfall values between gages. The ABRFC rainfall estimate depends on rain gages including the Mesonet, to calibrate radar signals. As distances from the Mesonet point measurements increase, the differences between the estimates may increase as well. This question was examined by separating the grid cells in the study area by distance groups and performing a separate correlation (r) on each group separately.

Each of the 11,132 4 x 4 kilometer cells in the study area was assigned a distance value based on the distance from the cell to its nearest Mesonet weather station. Please refer back to Figure 3.2 for a map of the location of the 114 Mesonet stations across the study area. This distance value was used to group the cells based on categories of distance. An example would be grouping all cells that are within 20 kilometers of a Mesonet station. By examining cells based on distance, the effects of distance on the two rainfall estimates can be examined.

The 4 x 4 kilometer cells were divided into four groups based on the cells distance from its nearest Mesonet site. The first group consists of all cells that are located within 5 kilometers of a Mesonet weathers station. A total of 453 cells out of the 11,132 cells in the study area fell into this group. Figure 4.56 illustrates the location of all cells that are within 5 kilometers of a Mesonet station.

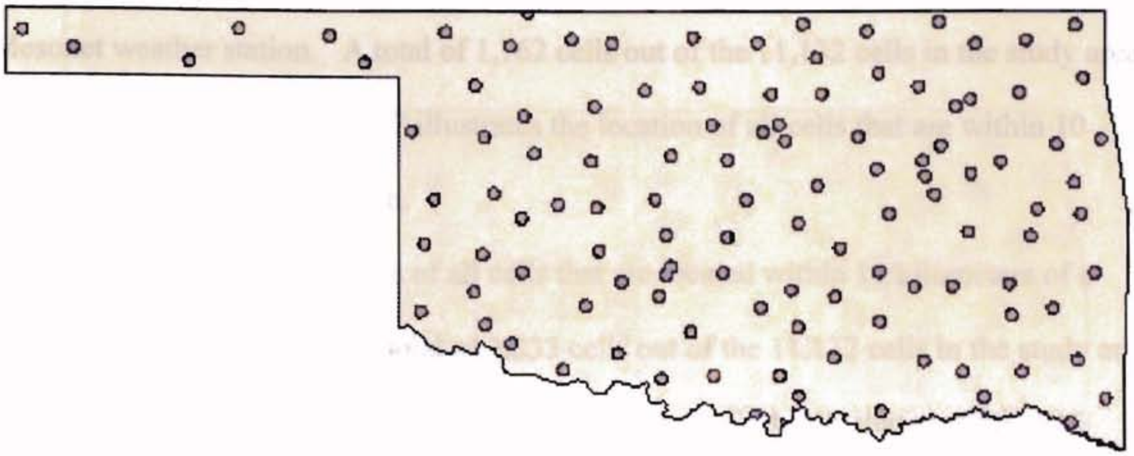

Figure 4.56: All cells within 5 Kilometers of a Mesonet Station.

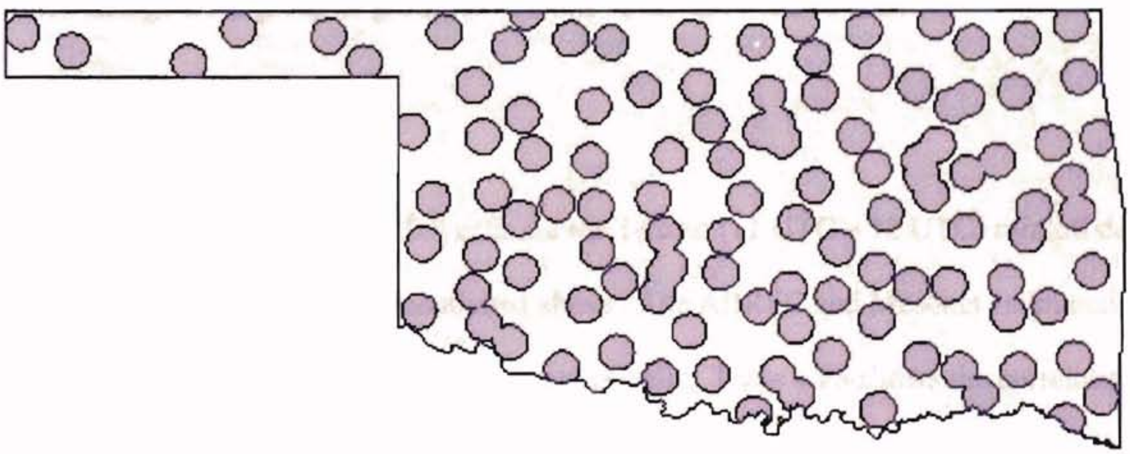

Figure 4.57: All cells within 10 Kilometers of a Mesonet Station.

The second group consists of all cells that are located within 10 kilometers of a Mesonet weather station. A total of 1,762 cells out of the 11,132 cells in the study area fell into this group. Figure 4.57 illustrates the location of all cells that are within 10 kilometers of a Mesonet station.

The third group consists of all cells that are located within 15 kilometers of a Mesonet weathers station. A total of 3,833 cells out of the 11,132 cells in the study area fell into this group. Figure 4.58 illustrates the location of all cells that are within 15 kilometers of a Mesonet station.

The fourth group consists of all cells that are located within 20 kilometers of a Mesonet weathers station. A total of 6,373 cells out of the 11,132 cells in the study area fell into this group. Figure 4.59 illustrates the location of all cells that are within 20 kilometers of a Mesonet station.

The ABRFC and Mesonet estimated rainfall values were correlated for each group of cells and repeated for the 1, 6 and 24 hour data. By examining how correlation values change from group to group, the effects of distance can be seen.

1 Hour Data

The 4 x 4 kilometer rainfall cells for the 1-Hour (11 UTC – 12 UTC) rainfall data were divided in into groups as mentioned above. The ABRFC and Mesonet estimated rainfall values were correlated for each group of cells. Table 4.28 shows the correlation values for the 1-hour data on each of the nine study dates. These values were plotted on the line graph in Figure 4.60.

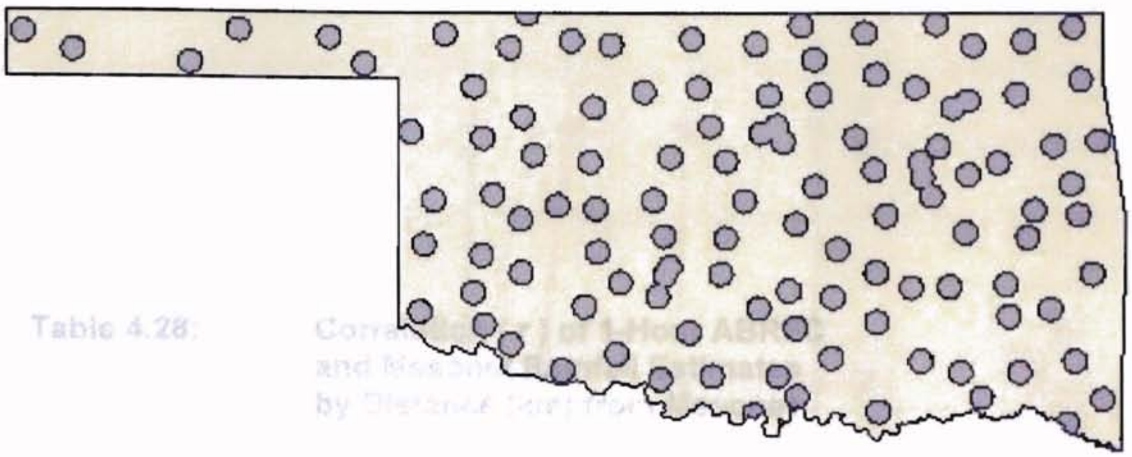

Figure 4.58: All cells within 15 Kilometers of a Mesonet Station.

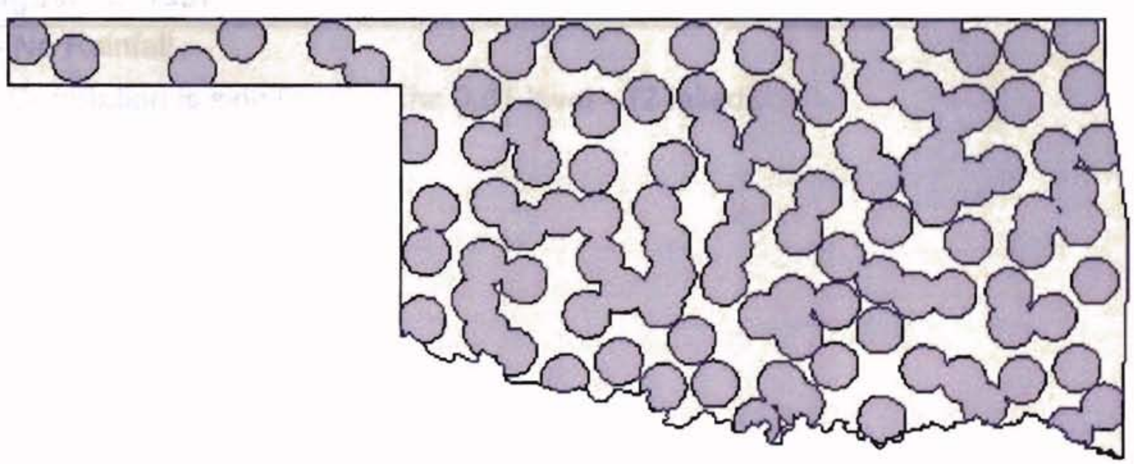

Figure 4.59: All cells within 20 Kilometers of a Mesonet Station.

Table 4.28: Correlation (r) of 1-Hour ABRFC and Mesonet Rainfall Estimates by Distance (km) from Mesonet

	Distance (km)				
Study Dates	**5**	**10**	**15**	**20**	**State**
June 9, 1997	0.717**	0.682**	0.640**	0.583**	0.536**
June 24, 1997	0.462**	0.392**	0.327**	0.297**	0.284**
June 28, 1997	0.923**	0.815**	0.676**	0.605**	0.515**
July 11, 1997	0.954**	0.908**	0.809**	0.724**	0.605**
July 16, 1997	*	*	*	*	*
July 18, 1997	0.939**	0.895**	0.814**	0.752**	0.728**
August 13, 1997	*	*	*	*	*
August 19, 1997	0.915**	0.842**	0.784**	0.758**	0.742**
August 22, 1997	0.939**	0.924**	0.902**	0.890**	0.874**

* - No Rainfall

** - Correlation is significant at the 0.01 level – (2 tailed).

Figure 4.60:
Correlation of 1-Hour ABRFC and Mesonet Estimated Rainfall by Distance (km) from Mesonet

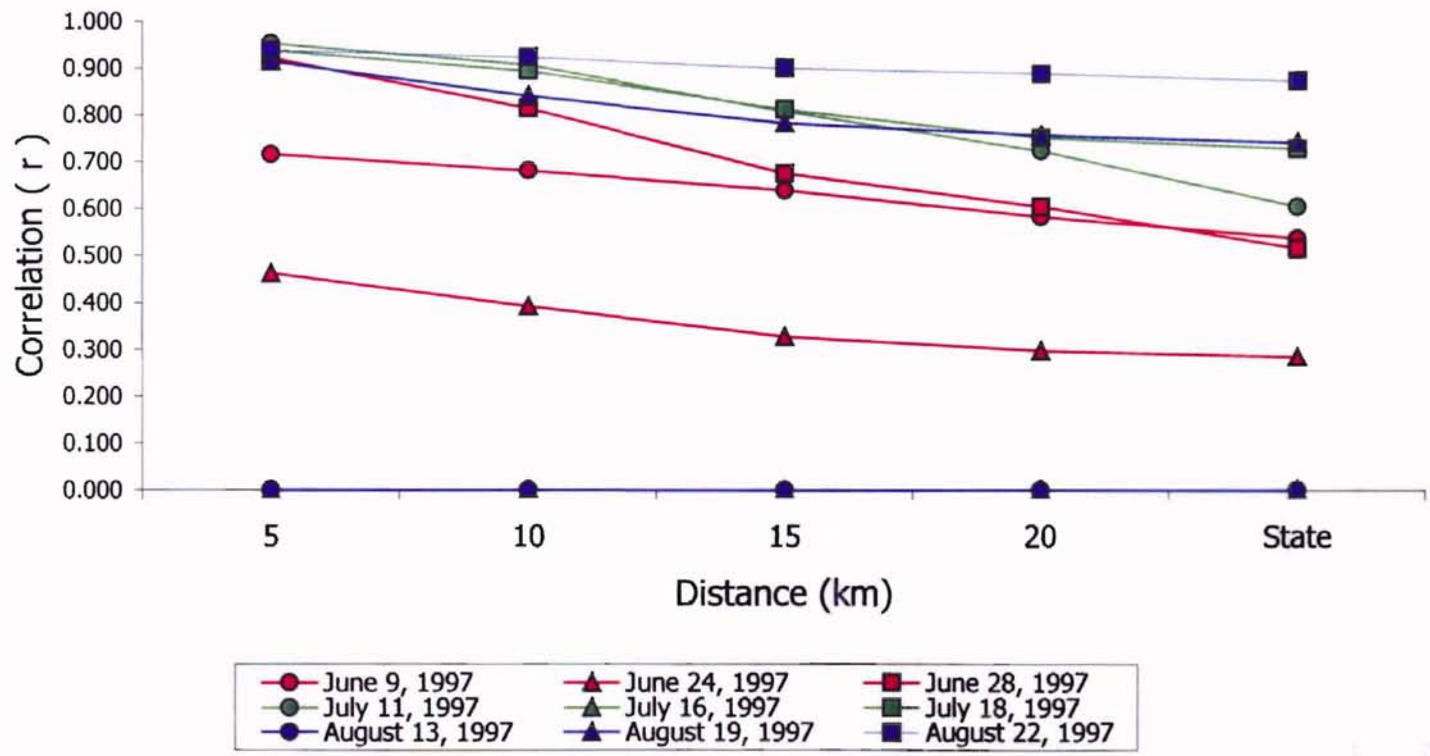

6 Hour Data

The 4 x 4 kilometer rainfall cells for the 6-Hour (6 UTC - 12 UTC) rainfall data were divided in into groups as mentioned above. The ABRFC and Mesonet estimated rainfall values were correlated for each group of cells. Table 4.29 shows the correlation values for the 6-hour data on each of the nine study dates. These values were plotted on the line graph in Figure 4.61.

24 Hour Data

The 4 x 4 kilometer rainfall cells for the 24-Hour (12 UTC - 12 UTC) rainfall data were divided in into groups as mentioned above. The ABRFC and Mesonet estimated rainfall values were correlated for each group of cells. Table 4.30 shows the correlation values for the 24-hour data on each of the nine study dates. These values were plotted on the line graph in Figure 4.62.

24-Hour Data by Distance Class

The 11,132 4 x 4 kilometer cells were once again divided into groups based on their distance from the nearest Mesonet station. However, rather than dividing the cells as done in the previous section (within 5, 10, 15, and 20 kilometers), the cells were divided into distance classes (0-10 kilometer and 10-20 kilometers). This was done only for the 24-hour rainfall data.

The first group consists of all cells that are located between 0 and 10 kilometers from a Mesonet weathers station. A total of 1,762 cells out of the 11,132 cells in the

Table 4.29: Correlation (r) of 6-Hour ABRFC and Mesonet Rainfall Estimates by Distance (km) from Mesonet

	Distance (km)				
Study Dates	**5**	**10**	**15**	**20**	**State**
June 9, 1997	0.899**	0.865**	0.815**	0.750**	0.691**
June 24, 1997	*	*	*	*	*
June 28, 1997	0.870**	0.771**	0.627**	0.555**	0.450**
July 11, 1997	0.954**	0.924**	0.880**	0.818**	0.731**
July 16, 1997	0.642**	0.564**	0.572**	0.492**	0.396**
July 18, 1997	0.760**	0.721**	0.698**	0.672**	0.646**
August 13, 1997	0.464**	0.443**	0.441**	0.448**	0.446**
August 19, 1997	0.945**	0.916**	0.886**	0.860**	0.834**
August 22, 1997	0.902**	0.891**	0.882**	0.877**	0.865**

* - No Rainfall

** - Correlation is significant at the 0.01 level (2 tailed).

Figure 4.61:
Correlation of 6-Hour ABRFC and Mesonet Estimated Rainfall by Distance (km) from Mesonet

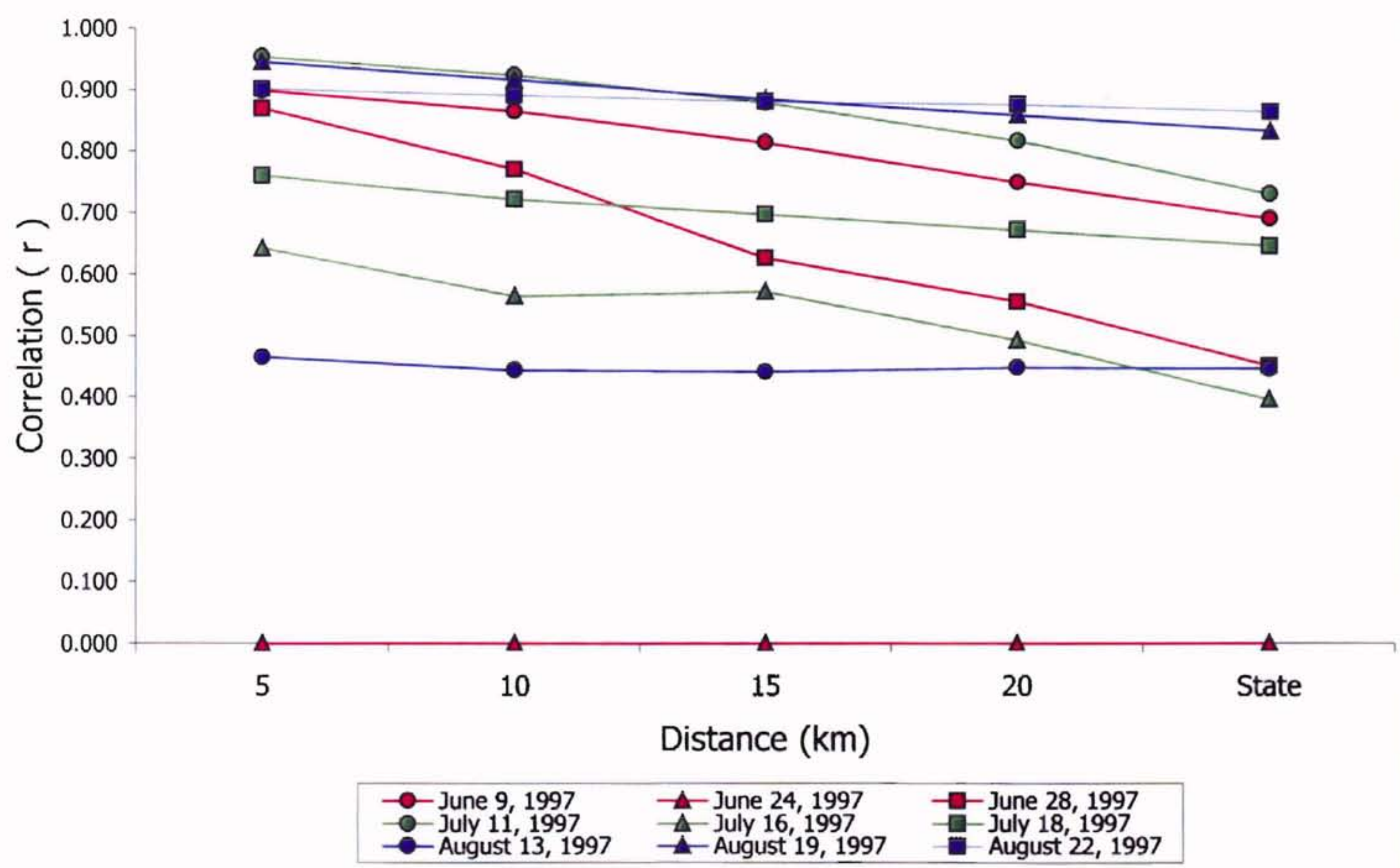

Table 4.30: **Correlation (r) of 24-Hour ABRFC and Mesonet Rainfall Estimates by Distance (km) from Mesonet**

	Distance (km)				
Study Dates	**5**	**10**	**15**	**20**	**State**
June 9, 1997	0.805**	0.764**	0.700**	0.679**	0.654**
June 24, 1997	0.857**	0.820**	0.779**	0.751**	0.676**
June 28, 1997	0.811**	0.702**	0.561**	0.471**	0.380**
July 11, 1997	0.848**	0.835**	0.802**	0.761**	0.701**
July 16, 1997	0.813**	0.723**	0.597**	0.511**	0.454**
July 18, 1997	0.879**	0.859**	0.849**	0.837**	0.823**
August 13, 1997	0.907**	0.877**	0.849**	0.823**	0.785**
August 19, 1997	0.901**	0.872**	0.839**	0.810**	0.778**
August 22, 1997	0.903**	0.891**	0.881**	0.876**	0.865**

* - No Rainfall

** - Correlation is significant at the 0.01 level (2 tailed).

Figure 4.62:
Correlation of 24-Hour ABRFC and Mesonet Estimated Rainfall by Distance (km) from Mesonet

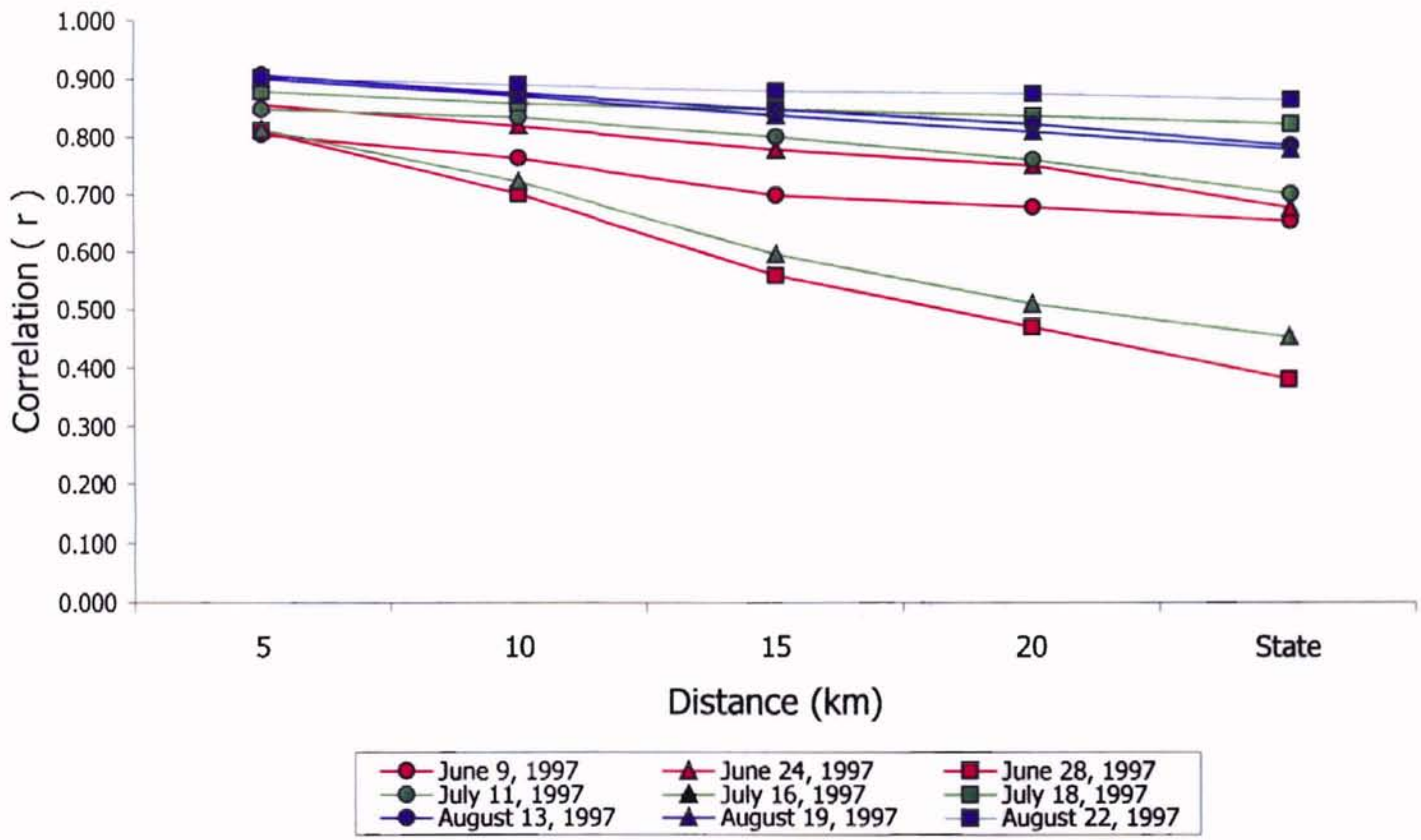

study area fell into this group. The second group consists of all cells that are located between 10 and 20 kilometers from a Mesonet weathers station, a total of 5,313 cells. The third group consists of all cells that are located between 20 and 30 kilometers from a Mesonet weathers station, a total of 3,076 cells. The fourth group consists of all cells that are located between 30 and 40 kilometers from a Mesonet weathers station, a total of 430 cells. The fifth group consists of all cells that are located between 20 to 30 kilometers from a Mesonet weathers station, a total of 65 cells.

The ABRFC and Mesonet estimated rainfall values were correlated for each group of cells. The correlation values for each study date and class range are presented in Table 4.31. These values were plotted in a line graph in Figure 4.63.

Mean and Standard Deviation by Distance Class

To further examine the effects of cell distance from Mesonet, the means and standard deviations of both the ABRFC and Mesonet were obtained for each study date and distance range. By examining how basic statistical measures vary with distance, the effects of distance on the ABRFC and Mesonet rainfall estimates may become apparent. To illustrate any spatial patterns, the statistical values for each study date were then plotted in a line graph.

Table 4.31: Correlation of 24-Hour ABRFC and Mesonet Rainfall Estimates by Distance (km) from Mesonet

	Distance (km)			
	0-10	10-20	20-30	30-40
June 9, 1997	0.764**	0.647**	0.618**	0.575**
June 24, 1997	0.820**	0.715**	0.605**	0.288**
June 28, 1997	0.702**	0.313**	0.189**	0.130**
July 11, 1997	0.835**	0.730**	0.625**	0.253**
July 16, 1997	0.723**	0.405**	0.424**	0.316**
July 18, 1997	0.859**	0.834**	0.818**	0.698**
August 13, 1997	0.877**	0.795**	0.673**	0.607**
August 19, 1997	0.872**	0.779**	0.728**	0.710**
August 22, 1997	0.891**	0.875**	0.857**	0.760**

** - Correlation is significant at the 0.01 level (2 tailed).

Figure 4.63:
Correlation of 24-Hour ABRFC and Mesonet Estimated Rainfall by Distance (km) from Mesonet

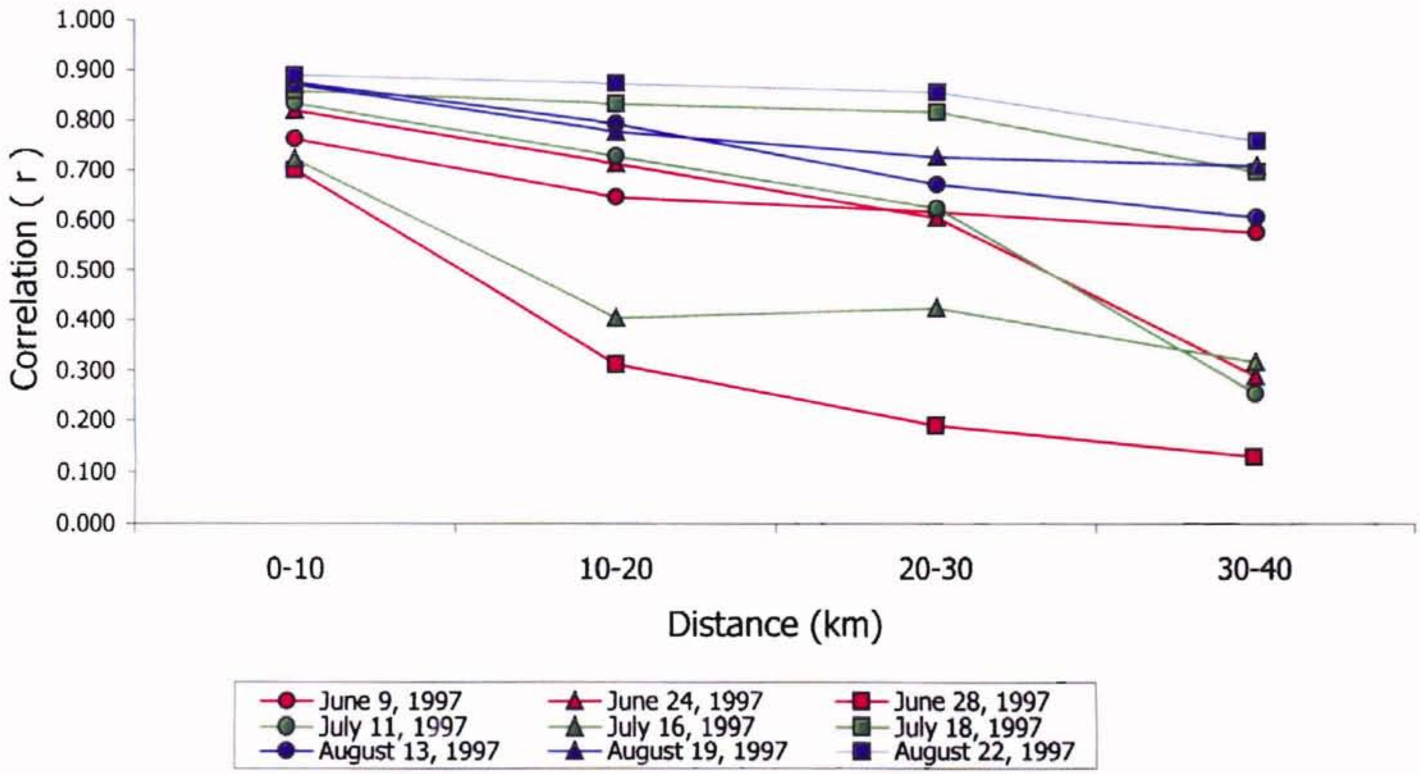

For each of the nine study dates (24 hour data), the ABRFC mean and standard deviation as well as the Mesonet mean and standard deviation for each distance class were calculated. These values are presented in Table 4.32 through Table 4.40. The mean and standard deviation by distance class for both estimates were then plotted on the line graphs presented in Figure 4.64 through Figure 4.72.

Table 4.32: **June 9, 1997 – Mean and Standard Deviation By Distance From Mesonet**

	Distance (km)				
	0-10	**10-20**	**20-30**	**30-40**	**40-50**
ABRFC Mean	4.514	4.276	4.342	3.679	1.520
Mesonet Mean	3.420	3.477	3.587	3.864	3.388
ABRFC St. Dev.	6.600	7.013	6.152	5.465	2.580
Mesonet St. Dev	4.280	2.960	2.360	1.816	0.817

Figure 4.64: June 9, 1997 ABRFC and Mesonet Mean and Standard Devation by Distance Class

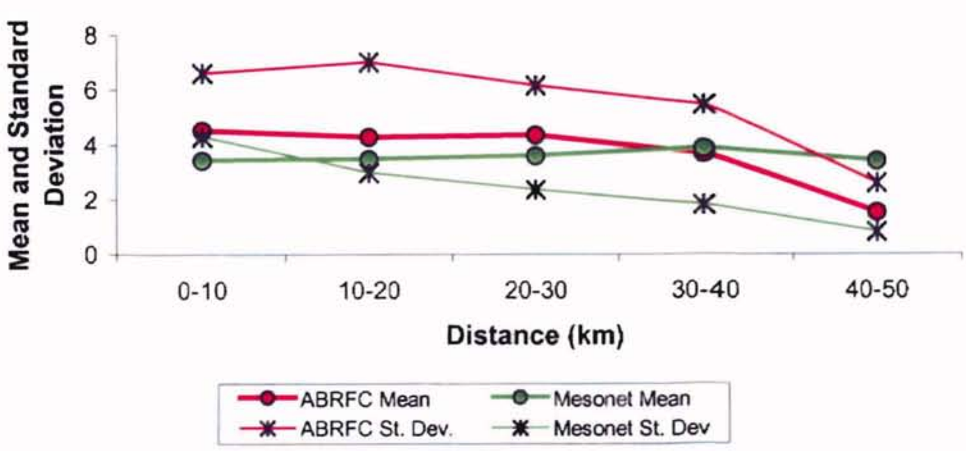

Table 4.33: **June 24, 1997 - Mean and Standard Deviation By Distance From Mesonet**

	Distance (km)				
	0-10	10-20	20-30	30-40	40-50
ABRFC Mean	5.144	4.940	4.303	3.610	9.275
Mesonet Mean	4.817	4.796	4.560	3.564	2.155
ABRFC St. Dev.	5.766	5.691	5.378	5.182	10.071
Mesonet St. Dev	4.708	2.962	2.219	1.809	1.074

Figure 4.65: June 24, 1997 ABRFC and Mesonet Mean and Standard Devation by Distance Class

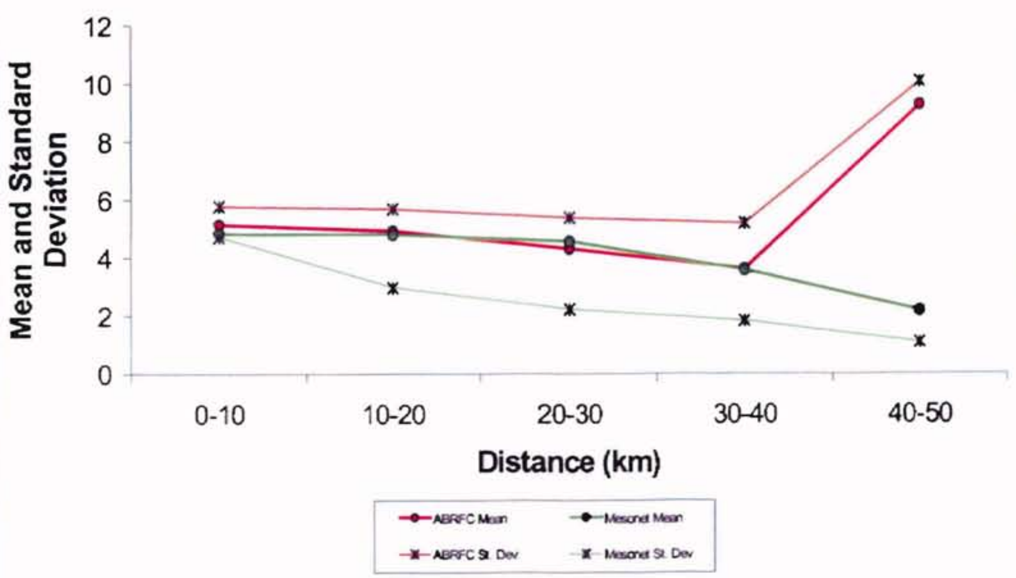

Table 4.34: **June 28, 1997 - Mean and Standard Deviation By Distance From Mesonet**

	Distance (km)				
	0-10	10-20	20-30	30-40	40-50
ABRFC Mean	3.140	3.236	3.068	1.259	0.026
Mesonet Mean	2.164	2.164	2.085	1.698	0.702
ABRFC St. Dev.	6.356	6.589	6.594	3.947	0.061
Mesonet St. Dev	4.291	2.489	1.728	1.909	0.436

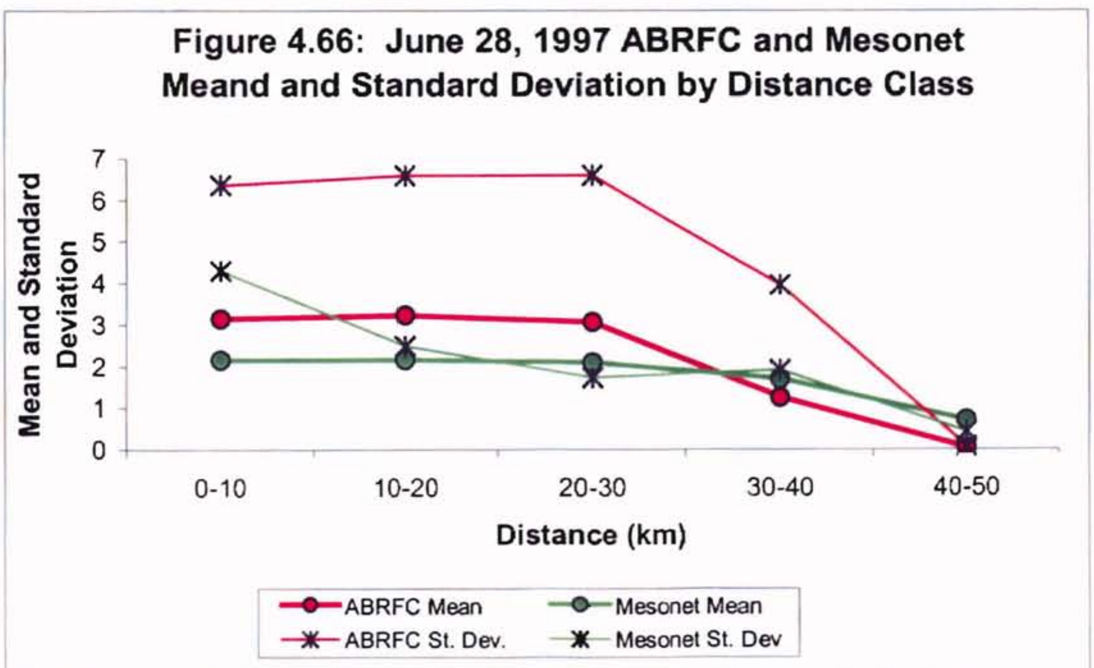

Table 4.35: July 11, 1997 - Mean and Standard Deviation By Distance From Mesonet

	Distance (km)				
	0-10	10-20	20-30	30-40	40-50
ABRFC Mean	9.276	9.578	8.684	4.636	1.797
Mesonet Mean	6.515	6.458	6.144	4.029	2.156
ABRFC St. Dev.	16.891	17.641	17.251	8.759	5.478
Mesonet St. Dev	9.971	5.819	4.067	2.550	0.925

Figure 4.67: July 11, 1997 ABRFC and Mesonet Mean and Standard Deviation by Distance Class

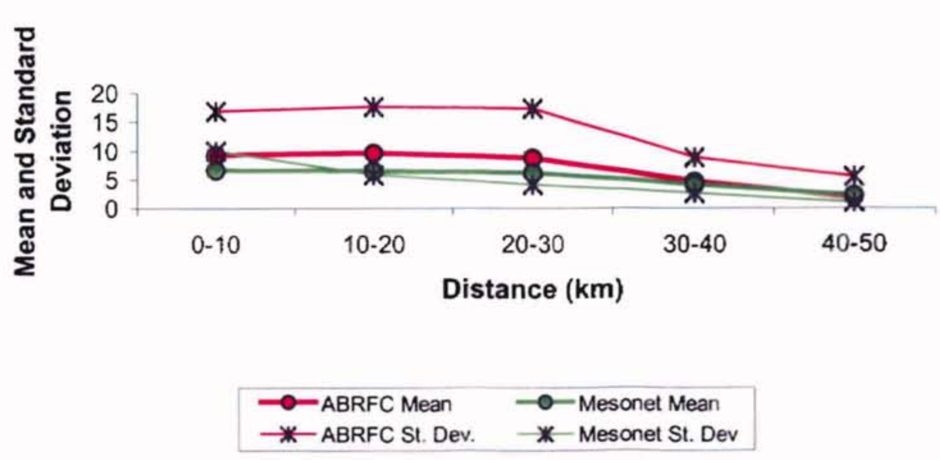

Table 4.36: **July 16, 1997 - Mean and Standard Deviation By Distance From Mesonet**

	Distance (km)				
	0-10	**10-20**	**20-30**	**30-40**	**40-50**
ABRFC Mean	3.516	4.474	4.982	3.887	1.825
Mesonet Mean	1.985	1.968	1.920	1.249	0.606
ABRFC St. Dev.	8.493	9.381	9.766	7.431	3.228
Mesonet St. Dev	4.829	2.558	1.716	1.148	0.365

Figure 4.68: July 16, 1997 ABRFC and Mesonet Mean and Standard Deviation by Distance Class

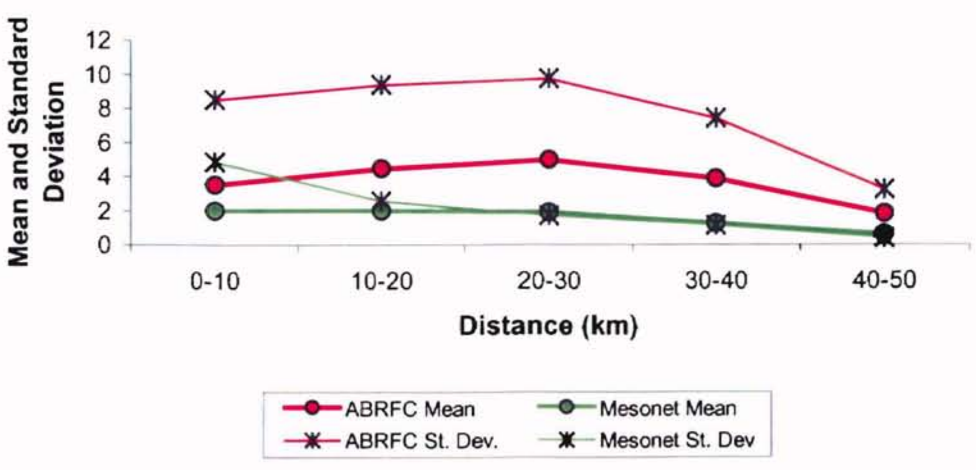

Table 4.37: **July 18, 1997 - Mean and Standard Deviation By Distance From Mesonet**

	Distance (km)				
	0-10	10-20	20-30	30-40	40-50
ABRFC Mean	13.691	13.621	11.230	2.752	0.587
Mesonet Mean	13.270	13.217	12.314	5.931	2.582
ABRFC St. Dev.	28.761	29.629	25.792	7.778	2.374
Mesonet St. Dev	24.903	17.777	13.748	5.334	1.424

Figure 4.69: July 18, 1997 ABRFC and Mesonet Mean and Standard Deviation by Distance Class

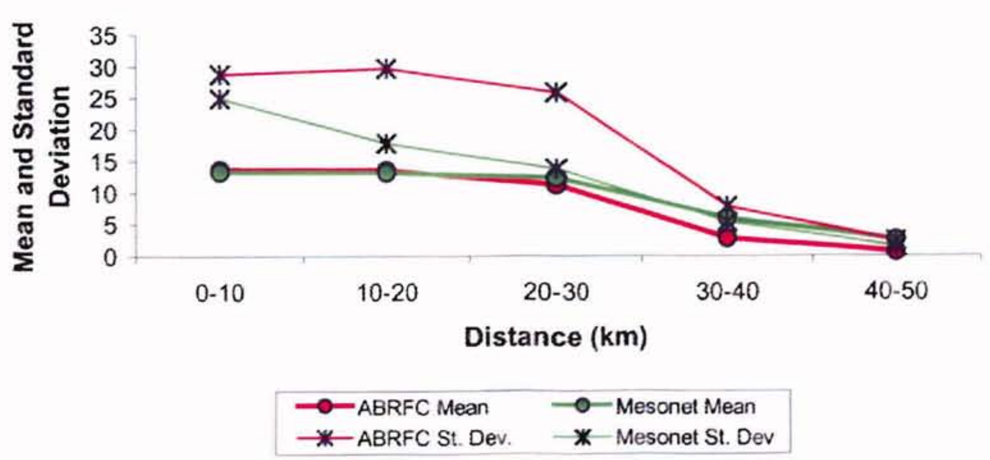

Table 4.38: **August 13, 1997 - Mean and Standard Deviation By Distance From Mesonet**

	Distance (km)				
	0-10	10-20	20-30	30-40	40-50
ABRFC Mean	5.587	5.681	4.830	2.462	0.030
Mesonet Mean	5.292	5.391	4.920	3.001	0.948
ABRFC St. Dev.	7.734	7.302	6.133	4.182	0.089
Mesonet St. Dev	7.164	4.800	3.419	2.563	1.113

Figure 4.70: August 13, 1997 ABRFC and Mesonet Mean and Standard Deviation by Distance Class

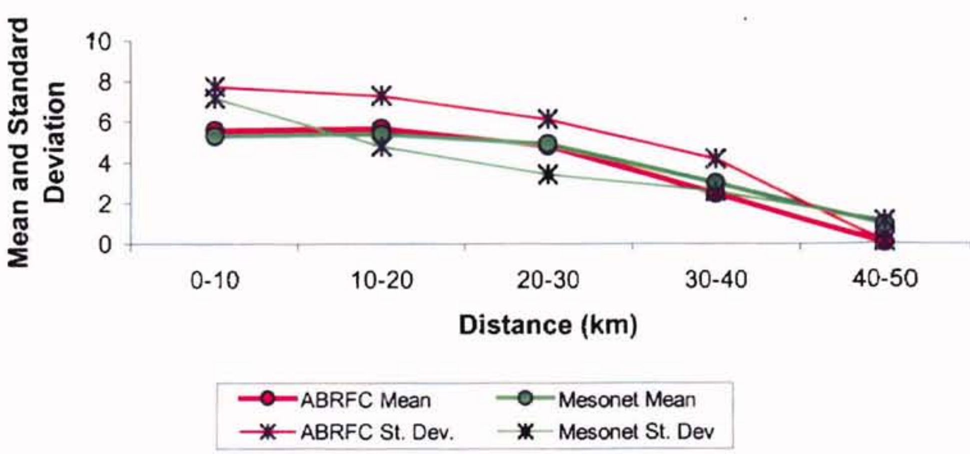

Table 4.39: **August 19, 1997 - Mean and Standard Deviation By Distance From Mesonet**

	Distance (km)				
	0-10	10-20	20-30	30-40	40-50
ABRFC Mean	21.237	20.489	18.121	10.730	7.608
Mesonet Mean	20.538	20.563	19.940	15.525	10.648
ABRFC St. Dev.	20.064	18.663	17.400	13.752	6.256
Mesonet St. Dev	17.202	10.728	8.263	7.050	2.331

Figure 4.71: August 19, 1997 ABRFC and Mesonet Mean and Standard Deviation by Distance Class

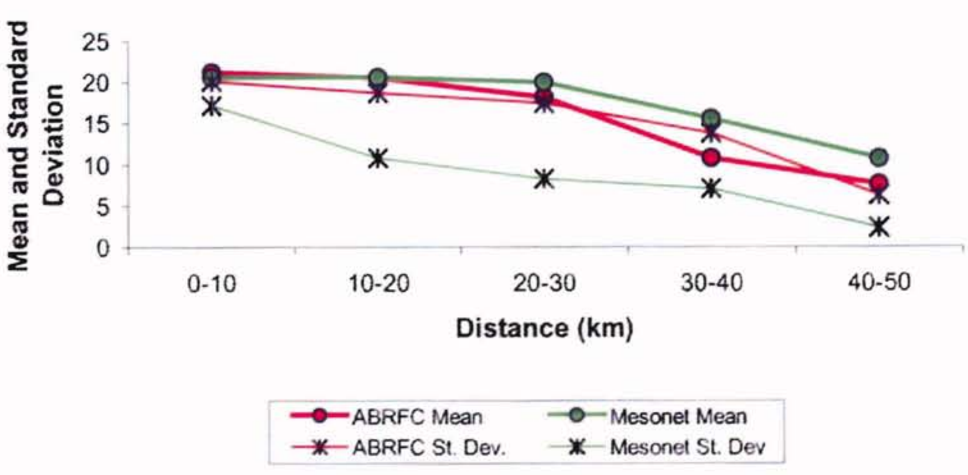

Table 4.40: **August 22, 1997 - Mean and Standard Deviation By Distance From Mesonet**

	Distance (km)				
	0-10	**10-20**	**20-30**	**30-40**	**40-50**
ABRFC Mean	14.334	14.575	13.408	5.574	0.031
Mesonet Mean	13.735	14.051	13.917	10.711	6.245
ABRFC St. Dev.	12.521	12.731	12.472	11.283	0.175
Mesonet St. Dev	10.661	8.877	8.121	7.493	2.305

Figure 4.72: August 22, 1997 ABRFC and Mesonet Mean and Standard Deviation by Distance Class

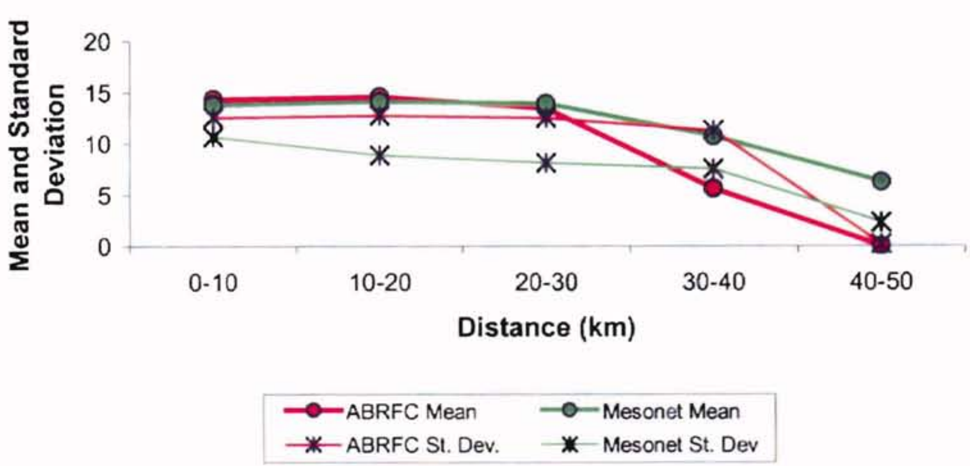

4.3 Distance From Radar

One of the goals of this study was to examine how distance from the WSR-88D Doppler radar sites affects the difference between the ABRFC and the Mesonet interpolated rainfall estimates. Due to the curvature of the earth, the radar signal can undershoot atmospheric moisture at close distances and overshoot them at farther distances. Smith (et al., 1996) document the close and far range bias in radar rainfall measurements. And Wilson and Brandes (1979) found that agreement between radar and surface (gage) rainfall estimates generally decreases with increasing radar range. By dividing the grid cells into different distance groups and performing a correlation on those groups separately, the effects of distance on estimate difference can be examined.

Each of the 11,132 4 x 4 kilometer cells in the study area was assigned a distance value based on the distance from the cell to its nearest radar station. Please refer back to Figure 3.18 for a location map of the various radar facilities used to produce the ABRFC rainfall estimate.

This distance value was used to group the cells based on categories of distance. An example would be grouping all cells that are within 100 kilometers of a Radar facility. By examining cells based on distance, the effects of distance on the two rainfall estimates can be examined.

The 4 x 4 kilometer cells were divided into three groups based on the cells distance from its nearest radar site. The first group consists of all cells that are located within 50 kilometers of a radar facility. A total of 1,519 cells out of the 11,132 cells in the study area fell into this group. Figure 4.73 illustrates the location of all cells that are within 50 kilometers of a Radar facility.

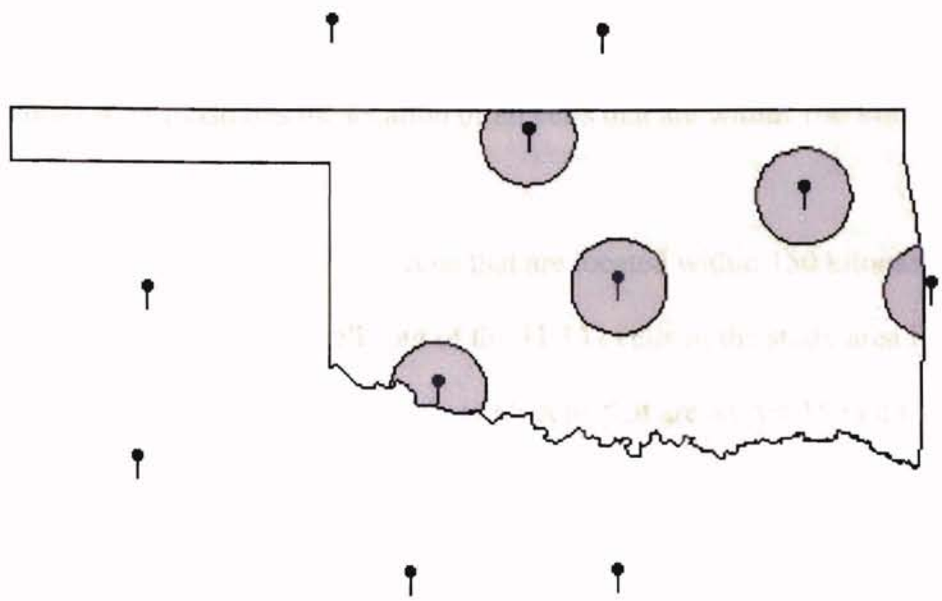

Figure 4.73: All cells within 50 Kilometers of a Radar Facility.

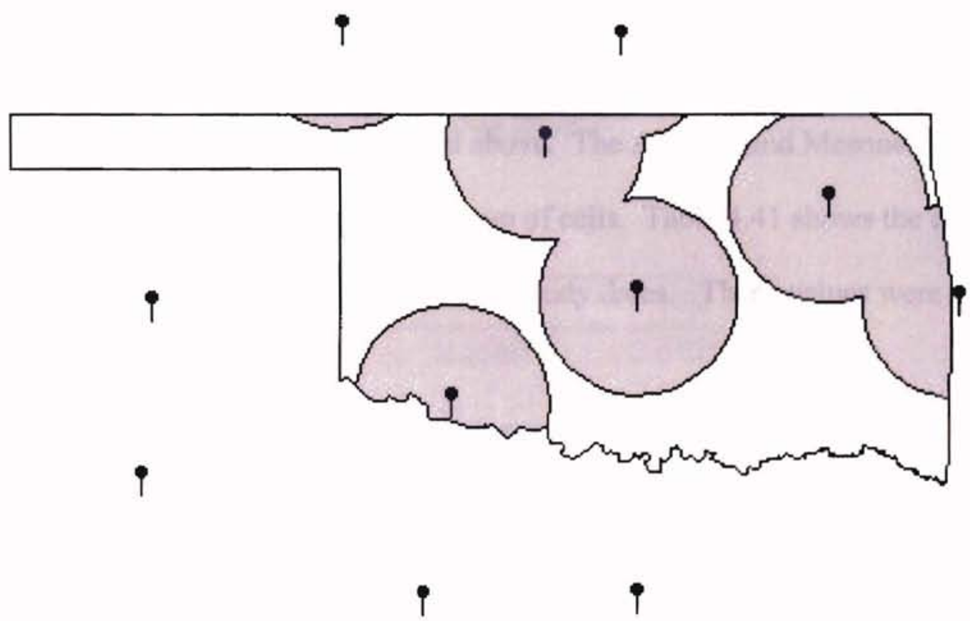

Figure 4.74: All cells within 100 Kilometers of a Radar Facility.

The second group consists of all cells that are located within 100 kilometers of a radar facility. A total of 5,627 cells out of the 11,132 cells in the study area fell into this group. Figure 4.74 illustrates the location of all cells that are within 100 kilometers of a radar facility.

The third group consists of all cells that are located within 150 kilometers of a radar facility. A total of 9,214 cells out of the 11,132 cells in the study area fell into this group. Figure 4.75 illustrates the location of all cells that are within 150 kilometers of a radar facility.

The ABRFC and Mesonet estimated rainfall values were correlated for each group of cells and repeated for the 1, 6 and 24-hour data. By examining how correlation values change from group to group, the effects of distance can be seen.

1 Hour Data

The 4 x 4 kilometer rainfall cells for the 1-Hour (11 UTC - 12 UTC) rainfall data were divided in into groups as mentioned above. The ABRFC and Mesonet estimated rainfall values were correlated for each group of cells. Table 4.41 shows the correlation values for the 1-hour data on each of the nine study dates. These values were plotted on the line graph in Figure 4.76.

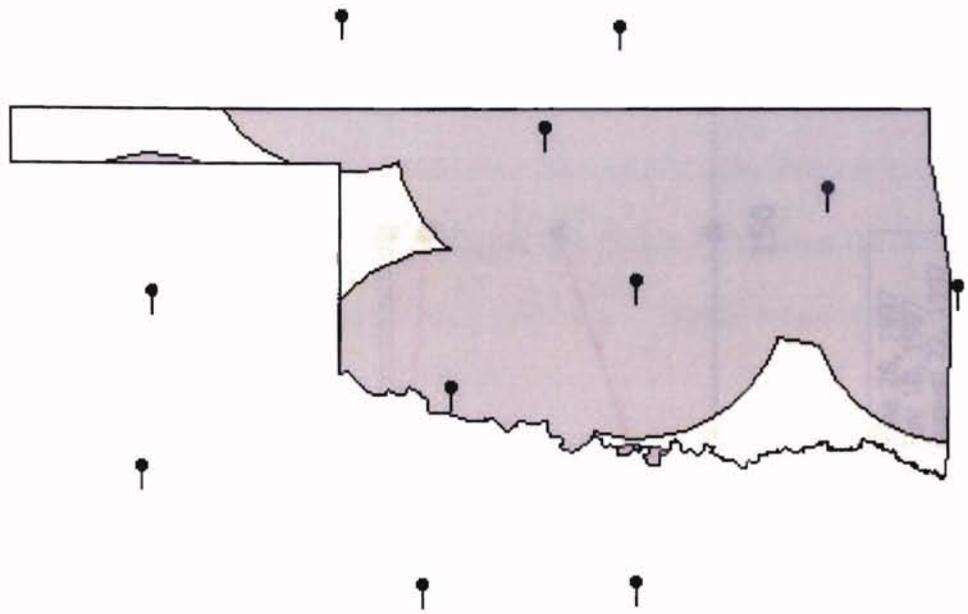

Figure 4.75: All cells within 150 Kilometers of a Radar Facility.

Table 4.41: Correlation of 1-Hour ABRFC and Mesonet Rainfall Estimates by Distance (km) from Radar

	Distance (km)		
Study Date	**50**	**100**	**150**
June 9, 1997	0.708**	0.586**	0.582**
June 24, 1997	*	*	0.284**
June 28, 1997	0.021	0.595**	0.515**
July 11, 1997	0.539**	0.593**	0.604**
July 16, 1997	*	*	*
July 18, 1997	0.704**	0.736**	0.727**
August 13, 1997	*	*	*
August 19, 1997	0.610**	0.760**	0.741**
August 22, 1997	0.880**	0.876**	0.871**

* - No Rainfall

** - Correlation is significant at the 0.01 level (2 tailed).

Figure 4.76:
Correlation of 1-Hour ABRFC and Mesonet Estimated Rainfall by Distance (km) from Radar

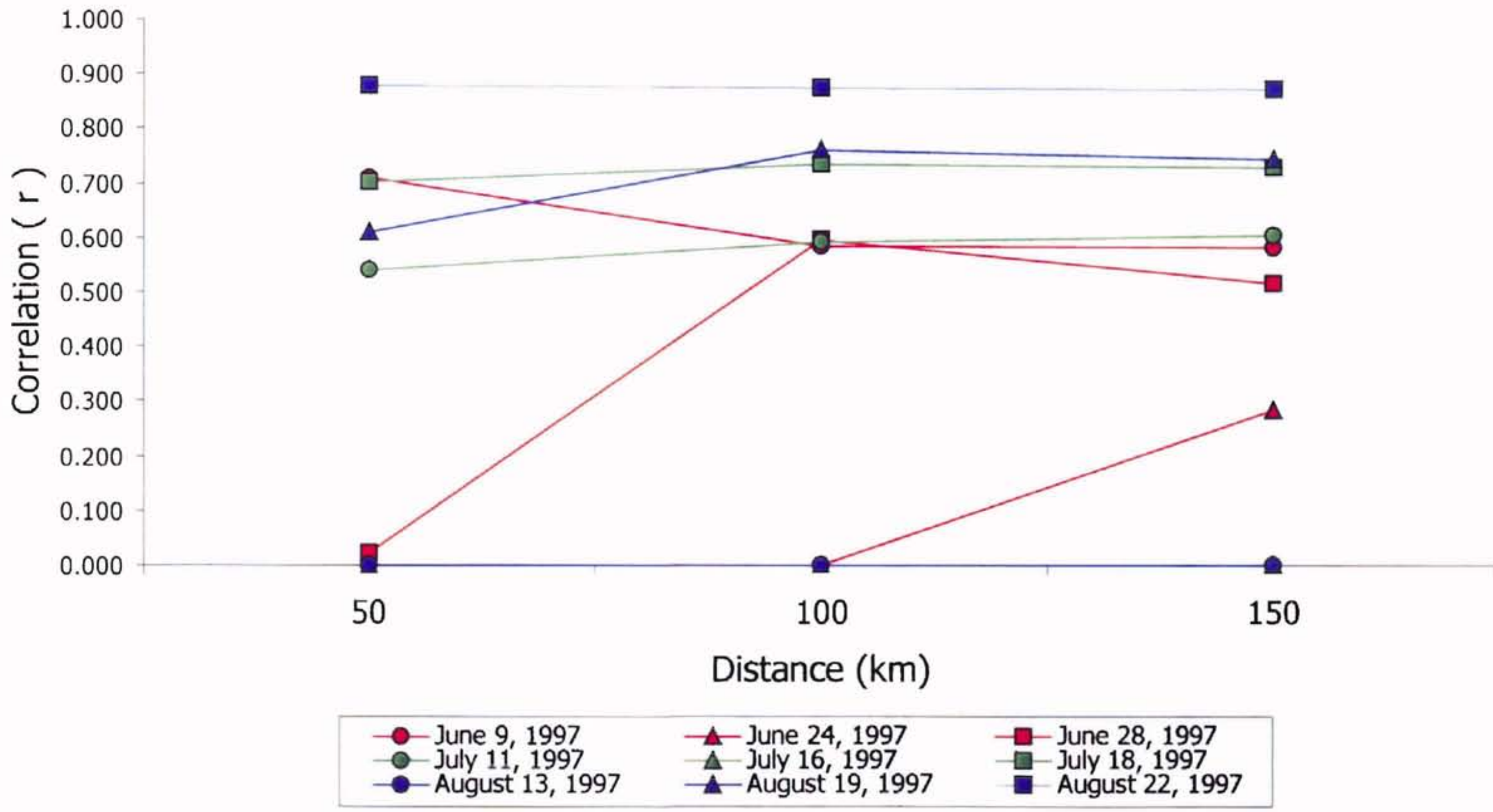

6 Hour Data

The 4 x 4 kilometer rainfall cells for the 6-Hour (6 UTC - 12 UTC) rainfall data were divided in into groups as mentioned above. The ABRFC and Mesonet estimated rainfall values were correlated for each group of cells. Table 4.42 shows the correlation values for the 6-hour data on each of the nine study dates. These values were plotted on the line graph in Figure 4.77.

24 Hour Data

The 4 x 4 kilometer rainfall cells for the 24-Hour (12 UTC - 12 UTC) rainfall data were divided in into groups as mentioned above. The ABRFC and Mesonet estimated rainfall values were correlated for each group of cells. Table 4.43 shows the correlation values for the 24-hour data on each of the nine study dates. These values were plotted on the line graph in Figure 4.78.

Table 4.42: Correlation of 6-Hour ABRFC and Mesonet Rainfall Estimates by Distance (km) from Radar

	Distance (km)		
Study Date	**50**	**100**	**150**
June 9, 1997	0.762**	0.765**	0.728**
June 24, 1997	*	0.110**	0.011
June 28, 1997	0.457**	0.473**	0.443**
July 11, 1997	0.557**	0.718**	0.729**
July 16, 1997	*	0.567**	0.453**
July 18, 1997	0.917**	0.896**	0.809**
August 13, 1997	0.574**	0.561**	0.465**
August 19, 1997	0.705**	0.804**	0.816**
August 22, 1997	0.861**	0.843**	0.846**

* - No Rainfall

** - Correlation is significant at the 0.01 level (2 tailed).

Figure 4.77:
Correlation of 6-Hour ABRFC and Mesonet Estimated Rainfall by Distance (km) from Radar

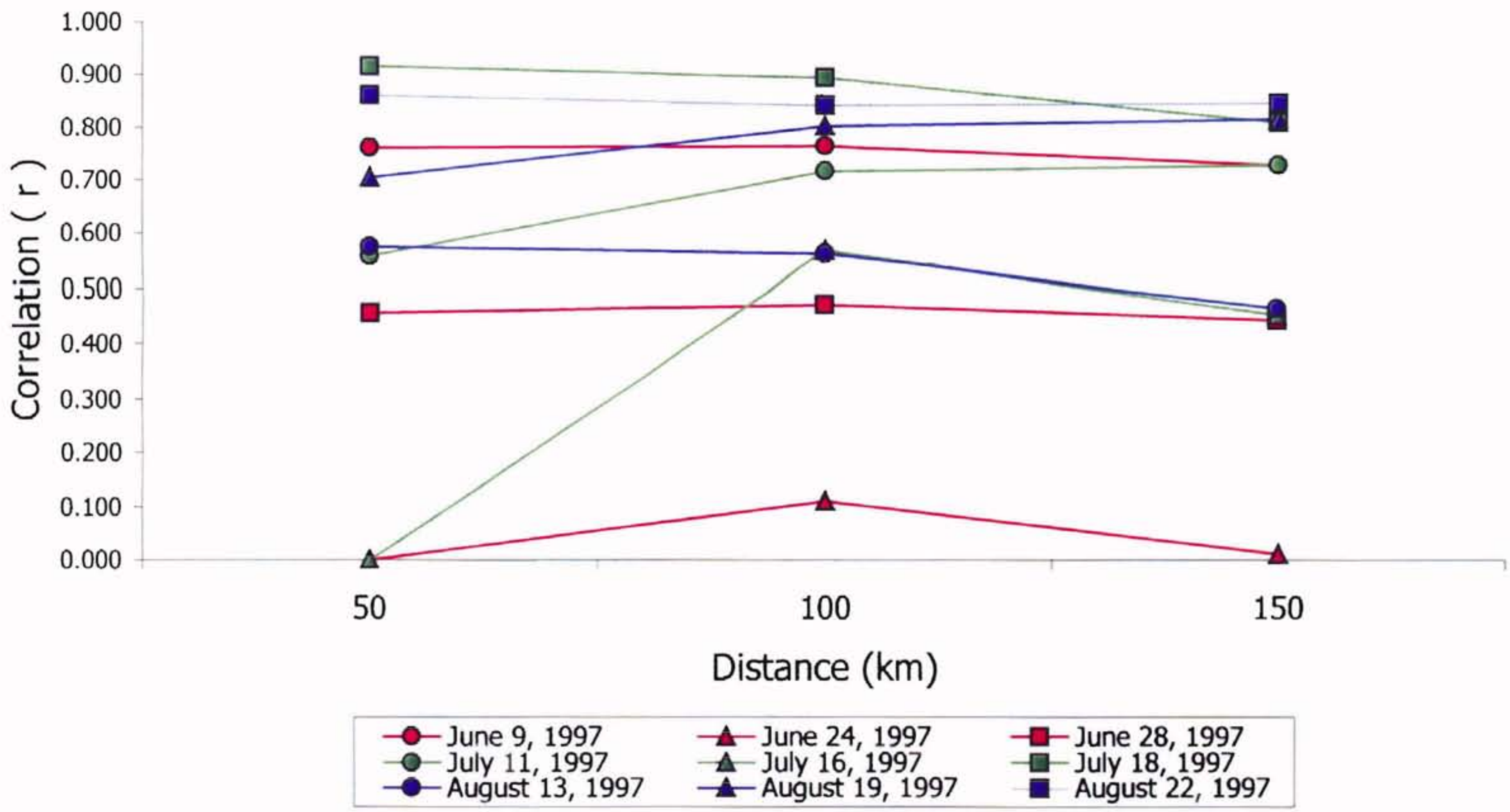

Table 4.43: Correlation of 24-Hour ABRFC and Mesonet Rainfall Estimates by Distance (km) from Radar

	Distance (km)		
Study Date	**50**	**100**	**150**
June 9, 1997	0.692**	0.635**	0.647**
June 24, 1997	0.552**	0.658**	0.681**
June 28, 1997	0.069**	0.336**	0.366**
July 11, 1997	0.762**	0.658**	0.683**
July 16, 1997	0.425**	0.509**	0.472**
July 18, 1997	0.926**	0.901**	0.878**
August 13, 1997	0.521**	0.785**	0.785**
August 19, 1997	0.725**	0.728**	0.760**
August 22, 1997	0.855**	0.850**	0.850**

** - Correlation is significant at the 0.01 level (2 tailed).

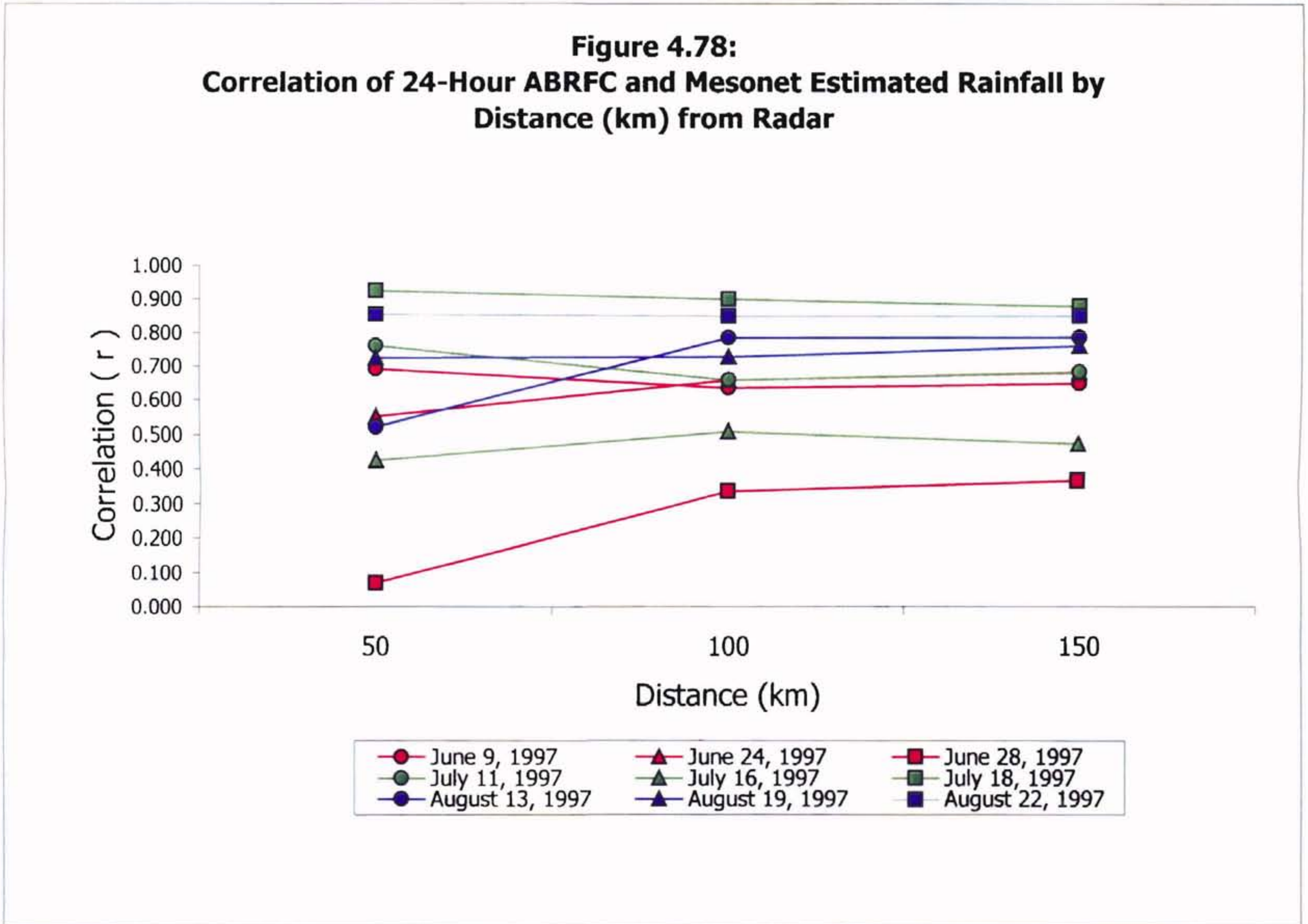
Figure 4.78:
Correlation of 24-Hour ABRFC and Mesonet Estimated Rainfall by Distance (km) from Radar
1.000
0.900
0.800
0.700
0.600
0.500
0.400
0.300
0.200
0.100
0.000
Correlation (r)
50
100
150
Distance (km)
June 9, 1997
June 24, 1997
June 28, 1997
July 11, 1997
July 16, 1997
July 18, 1997
August 13, 1997
August 19, 1997
August 22, 1997

4.4 Results Summary

Nine study dates, from a broad range of rainfall types, were compared on a visual as well as a statistical basis. Side by side maps of ABRFC and Mesonet interpolated rainfall illustrated the difference in how these two estimates spatially describe the same rainfall event. The cell by cell volumetric difference was mapped to illustrate where difference occurred and the quantity of that difference. A correlation (r) of the two estimates provided a statistical measure of the difference between the rainfall estimates.

The effects of distance, on the difference between the ABRFC and Mesonet interpolated rainfall estimates, was explored. The effects of cell distance from the Mesonet gages was examined by dividing the grid cells into distance groups according to their distance from the nearest Mesonet gage and performing separate correlation on those groups. Common statistical measures, such as mean and standard deviation were also examined on the basis of these same distance groups. The effects of cell distance from their nearest radar site was examined by dividing the grid cells into distance groups according to their distance from the nearest WSR-88D Doppler radar facility.

In the next chapter, these results will be used to examine the visual and statistical differences between the rainfall estimates. The correlation values of the previously mentioned distance groups will be used to draw conclusions on the effects of both the distance from Mesonet and the distance from radar on the difference between the two rainfall estimates. The broad range of rainfall types represented by the study dates will be used to draw conclusion about the impact of storm rainfall type on estimate difference. The results were repeated for 1, 6, and 24 hour time periods. The change in results between time scales will be used to draw conclusion about the effects of time scale on estimate difference.

CHAPTER 5

CONCLUSIONS AND DISCUSSION

5.1 Conclusions

Difference between Estimates

Differences between the Arkansas-Red Basin River Forecast Center (ABRFC) and Mesonet rainfall estimates are due to the differing nature of the estimation methods. The ABRFC estimate is calculated from returned radar signals, calibrated with Mesonet and other rain gages, and translated into estimated rainfall amounts for each grid cell in the HRAP coverage area, resulting in an estimation of rainfall in 4 km grid cells. The Mesonet estimate, however, directly measures rainfall at 114 points and then uses interpolation to estimate the amount of rainfall between these points.

Because the Mesonet rainfall measurements are used in the calibration of the ABRFC estimate, both estimates have similar rainfall measurements at or near each Mesonet location. This is evident in almost all the maps of difference, where "islands" of little or no difference (white) can be seen around many Mesonet locations. See Figure 4.35 for an example of this.

However, for the area between the Mesonet stations, the ABRFC estimate is relying on spatially continuous measurements whereas the Mesonet estimate is "blindly" calculating the amount of rainfall between the gages through the process of interpolation.

The difference between the two rainfall estimates in these areas often depends on where the rainfall occurs and the locations of the Mesonet gages.

Most of the difference between the rainfall estimates can be attributed to the following scenarios:

1. Rainfall detected by the ABRFC estimate, occurs between Mesonet gages and therefore goes undetected by the Mesonet rainfall estimate. This results in greater ABRFC estimated rainfall (red) on the difference maps presented in Chapter 4.
2. A Mesonet gage detects rainfall at the very edge of an ABRFC estimated rainfall event. The detected rainfall is interpolated outward and beyond the rainfall event boundaries estimated by the ABRFC. This results in greater Mesonet estimated rainfall (blue) on the difference maps presented in Chapter 4.
3. A rainfall event is detected by the Mesonet estimate and the ABRFC estimate but, the ABRFC describes the event as concentrated while the Mesonet estimate describes a smooth, homogenous event. The Mesonet interpolates this rainfall outward to areas where little or no rainfall is estimated by the ABRFC. This results in greater Mesonet estimated rainfall (blue) on the difference maps.

The following study dates contain examples of each cause of difference mentioned above.

The July 16, 1997 study date (24-hour) provides a good example of the difference that occurs when ABRFC estimated rainfall occurs between Mesonet gages. Figure 5.1 contains an ABRFC and Mesonet estimated rainfall map of a rainfall event in the northwest quarter of the study area. A map of the difference between the two estimates is also provided. For the purposes of comparison, the Mesonet gage locations are shown in each map as reference points.

Figure 5.1: 24 Hour rainfall event on the July 16, 1997 study date as estimated by ABRFC and Mesonet.

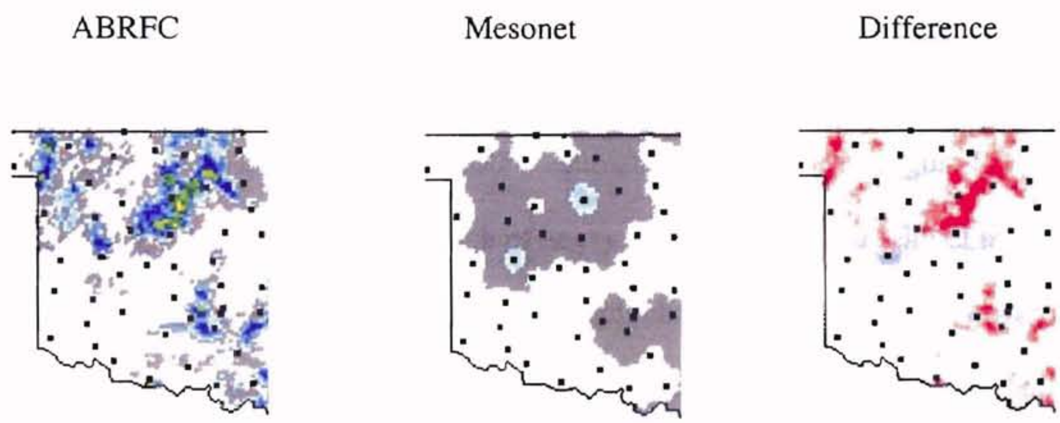

Notice how almost all of the heaviest ABRFC estimated rainfall for this event falls between the Mesonet locations. As can be seen in the map of Mesonet estimated rainfall, only a small portion of the ABRFC estimated rainfall is reflected in the Mesonet estimate. The disagreement between the estimates can be seen in the map of difference, where red indicates a greater ABRFC estimated rainfall and blue indicates a greater Mesonet estimated rainfall. When ABRFC estimated rainfall occurs between Mesonet gage locations, there is a two-fold consequence. First, rainfall is not detected by the

Mesonet gages and therefore not interpolated, resulting in a lower estimate of rainfall that the ABRFC. Secondly, the ABRFC estimate does not receive the benefit of the Mesonet gages in calibrating its estimate. For this rainfall event alone, the ABRFC estimates a total volume of 8.8 million cubic meters of rainfall while the Mesonet estimates only 2.8 million cubic meters of rainfall. The interpolated Mesonet estimate indicates approximately a third of the rainfall volume of the ABRFC estimate. When applied to hydrologic modeling efforts, this difference can be significant. Individual grid cells in this area may show only a 20 to 25 mm difference but, across a large watershed or the whole state, these differences will accumulate, resulting in potentially significant impacts on hydrologic models.

The July 11, 1997 (24-hour) study date provides a good example of a Mesonet gage detecting only the edge of an ABRFC estimated rainfall event. Figure 5.2 provides an ABRFC and Mesonet map of a patch of heavy ABRFC estimated rainfall in the southwest quarter of the study area falls in the neighborhood of several Mesonet gages. The two estimates are similar but the Mesonet estimate does not have ABRFC ability to spatially describe the edge of a storm. As a result, the Mesonet gages on the eastern and southeastern edge of the event, interpolate the rainfall outward and past the boundaries estimated by the ABRFC. This disagreement can be seen in the map of difference in the form of an intense blue plume extending outward from the rainfall event.

Figure 5.2: 24 Hour rainfall event on the July 11, 1997 study date as estimated by ABRFC and Mesonet.

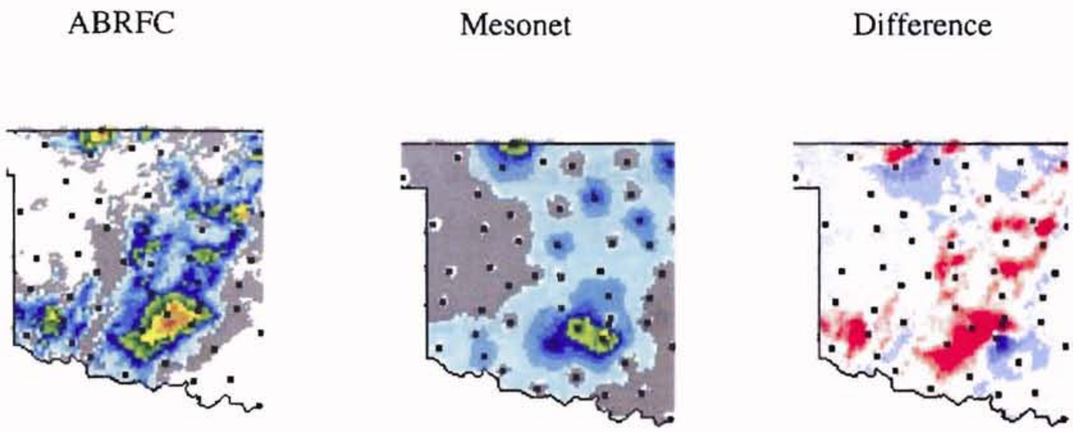

For this rainfall event alone, the ABRFC estimates a total volume of 3.4 billion cubic meters of rainfall while the Mesonet estimates 2.2 billion cubic meters of rainfall. For the area under consideration, the interpolated Mesonet estimate indicates almost 65% of the rainfall volume of the ABRFC estimate. However, the placement of this volume by the Mesonet estimate may produce a bigger hydrologic impact than any underestimated volume. The plume of bright blue (greater Mesonet estimated rainfall) indicates that the Mesonet estimate is estimating a large amount of rainfall volume where the ABRFC estimate indicates little or no rainfall. If this rainfall is misplaced over an individual watershed, the hydrologic input for the watershed could be overestimated. As mentioned in Chapter 2, one of the benefits of radar rainfall measurement over gage network measurement is its ability to delineate areas of no rainfall or areas of high rainfall.

The June 28, 1997 (24-hour) study date provides a good example of a rainfall event detected by both the ABRFC and Mesonet rainfall estimates, but spatially described in different ways. Figure 5.3 provides an ABRFC and Mesonet estimated rainfall map of a rainfall event along the eastern border of the state. The area of interest is circled in the ABRFC map.

This rainfall event is detected by the ABRFC and Mesonet rainfall estimates. Mesonet gages are present where the ABRFC estimated rainfall is indicated and also present where the ABRFC estimate indicates little or no rainfall.

Figure 5.3: 24 Hour rainfall event on the July 11, 1997 study date as estimated by ABRFC and Mesonet.

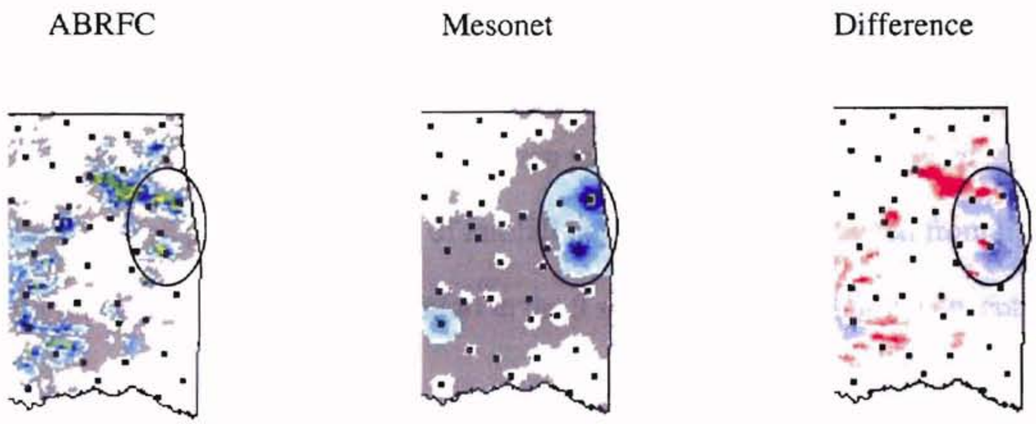

The ABRFC estimate indicates a rainfall event with high spatial variation. The rainfall appears to occur in small concentrated patches with little or no rainfall in between. The Mesonet estimate detects the same patches of rainfall but the rainfall is interpolated outward to areas where little or no rainfall is indicated by the ABRFC estimate. The Mesonet estimate also indicates a much more homogenous rainfall event. The resulting difference can be seen in the difference map. The example area is dominated by blue, indicating greater Mesonet estimated rainfall for the area. For this rainfall event alone, the ABRFC estimates a total volume of 1.3 billion cubic meters of rainfall while the Mesonet estimates 1.6 billion cubic meters of rainfall. Although, the total volume indicated by the two estimates are similar, the two rainfall estimates disagree on where this rainfall occurred. For hydrologic modeling applications, the difference in the spatial variability of rainfall described by two rainfall inputs can significantly impact model outputs even if the same average volume for the area is used. As mentioned in Chapter 2, Wilson (et al. 1979) concluded that ignoring the spatial variability of precipitation input, given when the total depth of rainfall is preserved, could have significant influences on the runoff hydrograph.

Storm Type and Correlation

The study dates were purposely chosen to represent of a broad range of storm types and rainfall patterns. The rate of rainfall in the 9 study dates ranged from light to heavy. The spatial pattern of the rainfall in the 9 study dates ranged from concentrated to homogenous.

As demonstrated above, the location of the rainfall in reference to Mesonet gages has an impact on how well the two rainfall estimates agree. The Mesonet locations are an average of 33 kilometers apart. The more even and widespread the rainfall, the more likely it is to be detected by the Mesonet gages. If the rainfall occurs in small, scattered patches less than 33 kilometers in size, it is more likely to fall between Mesonet gages and go undetected.

Figure 5.4 illustrates the storm type of each study date. Each study date was scored from 1 to 10 according the intensity of the rainfall, from low rainfall to high rainfall. The study dates were also ranked from 1 to 9 according to the amount of spatial

Figure 5.4: Scatterplot of storm rainfall rate versus storm spatial variability. Each study date was scored from 1 to 10 according to the intensity of rainfall and ranked from low to high according to its spatial variability. Each point is labeled with its corresponding date and correlation (r) value, all of which were significant at the 0.01 significance level (2 tailed).

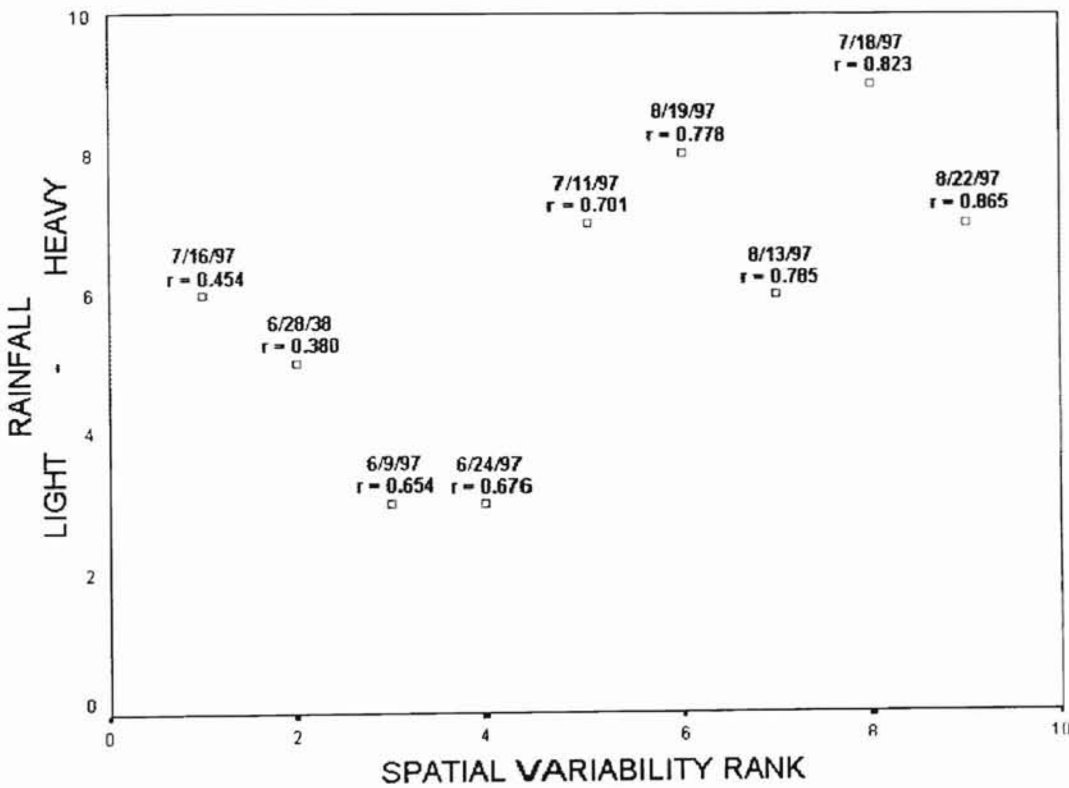

variability in the rainfall. The dates were plotted accordingly on the scatterplot in Figure 5.4.

There was a noticeable pattern in where the study dates appeared on the scatterplot. The dates with the highest correlation (r) between the ABRFC and the interpolated Mesonet estimates, tended to be the dates with higher rainfall and the lowest spatial variability. The study dates with the highest correlation between the estimates were July 18, 1997 and August 22, 1997. The rainfall maps for these dates are displayed in Figure 4.37 and Figure 4.55 respectively. The ABRFC rainfall estimate for both of these dates exhibited a smooth rainfall pattern. Although the rainfall intensity is high, the transition from areas of high rainfall to areas of low rainfall is gradual. This rainfall pattern closely matches the pattern that results from the interpolation of point rainfall measurements.

Because the ABRFC rainfall estimate uses radar, it has an advantage over the Mesonet estimate when describing the spatial variability of rainfall events. However, for spatially smooth, homogenous rainfall events, interpolated gage data can provide a description of spatial variability that is comparable to that of gage calibrated radar estimates. Therefore it can be concluded that the differences between the ABRFC and Mesonet rainfall estimates will be less significant when spatially uniform rainfall is being examined.

Distance from Mesonet

The distance to the nearest Mesonet weather station was determined for all of the 11,131 grid cells in the study area. The cells were grouped by distance, and the rainfall values for all cells were correlated, to determine if agreement between the ABRFC and Mesonet rainfall estimate would diminish with distance from the Mesonet locations.

When comparing the ABRFC and Mesonet rainfall estimates by distance group, a clear pattern emerges. There is a negative relationship between distance from Mesonet and the correlation (*r*) value of the cells in a given distance group. This pattern was present in the 1 hour, 6 hour and 24 hour data.

Referring back to the 1 hour data in Figure 4.60, it is apparent that the correlation (*r*) value of each distance group decreases as the distance to Mesonet increases. This negative trend clearly increases as more time is included. The same pattern, only stronger, is evident in the 6 hour data in Figure 4.61. The trend becomes even stronger in the 24 hour data in Figure 4.62. From this trend, it can be concluded that the differences between the ABRFC and Mesonet rainfall estimates are greater with increasing distance from the Mesonet gages. This result should be considered of practical significance when considering watershed or catchment areas that exist between gages.

Storm type comes into play when examining the effects of distance from Mesonet. In the previous section, it was noted that the most homogenous rainfall events exhibited the highest correlation between the ABRFC and Mesonet rainfall estimates. The same pattern emerges in Figure 4.62. The most homogenous rainfall dates exhibit the highest correlation (*r*) values across all distance groups. Also, the trend of decreasing correlation (r) values with distance is less pronounced for uniform, homogenous rainfall events. In contrast, the rainfall dates with the most random, scattered rainfall pattern exhibit a rapid drop in correlation as distances from Mesonet increase. This indicates that the effects of distance from the Mesonet gages are less significant when homogenous, uniform rainfall events are considered.

Distance from Radar

There was no clear pattern of decreasing correlation values associated with a cells distance from the radar facilities. Referring to the one-hour data in Figure 4.76, none of the study dates exhibit a downward trend with distance. The same results can be seen in the six-hour data in Figure 4.77. The twenty-four hour data in Figure 4.78 shows steady correlation values with distance from radar.

The effects of rainfall type can, once again, be seen in the 1 hour, 6 hour, and 24 hour data when examining the effects of distance from radar on correlation values. The study dates appear in much the same order as they appeared in the previously mentioned Mesonet charts in Figure 4.60, Figure 4.61, and Figure 4.62. Study dates that exhibit homogenous rainfall patterns, appear toward the top of the charts while those dates exhibiting random, scattered rainfall patterns appear near the bottom.

Time Scale and Correlation

There was not a clear trend associating the time scale (1, 6 or 24 hour time periods) with higher correlation. However, the patterns of decreasing correlation with distance became clearer as longer time periods were considered. For example, when examining the effects of distance from Mesonet on correlation in Figure 4.60, the trend was already evident at the 1 hour time scale. But the distance trend became clearer when

6 hours of accumulated rainfall was considered in Figure 4.61. The distance trend became even clearer for the 24 hour time scale in Figure 4.62.

This supports some of the findings in a study by Finnerty and Johnson (1997) that examined the effects of different rainfall time intervals on hydrologic model outputs. Finnerty and Johnson (1997) compared radar and gage derived rainfall accumulations in 1 and 6 hour time intervals over a 7 month period to help determine if a difference in the time scale would have an effect on model output. He determined that the 6-hour radar and gage rainfall data had similar estimates of the timing of rainfall events, and that the 1-hour radar and gage rainfall data showed more discrepancies in the timing of events. He also determined that the radar rainfall data captured more of the variability in the precipitation fields than the gage rainfall data for the 1-hour time steps. However, the variability of the radar and gage rainfall data was nearly equal at the 6-hour time step.

5.2 Problems and Discussion

There were many statistical tests that were not available simply because the ABRFC and Mesonet data were not normally distributed and no statistical test exists to compare surfaces. Simple correlation was the most straightforward means to test the correspondence between the two rainfall estimates.

The examination of radar distance effects was complicated by the fact that multiple WSR-88D radar sites could be used to provide a total rainfall measurement for a particular point. If a grid cell is overlapped by many radar coverage areas, an average of all the radar signals for that point was used to calculate an ABRFC rainfall estimate. The ArcView GIS software would only allow the distance to the nearest radar facility to be applied. Grid cells that were relatively near a radar location could also have more distant radar facilities involved in calculating the rainfall for that point. With further programming, the ArcView GIS software could be manipulated to include multiple radar distances.

In contrast to the findings of this study, some distance from radar effects were found by Pereira et. al. (1998) in his study of the ABRFC product. He found that, at the fringes of radar coverage by several radars, grid cells located at the maximum range of the WSR-88D often exhibited spurious rainfall gradients. Pereira et. al. (1998) also found that in these overlapping, fringe areas, the WSR-88D produced an underestimate of rainfall accumulation as much as 30%.

The examination of time scale was inhibited by the fact that the different time periods were not associated by rainfall type. Even though twenty-four hour rainfall estimate included rainfall from the one and six hour rainfall periods, they were not associated as far as storm type. The different time data for the same date could exhibit completely different rainfall volume and spatial qualities.

Comparison of these two rainfall estimates is hindered by the fact that they are linked by the rain gage data involved. The ABRFC estimate depends on over 500 gage measurements, including measurement from the Mesonet rainfall gages, to calibrate the final product. This association complicates any comparison of the two estimates. Also, there is no meta-data available to tell the user which and how many of the Mesonet gages are used for a particular study date.

The ArcInfo GIS software was limited in its interpolation capabilities. There were only a few interpolation methods available and it would be valuable to include the other methods alongside the inverse distance weighted method to see which one would most closely compare with the ABRFC estimate.

The main goal of the study was to determine if the spatial differences between the ABRFC and Mesonet rainfall estimates are significant. This goal is reflected in the research hypothesis mentioned in Section 1.2 of Chapter 1. Several factors, such as storm type, distance from Mesonet gages, distance from radar sites, and time scale, were examined to aid in this determination.

The storm type, or spatial variability of the rainfall event, was found to have an effect on the difference between the two rainfall estimates. The differences between the estimates increased as the spatial variability of the rainfall events increased. The Mesonet estimate was limited in its ability to capture the spatial variability of rainfall while the ABRFC estimate was able to describe the spatial variability of the rainfall in great detail. The study area frequently experiences intense, variable rainfall events, therefore, the differences between the estimates are of practically significance to any hydrologic study to which these rainfall inputs may be applied.

The distance of a grid cell from the nearest Mesonet gage was found to have an effect on the difference between the two rainfall estimates. The differences between the estimates increased with distance from the Mesonet gages. Again, the Mesonet estimate was limited in its ability to describe the spatial variability of rainfall between the gages. The ABRFC estimate could rely on its radar signal to fill in the information between the gages while the Mesonet estimate depended on the interpolation of the gage measurements alone. The trend, however, was tempered by the influence of storm type. The difference between the estimates did not increase significantly with distance when uniform, homogenous rainfall events were examined. If most of the area in a small watershed falls between the Mesonet gages, the difference in rainfall volume predicted by the two estimates could be practically significant.

The difference between the two rainfall estimates was not found to be associated with the distance of a grid cell from the nearest radar site. The difference between the estimates did not significantly increase as distance to radar sites increased.

The difference between the two rainfall estimates was not found to be associated with the temporal resolution (1, 6, and 24 hour periods). The previously mentioned trends did not change when longer time periods were examined.

Overall, the differences in how the ABRFC and the Mesonet rainfall estimates spatially describe the same rainfall event are of practical significance in a number of hydrologic applications. The spatial differences often translate into volumetric differences that could affect hydrologic modeling. Even when the two estimates predict the same volume of rainfall, the difference in where that rainfall is predicted can affect runoff hydrographs or soil moisture models.

5.3 Further Studies

There are several areas in this project that could be explored for further insight. Only one type of interpolation, inverse distance weighted, was used in comparison with the ABRFC rainfall data. What effect would different interpolation methods have on the correlation values? A study by Yuen (1994) examined the differences between several different interpolation methods in estimating evapotranspiration. Yuen (1994) used many different techniques to interpolate Mesonet weather parameters such as temperature, solar radiation, wind speed and direction. He determined that there was no significant difference between the results of the different interpolation methods. It seems likely that this would hold true for rainfall data as well. But it would be useful to examine how rainfall estimates differ with interpolation method and the effort would help to either support or refute Yuen's (1994) conclusions.

Only one spatial resolution (4x4 kilometers) was used to examine the rainfall estimates. The effects of spatial resolution could be examined by creating Mesonet and ABRFC rainfall grids of several different sizes. Perhaps using a 16 by 16 kilometer cell size rather than the 4 by 4 kilometer cell size would have different results.

One difficulty in comparing the two rainfall estimates was that neither estimate could be referred to as the "true" estimate. The estimates need to be compared to actual rainfall to determine which estimate is more accurate at estimating the total amount of rainfall falling in a given area. Other data sources, such as a dense gage network, could be used to compare the Mesonet and ABRFC estimates. The ABRFC and Mesonet rainfall estimates could be compared using the dense gage network as a benchmark reference to determine which rainfall estimate more accurately describes the rainfall for that area.

Bibliography

ABRFC. 1999. Arkansas-Red Basin River Forecast Center. Radar precipitation products. (http://info.abrfc.noaa.gov/index.html).

Bevon, K.J. and G.M. Hornberger. 1982. Assessing the effect of rainfall pattern of precipitation on modeling stream flow hydrographs. *Water Resources Bulletin* 18(5):823-829.

Brandes, E.A. 1975. Optimizing rainfall estimates with the aid of radar. *Journal of Applied Meteorology* 14:1339-1345.

Brock, F., K. Crawford, R. Elliott, G. Cuperus, S. Stadler, H. Johnson, and M. Eilts. 1995. The Oklahoma Mesonet: A technical overview. *Journal of Atmospheric and Oceanic Technology* 12:5-19.

Cederwall, R.T. 1999. Estimates of precipitation for the SGP97 study area based on WSR-88D radar products and ARM observations. 14th Conference on Hydrology. American Meteorological Society.

Choubey, I. 1997. Effect of spatial variability of rainfall on modeling hydrologic/water quality processes. Ph.D. Dissertation. Oklahoma State University, Stillwater, OK.

Collier, C.G. 1986a. Accuracy of rainfall estimates by radar; Part I, Calibration by telemetering raingauges. *Journal of Hydrology* 83:207-223.

Collier, C.G. 1986b. Accuracy of rainfall estimates by radar; Part II, Comparison with rain gauge network. *Journal of Hydrology* 83:225-233.

Corradini, C. and V.P. Singh. 1985. Effect of spatial variability of effective rainfall on direct runoff by geomorphic approach. *Journal of Hydrology* 81:27-43.

Cruten, J.D. and C. Obled. 1982. Objective analyses and mapping techniques for rainfall fields: an objective comparison. *Water Resources Research* 18:413-431.

Dawdy, D. R. and J.M. Bergman. 1969. Effect of rainfall variability on stream flow simulation. *Water Resources Research* 5(5):958-969.

Duncan, M.R., B. Austin, F. Fabry, and G.L. Austin. 1993. The effect of gage sampling density on the accuracy of streamflow prediction for rural catchments. *Journal of Hydrology* 142:445-476.

ESRI. 1999. The Environmental Systems Research Institute. ARC/INFO and ArcView GIS computer software. Redlands, California.

Finnerty, B.D., and D. Johnson. 1997. Comparison of mean areal precipitation estimates derived from NEXRAD radar vs. rain gage networks. International Association for Hydraulic Research. August 15, 1997. Pages 601-606.

Finnerty, B.D., M.B. Smith, D.J. Seo, V. Koren, and G.E. Moglen. 1997. Space-time scale sensitivity of the Sacramento model to radar-gage precipitation inputs. *Journal of Hydrology* 203:21-38.

Fulton, R.A., J.P. Breidenbach, D.J. Seo, D.A. Miller, T. O'Bannon. 1997. The WSR-88D rainfall algorithm. Submitted to *Weather and Forecasting*.

Greene, D.R., M.D. Hudlow, R.K. Farnsworth. 1979. A multiple sensor rainfall analysis system. Preprint volume: Third Conference on Hydrometeorology (Bogata), American Meteorological Society, Boston, MA, pp. 44-53.

Greene, D.R., and M.D. Hudlow. 1982. HRAP project. National Weather Service, Hydrologic Research Laboratory, Silver Spring, MD, internal publication.

Groisman, P.Y., and D.R. Legates. 1994. The accuracy of United States Precipitation Data. *Bulletin of the American Meterorological Society* 75(3):215-227.

Hildebrand, P.H., N. Towery, and M.R. Snell. 1979. Measurement of convective mean rainfall over small areas using high density raingages and radar. *Journal of Applied Meteorology* 18:1316-1326.

Hudlow, M.D. 1988. Technological developments in real-time operational hydrologic forecasting in the United States. *Journal of Hydrology* 102:69-92.

Klazura, G.E., and D.A. Imy. 1993. A description of the initial set of analysis products available from the NEXRAD WSR-88D system. *Bulletin of the American Meteorological Society* 74(7):1293-1311.

Legates, D.R., and T.L. Deliberty. 1993. Precipitation measurement biases in the United States. *Water Resources Bulletin* 29(5):855-861.

Legates, David R., Kenneth R. Nixon, Thomas D. Stockdale, and Geoffrey Quelch. 1996. Soil water modeling using a water resource decision support system with calibrated WSR-88 precipitation estimates and meteorological inputs. American Water Resources Association. Symposium Proceedings: GIS and Water Resources.

Legates, D.R. 2000. Real-time calibration of radar precipitation estimates. *Professional Geographer* 52(2):235-246.

McGrew, J.C., and C.B. Monroe. 1993. An Introduction to Statistical Problem Solving in Geography. McGraw-Hill. Boston, MA.

Morrissey, M.L., J.A. Maliekal, J.S. Greene, and J. Wang. 1995. The uncertainty of simple spatial averages using rain gage networks. *Water Resources Research* 31:2011-2017.

NetCDF. 1999. NetCDF data archive software. http://www.unidata.ucar.edu/packages/netcdf.

Obled, C., J. Wending, and K. Beven. 1994. The sensitivity of hydrological models to spatial rainfall patterns: an evaluation using observed data. *Journal of Hydrology* 159:305-333.

Pereira, A.J., K.C. Crawford, and C.L. Hartzell. 1998. Improving WSR-88D hourly rainfall estimates. American Meteorological Society.

Pereira, A.J., and K.C. Crawford. 1995. Integrating WSR-88D estimates and Oklahoma Mesonet measurements of rainfall accumulation: A statistical approach. 27th Conference on Radar Meteorology. American Meteorological Society.

Rudra, R.P., W.T. Dickinson, and E.L. Von Euw. 1993. The importance of precise rainfall inputs in non-point source pollution modeling. *American Society of Agricultural Engineering* 36(2):445-450.

Seo, D.J., and J.A. Smith. 1996. Characterization of climatological variability of mean areal rainfall through fractional coverge. *Water Resources Research* 33(7):2087-2095.

Seo, D.J. 1998. Real-time estimation of rainfall fields using radar rainfall and rain gage data. *Journal of Hydrology* 208:37-52.

Shanhltz, V.O., B.B. Ross, and J.F. Carr. 1981. Effect of spatial variability on the simulation of overland and channel flow. *Transactions of the ASAE* 24(1):124-138.

Smith, J.A., D.J. Seo, M.L. Baech, and M.D. Hudlow. 1996. An intercomparison study of NEXRAD precipitation estimates. *Water Resources Research* 32(7):2035-2045.

SPSS. 1996. SPSS 7.5 for Windows Statistical Software. December 20, 1996.

Yuen, Oi-Ming Daniel. 1994. Estimating Regional Reference Evapotranpiration From Meso-Dimensional Meteorological Data. M.S. Thesis. Oklahoma State University.

Wilson, J.W. 1970. Integration of radar and rain gage data for improved rainfall measurement. *Journal of Applied Meteorology* 9:489-497.

Wilson, J.W. and E.A. Brandes. 1979. Radar measurement of rainfall – A summary. *Bulletin of the American Meteorological Society* 60:1048-1058.

Wilson, C.B., J.B. Valdes, and I. Rodriquez-Iturbe. 1979. On the influence of the spatial distribution of rainfall on storm runoff. *Water Resources Research* 15(2):321-328.

Woodley, W.L., A.R. Olsen, A. Herndon, and V. Wiggert. 1975. Comparison of gauge-radar methods of convective rain measurements. *Journal of Applied Meteorology* 14:909-928.

APPENDIX A

APPENDIX A-TABLE OF MESONET WEATHER STATIONS WITH GEOGRAPHIC COORDINATES AND FOUR LETTER IDENTIFIER

SITE	LATITUDE	LONGITUDE
ACME	34.8056	-98.0056
ADAX	34.7989	-96.6692
ALTU	34.5872	-99.3378
ALVA	36.7797	-98.6717
ANTL	34.2242	-95.7006
APAC	34.9139	-98.2917
ARDM	34.1922	-97.0850
ARNE	36.0728	-99.9014
BBOW	34.0144	-94.6131
BEAV	36.8022	-100.5300
BESS	35.4017	-99.0589
BIXB	35.9625	-95.8661
BLAC	36.7544	-97.2539
BOIS	36.6925	-102.4927
BOWL	35.1717	-96.6314
BREC	36.4119	-97.6942
BRIS	35.7808	-96.3539
BUFF	36.8314	-99.6408
BURB	36.6342	-96.8111
BURN	33.8909	-97.2692
BUTL	35.5914	-99.2706
BYAR	34.8497	-97.0033
CALV	34.9925	-96.3342
CAMA	36.0283	-99.3464
CATO	36.2619	-95.7572
CENT	34.6086	-96.3331
CHAN	35.6528	-96.8042
CHER	36.7481	-98.3628
CHEY	35.5458	-99.7275
CHIC	35.0319	-97.9144
CLAR	36.3172	-95.6417
CLAY	34.6556	-95.3281
CLOU	34.2231	-95.2494
COOK	35.6794	-94.8486
COPA	36.9097	-95.8853
DURA	33.9206	-96.3200
ELRE	35.5481	-98.0358
ERIC	35.2047	-99.8033
EUFA	35.3000	-95.6583
FAIR	36.2636	-98.4978
FORA	36.8403	-96.4278
FREE	36.7256	-99.1422
FTCB	35.1492	-98.4667
GOOD	36.6017	-101.6014
GRAN	34.2392	-98.7397
GUTH	35.8489	-97.4800
HASK	35.7475	-95.6400
HECT	35.8436	-96.0056
HINT	35.4844	-98.4822
HOBA	34.9897	-99.0525
HOLL	34.6881	-99.8339
HOOK	36.8553	-101.2253
HUGO	34.0308	-95.5400
IDAB	33.8303	-94.8806
JAYX	36.4817	-94.7831
KENT	36.8297	-102.8781
KETC	34.5289	-97.7647
KING	35.8806	-97.9111
LAHO	36.3844	-98.1114
LANE	34.3086	-95.9975
MADI	34.0361	-96.9431
MANG	34.8361	-99.4239
MARE	36.0644	-97.2128
MARS	36.1186	-97.6014
MAYR	36.9869	-99.0111
MCAL	34.8819	-95.7808
MEDF	36.7922	-97.7456
MEDI	34.7292	-98.5667
MIAM	36.8886	-94.8447
MINC	35.2722	-97.9556
MTHE	34.3108	-94.8228
NEWK	36.8981	-96.9106
NINN	34.9678	-97.9514
NORM	35.2556	-97.4836
NOWA	36.7436	-95.6078
OILT	36.0314	-96.4972
OKEM	35.4317	-96.2628
OKMU	35.5811	-95.9150
PAUL	34.7156	-97.2294
PAWN	36.3611	-96.7697
PERK	35.9983	-97.0481
PRES	35.7247	-95.9886
PRYO	36.3669	-95.2717
PUTN	35.8992	-98.9603
REDR	36.3558	-97.1531
RETR	35.1231	-99.3597
RING	34.1939	-97.5883
SALL	35.4381	-94.7978
SEIL	36.1903	-99.0406
SHAW	35.3650	-96.9483
SKIA	36.4147	-96.0372
SLAP	36.5969	-100.2619
SPEN	35.5422	-97.3411
STIG	35.2653	-95.1814
STIL	36.1211	-97.0950
STUA	34.8764	-96.0700
SULP	34.5661	-96.9506
TAHL	35.9728	-94.9869
TALI	34.7106	-95.0117
TIPT	34.4394	-99.1375
TISH	34.3328	-96.6794
TULL	35.8397	-95.4133
VINI	36.7753	-95.2211
WALT	34.3647	-98.3206
WASH	34.9817	-97.5208
WATO	35.8422	-98.5261
WAUR	34.1678	-97.9878
WEAT	35.5081	-98.7753
WEBB	35.4728	-95.1322
WEST	36.0111	-94.6450
WILB	34.9008	-95.3478
WIST	34.9847	-94.6881
WOOD	36.4233	-99.4189
WYNO	36.5172	-96.3422

VITA

Scott A. Woodruff

Candidate for the Degree of

Master of Science

Thesis: SPATIAL COMPARISON OF TWO OKLAHOMA RAINFALL ESTIMATES AS POTENTIAL INPUTS FOR AN EVAPOTRANSPIRATION MODEL

Major Field: Geography

Biographical:

Education: Graduated from Colcord High School, Colcord, Oklahoma in May 1987; received Bachelor of Science degree in Biology from Northeastern State University, Tahlequah, Oklahoma in December of 1992. Completed the requirements for the Master of Science degree with a major in Geography at Oklahoma State University in December, 1999.

Experience: Water Quality Specialist with the Oklahoma Conservation Commission; Laboratory Analyst with the City of Miami, Oklahoma Water and Wastewater Department; Geographic Information Systems Analayst with the City of Norman, Oklahoma.

Professional Memberships: National Geographic Society, South Central Arc Users Group, American Fisheries Society.